

Thesis
5/1/07

**Stochastic Modelling of Phosphorus Transfer from Agricultural
Land to Aquatic Ecosystems**

By
Emma Gillian Murdoch

Submitted to
The Faculty of Natural Sciences, University of Stirling, May 2006

For the degree of
Doctor of Philosophy

This research was undertaken at
The School of Biological and Environmental Sciences
University of Stirling, Stirling, UK

05/07

ProQuest Number: 13917093

All rights reserved

INFORMATION TO ALL USERS

The quality of this reproduction is dependent upon the quality of the copy submitted.

In the unlikely event that the author did not send a complete manuscript and there are missing pages, these will be noted. Also, if material had to be removed, a note will indicate the deletion.



ProQuest 13917093

Published by ProQuest LLC (2019). Copyright of the Dissertation is held by the Author.

All rights reserved.

This work is protected against unauthorized copying under Title 17, United States Code
Microform Edition © ProQuest LLC.

ProQuest LLC.
789 East Eisenhower Parkway
P.O. Box 1346
Ann Arbor, MI 48106 – 1346

Statement of Originality

I hereby confirm that this research was carried out by the undersigned and that all research material has been duly referenced and cited.

Emma Gillian Murdoch

30th May 2006

Abstract

Phosphorus is a limiting nutrient in many freshwater ecosystems and increases in its concentration can lead to eutrophication. Effective management of P in freshwaters requires quantitative estimates of P supply from all significant sources. Simple export coefficient models aim to predict annual diffuse-source nutrient transfers from catchments on the basis of constituent land use. They are attractive water quality management tools, largely due to their low input data requirements. However, the export coefficient for each land use (designed to account for all the controls on P loss including soil type, topography and prevailing meteorological conditions) must be selected from a wide range of published values. This selection is uncertain as although some sort of calibration (to match predicted with observed fluxes by altering export coefficients) may be performed, this will be poorly constrained as different combinations of export coefficients may produce similar predicted fluxes. In addition, this simple approach does not account for inter-annual variations in P losses due to climatic variations and does not explicitly account for topographic controls, distance of fields to the receiving water body or soil type.

The overall aim of this thesis was to investigate modifications to the basic export coefficient model which would improve its applicability to ungauged catchments whilst retaining low, readily obtainable data requirements, without the need for extensive calibration. The modified model, “Stochastic Estimation of Phosphorus Transfer In Catchments” (SEPTIC), has been developed using GIS to exploit spatially referenced information on

- Slope and specific cumulative area drained, derived from digital elevation data. For any given land use, fields on steep slopes adjacent to the stream network are likely to contribute more phosphorus than those on shallow slopes far from streams.
- Soil type, using the UK Hydrology of Soil Types (HOST) classification to estimate “standard percentage runoff” which, in turn, is used to estimate the propensity of a given soil type for exporting phosphorus.

This information was used to constrain the export coefficients, which are randomly sampled from probability distributions, constructed from the range of published values, in a large number of iterations (Monte Carlo simulation). Meteorological data (hydrologically effective rainfall) is also used in the model to predict for inter-annual variations driven by changes in hydrology. The model produces frequency distributions of outputs which can be compared with the sample statistics (mean and confidence intervals) of observed fluxes. A field experiment was carried out to explore P distribution in soil and sediment deposited at field boundaries and to determine whether the model would require refinement to include these.

The model has been applied to two catchments in Scotland (Greens Burn and Leet Water) for which a limited amount of data on observed P losses are available. For the Greens Burn, the model performs well in the years of application, with the predicted load always within the measured load mean \pm 1SEM. For the Leet Water, the model performs reasonably well, with an overlap between the standard deviation of the predicted load and the standard error of the mean of the estimated measured load for many years. Although there is room for further development and improvement, SEPTIC represents a step forward in export coefficient modelling and is a useful screening tool for environmental managers.

Acknowledgements

Thank you to my supervisors, Dr Michael Whelan and Dr Ian Grieve, for their invaluable guidance and support. Thank you to the University of Stirling and Unilever for funding this research.

The assistance of the following people is much appreciated: Bill Jamieson and David Aitchison for their cartography expertise and for “the banter”; Scott Jackson and John McArthur for “saving the day” amidst many a computer crisis; Helen Ewan for her advice on laboratory techniques; Christian Spring for his assistance in the field; Jonathan Bowes for solving GIS glitches; Brian D’Arcy and Jannette MacDonald for providing me with information and the contacts for data (for the Greens Burn and Leet catchments); Will Dryburgh for sharing his considerable knowledge of the Leet catchment with me; Adrienne Clement for providing me with the Zala catchment data and Stanley Bayne for allowing access to his fields to take samples.

Thanks also to fellow colleagues, past and present, in the School of Biological and Environmental Sciences. In particular, Hannah Bishop, Lisa Cahan, Lorna English, Kevin Jones, Jo McKenzie and Christian Spring for helping me through the highs and lows.

Finally, I wish to thank my mum and dad for their support and Neil for his assistance and encouragement.

Table of Contents

Abstract	i
Acknowledgements	ii
Table of Contents	iii
List of Figures	vi
List of Tables	xii
Chapter 1. Introduction	1
1.1. Rationale	1
1.2. Phosphorus in soils	3
1.2.1. <i>P cycle</i>	3
1.2.2. <i>Factors affecting the form of P in soil and soil solution</i>	5
1.2.3. <i>P distribution with depth</i>	8
1.2.4. <i>Temporal Variation in P concentrations</i>	8
1.3. P transfer to water	10
1.3.1. <i>Pathways</i>	10
1.3.2. <i>Forms</i>	11
1.3.3. <i>Factors controlling P loss</i>	12
1.3.4. <i>P transformations</i>	13
1.4. Approaches to modelling diffuse-source P transfers	14
1.5. Main aims of this work	16
Chapter 2. Export Coefficient Modelling	18
2.1. Introduction	18
2.2. Application to the Greens Burn catchment	20
2.2.1. <i>The Loch Leven Catchment</i>	23
2.2.2. <i>The Greens Burn Catchment</i>	25
2.3. Model inputs	29
2.3.1. <i>Land use data</i>	29
2.3.2. <i>Animal data</i>	33
2.4. Simple (deterministic) export coefficient modelling	33
2.5. Stochastic export coefficient modelling, with spatial referencing	34
2.5.1. <i>Monte Carlo simulation</i>	34
2.5.2. <i>Spatially referenced input data</i>	35
2.5.3. <i>Model assumptions</i>	38
2.5.4. <i>Optimum number of iterations</i>	39
2.5.5. <i>Model results</i>	40
2.6. Investigation into using measured data to estimate annual load	43
Chapter 3. Development of the SEPTIC model	48
3.1. Model inputs	48
3.1.1. <i>Slope and Cumulative Area</i>	48
3.1.2. <i>Soil type</i>	56
3.1.3. <i>Hydrological and meteorological data</i>	62
3.2. Results	64
3.2.1. <i>Initial Results (with animals included explicitly)</i>	64
3.2.2. <i>Examination of the different stages of the model</i>	66
3.2.3. <i>Model Results</i>	74
Chapter 4. Investigation into P distribution in fields	78
4.1. Introduction	78

4.1.1.	<i>Delivery of sediment-associated phosphorus to the watercourse</i>	78
4.1.2.	<i>Distribution of phosphorus in the field</i>	79
4.2.	Aims.....	82
4.3.	Field Sites	82
4.4.	Field Site 1	83
4.4.1.	<i>Sampling Strategy (October 2002)</i>	87
4.4.2.	<i>Number of samples</i>	87
4.4.3.	<i>Conditions</i>	88
4.4.4.	<i>Sampling Locations and Samples Taken</i>	92
4.5.	Laboratory Analysis.....	99
4.5.1.	<i>pH</i>	99
4.5.2.	<i>Water Content</i>	101
4.5.3.	<i>Bulk Density</i>	102
4.5.4.	<i>Texture</i>	104
4.5.5.	<i>Organic Matter Content</i>	105
4.5.6.	<i>Total Phosphorus</i>	106
4.6.	Statistical Analysis.....	111
4.6.1.	<i>Correlation</i>	111
4.6.2.	<i>Difference between deposit and source samples</i>	111
4.7.	Discussion.....	112
4.7.1.	<i>pH</i>	112
4.7.2.	<i>Organic Matter Content</i>	112
4.7.3.	<i>Total Phosphorus</i>	112
4.8.	Field site 2.....	112
4.8.1.	<i>Sampling regime</i>	118
4.9.	Analysis	118
4.9.1.	<i>Texture</i>	118
4.9.2.	<i>pH</i>	119
4.9.3.	<i>Total Phosphorus</i>	120
4.9.4.	<i>Deposit Depths and Estimation of Deposit Volume</i>	121
4.10.	Correlation	122
4.11.	Discussion.....	123
4.11.1.	<i>Implications for modelling</i>	123
4.12.	Conclusions	125
Chapter 5.	Modelling using readily available data	126
5.1.	Alternative land use data	126
5.1.1.	<i>Agricultural Census Data</i>	126
5.1.2.	<i>Land Cover Map 2000</i>	128
5.2.	Is it possible to use LCM2000?	130
5.2.1.	<i>The effect of using less detailed land classes</i>	130
5.2.2.	<i>Model sensitivity to land use change</i>	132
5.3.	Readily available data for the Greens Burn catchment	134
5.3.1.	<i>Catchment boundary</i>	134
5.3.2.	<i>Slope and Cumulative Area (Digital Elevation Model)</i>	135
5.3.3.	<i>Land Use</i>	137
5.3.4.	<i>HOST</i>	138
5.3.5.	<i>HER (Rainfall and Actual Evapotranspiration)</i>	140
5.4.	Model results using the readily available data in the Greens Burn catchment.....	141
5.5.	Application of SEPTIC to the Leet Water catchment	141

5.5.1.	<i>The Tweed Catchment</i>	142
5.5.2.	<i>The Leet Catchment</i>	144
5.6.	Data for the Leet catchment – Model inputs	151
5.6.1.	<i>Data to derive slope and cumulative area</i>	152
5.6.2.	<i>Land use data</i>	154
5.6.3.	<i>HOST data</i>	154
5.6.4.	<i>Rainfall data</i>	155
5.7.	Measured data for the Leet catchment.....	156
5.8.	Application of the SEPTIC model to the Leet catchment	158
5.8.1.	<i>Numerical Results</i>	158
5.8.2.	<i>Spatial Results</i>	164
5.8.3.	<i>Assessment of model performance</i>	166
Chapter 6.	Discussion	167
6.1.	Summary of overall aims.....	167
6.2.	Model performance.....	168
6.3.	Further work on model	170
6.3.1.	<i>Soil type</i>	170
6.3.2.	<i>Rainfall and runoff</i>	171
6.3.3.	<i>Connectivity</i>	173
6.3.4.	<i>Selection of export coefficients – different distributions</i>	175
6.4.	Issues not included in model.....	176
6.4.1.	<i>Artificial drainage</i>	176
6.4.2.	<i>In-stream changes</i>	178
6.5.	The value of SEPTIC.....	178
Chapter 7.	Conclusions	180
References		183
Appendices		192

List of Figures

Figure 1.1. The phosphorus cycle in soils. The boxes represent pools of the various forms of phosphorus in the cycle, while the arrows represent translocations and transformations among these pools. The three largest boxes indicate the principal groups of phosphorus-containing compounds found in soils. Within each of these groups, the less soluble, less available forms tend to dominate. (From Brady & Weil, 1999, p. 549.).....	4
Figure 1.2. Transformation of Organic P. (Adapted from Brady & Weil, 1999, p.554.).....	5
Figure 1.3. Phosphorus balance in surface soils (Ultisols) of adjacent forested and agricultural watersheds. The forest consisted primarily of mature hardwoods that had remained relatively undisturbed for 45 or more years. The agricultural land was producing row crops for more than 100 years. It appears that in the agricultural soil about half of the organic phosphorus has been converted into inorganic forms or lost from the system since cultivation began. At the same time, substantial amounts of inorganic phosphorus accumulated from fertiliser inputs. Compared to the forested soil, mineralisation of organic phosphorus was about four times as great in the agricultural soil, and the amount of phosphorus lost to the stream was eight times as great. Flows of phosphorus, represented by arrows, are given as $\text{kg ha}^{-1} \text{a}^{-1}$. Although not shown in the diagram, it is interesting to note that nearly all (95%) of the phosphorus lost from the agricultural soil was in particulate form, while losses from the forest soil were 33% dissolved and 77% particulate. [Data from Vaithiyanathan and Correll (1992)] (From Brady & Weil, 1999, p.547.)	7
Figure 1.4. Seasonal variation in total, inorganic, organic, and available (Bray-1) P content of surface soil (0-50mm depth) from unfertilised and fertilised soil during 1981 and 1982. (From Sharpley, 1985, p.907.)	9
Figure 2.1. Hypothetical catchment to illustrate how the Export Coefficient Model works...	20
Figure 2.2. Map showing the location and extent of the Loch Leven catchment.....	24
Figure 2.3. Map showing the location of the Greens Burn catchment, Perth and Kinross.....	26
Figure 2.4. The Greens Burn catchment, looking eastwards from Newhill Farm (NW of catchment).....	27
Figure 2.5. The Greens Burn catchment, looking south towards the loch from Middleton Farm (centre of catchment).....	27
Figure 2.6. The burn at the centre of the catchment.	28
Figure 2.7. The gauging station on the Greens Burn, at Damleys Cottage (NGR 37 (NO) 157 040).	28
Figure 2.8. Discrepanies in the Greens Burn catchment boundary when derived using three different methods (O.S. 10m contour data, O.S. 5m contour data, provided by SEPA). ...	30
Figure 2.9. ArcView display, showing information for the selected field (shown in yellow), using the “inquiry cursor”.....	31
Figure 2.10. Demonstration of the basic principle of Monte Carlo simulation.....	35
Figure 2.11. Land use distribution in the Greens Burn catchment, 1996.	36
Figure 2.12. Land use distribution in the Greens Burn catchment, 1997.	36
Figure 2.13. Land use distribution in the Greens Burn catchment, 1998.	37
Figure 2.14. Land use distribution in the Greens Burn catchment, 1999.	37
Figure 2.15. Comparison of the means resulting from different numbers of iterations performed by the export coefficient model for the Greens Burn catchment for 1996.....	39

Figure 2.16. Histogram showing distribution of the model output (kg P a^{-1}) from 500 iterations and the spatial distribution of phosphorus export in the Greens Burn catchment, 1996.....	40
Figure 2.17. Histogram showing distribution of the model output (kg P a^{-1}) from 500 iterations and the spatial distribution of phosphorus export in the Greens Burn catchment, 1997.....	41
Figure 2.18. Histogram showing distribution of the model output (kg P a^{-1}) from 500 iterations and the spatial distribution of phosphorus export in the Greens Burn catchment, 1998.....	41
Figure 2.19. Histogram showing distribution of the model output (kg P a^{-1}) from 500 iterations and the spatial distribution of phosphorus export in the Greens Burn catchment, 1999.....	42
Figure 2.20. Measured discharge (Q) and total phosphorus (TP) from the Zala catchment in 1990.....	44
Figure 2.21. Estimated loads (kg P a^{-1}) from the Zala catchment in 1990 calculated from daily, weekly, fortnightly and monthly sampling regimes.....	44
Figure 3.1. Slope (degrees) in the Greens Burn catchment, calculated from the 25m DTM. .50	
Figure 3.2. Comparison of flow direction in the Greens Burn catchment calculated using the filled DTM and non-filled DTM.....	51
Figure 3.3. Diagram showing the binary convention employed by ArcView for Flow Direction.	51
Figure 3.4. Natural logarithm of the cumulative area in the Greens Burn catchment.	53
Figure 3.5. Distributions showing (a) histogram of q_s calculated for each cell during one run of the model, (b) histogram of $\ln q_s$, (c) histogram of $\ln (q_s+1)$, (d) histogram of $q_s/q_{s,\text{max}}$, (e) histogram of $\ln (q_s+1)/\ln (q_{s,\text{max}}+1)$ for the Greens Burn catchment.	55
Figure 3.6. Soil classes in the catchment (Macaulay Institute for Soil Research, Aberdeen). 56	
Figure 3.7. The Flood Studies Report method of flow separation (from Boorman <i>et al</i> , 1995, fig. 2.5, p. 8).....	59
Figure 3.8. Weighted SPR values, derived from HOST, for soil types in Greens Burn catchment.	61
Figure 3.9. Comparison of measured annual rainfall, hydrologically effective rainfall (HER) and TP load in the Greens Burn catchment, 1996-1999.	63
Figure 3.10. Comparison of the predictions of the SEPTIC model (treating organic inputs explicitly) with the measured data.	65
Figure 3.11. Comparison of the predictions of the SEPTIC model (treating organic inputs implicitly) with the measured data.....	66
Figure 3.12. Flow diagram summarising how the SEPTIC model works.....	67
Figure 3.13. Spatial distribution of predicted P export from the Greens Burn catchment in 1996 considering the effect of cropping (land use) only.	68
Figure 3.14. Spatial distribution of predicted P export from the Greens Burn catchment in 1996 considering the effect of cropping (land use) augmented by slope and cumulative area (the “prosser reduction factor”, PRF).....	68
Figure 3.15. Spatial distribution of predicted P export from the Greens Burn catchment in 1996 considering the effect of cropping (land use) augmented by slope and cumulative area (the “Prosser reduction factor”, PRF) and soil type (the “soil reduction factor”, SRF).	69
Figure 3.16. Spatial distribution of predicted P export from the Greens Burn catchment in 1996 considering the effect of cropping (land use) augmented by slope and cumulative	

area (the “Prosser reduction factor”, PRF) and soil type (the “soil reduction factor”, SRF) and <i>HER</i> (the “runoff factor”, ROF).....	69
Figure 3.17. The difference in P export (in 1996) from each cells as a result of including slope and cumulative area in the model compared to considering cropping alone (crops*PRF - crops).....	70
Figure 3.18. The difference in P export (in 1996) from each cell as a result of including soil type in the model compared to considering cropping, slope and cumulative area (crops*PRF*SRF – crops*PRF).....	71
Figure 3.19. The difference in P export (in 1996) from each cell as a result of including <i>HER</i> in the model compared to considering cropping, slope, cumulative area and soil type (crops*PRF*SRF*ROF – crops*PRF*SRF).....	72
Figure 3.20. The difference in P export (in 1998) from each cell as a result of including <i>HER</i> in the model compared to considering cropping, slope, cumulative area and soil type (crops*PRF*SRF*ROF – crops*PRF*SRF).....	73
Figure 3.21. Frequency distribution of predicted TP loads (500 iterations) compared with an estimate of the load derived from measured data (1 SEM) from the Greens Burn catchment for 1996 (a), 1997 (b), 1998 (c) and 1999 (d).....	75
Figure 3.22. Spatial distributions of phosphorus export predicted by the SEPTIC model output from the Greens Burn Catchment in 1996 (a), 1997 (b), 1998 (c) and 1999 (d)....	76
Figure 4.1. Olsen-P concentration in soil sampled between 0 and 85 cm depth, in drained and undrained plots (standard error bars are at the midpoint of the sample depth). (From Haygarth et al, 1998, p.68.).....	80
Figure 4.2. Available (sodium bicarbonate-soluble) soil P levels at various depth increments for manure and fertiliser treatments. The horizontal bars are standard errors. (From Eghball <i>et al</i> , 1996, p.1341.).....	81
Figure 4.3. Location of fields sampled in the Greens Burn Catchment.....	83
Figure 4.4. Topographic and recent land use data for field site 1. The location of boundary deposition observed in November 2001 is also depicted.....	83
Figure 4.5. Evidence of boundary deposition in field 1 in November 2001.....	84
Figure 4.6. Boundary deposition in field 1, November 2001.....	84
Figure 4.7. TP concentrations of surface soil (0-2cm) from samples taken from field 1 on 6 November 2001. Samples 1-7 were taken from the boundary deposit and samples 8-14 were taken from the surface horizon (0-5 cm) within the field.....	85
Figure 4.8. Fine deposition in field 1, Nov 2001.....	86
Figure 4.9. Coarser deposition in field 1, Nov 2001.....	86
Figure 4.10. Field site 1 in November 2001. Potatoes lifted September 2001, Winter Wheat sown October 2001.....	89
Figure 4.11. Field site 1 in October 2002. Winter Wheat cut September 2002.....	89
Figure 4.12. Daily rainfall measured in the Greens Burn catchment prior to the sampling dates (6 th November 2001 and 10 th October 2002), calculated as the average of the daily rainfall measured at the Balado and Portmoak rainguage sites.....	91
Figure 4.13. Sampling locations in field 1, for October 2002.....	92
Figure 4.14. Qualitative description of the soil profile at sampling locations 8 to 14, with 8 being taken 40 m from the top of the slope and 40 m intervals between the samples until 14 at the bottom of the slope.....	93
Figure 4.15. Visual comparison of soil colour changes with depth for core 8 at 0-5, 5-10, 10-15, 15-20, 20-25, 25-30, 30-35, 35-40 cm depths, dried at 30°C.....	94
Figure 4.16. Visual comparison of soil colour changes with depth for core 10 at 0-5, 5-10, 10-15, 15-20, 20-25, 25-30, 30-35, 35-40 cm depths, dried at 30°C.....	94

Figure 4.17. Visual comparison of soil colour changes with depth for core 14 at 0-5, 5-10, 10-15, 15-20, 20-25, 25-30, 30-35, 35-40 cm depths, dried at 30°C.	94
Figure 4.18. Deposit 1 (October 2002), formed at the end of a tramline, measuring 1.84 x 1.23 m, with an observed sandy layer (deposit) of 2cm. A sample (0-15cm) was taken from the centre of the deposit.	95
Figure 4.19. Deposit 2 (October 2002), formed at the end of a tramline, measuring 1.70 x 1.00 m, with an observed sandy layer (deposit) of 2 cm depth. A sample (0 - 15 cm) was taken from the centre of the deposit.....	96
Figure 4.20. Deposit 3 (October 2002), formed at the base of a rill, measuring 12.60 x 10.10 m. A core (to depth 20 cm) was taken from the centre of the deposit and two samples (0 - 15 cm) were taken from opposite edges of the deposit.....	97
Figure 4.21. View down a rill in field 1 (taken in October 2002), showing deposit 3 and the field boundary.	98
Figure 4.22. Visual comparison of soil colour changes with depth for the deposit 3 at 0-5, 5-10, 10-15, 15-20 cm depths, dried at 30°C.	99
Figure 4.23. pH measured at depths down soil and deposit cores sampled from Field 1.....	100
Figure 4.24. pH of surface soil (0-15cm) samples taken down three transects and deposits.	100
Figure 4.25. Change in bulk density with depth in soil cores.....	103
Figure 4.26 Organic matter content (measured as %LOI) of sub-samples with depth down three soil and one deposit cores in field 1.....	105
Figure 4.27. Organic matter content (measured as %LOI) of surface samples (0-15cm) taken down three transects and from deposits.	106
Figure 4.28. Graph showing the temporal variation in absorbance for molybdenum reactions for aliquots with 2 and 8 µgP.	107
Figure 4.29. TP concentrations of surface soil (0-15 cm) down three transects and deposit samples (0-15 cm) in Field 1.	108
Figure 4.30. TP concentrations with change in depth down soil and sediment cores sampled from Field 1.....	110
Figure 4.31. Topography and recent land use for field 2.....	113
Figure 4.32. View across the Greens Burn to field 2, showing source material being carried down a shallow (approximately 16 cm deep) gully (taken 14 th February 2003).	114
Figure 4.33. Gully from upslope in Field 2 (taken 14 th February 2003).	114
Figure 4.34. View from source area looking downslope to field boundary, along which sediment has accumulated (taken 14 th February 2003).....	115
Figure 4.35. Deposit along fence line, with buffer strip on other side (taken 14 th February 2003).	115
Figure 4.36. The deposit in field 2 in the corner of the field (topographic low point) with a clear route for the eroded sediment from the boundary to the burn (taken 14 th February 2003).	116
Figure 4.37. Corner of field 2, showing the removed deposit (28 th February 2003).....	117
Figure 4.38. Close up photograph, showing the depth of deposit removed (28 th February 2003).	117
Figure 4.39. Sampling locations in field 2.....	118
Figure 4.40. Diagram illustrating a section of the deposit used to estimate the volume.	122
Figure 4.41. Daily rainfall measured in the Greens Burn catchment in the year prior to the sampling date of Field 2 (28 th February 2003), calculated as the average of the daily rainfall measured at the Balado and Portmoak rainguage sites.	124
Figure 5.1. The Greens Burn catchment in relation to the Parishes in the area, reproduced from the Adminisitrative Areas Diagram Scotland.....	127

Figure 5.2. The predicted annual phosphorus export from the Greens Burn catchment in 1996-99 using discrete cereals and row crop export coefficients and an amalgamated “arable” coefficient.	131
Figure 5.3. The difference in predicted P export from each cell (kg/625m ² cell), when cereals and row crops are treated discretely (C+R) and when cereals and row crops are amalgamated (C=R) for a) 1996; b) 1997; c) 1998 and d) 1999. Positive values show areas where amalgamating arable crops underestimates export relative to the reference predictions. Negative values indicate overestimates.....	132
Figure 5.4. Predicted P export (kg/a) from the Greens Burn catchment for 1996-1999 when land use is kept constant (1996) and when land use is allowed to change between years.	133
Figure 5.5. Spatial distributions of the difference between the model output (kgP/cell) obtained using land use data for the current year or land use for 1996 (given as P export using land use in current year – P export using land use in 1996) for a) 1997; b) 1998; c) 1999. d) shows the difference (resulting from stochasticity) between two “identical” runs of the model for 1996.....	134
Figure 5.6. Greens Burn catchment boundary supplied by CEH (derived from IHDTM drainage direction grid) and the boundary derived from 5m contour data (as used in Chapters 2 and 3).	135
Figure 5.7. DTM for the Greens Burn data (using CEH boundary).....	136
Figure 5.8. Slope in the Greens Burn catchment, derived from CEH DTM.	136
Figure 5.9. Natural logarithm of the specific area (calculated using flow accumulation derived using DTM).....	137
Figure 5.10. LCM 2000 Subclasses in the Greens Burn catchment.	138
Figure 5.11. HOST data supplied by CEH (1km cell size).	139
Figure 5.12. Host (50m cell size) derived from the 1km data set supplied by CEH.	139
Figure 5.13. The Tweed Catchment.	142
Figure 5.14. Geology of the Tweed Catchment (from Robson <i>et al</i> , 1996, p.7).	143
Figure 5.15. The Leet Catchment.	145
Figure 5.16. The Leet catchment, taken from Hume Castle (NT 706 413) towards Hume, 23-03-06.	146
Figure 5.17. Kennetsideheads Dairy Farm (NT 729 412) - reed bed and settlement pond, 23-03-06.	147
Figure 5.18. Greenriggs Poultry Unit in the Leet catchment (NT 833 482), 23-03-06.	148
Figure 5.19. The Leet Water at Swinton Bridge (NT 832 475) with views upstream (a) and downstream (b), 23-03-06.....	149
Figure 5.20. Gauging station at Coldstream (NT 839 396), 23-03-06.	150
Figure 5.21. Maximum and minimum daily mean flows from 1970 to 2003 excluding those for the featured year (solid line), 2004: mean flow = 1.03 m ³ s ⁻¹ (2004 runoff = 288 mm). Sourced from http://www.nwl.ac.uk/ih/nrfa/station_summaries/021/023.html	150
Figure 5.22. The convergence of the Leet and the Tweed, just south of the gauging station at Coldstream, 23-03-06.	151
Figure 5.23. DTM of the Leet catchment. (Elevations are in metres above sea-level.)	152
Figure 5.24. Distribution of slope (degrees) in the Leet Catchment.	153
Figure 5.25. Distribution of the natural logarithm of specific area in the Leet Catchment...	153
Figure 5.26. Distribution of land use (LCM2000) in the Leet catchment.	154
Figure 5.27. Distribution of HOST classes in the Leet catchment (Note: for each cell, only the dominant HOST class is given).	155

Figure 5.28. Regression between o-P and TP measured at Coldstream gauging station (n = 38).	156
Figure 5.29. Comparison of SEPTIC model predictions with the estimated load, based on measured concentrations and flows, from the Leet catchment, 1996-2004.....	159
Figure 5.30. Comparison between the trends in estimated load (kg P a^{-1}) and <i>HER</i> (mm) for 1996-2004.	159
Figure 5.31. Comparison between <i>HER</i> (mm) and runoff (mm) for the Leet catchment, 1996-2004.....	160
Figure 5.32. Comparison of SEPTIC model predictions (using annual runoff instead of <i>HER</i> as the inter-annual driver) with the estimated load, from the Leet catchment, 1996-2004.	160
Figure 5.33. Histograms of the predicted model outputs (kg P a^{-1}) with the estimated measured load (kg P a^{-1}) for comparison, for the Leet catchment, 1996-2004.....	162
Figure 5.34. Spatial distribution of predicted P export from the Leet catchment, 1996.	165
Figure 5.35. Spatial distribution of predicted P export from the Leet catchment, 2000.	165
Figure 6.1. Natural log of specific area without including the effects of field boundaries in the DTM.....	174
Figure 6.2. Natural log of specific area when field boundaries are added onto the DTM. ...	174
Figure 6.3. Histogram of measured arable (cereals and row crops) export coefficients (Detailed in Appendix 1), n = 38. (x-axis shows the mid-point of the export coefficient classes.).....	175
Figure 6.4. Histogram of measured grassland export coefficients (Detailed in Appendix 1), n = 31. (x-axis shows the mid-point of the export coefficient classes.).....	176

List of Tables

Table 2.1. Area of each land use (ha) within the Greens Burn catchment (total area = 1087.1 ha) and organic inputs, 1995-1999.....	32
Table 2.2. Range of export coefficients measured for different crops and cited in the literature.	32
Table 2.3. Phosphorus Inputs from each organic source in the Greens Burn catchment.	33
Table 2.4. Estimated phosphorus export from the Greens Burn catchment, 1996-99 (using the minimum, maximum and average values for each input) and the measured annual load.	33
Table 2.5. Summary of the model output for 500 iterations and comparison to the measured load, 1996-99.	42
Table 2.6. Sampling regimes investigated to estimate annual P load from the Zala catchment in 1990.	45
Table 3.1. Key from Soil Survey of Scotland, Sheet 5, Eastern Scotland Soil, 1 : 250 000, The Macaulay Institute for Soil Research, Aberdeen, 1982.	57
Table 3.2. Soil and corresponding HOST classes and recommended Standard Percentage Runoff (SPR) coefficients (from Report No. 126, Hydrology of Soil Types: a hydrologically based classification of the soils of the United Kingdom, Inst. Of Hydrology, 1995, Appendix B).	60
Table 3.3. Average values of SPR for each soil class in the Greens Burn catchment.....	60
Table 3.4. Comparison of TP loads (1996-1999) from the Greens Burn catchment predicted by the basic export coefficient model (SD) and the SEPTIC model (SD), with animals included explicitly, with measured data (SEM).....	64
Table 3.5. Numerical Results (1996-1999) from each stage of the model: P export (kgP a ⁻¹) from just considering crops; from considering crops, slope and cumulative area (Crops*PRF); from crops, slope, cumulative area and soil type (Crops*PRF*SRF) and from crops, slope, cumulative area, soil type and <i>HER</i> (Crops*PRF*SRF*ROF) and the measured data for comparison.	73
Table 3.6. Summary of the mean and standard deviation of the distributions produced by the model predictions and the load estimated from the measured data for the Greens Burn catchment, 1996-1999.....	74
Table 4.1. Number of samples (n) required to achieve the specified limit ($D = p \cdot m$).....	88
Table 4.2. Water content (expressed as a percentage of the oven dried (105°C) soil weight) of the soil samples.	101
Table 4.3. Textural classes for the core and surface (0-15cm) soil samples taken in Field 1. The range (average) of the constituent sand, silt and clay for each textural class are: Loamy Sand: 70-90 (80), 0-30 (15), 0-15 (7.5); Sandy Loam: 43-85 (64), 0-50 (25), 0-20 (10); Sandy Clay Loam: 45-80 (62.5), 0-29 (14.5), 20-36 (28); Sandy Clay: 45-65 (55), 0-20 (10), 36-55 (45.5).....	104
Table 4.4. Spearman rank correlation coefficient (<i>p-value</i>) results for samples taken from Field 1.	111
Table 4.5. Soil texture results for samples taken from Field 2.	119
Table 4.6. pH of samples taken from source area and deposited sediment.	120
Table 4.7. TP concentrations (mgP kg oven-dried soil ⁻¹) of the soil samples following digestion and Molybdenum Blue analysis.	120
Table 4.8. Depth of deposit along fence-line.....	121
Table 5.1. Agricultural Census data for Orwell and Portmoak Parishes in 2000. (Note: To prevent disclosure of information about individual holdings, entries relating to less than	

five holdings, or those where two or less account for 85% or more of the information, have been replaced with an asterisk. Some of the data in the tables may not, by itself, be disclosive, but the information has been withheld to prevent disclosure by deduction.) 128

Table 5.2. LCM subclasses (number and description).	129
Table 5.3. Comparison of predicted annual phosphorus export from the Greens Burn catchment using readily available data and more detailed data as input into the model (500 iterations were used in each run).	141
Table 5.4. Measured annual rainfall (mm) in the Leet catchment, along with <i>AET</i> (mm) and <i>HER</i> (mm) estimates for 1996-2004. Average <i>HER</i> (1996-2004) = 198 mm.	156
Table 5.5. Estimated annual TP load (kgP a ⁻¹) from the Leet catchment in 1990 and 1991 using measured TP data and TP estimated from measured o-P data.	157
Table 5.6. Estimated annual TP loads from the Leet catchment in 1996-2004 using measured TP concentrations estimated from o-P concentrations.....	158
Table 5.7. Comparison between SEPTIC outputs when using <i>HER</i> or annual runoff as the inter-annual driver. Average predicted loads are compared to the average estimated load, with the % difference (calculated as ((predicted-estimated)/estimated)*100) shown for both outputs (using <i>HER</i> or annual runoff) for each year, 1996-2004.	161
Table 5.8. Numerical results (1996-2004) from each stage of the model: P export (kgP a ⁻¹) just considering crops; considering crops, slope and cumulative area (Crops*PF); from crops, slope, cumulative area and soil type (Crops*PF*SF) and from crops, slope, cumulative area, soil type and <i>HER</i> (Crops*PF*SF*RF).	163

Chapter 1. Introduction

1.1. Rationale

Phosphorus (P) is a major limiting nutrient in freshwater systems (e.g. Foy & Bailey Watts, 1998). Increases in its availability can cause increased primary productivity leading to eutrophication, characterised by enhanced growth of algae and/or aquatic macrophytes and reductions in dissolved oxygen concentrations. Eutrophication can adversely affect

- water chemistry (reduced dissolved oxygen levels caused by decomposition of dead algal biomass combined with algal respiration at night).
- fish stocks in lakes (the reduction of dissolved oxygen concentrations can result in salmonids being replaced by cyprinids, which are less demanding of high dissolved oxygen concentrations). In addition, at lake margins, algal blooms can out-compete macrophyte communities (which are used by fish for spawning and habitat), with the resulting decline in fish numbers.
- birds and other fish eating predators (through the reduction in food supplies).
- drinking water quality (small algae, which remain after treatment, can badly affect water taste and smell).
- recreational activity (some species of algae (cyanobacteria) produce toxins, which can cause skin rashes and gastrointestinal complaints in humans and may kill small animals)
- tourism (poor water quality, both visually and aromatically)

(e.g. Cooke, 1976; Marsden *et al*, 1995; Mason, 1996; LLCMP, 1999).

There are generally two dominant sources of P in freshwaters: point sources (sewage and, occasionally, leaking animal waste storage facilities) and diffuse sources (transfers from land to water).

Recent research (Jarvie *et al*, 2006) has highlighted evidence that indicates that point (effluent) sources rather than diffuse (agricultural) sources of phosphorus provide the most significant risk for river eutrophication. The incidence of nuisance algal growth in rivers is primarily linked to phosphorus concentrations during periods of ecological sensitivity i.e.

spring and summer low flows when biological activity is at its highest (Mainstone & Parr, 2002), which will be governed more by soluble reactive phosphorus (SRP) from sewage effluents. Although particulate phosphorus (PP) may form a significant proportion of the phosphorus load to rivers, particularly during winter storm events, this is of questionable relevance to river eutrophication (Jarvie *et al*, 2006). It is therefore important to better control point source inputs, especially the smaller sewage treatment works (STWs) discharging to ecologically sensitive/rural tributaries (Wheater & Dandolf, 2003 *in* Jarvie *et al*, 2006).

Although point-source discharges can contribute high P loads to surface waters, these loads can often be controlled (e.g. via the installation of tertiary treatment, which usually involves sulphate additions which causes P to precipitate as a solid). Furthermore, many laundry detergents now use alternative builder formulations (e.g. zeolites) to sodium tri poly phosphate (STPP) which has reduced the detergent P contribution. The net result is that the contribution of P from many STWs has been falling in recent years (Cooper *et al*, 2002a). As a result, complimentary mechanisms to control diffuse phosphorus from agriculture may also be required in catchments where STWs are less dominant or their effluents have been improved (Withers *et al*, 2000).

Diffuse sources, which are essentially agricultural, are much more difficult to manage. This is partly due to the complex and ubiquitous nature of the contributing processes, including surface runoff (Hortonian and saturation-excess overland flow), erosion, throughflow and leaching and their interactions with land management practices (e.g. fertiliser use, stocking and tillage operations). Diffuse source P transfers are believed to be rising slowly in the UK (Cooper *et al*, 2002b).

In many areas of the world (and in much of the UK), diffuse sources are now believed to be the dominant source of P for surface waters and any resulting adverse effects on water quality (Frossard *et al*, 2000; The Royal Society, 1983). As a consequence, a large amount of scientific and regulatory effort has been invested to try to better understand and manage diffuse-source transfers and a range of strategies have been developed including reducing fertiliser applications, changing land use and changing cultivation methods. Numerical modelling has become a vital component of this effort. Models essentially represent a

quantitative synthesis of our conceptual understanding of processes. This can be at a number of different levels from very detailed mechanistic understanding to “broad-brush” hypotheses (e.g. relating nutrient export to land use). The ultimate output is a prediction of water concentrations and loads in response to changes in controlling factors. As such they can be used to explore the implications of different environmental management strategies (e.g. land use controls, fertiliser inputs, encouraging the adoption of near-stream buffer zones) and changes in natural forcing factors (such as climate).

1.2. Phosphorus in soils

Typically, soils contain between 100 and 3000 mg P kg⁻¹ soil, most of which is present as orthophosphate compounds. Between 30 and 65 % of the total soil P is present in organic forms which, like the inorganic forms, have low water solubility. This means that they are not readily available for plant uptake and only slowly contribute to P in the soil solution. The soil solution in agricultural soils, which is the main source of P for plant roots, contains between 0.01 and 3.0 mg P l⁻¹. The quantity of P present in the soil solution represents only a small fraction of plant needs and the remainder must be obtained from the solid phase by a combination of abiotic and biotic processes. The main processes involved in soil P transformation are precipitation-dissolution and adsorption-desorption which control the abiotic transfer of P between the solid phase and soil solution, and biological immobilisation-mineralisation processes that control the transformations of P between inorganic and organic forms (Frossard *et al*, 2000).

1.2.1. P cycle

The forms and relative fractions of P present in soil are dependent on many factors, including soil texture, pH, organic matter content and land use. The interaction between these phosphorus forms is illustrated in Figure 1.1, which shows the cycling of P within the soil, from soil to plants and back to the soil.

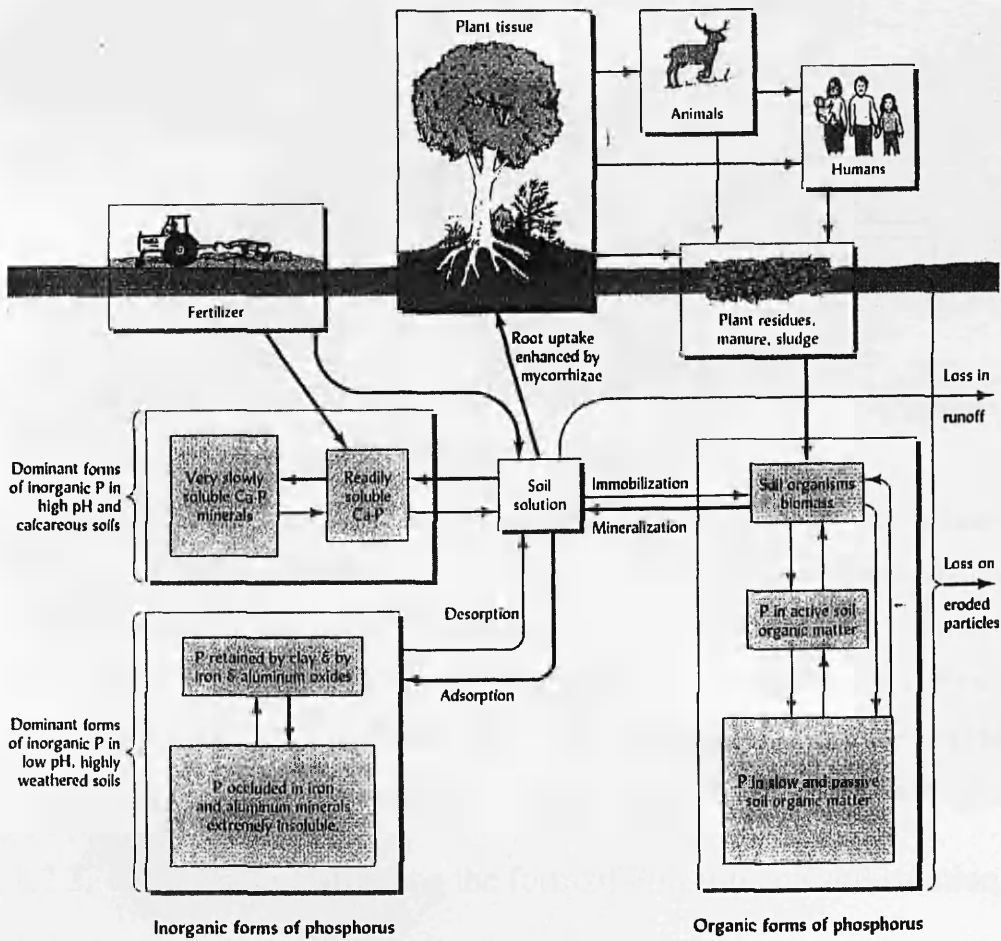


Figure 1.1. The phosphorus cycle in soils. The boxes represent pools of the various forms of phosphorus in the cycle, while the arrows represent translocations and transformations among these pools. The three largest boxes indicate the principal groups of phosphorus-containing compounds found in soils. Within each of these groups, the less soluble, less available forms tend to dominate. (From Brady & Weil, 1999, p. 549.)

Plants uptake phosphate via their roots or associated mycorrhizal fungi. This is then returned to the soil as litter where it is broken down, by the micro-fauna and fauna of the soil, into P containing soil organic matter (SOM), where upon it is ready for future, slow release to soluble forms (Figure 1.2).

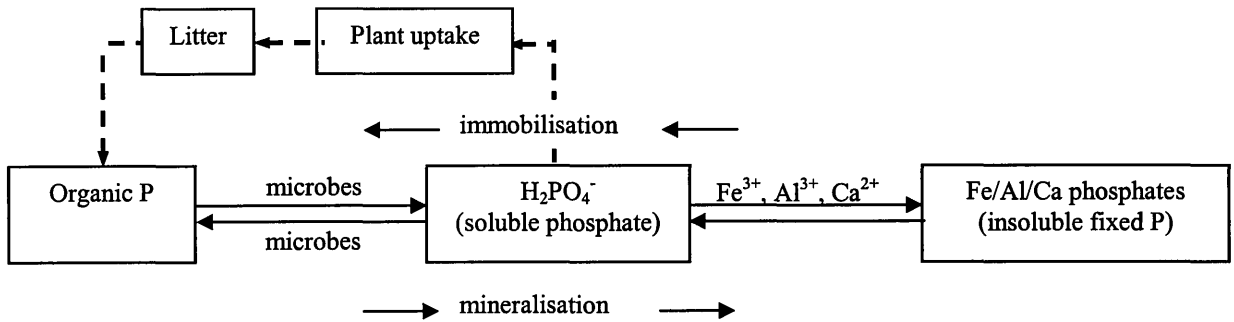


Figure 1.2. Transformation of Organic P. (Adapted from Brady & Weil, 1999, p.554.)

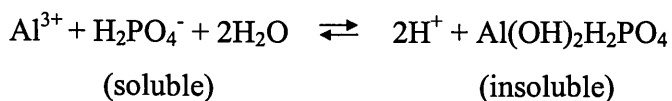
The rate of P mineralisation in soil is dependent, for example, on temperature, moisture content and tillage. Whether there is net immobilisation or mineralisation depends on the carbon (C) content in the soil. In soils with a high C:P ratio (>300:1), microbes will increase their activity and immobilise the phosphorus in their biomass. A low C:P ratio (<200:1) will result in net mineralisation (Brady & Weil, 1999). Soluble phosphate can either be taken up by plants, as already discussed, or transformed further into insoluble Fe/Al/Ca phosphates.

1.2.2. Factors affecting the form of P in soil and soil solution

1.2.2.1. *pH*

The form of phosphate in the soil solution is dependent on the pH of the soil solution. In acidic solutions, the monovalent anion H_2PO_4^- dominates whereas in alkaline solutions, the divalent anion HPO_4^{2-} dominates. In neutral soil, both anions occur. It is thought that the monovalent anion might be more available to plants (Brady & Weil, 1999).

In soils, the form of P is also determined by the pH. In acid soils, the phosphate fixes with Iron (Fe^{3+}), Aluminium (Al^{3+}) and, to a lesser extent, Manganese (Mn^{3+}) in either a precipitation reaction (Equation 1.1 shows such a reaction for Aluminium) or, more commonly, the phosphate ion is exchanged with an anion or hydroxyl group on the surface of insoluble oxides of Fe, Al and Mn.



Equation 1.1

Worthy of note is the tendency of Fe^{3+} to be reduced to Fe^{2+} under water-logged (anaerobic) conditions, e.g. saturated hollows, wetlands or river/lake sediments. This reduction makes the iron-phosphate complex more soluble, with the subsequent release of P into solution (Brady & Weil, 1999).

In alkaline soils, calcium-bound inorganic phosphorus dominates. Under alkaline conditions, in the presence of free calcium carbonate (CaCO_3), adsorption of $\text{H}_2\text{PO}_4^-/\text{HPO}_4^{2-}$ on to calcite occurs by replacement of water, bicarbonate (HCO_3^-) or OH^- ions present on the calcite particles (Morgan, 1997).

In neutral soils, the P fixation is relatively low as Al/Fe/Mn phosphates are more soluble above pH 5-6 and Ca phosphates are more soluble at pH less than 6-8 (Brady & Weil, 1999). For soils in the range pH 4-7.5, adsorption is the main mechanism of P retention (Heathwaite, 1997).

In addition to its CaCO_3 , Al, Fe and Mn content, the P-fixation capacity of a soil is related to its clay and soil organic matter content.

1.2.2.2. *Clay*

Retention/fixation of fertiliser P does not occur to the same degree in all soils. Since the adsorption component of the fixation process is associated with the clay ($< 2 \mu\text{m}$) and hydrous oxide fractions, it follows that P retention will be greater in soils of higher clay content (e.g. Morgan, 1997). Therefore, soils with similar pH and mineralogy, but with different texture, will have different degrees of P fixation. Relatively low P release can be expected for a soil with high clay content (Brady & Weil, 1999).

1.2.2.3. *Soil Organic Matter*

Organic matter has little capacity to strongly fix phosphate ions and will reduce P fixation as

- humic molecules adhere to clay and metal hydroxide particles, masking P-fixation sites and preventing interaction with P ions in solution.

- organic acids produced by plant roots and decay serve as organic anions, which are attracted to positive charges and hydroxyls on clay and hydrous oxide surfaces and hence compete with P ions for fixation sites.
- organic acids entrap reactive Al and Fe in stable organic complexes, called chelates, rendering the metals unavailable for reaction with the P ions in solution (Brady & Weil, 1999).

1.2.2.4. Land Use

The total amount of P in soil and the relative quantities of organic and inorganic P also depend on land use. For the study depicted in Figure 1.3, in an undisturbed, forested catchment, the ratio of inorganic to organic P tends to be 1:2.3. In an agricultural watershed, the ratio is more likely to be 1:0.3.

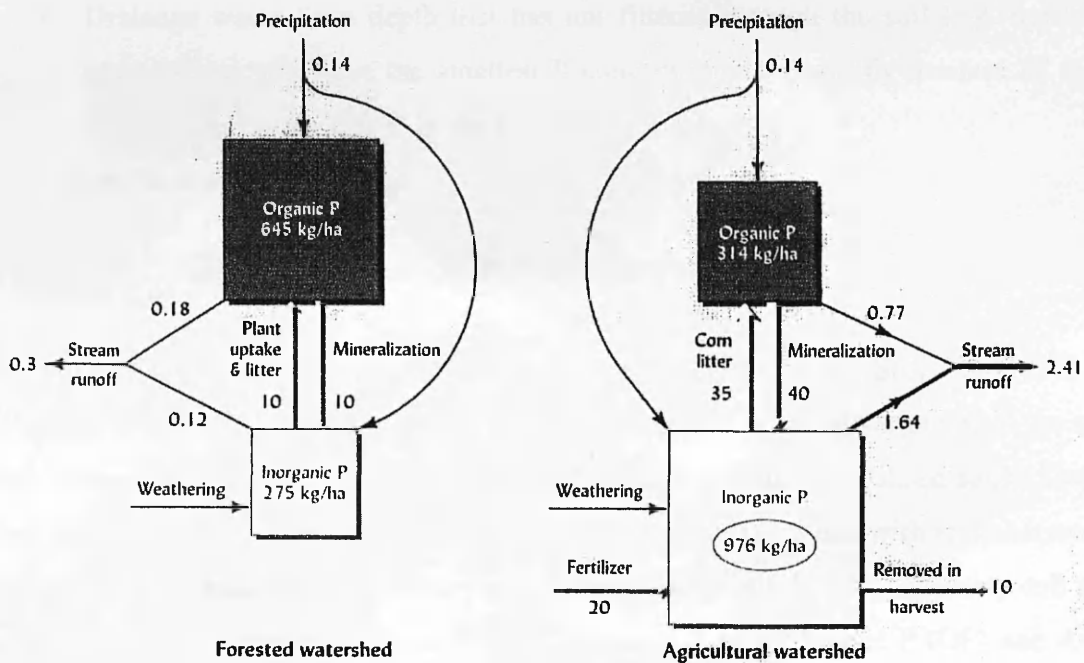


Figure 1.3. Phosphorus balance in surface soils (Ultisols) of adjacent forested and agricultural watersheds. The forest consisted primarily of mature hardwoods that had remained relatively undisturbed for 45 or more years. The agricultural land was producing row crops for more than 100 years. It appears that in the agricultural soil about half of the organic phosphorus has been converted into inorganic forms or lost from the system since cultivation began. At the same time, substantial amounts of inorganic phosphorus accumulated from fertiliser inputs. Compared to the forested soil, mineralisation of organic phosphorus was about four times as great in the agricultural soil, and the amount of phosphorus lost to the stream was eight times as great. Flows of phosphorus, represented by arrows, are given as $\text{kg ha}^{-1} \text{a}^{-1}$. Although not shown in the diagram, it is interesting to note that nearly all (95%) of the phosphorus lost from the agricultural soil was in particulate form, while losses from the forest soil were 33% dissolved and 77% particulate. [Data from Vaithiyanathan and Correll (1992)] (From Brady & Weil, 1999, p.547.)

1.2.3. P distribution with depth

Different experimental research has concluded that when phosphorus is added to the soil surface, the result is surface P enrichment, which reflects the accumulation of P from fertiliser and manure additions over time, the return of P in dead plants and storage in soil organic matter (Haygarth *et al*, 1998). Studies at Barnfield, UK have shown that fertiliser will have little enriching effect below 30cm depth but additions of manure will cause enrichment to 46cm, with little increase in soil P below this depth (Johnston, 1976). With depth, the P content reduces non-linearly (e.g. Nair *et al*, 1995; Eghball *et al*, 1996; Haygarth *et al*, 1998; Frossard *et al*, 2000) and is discussed further in Chapter 4. The implications for P transfer include

- The large concentration of P in surface soil, combined with the erosive, concentrated hydrological energy, will result in overland flow, when it occurs, being efficient in entraining P.
- Drainage water from depth that has not filtered through the soil (e.g. bypassed via macropores) will have the smallest P concentrations, probably because of the small concentrations of Olsen P in the lower horizons.

(Haygarth *et al*, 1998).

1.2.4. Temporal Variation in P concentrations

In response to conflicting research results reported in the literature, Sharpley (1985) carried out a two-year study in Oklahoma and Texas to investigate seasonal variations in the amounts and forms of P in several grassed and cropped, unfertilised and P-fertilised soils. During the two-year period, maximum rainfalls were measured in April – June, with temperatures rising from minima in January and February to maxima in July and August. Monthly soil samples were taken and measured for Total P (TP), Inorganic P (IP), Organic P (OP) and Available (Bray-1) P (AP). Details of these procedures can be found in Sharpley (1985). The results from the experiment are shown in Figure 1.4.

For the unfertilised sites, the TP and IP content of surface soil (0-50 mm) remained fairly constant throughout the study period. OP content was lower in summer (the growing season) compared with winter. AP is also at a minimum during the growing season but increases in

October and November. Over the winter months, AP content remains fairly constant due to the unfavourable soil conditions for biological activity.

For the fertilised sites, TP and IP content in surface soil increases after the P-fertiliser application in May and the OP content was, like the unfertilised sites, lower in summer than in winter, which is largely due to the crop uptake of P. The application of fertiliser also resulted in an increase in AP content but this is not maintained for long.

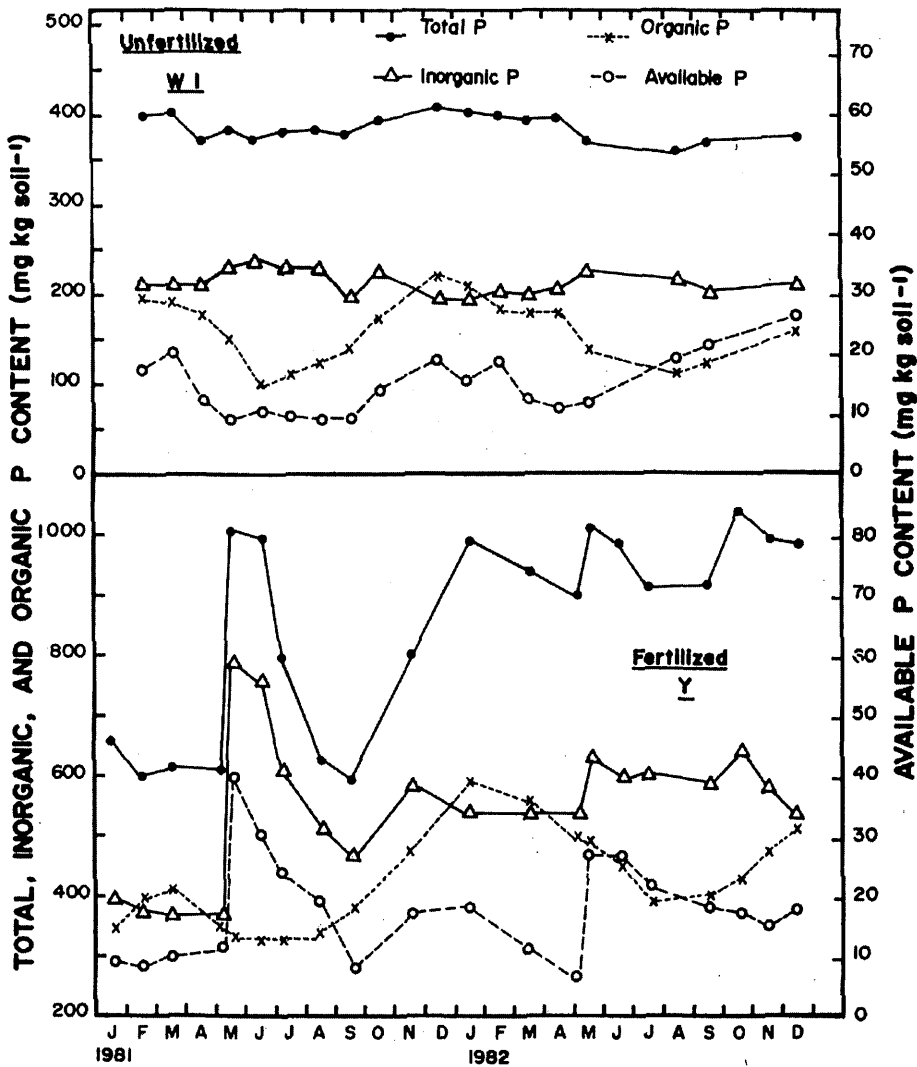


Figure 1.4. Seasonal variation in total, inorganic, organic, and available (Bray-1) P content of surface soil (0-50mm depth) from unfertilised and fertilised soil during 1981 and 1982. (From Sharpley, 1985, p.907.)

The results of this experiment indicate that the AP content of surface soil, for the study sites and study period, was significantly related to the OP content for unfertilised soils and to the IP content for fertilised soils.

The subsurface soil samples (50–150 mm) showed no consistent seasonal variation in IP, OP or AP in unfertilised soils. In fertilised soils, a slight increase in IP and AP content was observed following the P fertiliser application. This lack of seasonal variation in the subsurface soils may be attributed to smaller fluctuations in soil temperature and moisture which, along with low soil organic matter content and associated microbial biomass, reduce microbial activity. In addition, the low mobility of P in soil is also a part explanation.

Seasonal change in inorganic P concentrations extractable from field soils is documented elsewhere, e.g. Smith (1959) found a 3-fold increase in extractable inorganic P during the summer in an unfertilised plot in Scotland. Shand *et al* (1994) showed the maximum concentration of inorganic P occurred in August in the soil solutions of three P-deficient Cambisols in NE Scotland.

In coarse textured soils (where a large amount of the soil volume dries out in summer), a winter minimum and summer maximum in P concentrations has been observed (e.g. Smith, 1959, Weaver *et al*, 1988, Magid & Neilson, 1992). In fine soils, the reverse has been observed, with a winter maximum and summer minimum where P concentrations may be controlled by the reduction and release of P from ferric hydroxides during wet months (Jensen *et al*, 1998 in McDowell & Trudgill, 2000).

1.3. P transfer to water

1.3.1. Pathways

The principal pathways by which P is lost from the soil system are plant removal (5 – 50 kg ha⁻¹ annually in harvested biomass), erosion of P-carrying soil particles (0.1 – 10 kg ha⁻¹ annually on organic and mineral particles) and P dissolved in surface runoff water (0.01 – 3.0 kg ha⁻¹ annually). For each pathway, the higher figures cited for annual P loss are most likely to apply to cultivated soils (Brady & Weil, 1999). In undisturbed ecosystems, net phosphorus

losses from soils occur mainly by leaching at very low rates (Frossard *et al*, 2000), with P removal by plant uptake being returned, eventually, in litter fall.

1.3.2. Forms

Phosphorus in runoff and receiving waters is present as ions of inorganic orthophosphate in solution or in association with organic or inorganic colloidal and particulate material. Dissolved organic P (DOP) is generated from organic matter and organic biomass residues whereas dissolved inorganic P (DIP) is released through mineralisation, although some may be directly derived from agricultural sources, such as fertilisers (Heathwaite, 1997).

Dissolved P (DP) is important because it is immediately available for uptake by plants and algae in soil and water. Under some circumstances, grass and pasture systems can export a greater proportion of DP than cultivated systems (Caruso, 2000). Leaching of DOP can be significant in some areas, particularly in uplands which may have more sources of organic material (for example wastes from grazing animals, peat) because organic forms are less strongly adsorbed to soils, and hence are more mobile than soluble inorganic phosphates (Caruso, 2000; Brady & Weil, 1999). In the lower horizons of such soils, the DOP commonly makes up more than 50% of the total soil solution P. As a consequence, in heavily manured areas with sandy soils DOP can leach downward to nearly 2m. In fields with high water tables, the P can move with the groundwater to nearby lakes or streams and thereby contribute significantly to eutrophication (Brady & Weil, 1999).

Most subsurface transport of P is assumed to be in the soluble fraction, where typical concentrations of soluble P percolating through soil are of the order of 0.1 mg l^{-1} orthophosphate ($\text{PO}_4\text{-P}$), even where the soil-P concentrations are high. Recent research suggests that other P fractions may also be transported via this pathway. For example, for a single storm event it was found that the soluble inorganic fraction in subsurface and near-surface flow formed only 10% of the total P export in both undrained and tile-drained plots. Particulate P formed the bulk of total P mobilised for this event (Heathwaite, 1997). Particulate P clearly is potentially available given suitable conditions for its transformation. Ryding and Rast (1989 *in* Heathwaite, 1997) suggest that around one third of P associated with suspended sediment is biologically available.

1.3.3. Factors controlling P loss

1.3.3.1. *Climate*

Most P loss will occur during periods of high rainfall and when the soil is relatively wet (i.e. usually from autumn through to spring in the UK) (Heathwaite, 1997). Overland flow is periodically generated in UK catchments particularly during prolonged, intense rainfall events and can lead to soil erosion and sediment transport downslope. The efficiency of this pathway for the transport of sediment, with associated P, depends upon factors such as surface roughness, soil physical properties, vegetation cover and the steepness of slope (Johnes & Hodgkinson, 1998). Exceptional periods of loss include summer thunderstorms, which, owing to their intensity, may initiate large P losses, although these tend to be localised in extent (Heathwaite, 1997).

Nash *et al* (2000) concluded that eight storms, out of a total of thirty-two, accounted for 72% of the total P exported from a site in Darnum, Australia. Caruso (2000) also noted the importance of storms in exporting P from a site near Queenstown, New Zealand: One storm was responsible for exporting 23% of the annual TP load. Of the total P load, 47% was transported by baseflow and the remainder by snowmelt.

1.3.3.2. *Topography*

Catchments with steeper slopes are more prone to erosion and associated loss of particulate P. Nash *et al* (2000) compared two sites: For the catchment with steep slopes, loam over clay, only 14% of the TP was in dissolved form whilst for the flatter catchment, sand over clay; 76% of the TP was in dissolved form. This specific study supports the general trend that steeper slopes give rise to larger erosion and hence greater losses of particulate P.

1.3.3.3. *Application of fertiliser/manure*

Only 25%, or less, of the annual fertiliser/manure application is generally recovered by the growing crop. After dissolution in the soil water, the remainder is quickly immobilised by reactions with various soil constituents (i.e. usually minerals but also immobilisation by microorganisms) (e.g. Morgan, 1997). This results in a gradual accumulation of P as a result

of long-term inputs of excessive fertiliser P (e.g. Frossard *et al*, 2000). In some cases, the contribution of residual P (i.e. P not utilised in crop growth) to crop growth may last for 8-10 years. The benefit of residual P for growth will depend on a number of factors, including original rate of fertiliser application, amount of P already removed by growing crops, soil buffering capacity and soil pH (Morgan, 1997). It is important to establish the point at which the capacity of soil to adsorb P becomes saturated, because this will influence the potential for P export in drainage waters. The degree of saturation is dependent on the concentration of P in the soil solution. As the adsorption capacity of the soil approaches saturation, any additional P becomes held less strongly (Heathwaite, 1997). In soils that have low adsorption capacities, or where these have been exceeded, additional inputs of soluble P from fertilisers may be more vulnerable to leaching. This, together with the desorbed fractions, will tend to move vertically down the soil profile below the rooting zone (Johnes & Hodgkinson, 1998) until water is diverted laterally downslope at the water table or at a permeability discontinuity.

The timing of fertiliser application is significant. Intense rainfall shortly after fertiliser application can result in high losses (Haygarth *et al*, 1998). In addition, fertiliser application and heavy grazing when the soil is close to saturation can lead to large losses of both soluble or dissolved (DP) and particulate P (PP). Increasing stocking density can also increase P losses (Caruso, 2000) due, for example, to additional manure deposited per hectare and increased damage to land cover.

1.3.4. P transformations

Whilst phosphorus is being transferred from land to water, it can be transformed from one form to another. Below the ground surface, soil characteristics and P transformations along flow pathways become relatively more important in characterising P loss. Soil structure will influence P fractionation through its indirect control of the length of contact time between percolating water, soil water and soil particles. In this context, macropores, which exist in structured soils or develop through cracking during dry periods, enable rapid bypass flow through the soil. This will reduce the contact time between soil and percolating water. There is evidence to suggest that water moving through soil fissures may show elevated P concentrations. Bypass or macropore flow will probably transport P in a form similar to that recorded in surface runoff. However, it does not quite require the high rainfall intensity and

duration events characteristic of infiltration- or saturation-excess overland flow conditions. Thus P may be transported by macropore flow for relatively small storm events (McGechan, 2003). Similar arguments exist for artificial drainage pipes, which act as effectively large, more or less permanent, macropores in the soil (Heathwaite, 1997).

Once in the stream, P can be transformed from one form to another, which has implications for comparing measured water quality with predicted P loads or concentrations. These in-stream processes include bottom sediment remobilisation, uptake and release from bottom sediments during transport in the river and biological uptake of P by growing macrophytes (May *et al*, 2001). It has been suggested that P concentration in streams draining arable catchments may originate from in-stream processes e.g. Arheimer & Liden (2000) found that the P concentrations in drainage water from clayey fields within some studied catchments in Sweden were lower than at the catchment outlets. The P concentrations in streams may also be altered by stream-bank erosion, which may add directly to particulate P in runoff (Nash *et al*, 2000). This is compounded by livestock access to streams (Caruso, 2000).

1.4. Approaches to modelling diffuse-source P transfers

Various models for predicting the transfer of phosphorus from agricultural land to water courses have been described in the literature. These models vary in complexity, procedure and applicability.

In terms of attempting to represent the best available understanding of the processes governing P turnover and transport, physically-based models are most appropriate. The models include:

- AgNPS (Agricultural Non-Point Source pollution model) – a distributed event-based and continuous model (e.g. Tim & Jolly, 1994).
- ANSWERS (Areal Non-Point Source Watershed Environmental Response Simulation) (Fisher *et al*, 1997) – an event-orientated, process-based distributed model.
- GLEAMS (Groundwater Loading Effects of Agricultural Management Systems) (Yoon *et al*, 1994) – a continuous simulation model.
- SWAT (Soil and Water Assessment Tool) (Arnold *et al*, 1993) – a continuous, spatially distributed model.

Scientifically, these models are intuitively attractive because they attempt to describe how the system will respond to drivers, in theory, without the need for calibration and without many of the constraints which apply to empirical models (e.g. difficulties to extrapolate beyond the range of data used to construct the model). However, such models are generally expensive in terms of their input data and parameter requirements. In many cases the measurements required to calibrate them are not available or have to be replaced by less accurate surrogate data. Even where suitable input data exist, complex models often give little improvement in predictive capability over much simpler models (e.g. Whelan *et al*, 2002). In addition, they may be difficult to extend spatially to the catchment scale and temporally to give predictions over the appropriate time frame (e.g. making long term predictions).

At the other end of the spectrum of model complexity, a number of empirical models have been developed which include:

- The Export Coefficient Model (e.g. Johnes & O'Sullivan, 1989).
- PLUS (Phosphorus, Land Use and Slope) (MLURI & FRPB, 1995) – developed from the export coefficient approach.
- SPARROW (Spatially Referenced Regressions On Watershed Attributes (Alexander *et al*, 2002) – uses a mechanistic non-linear regression equation.
- STELLA (Cassell & Clausen, 1993) - an object-orientated program which calculates the P stored in soil at the field scale.

Although these models sacrifice detail (usually temporally but also spatially) and do not explicitly attempt to synthesise understanding of the processes involved, their minimal input data requirements can make them more attractive to environmental managers for providing indications of how certain factors (e.g. land use practices) are likely to affect phosphorus fluxes to watercourses.

A limitation of most models, of whatever hue (a notable exception being Hession & Storm, 2000), is that they are deterministic and give no appreciation of uncertainty in their predictions. Uncertainty (ignorance) about process mechanisms, parameter values and driving variables is often significant in environmental modelling. Similarly, parameter and driving variable variability (which is simply a characteristic of the system concerned and is, in

principle, knowable and thus distinct from uncertainty) can also contribute to variable outcomes (i.e. a spread of predictions rather than a single number). This means that deterministic models can give a false picture of (and, sometimes, over confidence in) predicted responses. A key element of this project is to incorporate a quantification of uncertainty, and to some extent variability, into model predictions.

1.5. Main aims of this work

The main aim of this work was to develop a model, which bridges the gap between simple, empirical models and more complex, physically-based models, to predict P loading from catchments. The starting point for this work was the simplest existing P export model: the export coefficient model. The export coefficient model (described more fully in Chapter 2) assumes that current land use is the major control of nutrient export and aims to predict total annual nutrient loading to surface waters by estimating the nutrient export by employing “export coefficients” assigned to the constituent land uses in the contributing catchment.

A weakness in the original export coefficient model (as described in Johnes & O’Sullivan, 1989) is the selection of export coefficients. A full verification of the selected export coefficients is not possible without considerable expenditure on field experimental work (Johnes and Heathwaite, 1997) and as a result the coefficients are chosen either by employing expert opinion or through obtaining a good fit between measured and modelled loads. As a result, the coefficients chosen will have a degree of uncertainty attached to them. So far, there has been little effort to take account of this uncertainty in the export coefficient model and the effects of this were explored using a stochastic modelling technique known as Monte Carlo Simulation.

The original export coefficient model also fails to explicitly include the effects of topography and soil type on the export of nutrients from the catchment, with the result that two fields with identical land uses will export the same amount of P regardless of the slope in the field and its position in the catchment. In addition, there is a failure to recognise explicitly the role of runoff in transporting P, such that a dry year will transport as much P as a wet year. This work attempted to address these weaknesses by incorporating the effects of slope, cumulative area, soil type and hydrologically effective rainfall into the model.

A further improvement to the model was the incorporation of GIS to give spatially referenced predictions of P export within the catchment. This has the benefit of aiding the interpretation of the model results, highlighting sensitive areas within the catchment which are more likely to be problematic in exporting P. This pictorial output will also aid discussion between interested parties (e.g. regulators and farmers) in the catchment and thus potentially enable cost effective management.

The target users for this developed model were land managers/ regulators and as such it is desirable that the model uses readily available input data. The ability for the model to make reasonable predictions given easily obtained data was therefore also explored.

Chapter 2. Export Coefficient Modelling

2.1. Introduction

In order to model phosphorus transfer from agricultural land to aquatic ecosystems, the starting point is the export coefficient model (e.g. Reckhow *et al*, 1980; Beaulac & Reckhow, 1982; Rast & Lee, 1983; Johnes & O'Sullivan, 1989; Johnes, 1996; Johnes & Heathwaite, 1997; Worrall & Burt, 1999; Wickham *et al*, 2000). This is the simplest description of P export available and assumes that present land use is the most significant control on nutrient export. Total annual nutrient (nitrogen and phosphorus) loading to surface waters is predicted by estimating export coefficients from each of the constituent land uses in the catchment, such that, for phosphorus

$$L_P = \sum_{i=1}^n c_i A_i + \sum_{j=1}^m \omega_j v_j$$

Equation 2.1

where

L_P	=	estimated P load (kg a ⁻¹)
c_i	=	export coefficient for land cover type i (kg ha ⁻¹ a ⁻¹)
A_i	=	area of land cover type i (ha)
ω_j	=	export coefficient for animal type j (kg cap ⁻¹ a ⁻¹)
v_j	=	number of animals of type j
n	=	number of land cover types in catchment
m	=	number of animal types in catchment

The export coefficients effectively integrate all controls on nutrient transfer (edaphic, hydrological and management). For phosphorus, the coefficients are expressed as mass ha⁻¹ a⁻¹ rather than as a proportion of the amount of P applied because phosphorus transfer is often independent of input rate in the short term, often being associated with sediment transfer (erosion) (Johnes *et al*, 1996; Johnes & Heathwaite, 1997).

Animals are usually included explicitly in Equation 2.1 (e.g. Johnes & O'Sullivan, 1989; Johnes, 1996) because stocking density is believed to be an important factor controlling P

export in many catchments. Substantial losses of P have been observed in grassland grazed by livestock (Hooda *et al*, 1999). However, since animal waste is essentially equivalent to a fertiliser application, which is itself included in the land use-based export coefficient, this extra and explicit contribution from animals may be superfluous. This will be discussed in Chapter 3.

A simple illustration of how the model works is shown in Figure 2.1, which considers the following hypothetical catchment. This catchment is divided into 4 land uses, with the respective areas shown, and there are 20 sheep grazing in the grassland area. The export coefficients that have been applied to these land uses are Potatoes = $0.7 \text{ kgP ha}^{-1} \text{ a}^{-1}$, Wheat = $0.6 \text{ kgP ha}^{-1} \text{ a}^{-1}$, Permanent Grass = $0.4 \text{ kgP ha}^{-1} \text{ a}^{-1}$ and Woodland = $0.02 \text{ kgP ha}^{-1} \text{ a}^{-1}$ and the P lost to the watercourse from sheep is assumed to be $0.05 \text{ kgP cap}^{-1} \text{ a}^{-1}$ (after Johnes, 1996). So the total P export from this catchment in one year is calculated as

$$\begin{aligned}
 \text{P export} &= L_P (\text{Potatoes}) + L_P (\text{Wheat}) + L_P (\text{Permanent Grass}) + L_P (\text{Woodland}) + L_P (\text{Sheep}) \\
 &= (c_{\text{Potatoes}} * A_{\text{Potatoes}}) + (c_{\text{Wheat}} * A_{\text{Wheat}}) + (c_{\text{Permanent Grass}} * A_{\text{Permanent Grass}}) + \\
 &\quad (c_{\text{Woodland}} * A_{\text{Woodland}}) + (\omega_{\text{Sheep}} * \nu_{\text{Sheep}}) \\
 &= (0.7 * 2.0) + (0.6 * 2.0) + (0.4 * 2.5) + (0.02 * 2.5) + (0.05 * 20) \\
 &= 4.65 \text{ kgP a}^{-1} \\
 &= 0.5 \text{ kgP ha}^{-1} \text{ a}^{-1}.
 \end{aligned}$$

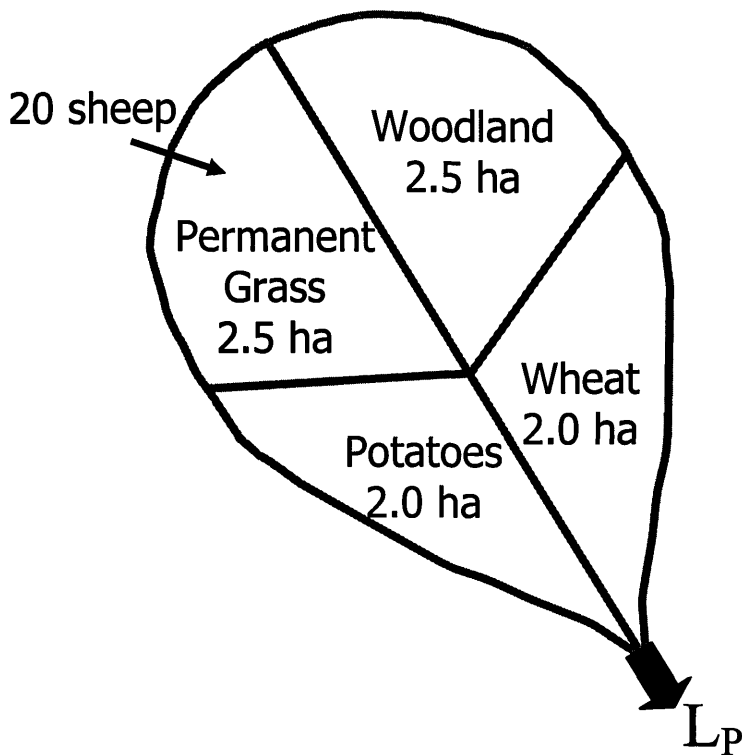


Figure 2.1. Hypothetical catchment to illustrate how the Export Coefficient Model works.

The simplicity, and consequently low data input requirements of this model, makes it an attractive management tool (Johnes, 1996). As a starting point, this model was applied to the Greens Burn catchment, which drains into Loch Leven in the Perth and Kinross region of southeast Scotland (Figure 2.3).

2.2. Application to the Greens Burn catchment

Loch Leven, with a surface area of 13.3 km², a mean depth of 3.9m and a maximum depth of 25.5m, is the largest natural eutrophic lake in Britain (Holden 1976; NCC, 1993; SNH, 2005). The loch has probably always been more productive than most Scottish lochs, with alkaline water in contrast to the acid waters of the Scottish Highlands (Holden, 1976).

Historically, the loch has been subject to change. The greatest change occurred between 1828-1832 when the loch was reduced in size by about one-quarter. This was undertaken to control the loch level, to ensure a regular supply of water to downstream mills and increase the land available to agriculture (Munro, 1994 *in* LLCMP, 1999). Today, the loch's level is

managed by the River Leven Trust for the provision of process water for industry in Fife (LLCMP, 1999).

The loch has a number of conservation designations (SSSI, National Nature Reserve, Ramsar Site, potential Special Protection Area) on account of its ecological significance. The loch and its margins comprise a rich and diverse range of habitats that support a broad variety of insects, plants and animals. Botanically, there are nine species of particular note, including two red data book species: *Hierochloa odorata* and *Juncus filiformis*. In addition, it is the only mainland site in Britain for the beetle, *Thanatophilus dispar* (NCC, 1993). Loch Leven is the most important grey goose roost in Britain with internationally important numbers of Greylag and Pink-footed Geese. It also holds nationally important wintering populations of several other species of wildfowl and has exceptionally high breeding duck numbers. Consequently, it was included in a list of European and North African Wetlands of particular importance to wildfowl published by the 1962 “MAR” International Conference on Wetlands (SNH, 2005). To ensure that there would remain an area for geese to graze, the Royal Society for the Protection of Birds established the Vane Farm Nature Centre and Reserve, on the south shore of the loch (SNH, 2005; RSPB, undated).

The ecology of the loch is threatened by its water quality. Blooms were reported in 1937, 1947, 1954, 1958 and 1961. A bloom beginning in April 1963 lasted until 1964 and there were annual dense blooms in the 1970s. Research during the 1970s clearly showed that eutrophication in the loch was adversely affecting insect life, fish and some wildfowl species e.g. from a maximum of almost 90,000 trout caught in 1960, the annual catch decreased to less than 20,000 fish in the 1970s (Cooke, 1976). Since then, there has been an action plan to reduce phosphorus inputs to the loch, which initially focussed on point-sources. Improvements to the quality of discharges from industry and the local Waste Water Treatment Works (WWTWs) reduced the annual phosphorus load from an estimated 11.6 tonnes in 1985 to about 3.3 tonnes in 1995. These improvements included the replacement of the ferric dosing plants at Milnathort and Kinross WWTWs and the diversion of Kinnesswood’s sewage out of the Loch Leven catchment. Reducing the input of diffuse phosphorus sources is the remaining challenge (LLCMP, 1999).

Following the severe algal bloom of 13th June 1992, known locally as “Scum Saturday”, the Loch Leven Area Management Advisory Group (LLAMAG) was established with the long-term objective of “achieving, by co-operation of interested parties, a water quality in Loch Leven which can form the basis for the loch’s long-term sustainable management, and use for local, national or international needs” (LLCMP, 1999). To induce a recovery of macrophytes and associated fauna in the loch, the LLAMAG derived, from various eutrophication models, a target of $40\mu\text{gl}^{-1}$ for the annual mean total phosphorus concentration. In addition, the group recommended that a Catchment Management Plan should be instigated to address the problem of diffuse phosphorus inputs to the loch. In the meantime, the loch was downgraded to Class 2 in SEPA’s 1995 Lochs Classification Scheme, due to the significant input of phosphorus from its catchment (LLCMP, 1999).

The Loch Leven Catchment Management Project was constituted under Section 5 of the Natural Heritage (Scotland) Act 1991. A project steering group (consisting of members from Scottish Natural Heritage (SNH), Scottish Agricultural College (SAC) and the predecessor bodies of Perth and Kinross Council (PKC) and Scottish Environmental Protection Agency (SEPA)) was appointed in 1995, with the aim of promoting sustainable management of the Loch Leven catchment area through the development, promotion and implementation of an integrated catchment management plan. To achieve this aim, eight objectives were defined:

1. To identify appropriate targets for water quality and phosphorus loading for the Loch Leven catchment.
2. To identify mechanisms and initiate practical management which would enable those targets to be met.
3. To establish guidelines which will enable an integrated approach from statutory consultees to the local planning authority on development issues and give clear guidance to potential developers.
4. To produce, and initiate implementation of, a river management strategy which would include the improvement of the habitat quality of the loch’s feeder burns.
5. To produce, and initiate implementation of, a practical land use strategy for the catchment.
6. To establish a framework for continued integrated catchment management.
7. To produce a Catchment Management Plan, documenting the above information.

8. To consult with other parties interested in the management of the Loch Leven catchment.

Working groups, which consisted of representatives from SNH, SAC, SEPA, PKC, East of Scotland Water Authority (ESWA), Institute of Freshwater Ecology (IFE), Farming and Wildlife Advisory Group (FWAG), Royal Society for the Protection of Birds (RSPB), and Forestry Authority (FA), were formed to address the issues of water quality, river management, planning & development and agriculture & forestry.

It is generally recognised that the production of algal biomass in the loch is dependent primarily on weather conditions and the loch's flushing rate and only secondarily by the concentration of nutrients. However, minimising phosphorus inputs currently appears to be the most practicable way that the loch's recovery can be managed (LLCMP, 1999).

2.2.1. The Loch Leven Catchment

The Loch Leven catchment has an area of 145km² and is delimited by the Lomand, Benarty, Cleish and Ochil hills (shown in Figure 2.2). There are two main aquifers in the catchment, one lying above the other. The lower one, with bedrock of Old Red Sandstone, underlies the whole basin and is largely sealed by overlying clay layers. It is fed by the surrounding hills, is generally of good quality and is thought to drain eastwards down the Leven valley. The upper aquifer lies above the clay layers on sand and gravel deposits and drains to the loch. It is often in close contact with surface waters and its quality is variable, greatly influenced by the activities in the catchment. The main concern in the upper aquifer is the phosphorus level in the groundwater, which can be at or above the phosphorus Water Quality Standard set for the loch itself (Sargent, 1996 *in* LLCMP, 1999, p.22).

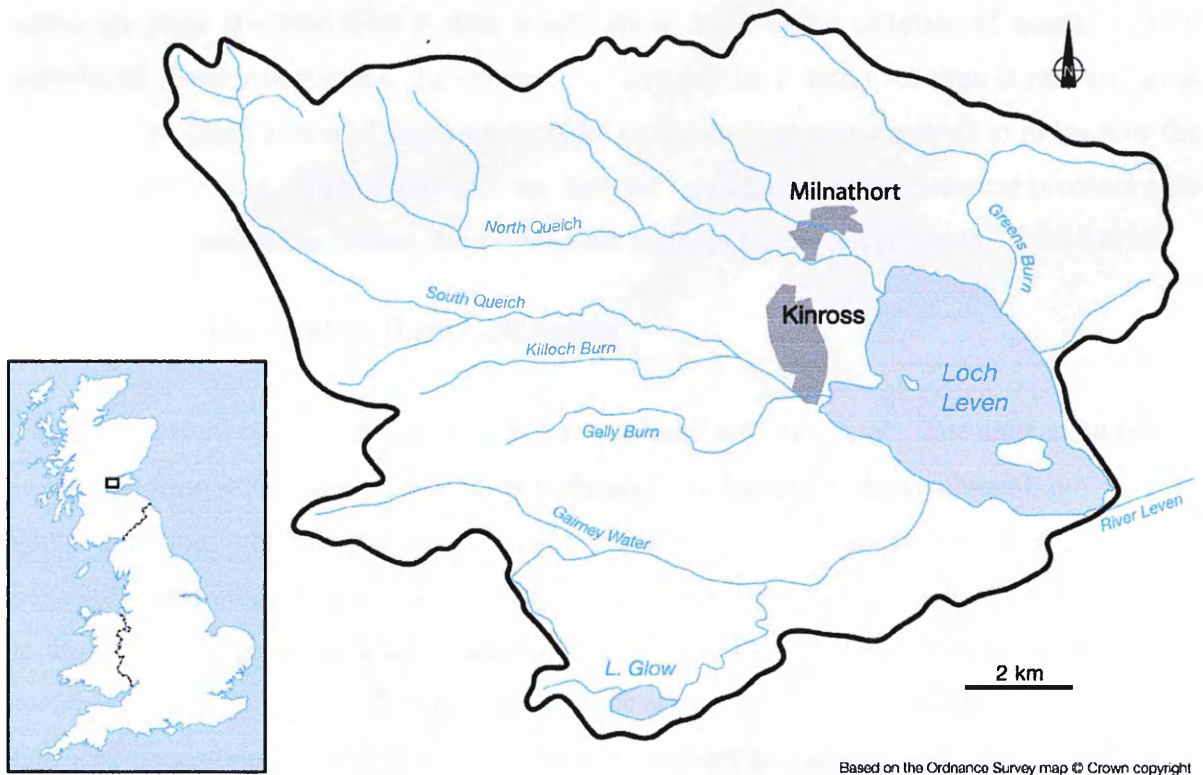


Figure 2.2. Map showing the location and extent of the Loch Leven catchment.

Five main watercourses drain the catchment: the North and South Queichs; the Gelly Burn; the Gairney Water and the Pows/Greens Burn. In the last 200 years, many sections of the burns flowing into the loch have been straightened and deepened to enhance drainage of lowland areas and in some cases to provide power for the mills (Soulsby and Soulsby, 1994 *in* LLCMP, 1999).

The Scottish Environmental Protection Agency (SEPA) has established a gauging site at the outlet of the Greens Burn catchment at Damley's Cottage (shown in Figure 2.7) where flow is measured and daily mean flow recorded. In addition, a grab sample is taken from this site on a monthly basis and tested for total P concentration, amongst other determinants. For each year, the average annual P load is estimated as the average of the annual load calculated for each of the 12 monthly samples (from the product of the P concentration and daily mean flow). Such an infrequent sampling regime leads to an uncertain estimated annual P load, as demonstrated in Section 2.6.

Although more frequent total P data would allow for a better estimate of annual total P transferred to the watercourse, the existence on any regular P data over time is rare and so at least a rough guide to total P exported from the catchment can be calculated to judge how the model is performing. This, along with the fact that Loch Leven has a historical problem with P enrichment, makes the Greens Burn catchment suitable for the development of the model.

2.2.2. The Greens Burn Catchment

The Greens Burn catchment (Figure 2.3) has a gauged area of 11km². The catchment ranges in altitude from 400m above sea level at Bishophill, in the east of the catchment, down to the gauging station, which is sited at 105m above sea level. According to Frost (1993, s.3), the soils within the study area are varied, ranging from peats and peat alluvial complex soils close to the Loch through fluvio-glacial sand and gravel deposits and areas of glacial till to shallow rocky skeletal soils on the hills. Parent materials are generally either sandstone or lava of the Old Red Sandstone age. Most of the soils are relatively coarse textured with freely drained soils predominating, except close to the loch, where shallow ground water gives rise to wet soils. For 1996-1999, the mean annual rainfall was 1000mm.

Land use in the catchment is predominately arable, although grass is grown in most crop rotations (Frost, 1993). The exception is on the steep hillsides, where the poor soil and gradient dictate rough grazing. Figures 2.4 – 2.6 show views of the catchment and Figure 2.7 shows the gauging station situated at Damleys Cottage on the Greens Burn.

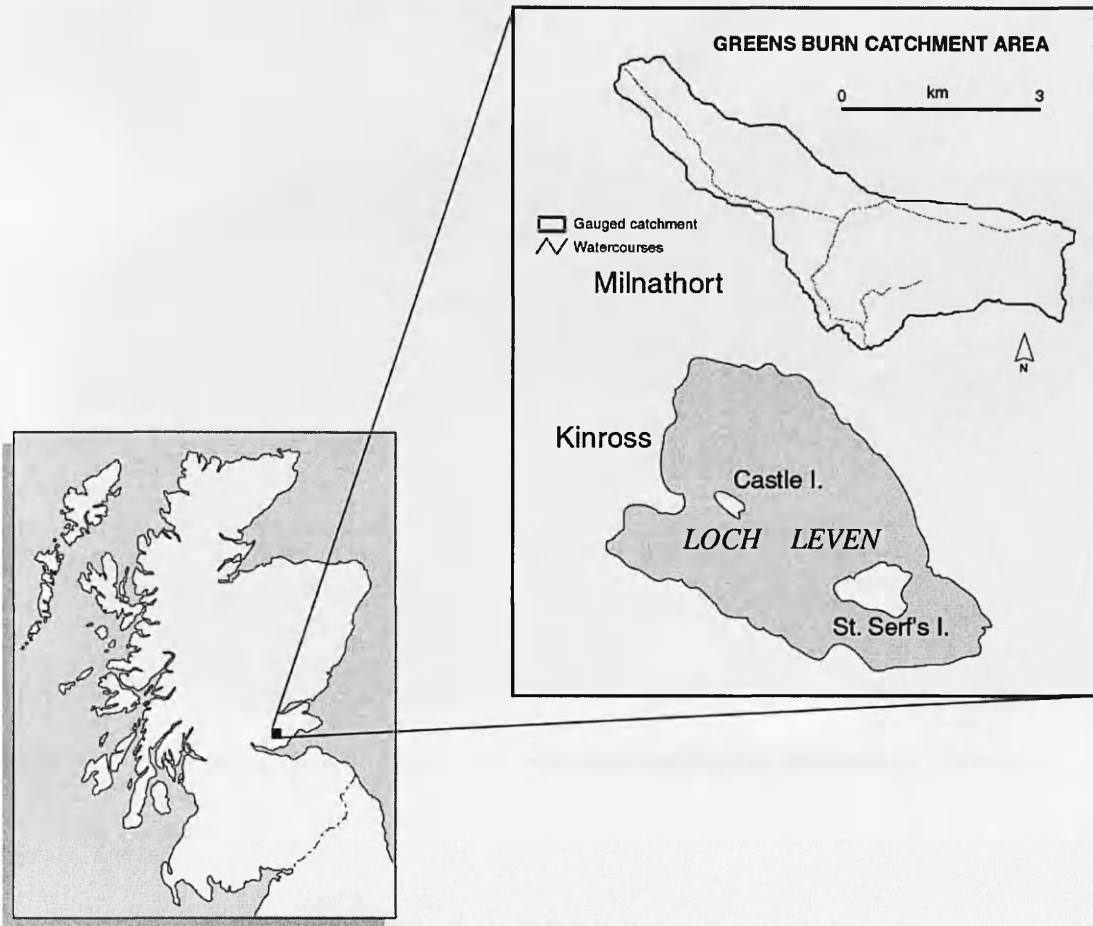


Figure 2.3. Map showing the location of the Greens Burn catchment, Perth and Kinross.



Figure 2.4. The Greens Burn catchment, looking eastwards from Newhill Farm (NW of catchment).



Figure 2.5. The Greens Burn catchment, looking south towards the loch from Middleton Farm (centre of catchment).



Figure 2.6. The burn at the centre of the catchment.



Figure 2.7. The gauging station on the Greens Burn, at Damleys Cottage (NGR 37 (NO) 157 040).

The catchment draining to the gauging site at Damley's Cottage was delimited in ArcInfo GIS program, using O.S. digitised 5m contour data for the area.

2.3. Model inputs

2.3.1. Land use data

To gain information on the land use in the Greens Burn catchment, an inventory of land use, fertiliser inputs and animal numbers was required. This information had previously been researched by Hope (2000), using a catchment boundary supplied by SEPA. Information on land tenure within the catchment was obtained from The Scottish Executive Rural Affairs Department (SERAD). Each farm within the catchment was visited and the farmer interviewed. Firstly, the farmer was shown an enlarged area of the catchment, which showed in detail the individual fields belonging to his/her farm. After clarifying the boundary of the farm within the catchment, the following questions were asked:

1. What crops were grown in each field for the previous five years (1995-1999)?
2. What was the average fertiliser application for each crop type? Please detail fertiliser brand/ratio.
3. Do you keep any cattle, sheep, pigs, poultry or horses? If so, please give a number for each type in the fields of interest for each year (1995-1999).
4. Do you apply any slurry, farmyard manure or silage effluent to the fields? If so, please estimate total amounts over the fields of interest in each year (1995-1999).

The answers to question 1 were recorded for each individual field, whereas the answers to questions 2-4 were recorded on a farm-by-farm basis.

From the 1991 population census, it was estimated that 130 people are resident in the catchment (Perth and Kinross Council, 2000). All domestic sewage in the area is treated via septic tanks (A. Crawford, *pers comm.*)

A map (Ordnance Survey Pathfinder 372 (NO 00/10), 1:25000 scale) showing the field boundaries in the catchment was scanned and geo-corrected (i.e. to assign spatial referencing) in ERDAS IMAGINE (Leica Geosystems Geospatial Imaging, Georgia, USA). The map was

then imported into ArcView (v.3.1, ESRI, California, USA) and the catchment boundary (provided by SEPA) superimposed.

For this new research, digital elevation models were derived (in ArcInfo) to show the catchment draining to the gauging station, using 10m O.S. digitised contour data and 5m O.S. digitised contour data. These derived catchment boundaries were subsequently imported into ArcView where it was noted that there were discrepancies between the catchment boundaries derived by these three methods (SEPA, 10m contour data and 5m contour data), as shown in Figure 2.8. A “ground-truthing” exercise confirmed that the boundary derived using the 5m O.S. digitised contour data was the most accurate. As a result of this “new” boundary, there was a lack of information in the farm surveys conducted by Hope (2000), which were based on the SEPA boundary, for the fields in the south-east of the catchment and a further survey filled in these gaps to give a complete land use data set for the entire catchment for 1995-99.

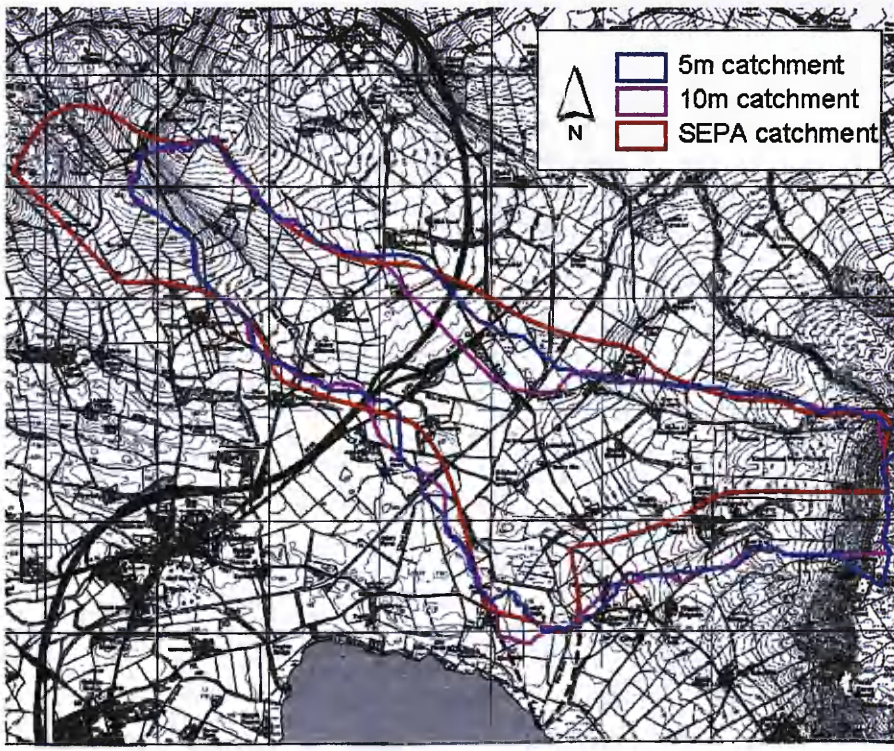


Figure 2.8. Discrepancies in the Greens Burn catchment boundary when derived using three different methods (O.S. 10m contour data, O.S. 5m contour data, provided by SEPA).

Using the correct catchment boundary, the field boundaries were digitised, in ArcView, as a new theme. This allowed the area of each field to be calculated. The land use data for each year (1995-1999) was then entered into the attribute table for the theme, allowing each field to be selected (using the inquiry cursor) and the information for that field (farm; land use in each year; area) to be displayed, as illustrated in Figure 2.9.

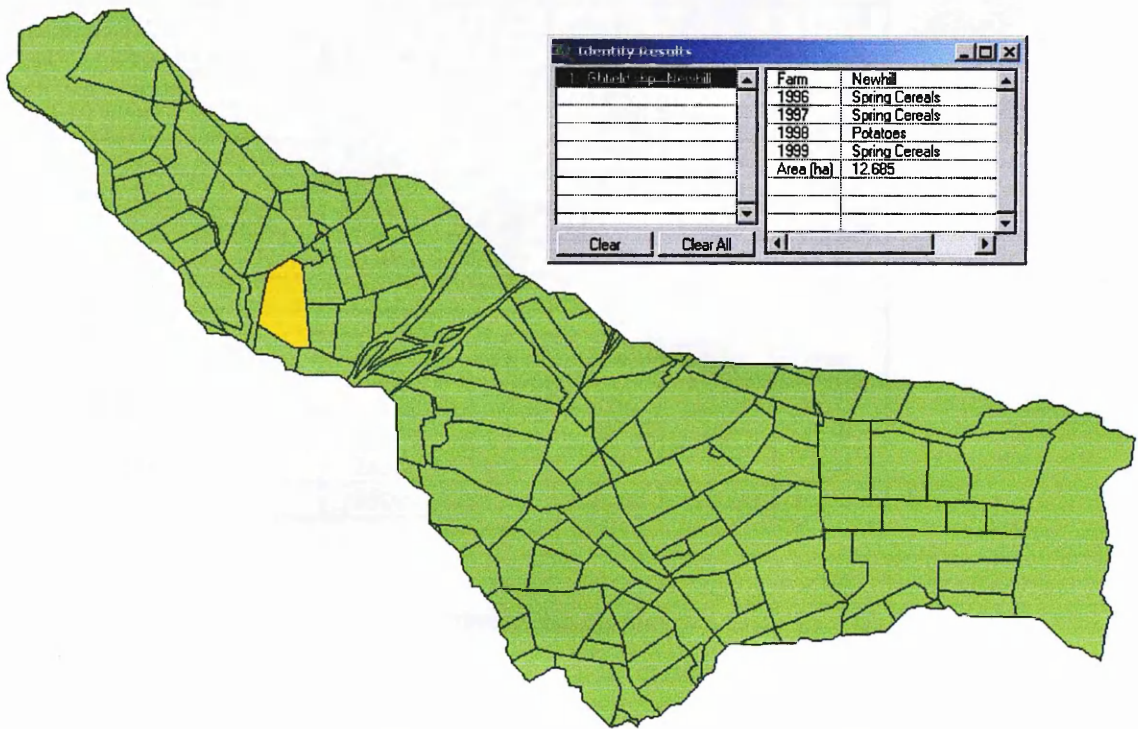


Figure 2.9. ArcView display, showing information for the selected field (shown in yellow), using the “inquiry cursor”.

Subsequently, the distribution of each land use within the catchment was determined for each year and is shown in Table 2.1.

Table 2.1. Area of each land use (ha) within the Greens Burn catchment (total area = 1087.1 ha) and organic inputs, 1995-1999.

YEAR	1995	1996	1997	1998	1999
LAND USE					
	AREA (HA)				
Permanent Grass	102.599	102.599	102.599	102.599	102.599
Temporary Grass	99.872	92.426	91.522	56.197	98.574
Spring Cereals	236.702	314.851	321.995	396.974	397.193
Winter Cereals	160.660	191.662	113.371	132.853	81.243
Spring Oilseed Rape	20.283	31.909	26.081	9.799	27.516
Winter Oilseed Rape	41.136	3.908	65.561	21.466	45.797
Field Vegetables	70.311	46.416	86.603	61.217	66.796
Peas	39.480	49.923	21.073	8.612	13.862
Potatoes	97.001	92.771	94.388	107.225	70.912
Root Crops	25.432	7.687	4.694	4.351	4.351
Rough Grazing/Set Aside	160.123	119.447	125.712	122.478	144.756
Buildings/Roads	33.475	33.475	33.475	33.475	33.475
ORGANIC INPUTS					
Cattle (no)	254	294	294	254	295
Sheep (no)	1550	1580	1580	1550	1580
Humans (no)	150	150	150	150	150
Hen pen (tonnes)	2824	1450	727	758	980
Slurry (litres)	198000	198000	198000	198000	198000

This information can be used to estimate the annual phosphorus export, for each year, from the catchment. There is a wide range of export coefficients published in the literature for different land uses and these are summarised in Table 2.2 (and detailed in Appendix 1). It should be noted that most of these measurements represent plot or field scale transport (i.e. are effectively mobilisation) and are not a measure of delivery to the stream.

Table 2.2. Range of export coefficients measured for different crops and cited in the literature.

Land Use	Export kg P ha ⁻¹ a ⁻¹		
	Average	Minimum	Maximum
Grass	0.93	0.02	4.90
Arable/Cereals	1.60	0.06	5.67
Row Crops	1.31	0.02	5.77

2.3.2. Animal data

In order to correctly calculate the animal inputs, information is needed on the phosphorus input from each source, how much of it is actually applied to the catchment and an estimate of how much of this is subsequently lost to runoff. Table 2.3 summarises this information, which is expressed in more detail in Appendix 1.

Table 2.3. Phosphorus Inputs from each organic source in the Greens Burn catchment.

Organic Source	Phosphorus Input Average (Range)	% applied to land Average (Range)	% lost to runoff Average (Range)
Cattle (per head)	10.18 (3.13 – 17.60)	95 (72 – 100)	3 (1 – 5)
Sheep (per head)	1.6 (1.47 – 1.80)	100	3 (1 – 5)
Humans (per head)	0.65 (0.30 – 1.00)	n/a	n/a
Hen Pen (per tonne)	10.5 (+/- 25%)	90 (68 – 100)	3 (1 – 5)
Slurry (per litre)	0.0007 (+/- 25%)	90 (68 – 100)	3 (1 – 5)

2.4. Simple (deterministic) export coefficient modelling

Using the most simple, deterministic version of the export coefficient model, the phosphorus export from the Greens Burn catchment for 1996-99 was calculated (in an EXCEL spreadsheet) for three “what if” scenarios: assuming the minimum, maximum and average values for each export coefficient input. The results are shown in Table 2.4.

Table 2.4. Estimated phosphorus export from the Greens Burn catchment, 1996-99 (using the minimum, maximum and average values for each input) and the measured annual load.

Year	Estimated Phosphorus Export (kg/a)			Measured P Load (kg/a)
	Minimum	Maximum	Average	
1996	190	6611	1985	528 ± 260
1997	153	6124	1781	574 ± 330
1998	153	6128	1781	664 ± 257
1999	166	6169	1822	528 ± 224

Clearly the model hugely over-predicts when the maximum values are used and also over-estimates when the average values are used. However, the measured load does lie within the range predicted by the model when using the minimum and maximum values, although the

large range between the scenarios makes it difficult to make any useful interpretation. The problem for the modeller is the correct selection of these input parameters from the published range. For any particular land use, phosphorus export will vary from year to year and from location to location. This is reflected in a wide range of measured values of phosphorus export reported in the literature (summarised in Table 2.2 and detailed in Appendix 1) and means that the basis for selecting a meaningful coefficient for each of the constituent land uses of a catchment will always be highly uncertain, particularly in the absence of site-specific measurements. A common approach is to invoke a calibration procedure, which involves adjusting the coefficients so as to obtain a good match between the observed and measured fluxes. However, this will be poorly constrained as several different combinations of export coefficients may generate similar fits to measured data. Alternatively, the selection of coefficients may be achieved subjectively, with expert opinion being sought to ascertain the likely export for land uses in a specific catchment. With both these approaches, the model parameters are set for a specific catchment and hence are not universally applicable.

An additional weakness with this model is that it takes no account of the position of the field within the catchment and does not provide the land manager with any spatial results, which would allow the identification of “hot spots” (areas prone to export most P) within the catchment and hence allow management P loss mitigation strategies to be targeted.

2.5. Stochastic export coefficient modelling, with spatial referencing

2.5.1. Monte Carlo simulation

One aim of this work is to modify the export coefficient model in an attempt to address these limitations. In order to account for the uncertainty in the export coefficients selected for each land use, Monte Carlo simulation (depicted in Figure 2.10) is employed (e.g. Vose, 1996). This involves making a large number of iterations of the deterministic model core. In each iteration, a value for each export coefficient is randomly selected from a probability distribution (e.g. uniform, normal, log-normal) constructed from the range of published coefficients for that land use. This will result in an output distribution which shows the range and likelihood of possible P export from a catchment.

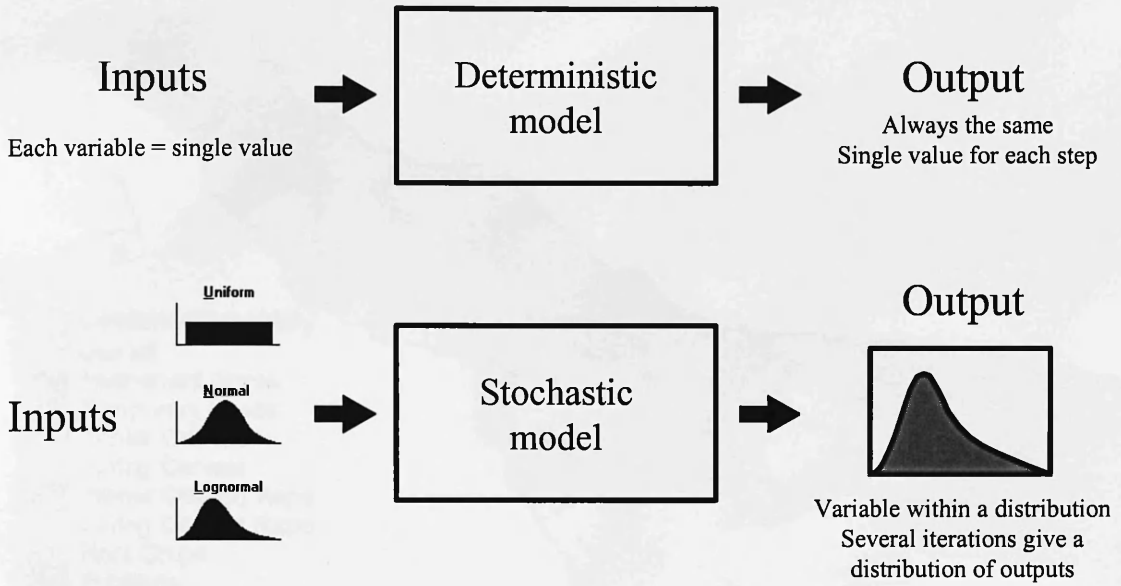


Figure 2.10. Demonstration of the basic principle of Monte Carlo simulation.

2.5.2. Spatially referenced input data

GIS is employed to provide spatial referencing, so that the position of each field can now be incorporated. Using the field boundaries theme created in ArcView GIS (which includes land use information for 1995-99), RASTER grids (cell size of 25m*25 m) were created showing the land use distribution in each year (1996-99) in the Greens Burn catchment. The cell size (25m*25m) was selected as providing a good level of catchment detail whilst recognising the constraints imposed by the quality of input data (O.S. 5m contour data). The resultant grids are shown in Figures 2.11 – 2.14.

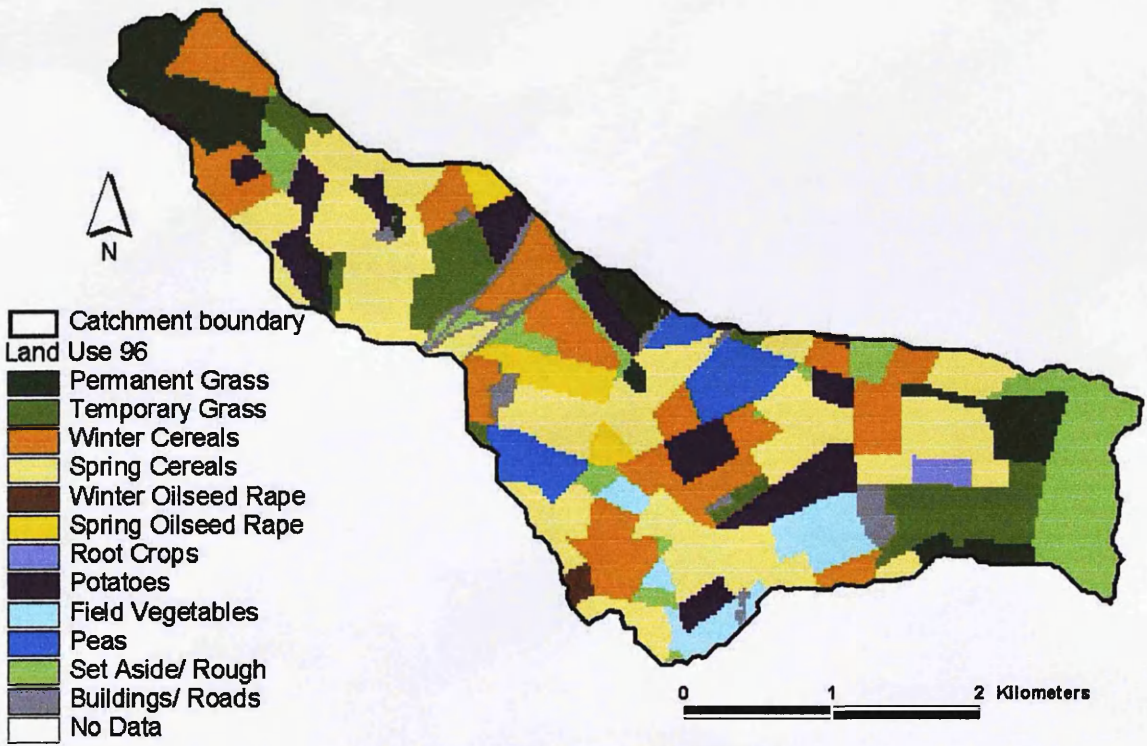


Figure 2.11. Land use distribution in the Greens Burn catchment, 1996.

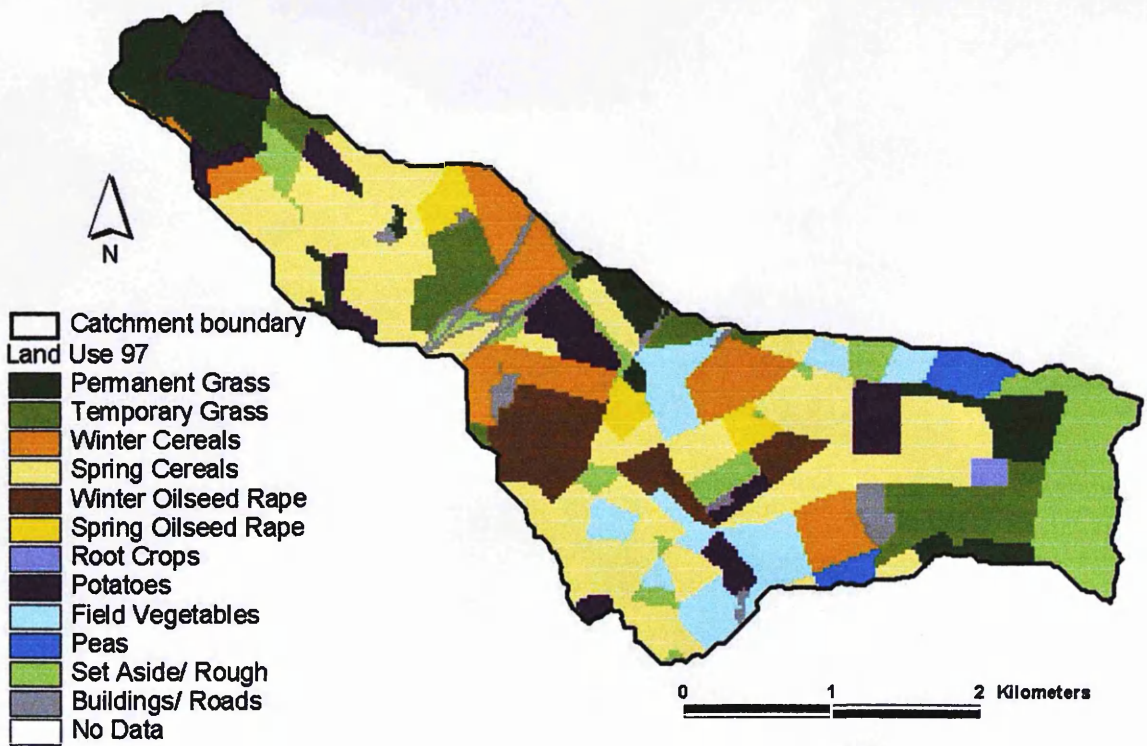


Figure 2.12. Land use distribution in the Greens Burn catchment, 1997.

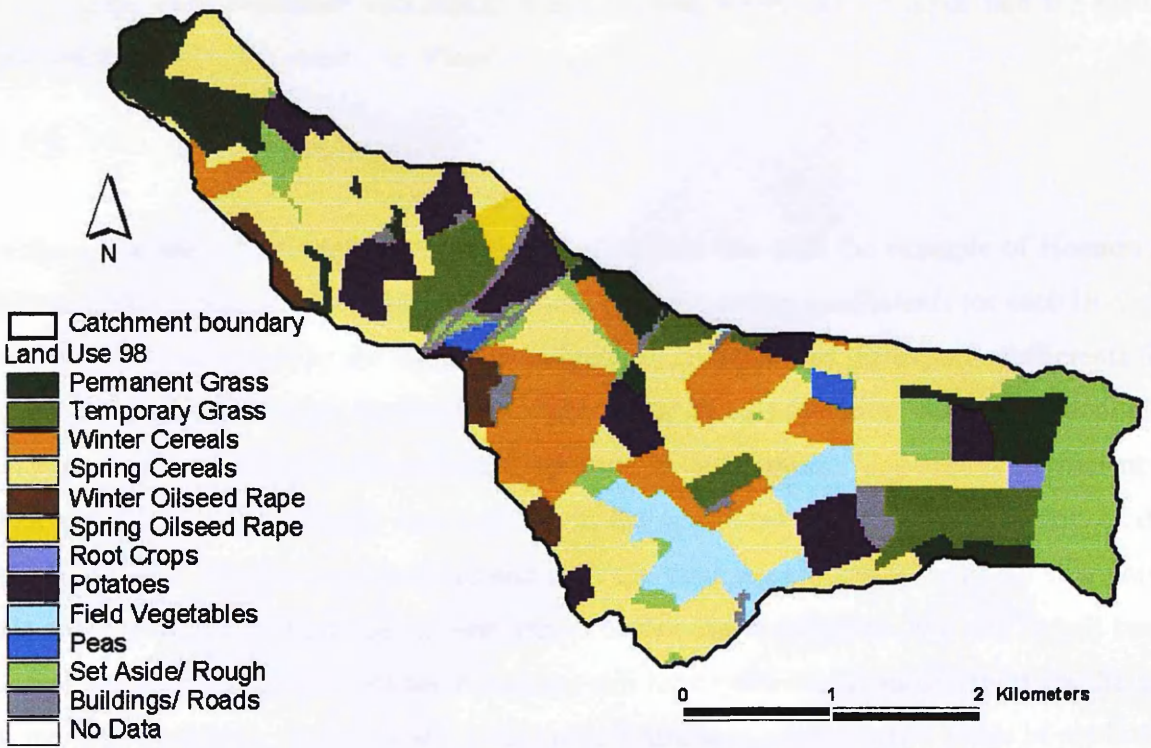


Figure 2.13. Land use distribution in the Greens Burn catchment, 1998.

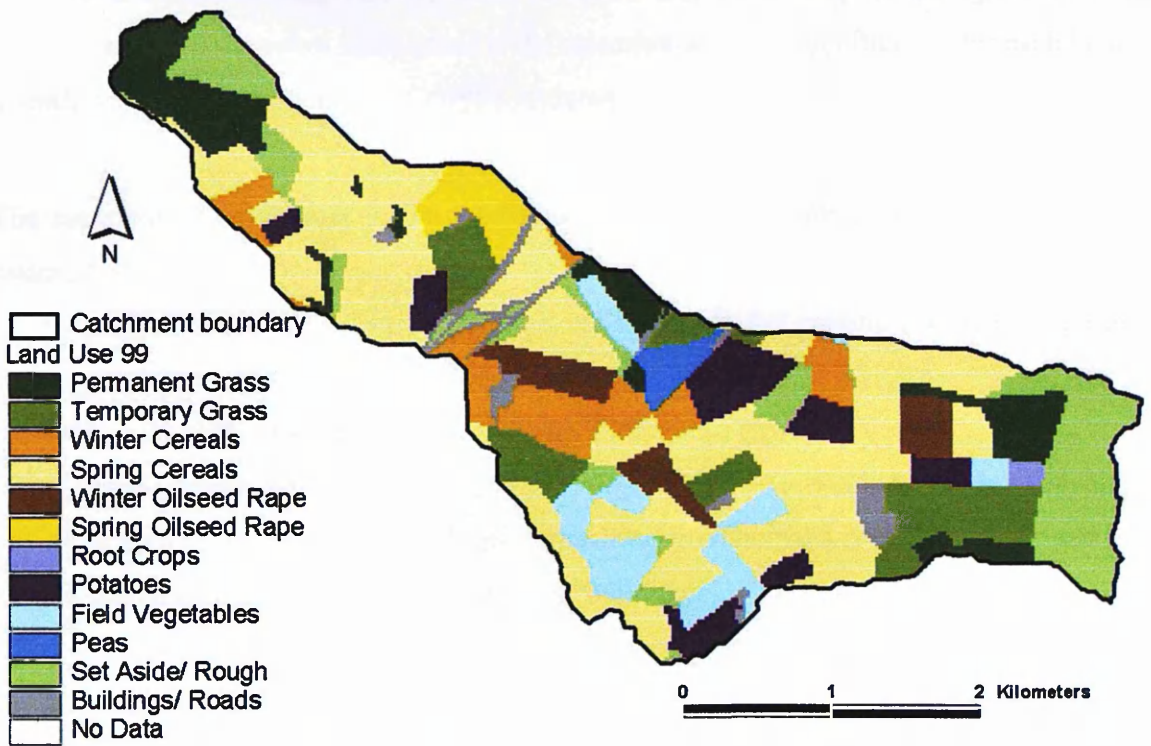


Figure 2.14. Land use distribution in the Greens Burn catchment, 1999.

These grids were converted into ASCII files: a format which can be input into the model (written in the EXCEL extension, Visual Basic).

2.5.3. Model assumptions

Without any site-specific export coefficient data, and in line with the example of Hession & Storm (2000), it was assumed that the distributions of the export coefficients for each land use were uniform, delimited by the minimum and maximum values for the export coefficients for each land use derived from the literature (Table 2.2). In each iteration, the model randomly selects an export coefficient for each land use from its distribution. This export coefficient is then applied to each cell with that land use in the catchment (i.e. for each iteration of the model, all cells with the same land use will have the same export coefficient). An alternative technique is to sample from the relevant export coefficient distribution on a cell by cell basis in each iteration (i.e. cells of the same land use will have different values of export coefficient in the same iteration). However, the latter method results in a very narrow range of predicted P fluxes from the catchment because high export coefficients in individual cells are always balanced by low export coefficients in others. Since the export coefficient is essentially an integration of contributing factors, some of which may be time specific (e.g. P availability may be seasonal), it makes more sense if the selection of export coefficients for each land use in each iteration is highly (or perfectly) correlated.

The contribution of animals to the total phosphorus export is included using the following assumptions:

- animals are evenly distributed in all cells suitable for grazing (i.e. temporary grass, permanent grass, rough grazing)
- manure and slurry are spread evenly on all land use types
- where information on the position of sewage outlets (e.g. septic tanks) is not available, as is the case for the Greens Burn, P resulting from humans is evenly distributed in the cells where their land use is classed as “buildings”.

Animal export coefficients are also randomly selected from uniform probability distributions constructed using measured data, as detailed in Table 2.3. For each P source, the % applied to land (takes into account P lost in storage) and % of P applied to land which is then lost to

runoff is also assigned from within the published range (detailed in Appendix 1). This allows the total amount of TP lost per cell as a result of organic inputs to be calculated.

2.5.4. Optimum number of iterations

With the input data ready for modelling, the next task was to decide how many iterations the model should be run for. There are few phosphorus models (e.g. Dunn, 1999; Dunn & Lilly, 2000; Hession & Storm, 2000; Whelan *et al*, 2002; Smith *et al*, 2005) which incorporate uncertainty in their input parameters and hence are stochastic in nature. The number of iterations performed by these models varies from 1000 to 10,000. However, all these models are more complex than this basic export coefficient model, with more uncertain input parameters. As a result, it is likely that they will require more iterations in order to provide numerical stability of the output distributions. Therefore, it was decided to investigate the number of iterations which would give confidence in the model output from this model. The model for 1996 was run ten times each for 10, 50, 100, 200, 300, 500, 1000 and 2000 iterations and the results are shown in Figure 2.15.

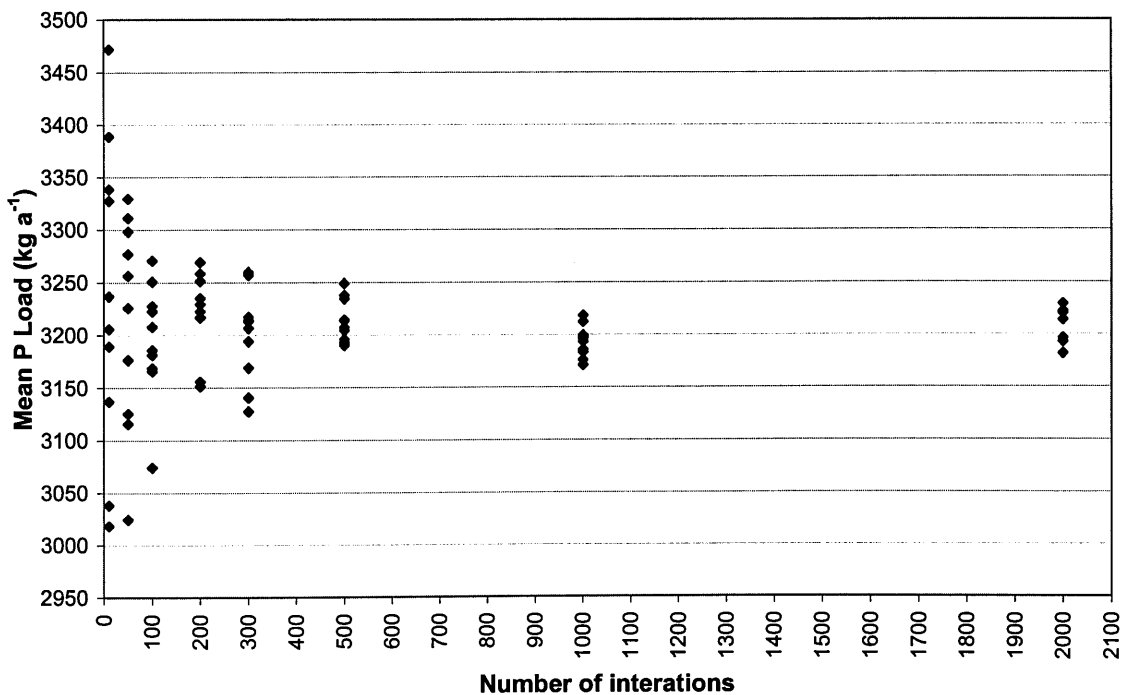


Figure 2.15. Comparison of the means resulting from different numbers of iterations performed by the export coefficient model for the Greens Burn catchment for 1996.

From the results it can be seen that, although there is an appreciable difference in the distributions formed by 10 runs for the lower numbers of iterations (< 500), there is not a great amount of difference in the distributions formed by 500 iterations and 2000 iterations. For 500 iterations, the mean of the 10 means = 2599 kgPa⁻¹ and the standard deviation of the 10 means = 21 kgPa⁻¹. For 2000 iterations, the mean of the 10 means = 2598 kgPa⁻¹ and the standard deviation of the 10 means = 13 kgPa⁻¹. In order to determine whether there is a statistically significant difference between the results obtained by 500 and 2000 iterations, the Mann Whitney non-parametric test was employed. This confirmed that there was no significant difference between the mean of the 10 means (p = 0.9698) or the standard deviation for the 10 means (p = 0.5708) for 500 and 2000 iterations. As a result of this analysis, it was decided that 500 iterations adequately sampled the parameter space and there was little gain in increasing the number of iterations, and computing time, beyond that.

2.5.5. Model results

This advanced model (moving on from a deterministic to stochastic approach for the selection of the export coefficients, with the advantage of spatial referencing) was run for 1996-99 and the results are shown in Figures 2.16 – 2.19 and summarised in Table 2.5.

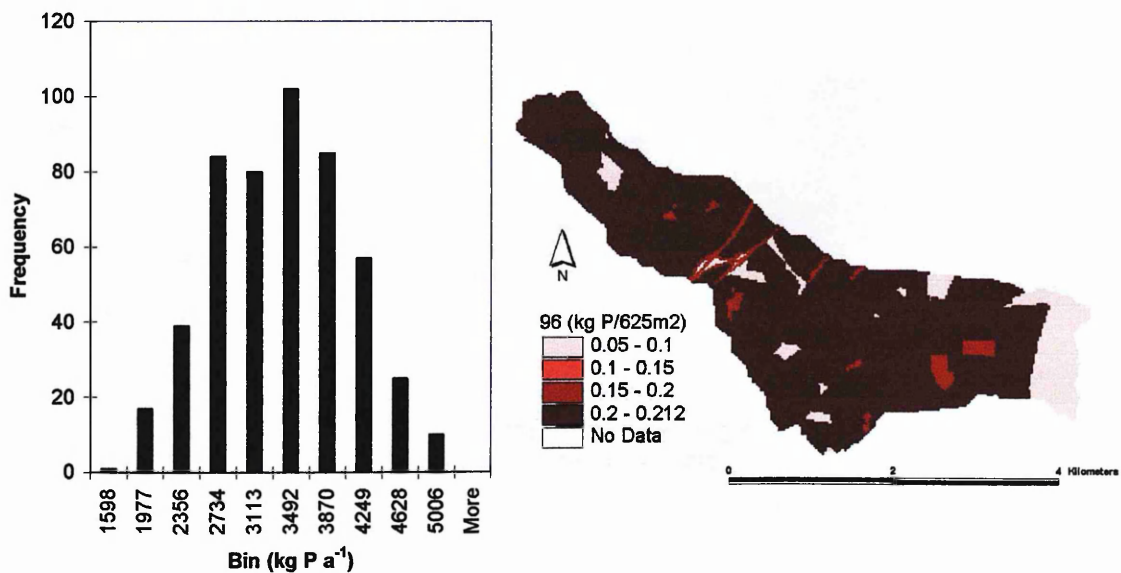


Figure 2.16. Histogram showing distribution of the model output (kg P a⁻¹) from 500 iterations and the spatial distribution of phosphorus export in the Greens Burn catchment, 1996.

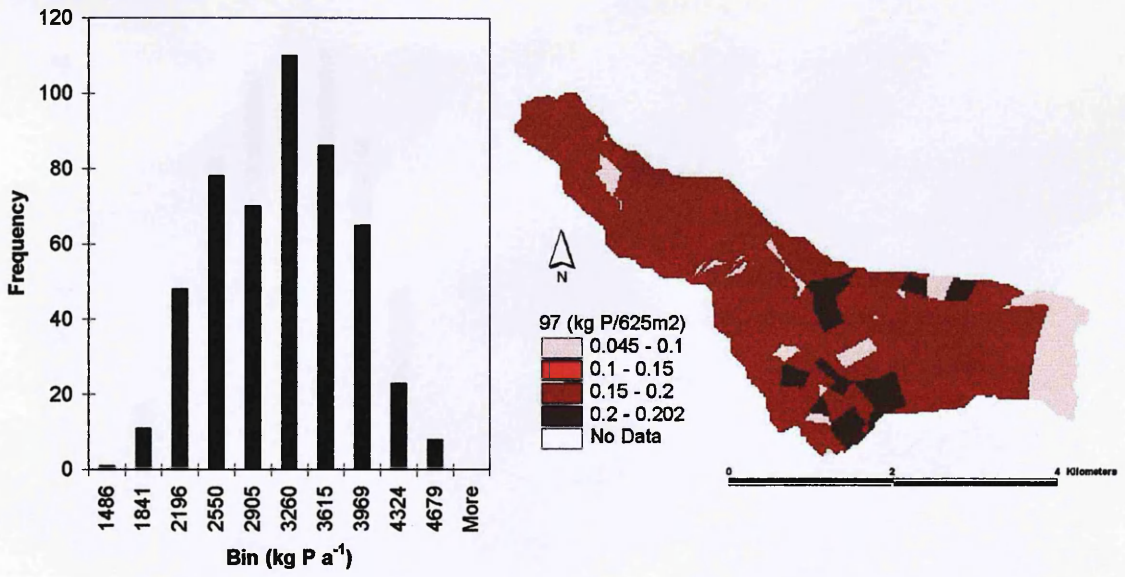


Figure 2.17. Histogram showing distribution of the model output (kg P a⁻¹) from 500 iterations and the spatial distribution of phosphorus export in the Greens Burn catchment, 1997.

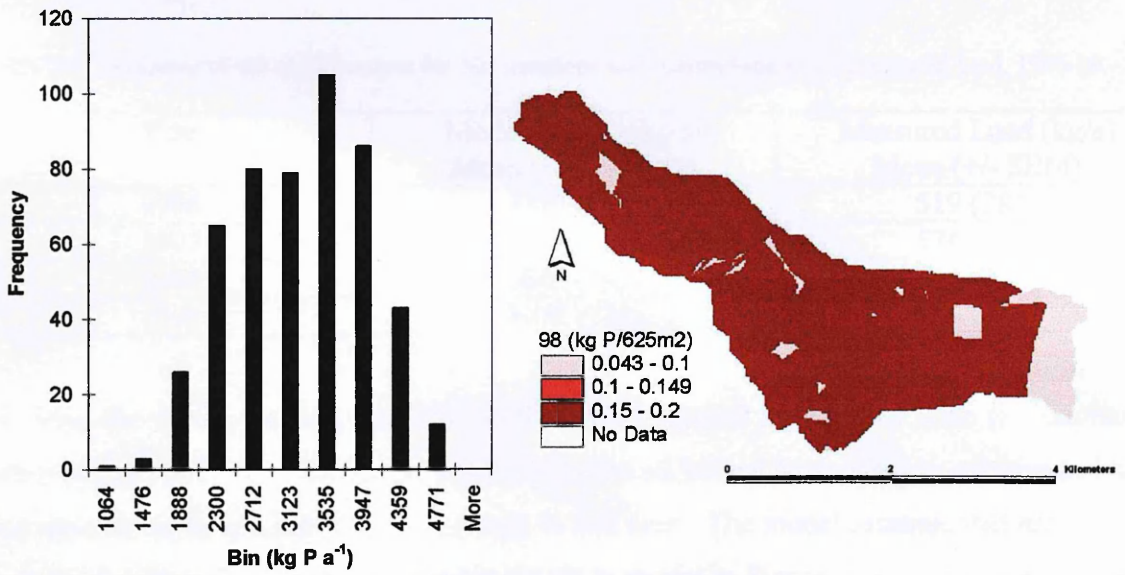


Figure 2.18. Histogram showing distribution of the model output (kg P a⁻¹) from 500 iterations and the spatial distribution of phosphorus export in the Greens Burn catchment, 1998.

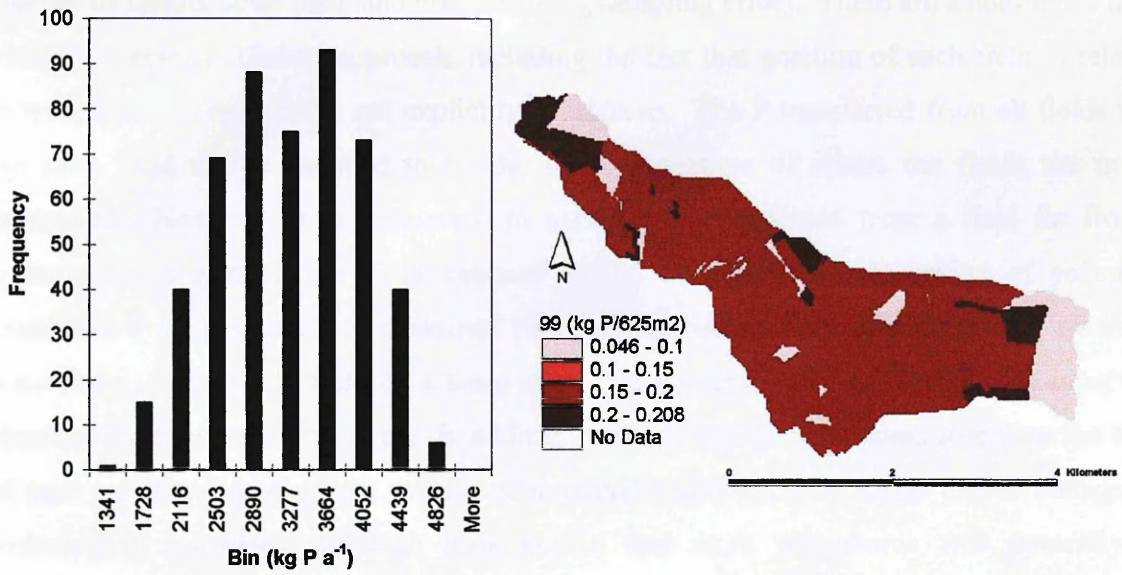


Figure 2.19. Histogram showing distribution of the model output (kg P a⁻¹) from 500 iterations and the spatial distribution of phosphorus export in the Greens Burn catchment, 1999.

Table 2.5. Summary of the model output for 500 iterations and comparison to the measured load, 1996-99.

Year	Model Output (kg/a) Mean (+/- Std Dev)	Measured Load (kg/a) Mean (+/- SEM)
1996	3220 (695)	519 (281)
1997	3008 (645)	574 (331)
1998	3046 (741)	664 (257)
1999	3058 (734)	529 (224)

In 1996, the model predicts that around 200 kg a⁻¹ more P is exported from the catchment compared to 1997-99. This can be attributed to the additional (compared to other years) hen-pen reported to be applied to the catchment in that year. The model assumes that the hen-pen is applied uniformly over the catchment, which is shown in Figure 2.16 by the overall darker red colour, indicating that more phosphorus is being exported from these cells.

The results show that, without expert-based selection of coefficients or optimisation, the export coefficient model is grossly over-predicting the phosphorus exported from the Greens Burn catchment in all years. Although it can be argued that the result for the basic model could be improved by optimising the coefficients, there are too few measurements to justify a

unique set of export coefficients, especially since changes in observed fluxes may be due to a number of factors other than land use (including sampling error). There are a number of flaws with the export coefficient approach, including the fact that position of each field in relation to receiving watercourses is not explicitly considered. The P transferred from all fields with the same land use is assumed to be the same, regardless of where the fields are in the catchment. However, it is reasonable to expect that P exported from a field far from a watercourse is more likely to be retained in the catchment (by deposition of sediment-associated P or adsorption of dissolved P) compared with a field adjacent to the receiving waterbody. Likewise, a field on a steep slope is more likely to export P than an otherwise identical field on a shallow slope. In addition, since P export is predicted solely on the basis of land use, the model cannot predict inter-annual variations in P losses due to changes in hydrological processes, although it is known that more phosphorus will generally be transferred in wet years than in dry years (e.g. Heathwaite, 1997). Similarly, it cannot predict spatial variations in hydrological response resulting from differences in soil type (e.g. Boorman *et al*, 1995). Efforts to address these weaknesses (through the inclusion of slope, distance to watercourse, soil type and hydrology) are detailed in Chapter 3.

2.6. Investigation into using measured data to estimate annual load

To investigate the issue of the quality of the measured data used to estimate the annual loads, data was obtained for the Zala catchment (1528 km²) in Hungary, where daily measurements of discharge (m³ s⁻¹) and total phosphorus (mg l⁻¹) are taken (data for 1990 is shown in Figure 2.20).

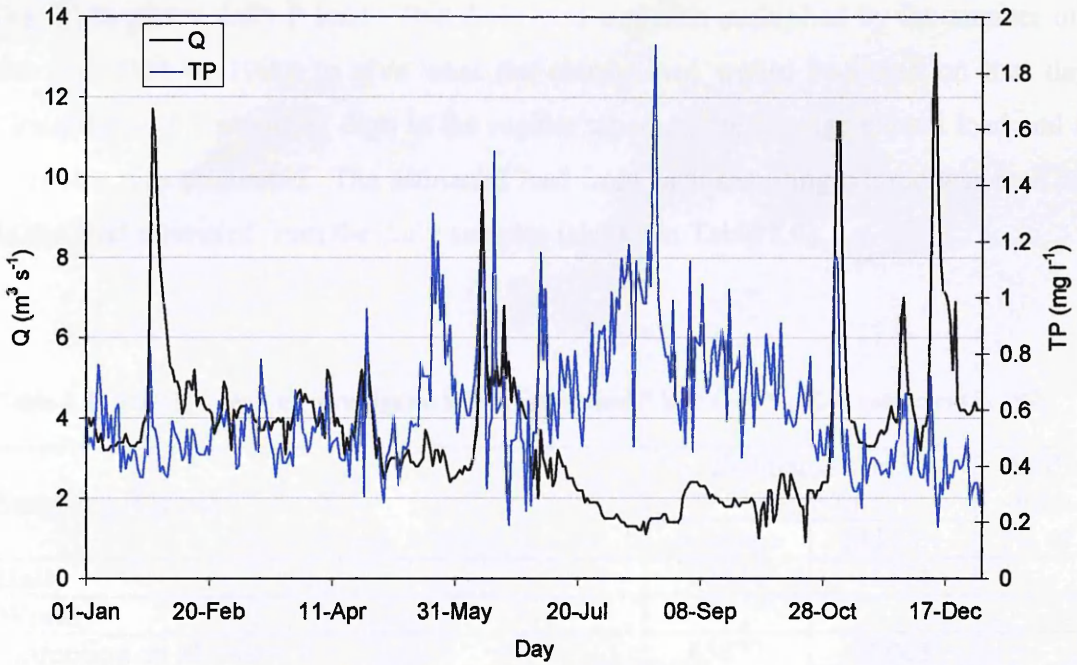


Figure 2.20. Measured discharge (Q) and total phosphorus (TP) from the Zala catchment in 1990.

The annual P load (kg a^{-1}) for 1990 from the catchment was then calculated assuming different sampling regimes (daily, weekly, fortnightly and monthly), as shown in Figure 2.21 and detailed in Table 2.6.

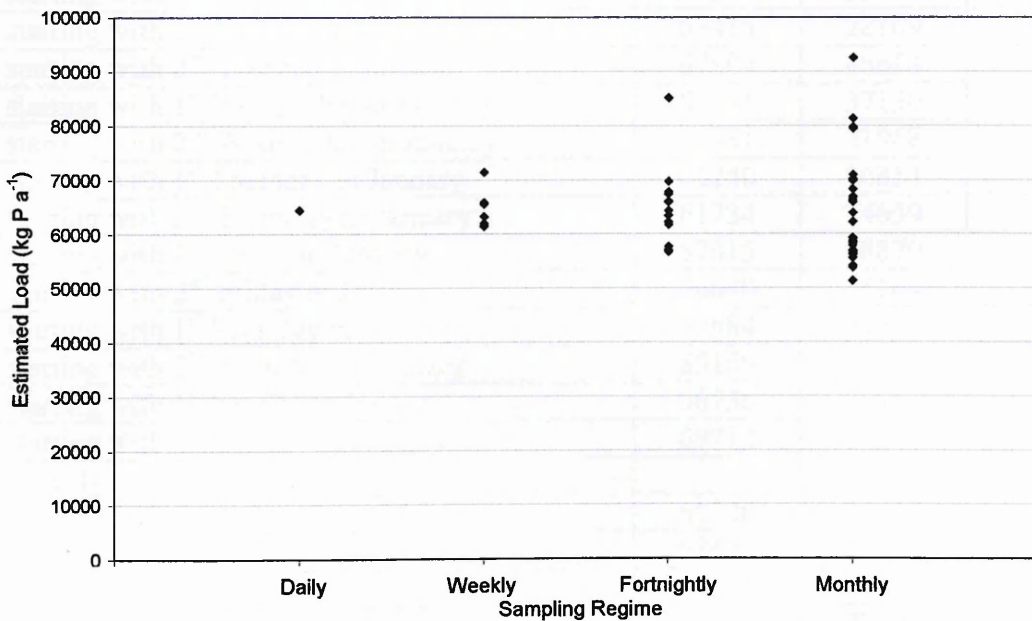


Figure 2.21. Estimated loads (kg P a^{-1}) from the Zala catchment in 1990 calculated from daily, weekly, fortnightly and monthly sampling regimes.

With each regime, the daily mean flow ($l\ d^{-1}$) was multiplied by the measured P concentration ($kg\ l^{-1}$) to give a daily P load. This daily load was then multiplied by the number of days in the year (365 in 1990) to give what the annual load would be based on that day alone. Grouping all the sampling days in the regime together, the average annual load and standard deviation was calculated. The estimated load from each sampling regime was then compared to the load estimated from the daily samples (shown in Table 2.6).

Table 2.6. Sampling regimes investigated to estimate annual P load from the Zala catchment in 1990.

Sampling Regime	Estimated Load (kg P/a)		Difference from daily (% of daily)
	Average	Std Dev	
Daily	64444	41824	-
Weekly			
- sampling on Monday	65872	48003	2
- sampling on Tuesday	65609	39379	2
- sampling on Wednesday	61431	34604	5
- sampling on Thursday	61992	25518	4
- sampling on Friday	61527	41073	5
- sampling on Saturday	71427	58810	11
- sampling on Sunday	63224	42574	2
Fortnightly			
- starting with 1 st Monday in January	67357	35905	5
- starting with 2 nd Monday in January	64330	58714	0
- starting with 1 st Tuesday in January	63415	28109	2
- starting with 2 nd Tuesday in January	67804	48614	5
- starting with 1 st Wednesday in January	65931	37130	2
- starting with 2 nd Wednesday in January	56931	31968	12
- starting with 1 st Thursday in January	62250	26854	3
- starting with 2 nd Thursday in January	61734	24639	4
- starting with 1 st Friday in January	57015	18870	12
- starting with 2 nd Friday in January	66040	55164	2
- starting with 1 st Saturday in January	57684	19698	10
- starting with 2 nd Saturday in January	85169	79213	32
- starting with 1 st Sunday in January	56736	29727	12
- starting with 2 nd Sunday in January	69712	52214	8
Monthly			
- 1 st Monday in month	65926	25574	2
- 1 st Tuesday in month	58420	19276	9
- 1 st Wednesday in month	54181	61610	16
- 1 st Thursday in month	62218	27804	2
- 1 st Friday in month	79526	76114	23
- 1 st Saturday in month	92592	101262	44

- 1 st Sunday in month	70903	62208	10
- 2 nd Monday in month	53800	20751	17
- 2 nd Tuesday in month	79762	68780	24
- 2 nd Wednesday in month	66848	42678	4
- 2 nd Thursday in month	66357	25172	3
- 2 nd Friday in month	57890	13525	10
- 2 nd Saturday in month	56195	16777	13
- 2 nd Sunday in month	63892	42573	1
- 3 rd Monday in month	81347	86934	26
- 3 rd Tuesday in month	59275	18231	8
- 3 rd Wednesday in month	56938	33434	12
- 3 rd Thursday in month	55585	12187	14
- 3 rd Friday in month	56754	19418	12
- 3 rd Saturday in month	70165	52650	9
- 3 rd Sunday in month	56368	20070	13
- 4 th Monday in month	59193	25018	8
- 4 th Tuesday in month	62244	27661	3
- 4 th Wednesday in month	69826	42026	8
- 4 th Thursday in month	58688	27211	9
- 4 th Friday in month	51338	19143	20
- 4 th Saturday in month	70007	43170	9
- 4 th Sunday in month	68252	44934	6

Considering the weekly sampling regime, it can be seen that a wide range of variability in the estimated average annual loads (61431 – 71427 kg P a⁻¹) occurs when sampling on different days within a weekly regime. A spread of results is also found when using a fortnightly (range: 53736 – 85169 kg P a⁻¹) or monthly (range: 51338 – 92592 kg P a⁻¹) regime, with the range of results getting wider as sampling occurs less often.

Looking at how the estimated annual load calculated from the various sampling regimes differs from the load estimated from the daily samples, it can be seen that for weekly sampling, the difference varies from 2 - 11%. For fortnightly sampling, the range is 0 – 32 % and for monthly sampling, the range is 1 – 44%. As sampling frequency decreases, there is more likelihood of the estimated load being further from the load estimated from daily sampling i.e. there is a greater chance that the estimated load will get skewed by sampling on a day with high flow and concentration (e.g. 3rd November 1990), which with monthly sampling will have a great effect on the estimated annual load.

In addition, it is clear that for each of these regimes (weekly, fortnightly and monthly), there is a strong element of chance in how good an estimate (compared to daily sampling) is achieved e.g. sampling on the first Monday of each month will result in a 2% variation (from the estimate from daily sampling) whereas sampling on the 3rd Monday of each month results in a 26% variation.

Even with daily sampling, there is error associated with estimating annual load, which is calculated from flow and P measurements. Measured flow ($\text{m}^3 \text{s}^{-1}$) is multiplied up to give the daily mean flow. The measured flow could be a snapshot of one second on the day (which means that an assumption is made that flow remains constant all day) or could be an average of the flow over the day. Measured P (mg l^{-1}) could be determined using one grab sample taken each day (with the assumption that P remains constant throughout the day) or from a mixture of hourly samples. With more frequent sampling, there is greater confidence that the estimated load is closer to the true load. However, the reality (time and cost) of undertaking high-frequency sampling regimes usually means that, unless the catchment is subject to intensive research, it is likely that monthly sampling is the best that a modeller can hope for and so the estimated load from a catchment in a particular year should be treated with caution.

Chapter 3. Development of the SEPTIC model

The basic export coefficient model has a number of weaknesses that have been identified in the literature e.g. MLURI & FRPB (1995) thought that slope was important in the export of P and should be incorporated; Johnes & Heathwaite (1997) recognised that proximity to streams was important and should be included and Worrall & Burt (1999) showed historical land use was important (converting grassland to arable would result in the release of large amounts of stored N) when modelling nitrogen export. With the aim of addressing weaknesses in the basic export coefficient model, the next step of this project was to include additional factors (known to influence soil erosion and P export) into the model. In addition to land use, this developed model (“Stochastic Estimation of Phosphorus Transfer In Catchments”, SEPTIC) includes information on topography (slope and cumulative area from the divide), soil type, annual precipitation and annual actual evapotranspiration, which are used to adjust export coefficients and to produce uncalibrated, catchment-specific predictions.

3.1. Model inputs

The model reads information on land use, slope, cumulative area (upslope area to the divide) and soil type which is stored in ASCII format. The ASCII files were all created in ArcView GIS with a RASTER grid cell size of 25m. In each iteration, the combined P export (cropping and animal) from each cell is corrected for topography (slope and cumulative area), soil type and annual hydrologically effective rainfall (*HER*).

3.1.1. Slope and Cumulative Area

Slope is important in the erosion of sediment (e.g. Heathwaite, 1997; Nash *et al*, 2000) so that, with all other factors remaining constant, steeper slopes pose a greater erosion risk and hence an elevated likelihood that sediment-associated phosphorus will be exported. The PLUS model (MLURI & FRPB, 1995) developed the basic export coefficient model in ARC/INFO GIS to attribute different export coefficient ranges for each land use category (determined using the MLURI LCS88 Digital Dataset) on the basis of slope (determined from

the OS 1:50,000 Digital Elevation Model) by assigning a maximum and minimum value to selected land cover categories for each of the flat ($<3^\circ$), medium ($3-13^\circ$) and steep ($>13^\circ$) slope categories. The output from PLUS gives a minimum and maximum predicted load from the catchment, thus giving an indication of the uncertainty in the predictions. The model assumes land cover and slope represent the most important factor determining P loss. Although the authors defend this generalisation for Scotland, they admit that there are circumstances where these factors may not adequately reflect the phosphorus dynamics within a catchment e.g. in lowland areas, factors such as soil type and proximity to a watercourse may be more important (MLURI & FRPB, 1995).

In addressing the importance of proximity to a watercourse, Johnes & Heathwaite (1997) applied different export coefficients to each land use class on the basis of proximity to streams ($<$ or $>$ 50m) with the understanding that P exported from land next to the stream is more likely to contribute to the P loading at the catchment outlet and hence should be assigned a higher export coefficient. This model, however, was not developed in GIS and each relevant export is applied to the total area of the applicable land use in the catchment (i.e. the export for permanent grass at a distance of more than 50m from a stream ($\text{kg ha}^{-1} \text{a}^{-1}$) is multiplied by the total area of such grass in the catchment.

Instead of assigning export coefficients on the basis of the particular slope (which requires subjective expert opinion), this model uses the values of the slope in each cell to adjust the randomly selected export coefficient in each iteration of the model such that cells with steeper slopes in the catchment will have a greater export coefficient in each iteration of the model compared to cells with shallower slopes with the same land use. With regards to proximity to stream, instead of choosing a boundary (from which a land use nearer the stream is assigned a greater export coefficient (which again requires a judgment to be made) than the same land use further away), this model employs the idea of drainage area. Greater drainage area (i.e. area drained to the divide) will result in greater surface and sub-surface discharge with more risk of erosion (e.g. Kirkby & Cox, 1995) and a greater chance of both sediment-associated and dissolved P being transported. In addition, since upslope area increases as cells get closer to the channel network, it can also be used as an inverse surrogate for distance to streams.

A digital terrain model (DTM), with a cell size of 25m, was created for the catchment in ArcInfo, using the 5m O.S. contour data and vector data containing the location of streams and catchment boundary. The DTM was then imported into ArcView where the slope was calculated (shown in Figure 3.1).

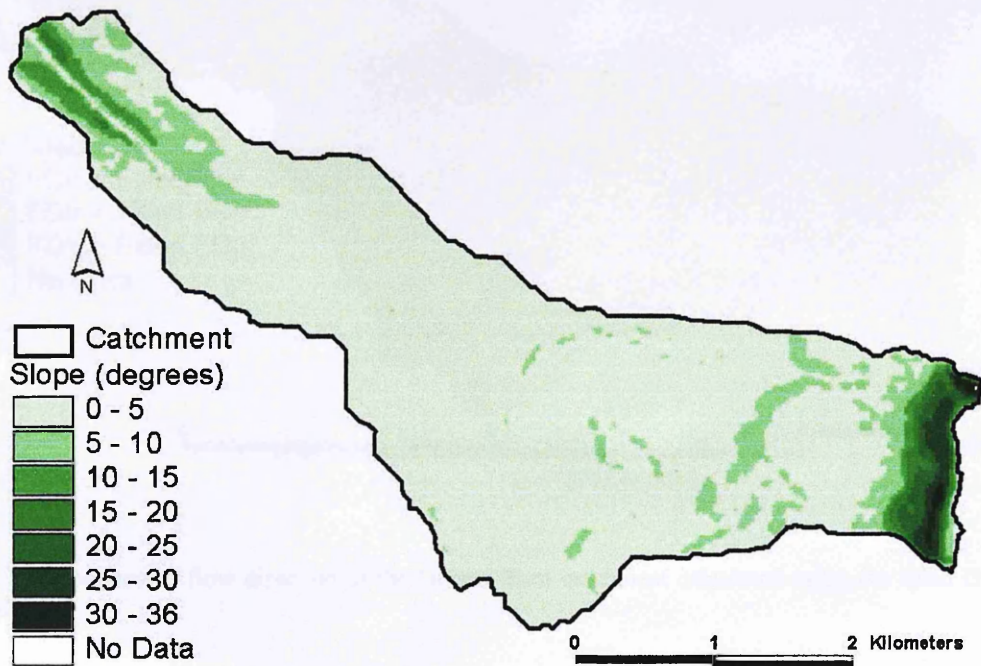


Figure 3.1. Slope (degrees) in the Greens Burn catchment, calculated from the 25m DTM.

The DTM for the catchment was also used to calculate flow direction and flow accumulation through the catchment, using the extension “Hydrologic Modeling v1.1” in ArcView. First the sinks (cells with undefined flow direction) were filled to create a “depressionless” DTM and then the flow direction calculated. Figure 3.2 shows the comparison of flow direction calculated with the filled DTM and the non-filled DTM. Clearly for most of the catchment, filling the sinks makes no difference. However, to create an accurate representation of flow direction and therefore accumulated flow, it is best to use a data set that is free of sinks.

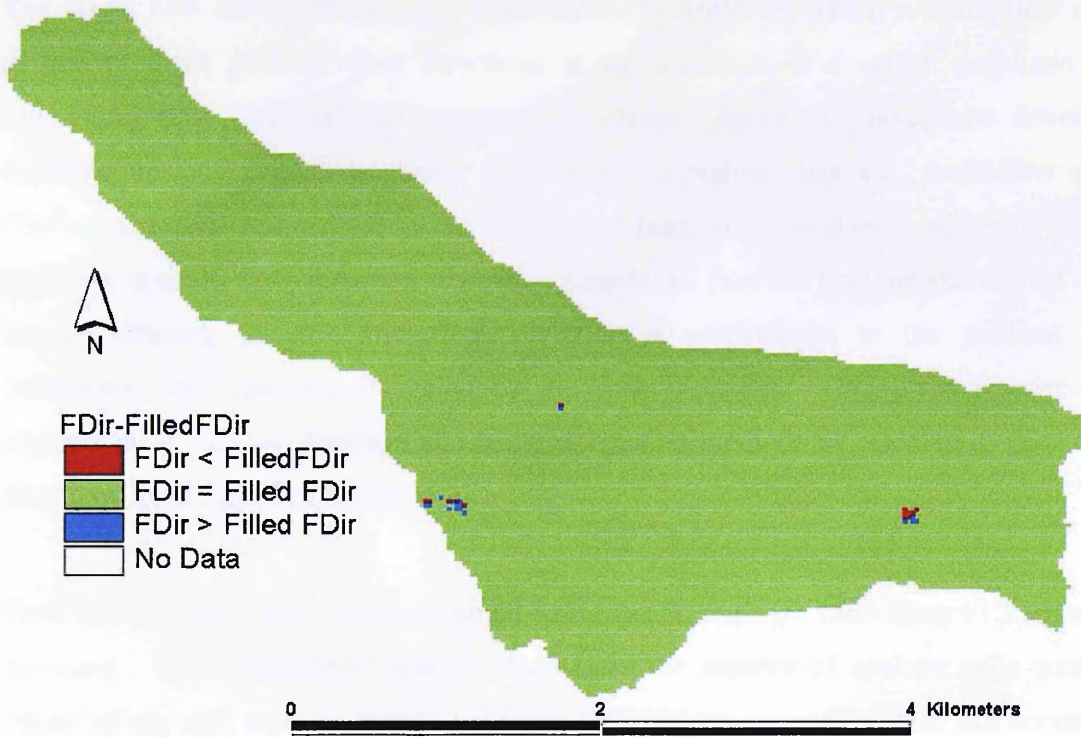


Figure 3.2. Comparison of flow direction in the Greens Burn catchment calculated using the filled DTM and non-filled DTM.

Flow direction is calculated according to the binary convention for direction, as shown in Figure 3.3. To decide the direction of flow, the slope to each of the adjacent cells is considered. If the direction of steepest slope is to the right of the cell, for example, then its flow direction would be coded as “1”. In the event that descent to all adjacent cells is the same, the neighbourhood is enlarged until the line of steepest descent is found.

32	64	128
16	cell	1
8	4	2

Figure 3.3. Diagram showing the binary convention employed by ArcView for Flow Direction.

The single flow direction algorithm implemented in ArcView, which restricts flow direction to one of eight possible flow directions at 45° intervals, is a rather simplistic way of calculating flow direction. A number of different algorithms have been developed to calculate upslope contributing area from digital elevation data e.g. multi-flow direction (Tarboton, 1997; Quinn *et al*, 1991). Instead of restricting the flow from a cell to just one direction, a multi-flow direction algorithm distributes flow so that the fraction of the total amount draining to each downslope direction is proportional to the gradient of each downslope flow path and weighted by the flow direction. This gives a more realistic representation of flow direction and using alternative methods of calculating flow direction should be investigated in further work.

Flow accumulation was also determined using the Hydrologic Modelling v1.1 extension in ArcView. The accumulated flow is based upon the number of upslope cells contributing “flow” to any cell, with the current processing cell not being considered in this accumulation. Cumulative area is calculated as the cells accumulated * cell area. In this case, the cell size is 25m so the cell area is 625m². Output cells with a high flow accumulation are likely to be close to, or part of, the stream network. The cumulative area is shown in Figure 3.4.

A widely used value is the specific area (contributing area per unit contour length), which in practice is the cumulative area/cell size. So, specific area can be calculated as flow accumulation * cell width (i.e. 25m in this case).

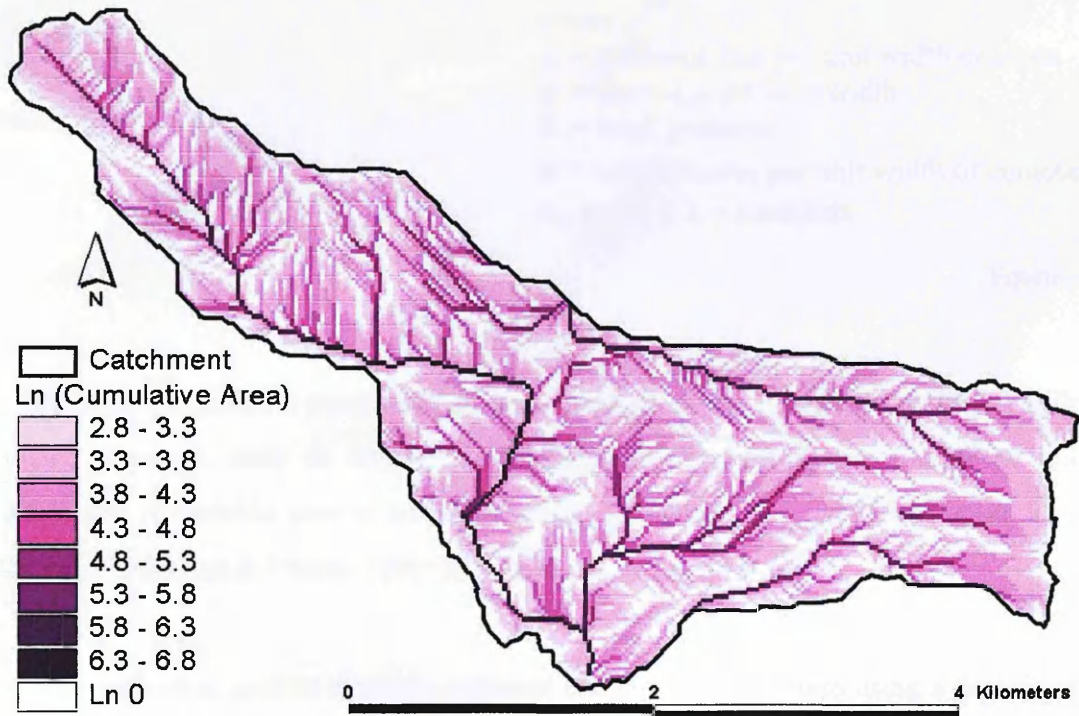


Figure 3.4. Natural logarithm of the cumulative area in the Greens Burn catchment.

Most geomorphological models assume overland flow erosion to be transport limited, with topography (slope and specific area) playing a central role in governing hillslope hydrological response (Desmet & Govers, 1995). Cumulative area influences water table coincidence with the surface and slope influences flow to create areas (variable source areas) where saturated excess overland flow will occur (Beven & Kirkby, 1979). Large cumulative area and steep slopes will lead to a high propensity for saturation-excess overland flow and near-surface flow, with greater chance of P transport (by whatever mechanism) to the channel. These assumptions are central to TOPMODEL (e.g. Beven, 1997) and these concepts were exploited by Whelan *et al* (2002, see Appendix 3).

Topographic controls are included in this model using generic empirically-based equations summarised by Rustomji & Prosser (2001), i.e.:

$$q_s = k_1 \cdot q^\beta \cdot S^\gamma$$

where $q = k_2 \cdot a^\lambda$

i.e. $q_s = k_1 (k_2 a^\lambda)^\beta S^\gamma$

where

q_s = sediment flux per unit width of slope

q = discharge per unit width

S = local gradient

a = hillslope area per unit width of contour

$k_1, k_2, \beta, \gamma, \lambda$ = constants

Equation 3.1

The following parameter values were chosen for hillslope hydrological conditions in humid temperate climates, such as Britain (i.e. dominated by subsurface throughflow and the development of variable source areas) based on guidelines given by Prosser & Rustomji (2000) (and Rustomji & Prosser (2001)): $k_1 = k_2 = \lambda = 1$; $\beta = \gamma = 1.4$.

Since it is difficult to predict absolute sediment and phosphorus fluxes using a generic model, the relative flux (RF , 0-1) is defined as:

$$RF = \frac{\ln(q_s + 1)}{\ln(q_s \text{ max} + 1)}$$

Equation 3.2

“ $q_s + 1$ ” is used rather than “ q_s ” to avoid negative values for the relative flux. Natural logarithms are used since there is a large scale of q_s which unlogged would produce minuscule, unrealistic numbers for the relative flux. Figure 3.5 shows the frequency distribution of q_s , $\ln q_s$, $\ln (q_s + 1)$, etc derived from the Greens Burn DEM.

This relative flux (termed the “Prosser Reduction Factor”, PRF) is used to adjust the selected export coefficient for each cell (see Figure 3.12).

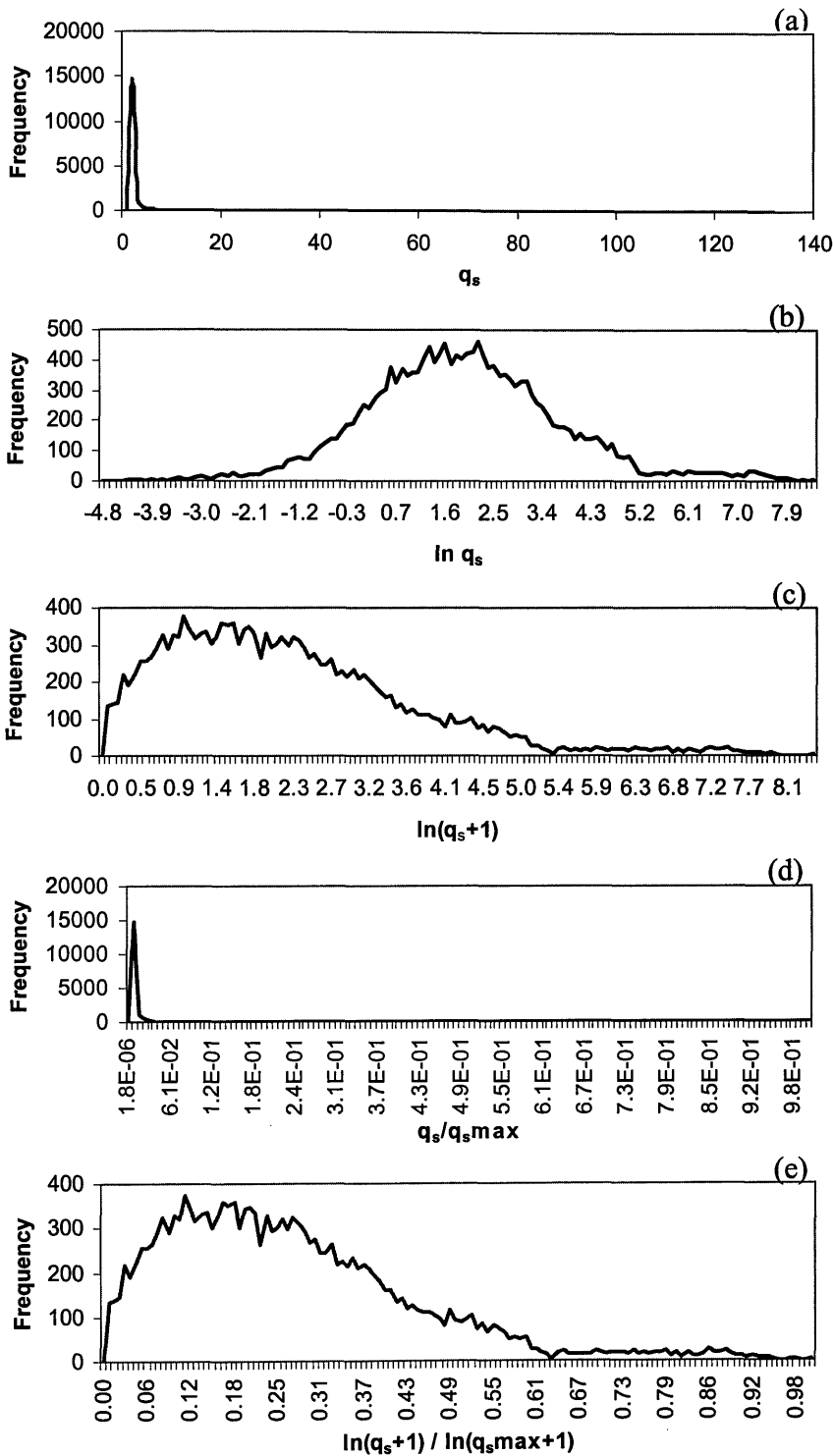


Figure 3.5. Distributions showing (a) histogram of q_s calculated for each cell during one run of the model, (b) histogram of $\ln q_s$, (c) histogram of $\ln (q_s+1)$, (d) histogram of $q_s/q_{s,max}$, (e) histogram of $\ln (q_s+1)/\ln (q_{s,max}+1)$ for the Greens Burn catchment.

3.1.2. Soil type

Soil properties (e.g. texture and organic matter content) are potentially important in the transfer of phosphorus (e.g. Morgan, 1997; Brady & Weil, 1999, Fraser *et al*, 1999).

Digital soils data for the catchment were obtained from the Macaulay Institute for Soil Research, Aberdeen and is shown in Figure 3.6, with additional information detailed in Table 3.1.

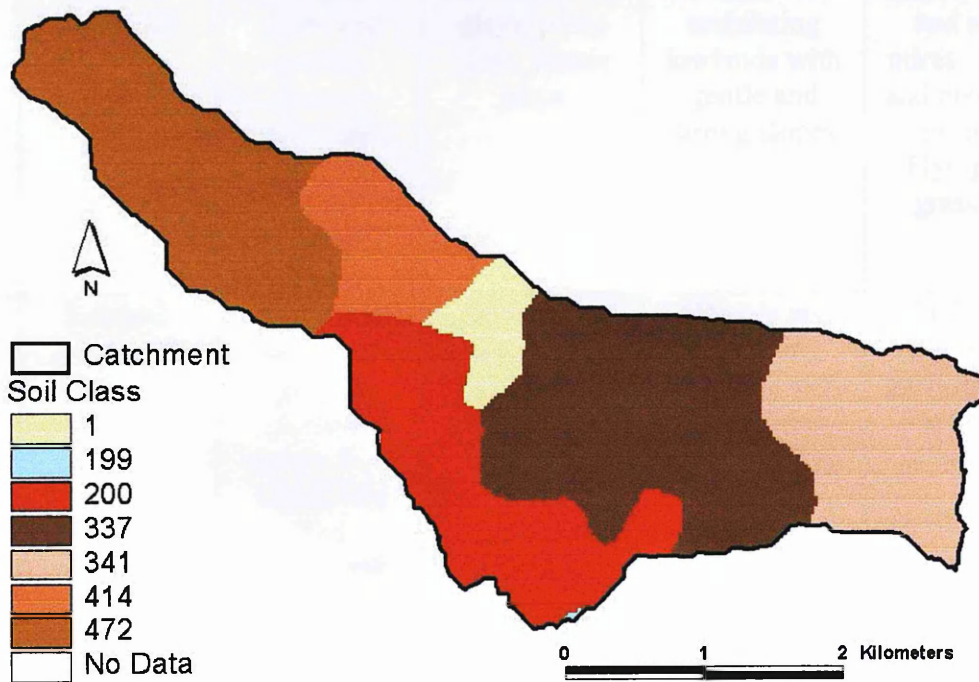


Figure 3.6. Soil classes in the catchment (Macaulay Institute for Soil Research, Aberdeen).

Table 3.1. Key from Soil Survey of Scotland, Sheet 5, Eastern Scotland Soil, 1 : 250 000, The Macaulay Institute for Soil Research, Aberdeen, 1982.

Soil Class	Soil Association	Parent Materials	Component Soils	Landforms	Vegetation
1	Alluvial soils	Recent riverine and lacustrine alluvial deposits	Alluvial soils	Flood plains, river terraces and former lake beds	Arable and permanent pastures. Rush pastures and sedge mires. Broadleaved woodland.
199	Eckford/ Innerwick	Fluvioglacial sands and gravels derived mainly from Upper Old Red Sandstone sediments	Noncalcareous gleys, peaty gleys, humic gleys	Mounds and undulating lowlands with gentle and strong slopes	Rush pastures and sedge mires. Arable and permanent pastures. Flying bent grassland.
200	Eckford/ Innerwick	Fluvioglacial sands and gravels derived mainly from Upper Old Red Sandstone sediments	Humus-iron podzols; some gleys and peaty podzols	Mounds and undulating lowlands with gentle and strong slopes	Arable and permanent pastures. Rush pastures and sedge mires.
337	Kippen/ Largs	Drifts derived mainly from Upper Old Red Sandstone sandstones	Brown forest soils; some gleys	Undulating lowlands with gentle and strong slopes; non-rocky	Arable and permanent pastures. Acid-bent fescue grassland. Oak and birchwood.
341	Kippen/ Largs	Drifts derived mainly from Upper Old Red Sandstone sandstones	Humus-iron podzols; some brown forest soils and gleys	Hills and valley sides with strong and steep slopes; moderately rocky	Dry Atlantic heather moor. White bent grassland. Dry birchwood.

414	Mountboy	Drifts derived from Old Red Sandstone lavas and sediments	Brown forest soils with gleying; brown forest soils; some gleys	Undulating lowlands and foothills with gentle and strong slopes	Arable and permanent pastures. Rush pastures and sedge mires.
472	Sourhope	Drifts derived from Old Red Sandstone intermediate lavas	Brown forest soils; some brown forest soils with gleying and gleys	Undulating lowlands and hills with strong slopes	Arable and permanent pastures. Acid-bent fescue grassland. Rush pastures and sedge mires.

To incorporate the effect of soil type into the model, a well-tested and readily available soils classification system was adopted. The UK Hydrology of Soil Types (HOST) classifies UK soils into 29 classes on the basis of hydrology and geology (Boorman *et al*, 1995; Dunn & Lilly, 2001; Maréchal & Holman, 2005). Soils from different HOST classes will respond differently to rainfall, producing varying degrees of runoff.

HOST predicts a standard percentage runoff (*SPR*) value for each HOST class. *SPR* is the percentage of the total rainfall that causes the short-term increase in flow seen at the catchment outlet (with the remaining rainfall causing an increase in baseflow or is lost to evaporation, detention on surface or retention in soil), such that:

$$\text{percentage runoff} = \frac{\text{quick response runoff}}{\text{total rainfall}} * 100$$

Equation 3.3

In HOST, the response runoff is calculated using the Flood Studies Report (FSR) method of flow separation, as shown in Figure 3.7.

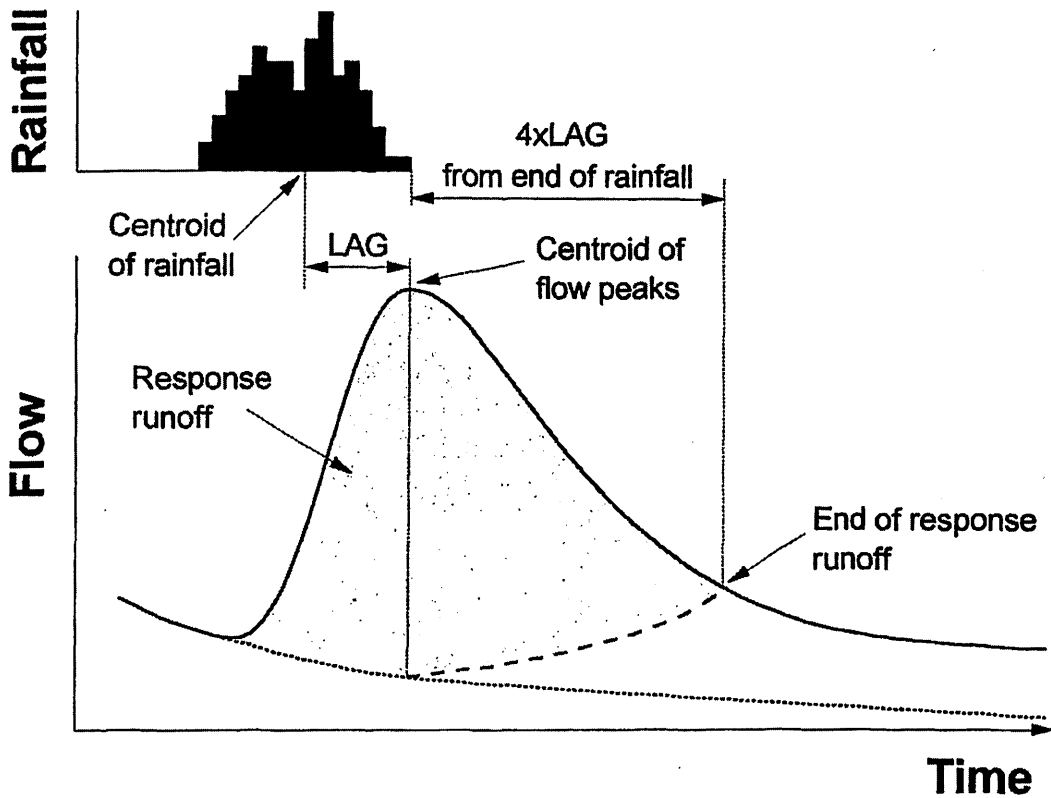


Figure 3.7. The Flood Studies Report method of flow separation (from Boorman *et al*, 1995, fig. 2.5, p. 8).

It should be noted, that by this definition, *SPR* will include interflow. Interflow will not contribute to surface erosion and sediment-associated P. However interflow will, presumably, transfer dissolved, sub-surface P and hence re-introduces the possibility of partially including a sub-surface component into the model.

For each soil class, which may contain a number of different HOST classes, a weighted average for *SPR* can be calculated. Table 3.2 shows the constituent HOST classes (and associated *SPR* values) for each soil class.

Table 3.2. Soil and corresponding HOST classes and recommended Standard Percentage Runoff (SPR) coefficients (from Report No. 126, Hydrology of Soil Types: a hydrologically based classification of the soils of the United Kingdom, Inst. Of Hydrology, 1995, Appendix B).

Soil Class	Soil Name	HOST Class	SPR value (%)	Percentage
1	Alluvial Soils	7	44.3	35.00
		8	44.3	15.00
		9	25.3	10.00
		10	25.3	20.00
		12	60.0	20.00
199	Eckford	10	25.3	100.00
200	Eckford	5	14.5	70.00
		12	60.0	30.00
337	Kippen	13	2.0	50.51
		17	29.2	49.49
341	Kippen	6	33.8	100.00
414	Mountboy	6	33.8	30.00
		18	47.2	70.00
472	Sourhope	17	29.2	100.00

The weighted SPR value for each soil class can be calculated by summing the SPR value * fraction of each HOST class.

e.g. for Soil Class 414 (Mountboy)

$$\text{weighted SPR value} = (33.8 * 0.3) + (47.2 * 0.7) = 43.2$$

The weighted SPR values for each soil class are shown in Table 3.3.

Table 3.3. Average values of SPR for each soil class in the Greens Burn catchment.

Soil Class	Soil Name	Weighted SPR value (%)
1	Alluvial Soils	41.7
3	Organic Soils	60.0
199	Eckford	25.3
200	Eckford	28.2
337	Kippen	15.5
341	Kippen	33.8
414	Mountboy	43.2
472	Sourhope	29.2

Figure 3.8 shows a map of weighted SPR values for the Greens Burn catchment, showing that soils in the centre of the catchment are predicted to produce less runoff than those to the east and west, all other factors remaining constant.

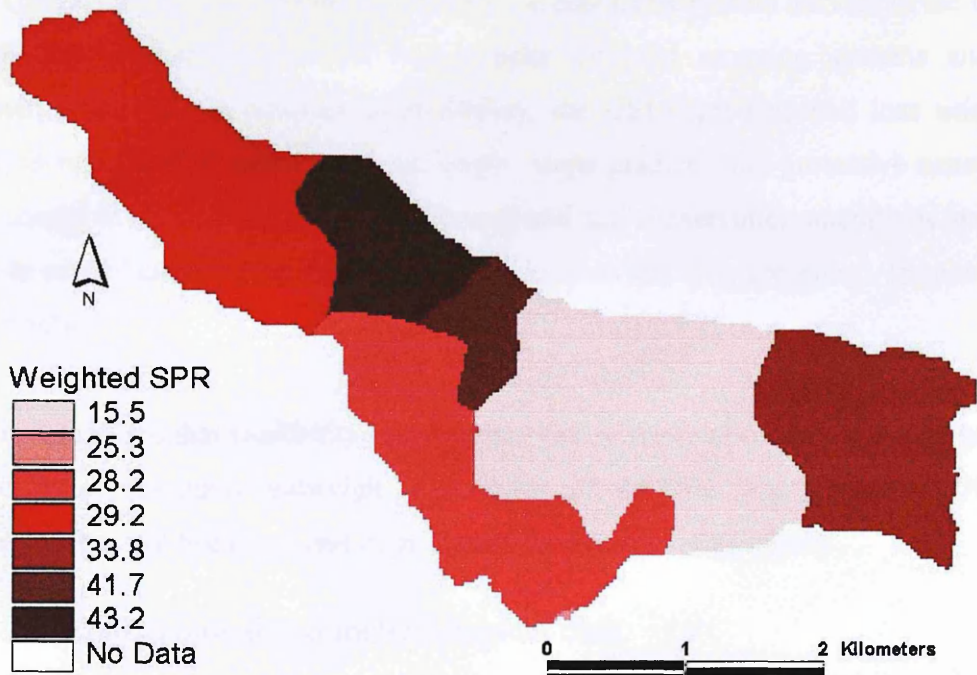


Figure 3.8. Weighted SPR values, derived from HOST, for soil types in Greens Burn catchment.

These *SPR* values are used in the model to further adjust the export coefficients such that soils with greater *SPR* will have a greater likelihood of transferring dissolved and sediment-associated phosphorus than otherwise similar cells (see Figure 3.12). The soil weighting factor (*SWF*) describing the relative transfer of P is defined as:

$$SWF = \left(\left[\frac{\max SWF - \min SWF}{\max SPR - \min SPR} \right] * SPR \right) + SWFi$$

Equation 3.4

where

$\max SWF$ = maximum *SWF*, as defined by the model user; default = 0.8

$\min SWF$ = minimum *SWF*, as defined by the model user; default = 1.2

$\max SPR$ = maximum *SPR* value in catchment

$\min SPR$ = minimum *SPR* value in catchment

SPR = *SPR* value for specific cell

SWFi = *SWF* intercept, defined by $\max SWF$, $\min SWF$, $\max SPR$, $\min SPR$

In addition to affecting hydrological response, soil type can also influence erodibility (i.e. the propensity of soil to erode). Erodibility is one parameter used in the Universal Soil Loss

Equation (USLE) which was adopted in 1958 by the Soil Conservation Service in the USA to make long-term assessments of soil losses under different cropping systems and land management practices. In addition to erodibility, the USLE predicts soil loss using five additional factors (rainfall erosivity; slope length; slope gradient; the protective canopy and organic material in direct contact with the ground; and soil conservation operations and other measures to control erosion (e.g. contour farming, terraces and strip cropping) (Sonneveld & Nearing, 2003).

Whilst it is recognised that erodibility may be important in many circumstances, it is believed that other factors probably outweigh it in much of the UK (e.g. Kirkby, 1979) and consequently it has not been included in the model for the sake of simplicity.

3.1.3. Hydrological and meteorological data

Daily rainfall is measured by SEPA at two raingauge sites in the catchment (Balado (NO 095 024) and Portmoak (NO 175 007)). The rainfall for the catchment adopted in the model is taken as the average of that measured at these two sites. The principal driver for phosphorus transport is runoff, defined here in its widest sense as the total transfer from land to surface waters regardless of mechanism (it includes water transfer by overland flow, throughflow, groundwater discharge and artificial drainflow). Annual hydrologically effective rainfall (*HER*), defined as the measured annual precipitation – annual actual evapotranspiration (*AET*) was used as an approximation of runoff. An annual time-step was chosen to be consistent with the annual TP load predicted by the model and for the sake of simplicity.

The estimation of *AET*, which includes interception losses, was derived from predictions made by the Meteorological Rainfall and Evapotranspiration Calculation System – *MORECS* (Thompson *et al*, 1981). *MORECS* divides the UK into 40km squares and makes potential evapotranspiration (*PET*), *AET* and soil moisture deficit calculations for a number of different crop and soil types in each cell. *MORECS* was revised in 1995 to take into account changes in cropping practices since the 1960s (i.e. a general increased coverage of winter cereals and oil-seed rape at the expense of spring barely and grass) and the availability of computerised soil databases for the calculation of actual soil moisture (Hough & Jones, 1997). Daily *PET* is calculated for each grid square for a range of surface covers from bare soil to forest using a

modified form of the Penman-Monteith equation (Monteith & Unsworth, 1990). The *PET* estimates are then converted to estimates of actual evaporation by progressively reducing the rate of water loss from the potential value to zero as the available water decreases from a fraction, p , of its maximum value to zero by increasing the bulk surface (canopy) resistance (p depends upon the soil crop combination and ranges from 60% for bare soil to 25% or less for some crops and soils) (Hough & Jones, 1997).

The Greens Burn catchment is contained within *MORECS* square 50. The information available for each square is detailed on the internet (<http://www.nerc-wallingford.ac.uk/ih/nrfa/yb/>). *MORECS* give a range of *AET* values (for grass cover) for square 50 for each year and as a default, the model uses the minimum *AET* value for each year.

For each year a relative weighting factor is calculated by dividing the *HER* for that year by the average *HER* for all years. This is based on the reasonable assumption that annual P flux (although not necessarily concentrations) will be directly proportional to *HER* (as shown in Figure 3.9).

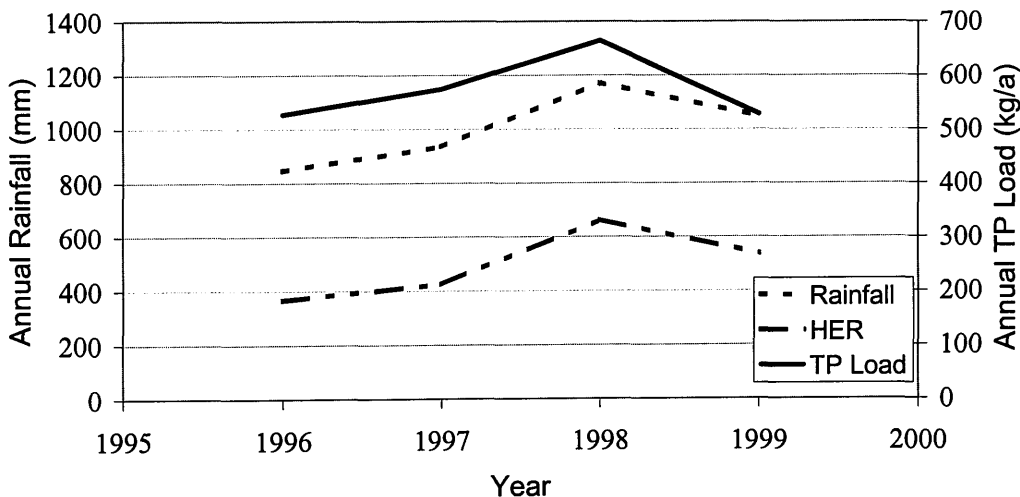


Figure 3.9. Comparison of measured annual rainfall, hydrologically effective rainfall (*HER*) and TP load in the Greens Burn catchment, 1996-1999.

The model output is adjusted for the amount of runoff in a year, by relating the hydrologically effective rainfall (*HER*) during the year in question to the average *HER* measured over time (i.e. the model output is multiplied by $HER/avHER$ – see Figure 3.12).

3.2. Results

3.2.1. Initial Results (with animals included explicitly)

Table 3.4 shows the results of the model predictions (kg P a^{-1}) for 1996 – 1999 for the basic export coefficient model and the SEPTIC model and comparison with the measured data.

Table 3.4. Comparison of TP loads (1996-1999) from the Greens Burn catchment predicted by the basic export coefficient model (SD) and the SEPTIC model (SD), with animals included explicitly, with measured data (SEM).

Year	Measured (SEM) (kg P a^{-1})	Basic Model Mean (SD) (kg P a^{-1})	SEPTIC Model Mean (SD) (kg P a^{-1})
1996	519 (281)	3224 (673)	576 (116)
1997	574 (331)	3024 (648)	625 (129)
1998	665 (257)	2947 (741)	942 (231)
1999	529 (224)	3016 (697)	783(178)

From Table 3.4, it can be appreciated that the SEPTIC model makes predictions closer to the measured data, suggesting that the adjustments made to incorporate the effects of topography, soil type and *HER* are sensible. Furthermore, the direction of change from year to year is captured by the SEPTIC model, such that 1998 is predicted as exporting more P compared to the other years, but not by the basic export coefficient model.

This is illustrated more clearly in Figure 3.10. From the figure, it can be appreciated that although the average value predicted by the SEPTIC model for 1998 and 1999 lies outwith the limits of the measured value \pm SEM, there is always an overlap between the measured mean \pm SEM and mean predicted flux \pm 1SD. However, a question which needs to be answered at this stage is whether the input from animals/manure should be included explicitly in the model. Further research into the published export coefficients revealed that in many grassland cases, the export coefficient was measured for grassland which was grazed and had manure added and that for many crops (root and cereals), the export coefficient was measured for land to which manure was added. Hence, the range of published export coefficients

contains values which reflect the presence of animals and the addition of manure. Therefore, adding animals into the model explicitly results in a double counting of animal inputs and is not required.

The model was re-run without the explicit inclusion of organic inputs and the results are shown in Figure 3.11.

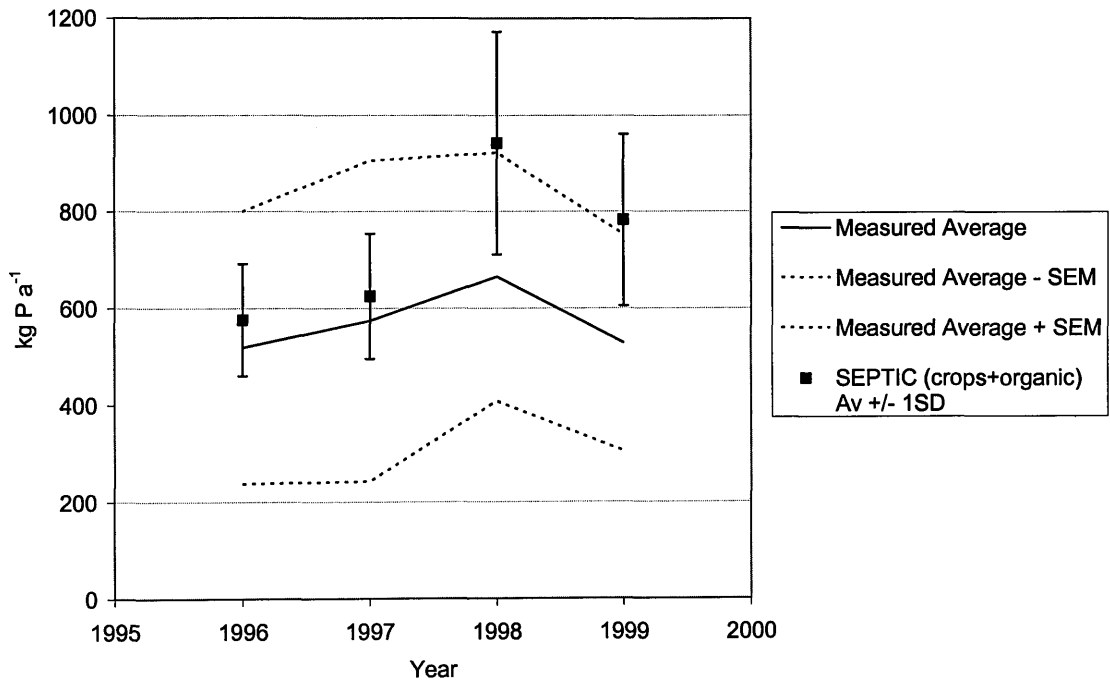


Figure 3.10. Comparison of the predictions of the SEPTIC model (treating organic inputs explicitly) with the measured data.

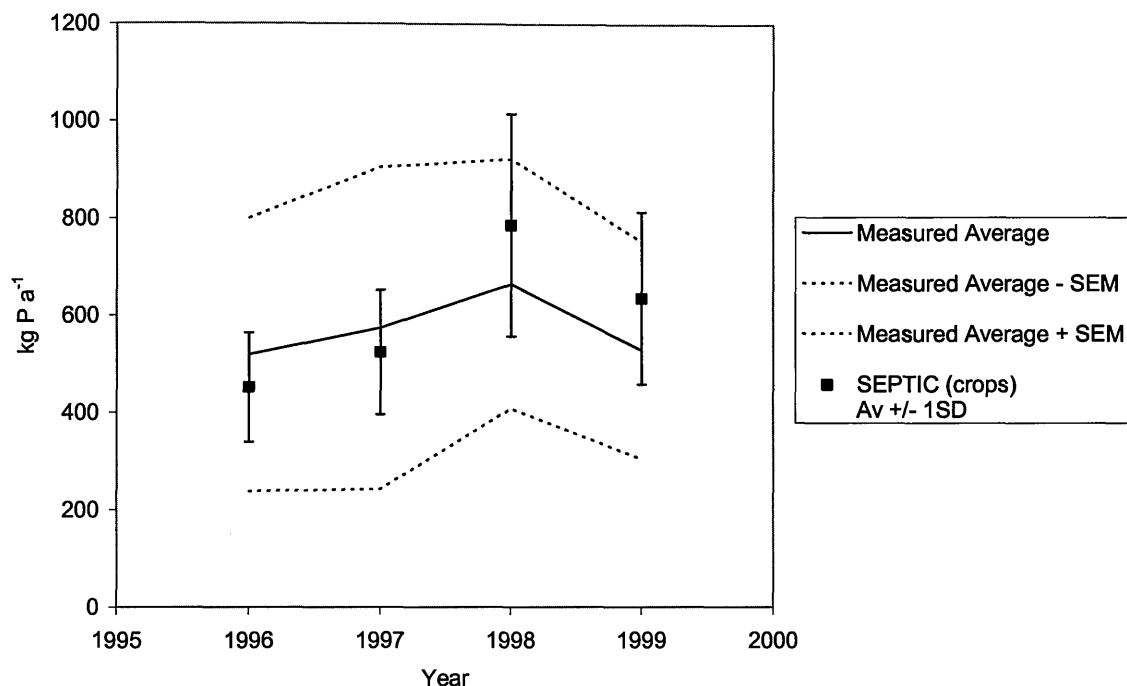


Figure 3.11. Comparison of the predictions of the SEPTIC model (treating organic inputs implicitly) with the measured data.

By not including organic inputs explicitly in the SEPTIC model (and instead assuming they are included implicitly in the range of published measured export coefficients), the model predictions for 96-99 all lie within the limits of the measured data \pm SEM. Hence the decision was made not to consider the impact of animals separately from the land use export coefficients.

3.2.2. Examination of the different stages of the model

Figure 3.12 summarises the different stages of the SEPTIC model. The model can be separated into its individual stages in order to inspect the effect that including the effects of slope, cumulative area, soil type and *HER* have on the model predictions. The impact of each of these “adjustments” is shown in Figures 3.13 – 3.16.

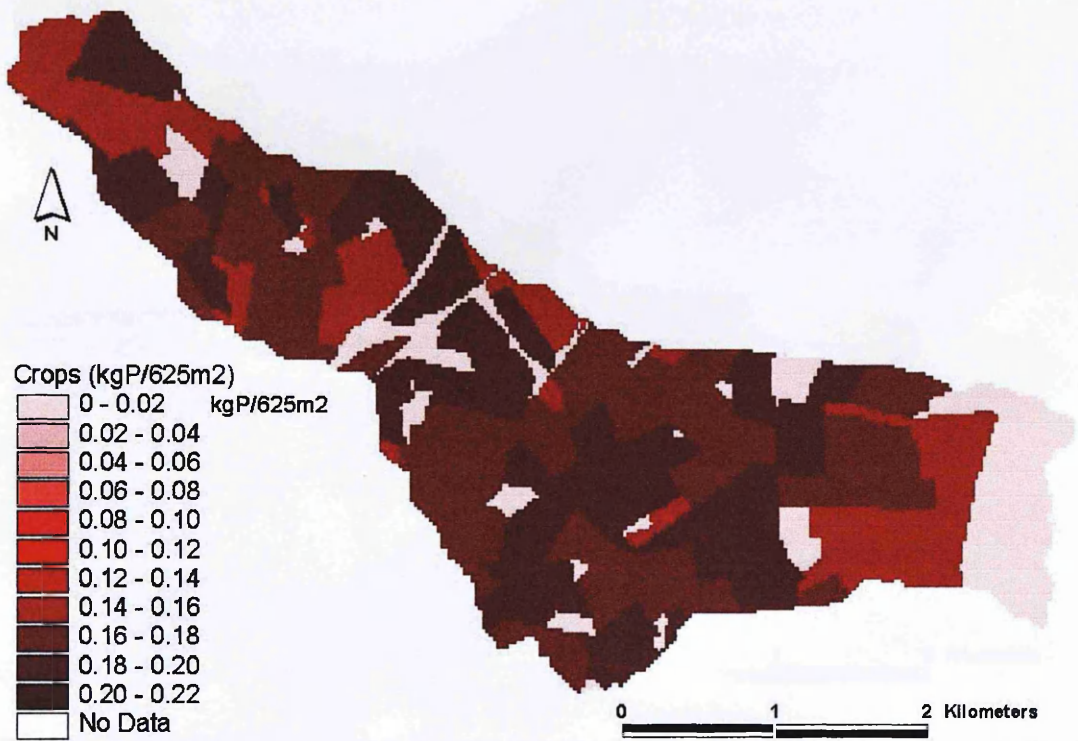


Figure 3.13. Spatial distribution of predicted P export from the Greens Burn catchment in 1996 considering the effect of cropping (land use) only.

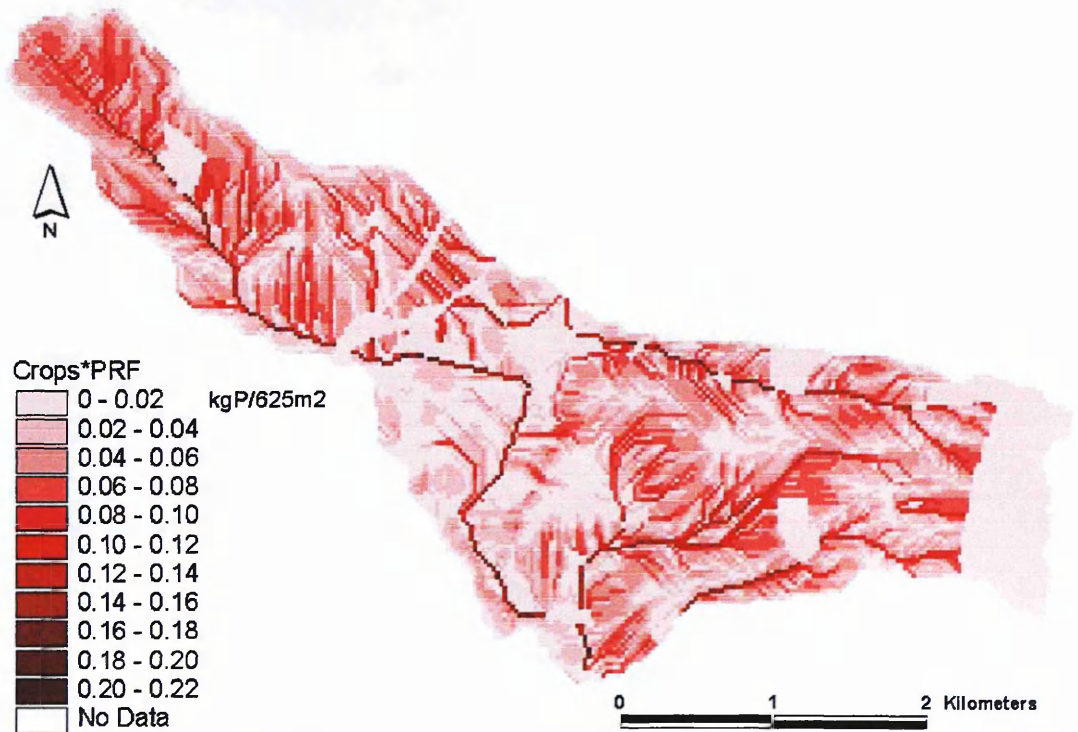


Figure 3.14. Spatial distribution of predicted P export from the Greens Burn catchment in 1996 considering the effect of cropping (land use) augmented by slope and cumulative area (the "prosser reduction factor", PRF).

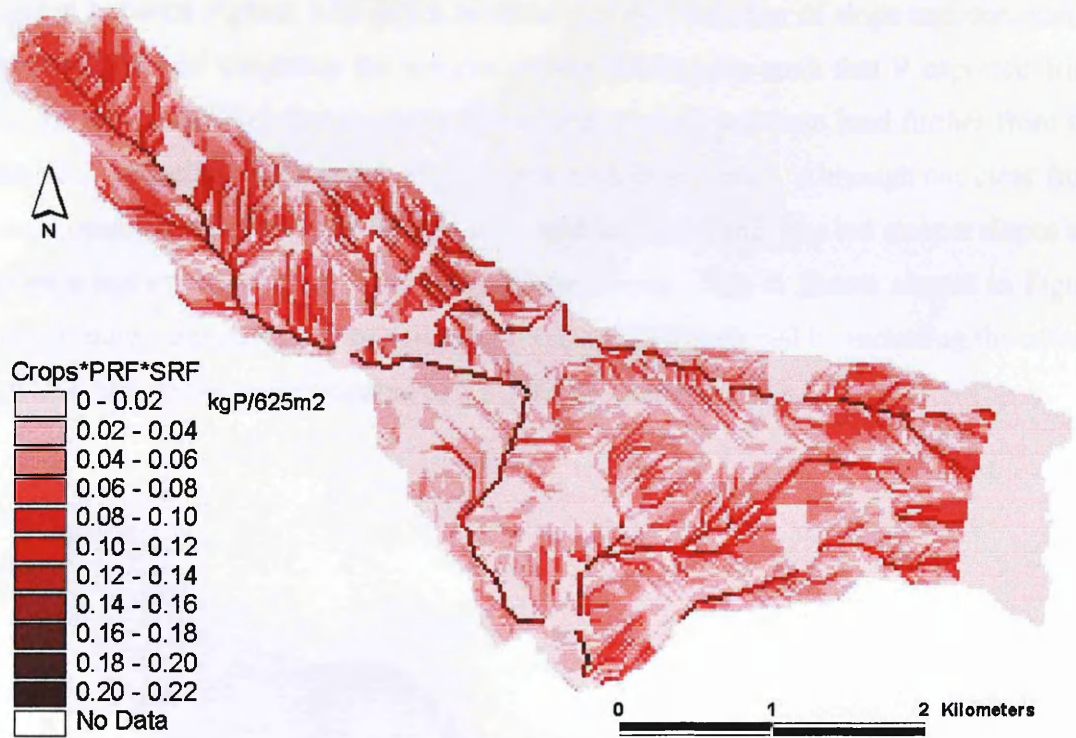


Figure 3.15. Spatial distribution of predicted P export from the Greens Burn catchment in 1996 considering the effect of cropping (land use) augmented by slope and cumulative area (the “Prosser reduction factor”, PRF) and soil type (the “soil reduction factor”, SRF).

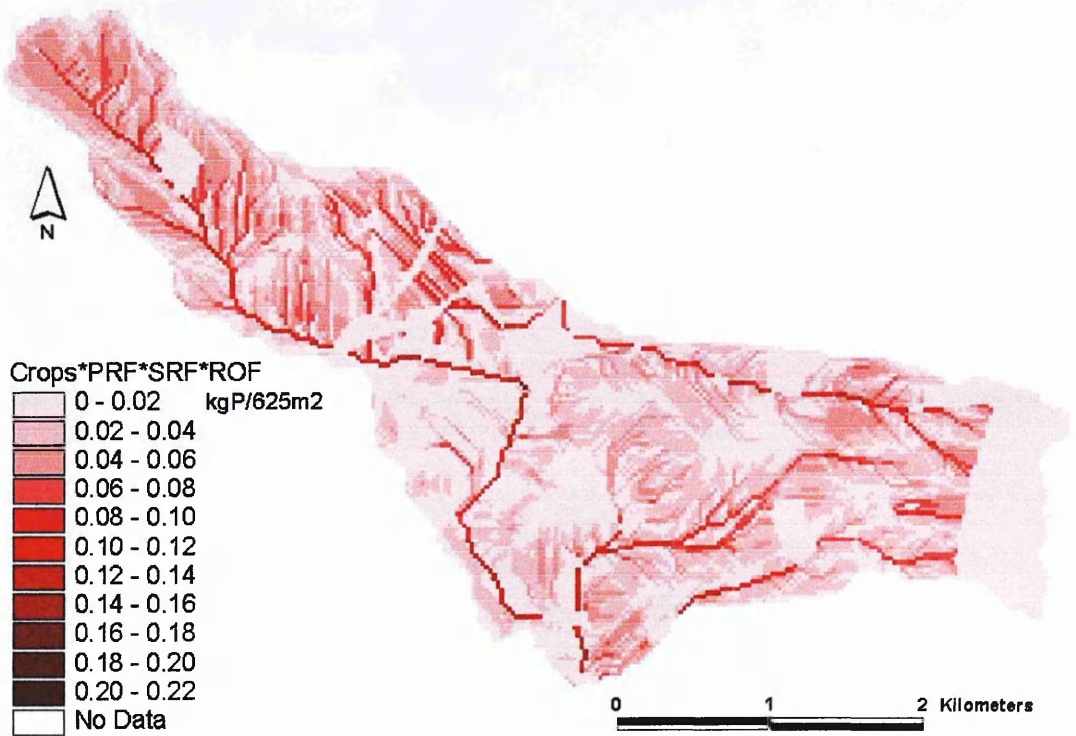


Figure 3.16. Spatial distribution of predicted P export from the Greens Burn catchment in 1996 considering the effect of cropping (land use) augmented by slope and cumulative area (the “Prosser reduction factor”, PRF) and soil type (the “soil reduction factor”, SRF) and *HER* (the “runoff factor”, ROF).

Comparison between Figures 3.13 and 3.14 show that the inclusion of slope and cumulative area has the effect of weighting the selected export coefficients such that P exported from close to the stream network has a greater impact than P exported from land further from the streams, thus supporting the concept of the sediment delivery ratio. Although not clear from the visual comparison between the figures, cells with identical land uses but steeper slopes are registering a higher export than those on shallower slopes. This is shown clearer in Figure 3.17, which shows the difference between the P export from each cell by including the effects of slope and cumulative area compared to considering cropping alone.

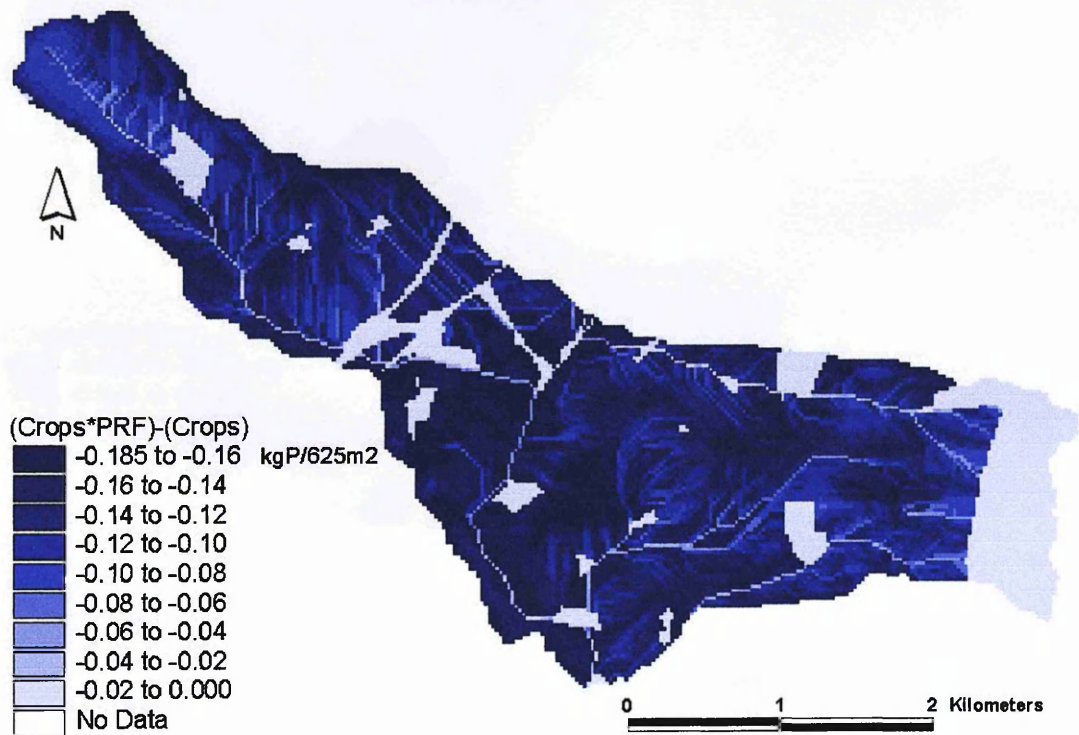


Figure 3.17. The difference in P export (in 1996) from each cells as a result of including slope and cumulative area in the model compared to considering cropping alone (crops*PRF - crops).

The difference is more marked (i.e. the export coefficient from land use has been more reduced) in the centre of the catchment, where slopes are shallower compared to the extremes of the catchment, where slopes are steeper. In addition, the difference is more marked in areas further from the stream network. The “block areas” of little change occur in areas which are designated as either buildings/roads or set aside in 1996 (Figure 2.11). These areas

had negligible export coefficients assigned to them and hence there was little room for any reduction in the export coefficients as a result of the effect of slope and cumulative area.

Visual comparison between Figures 3.14 and 3.15 gives little appreciation of the difference in the spatial distribution as a result of the further inclusion of the effect of soil type into the model. Figure 3.18 shows the difference in the P export from each cell as a result of including soil type in the model compared to just crops, slope and cumulative area.

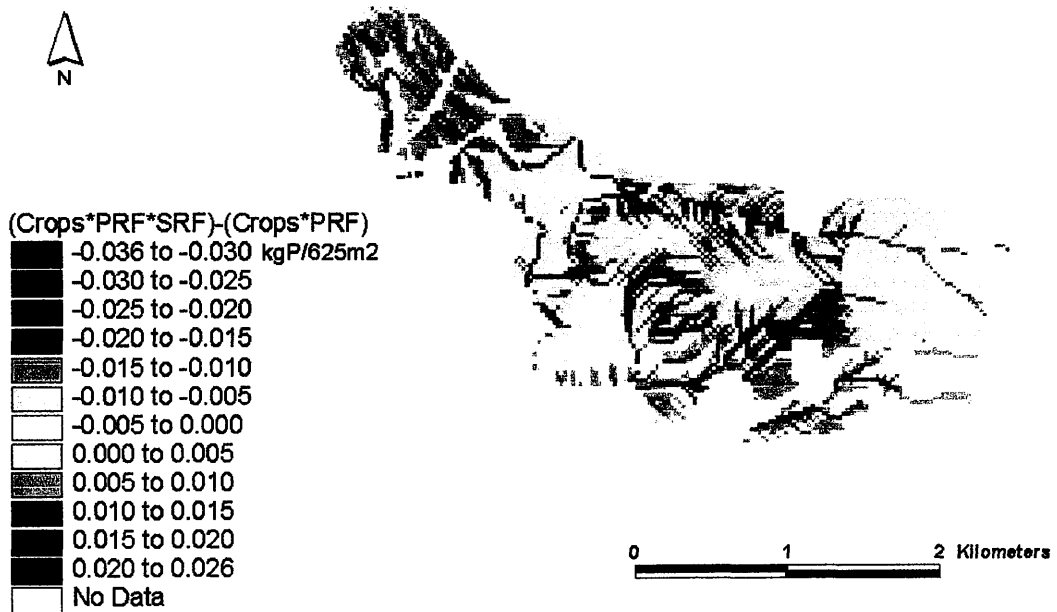


Figure 3.18. The difference in P export (in 1996) from each cell as a result of including soil type in the model compared to considering cropping, slope and cumulative area (crops*PRF*SRF – crops*PRF).

The inclusion of soil type (using weighted *SPR*) in the model acts only as a within-catchment relative factor, such that cells with near to average values of *SPR* in the catchment (Figure 3.8), experience little change in their P export whereas areas with higher than average values of *SPR* experience an increase in their P export and areas with lower than average values of *SPR* experience a decrease in their P export. This is in support of the idea that otherwise identical cells with a lower *SPR* value will be subject to less surface runoff (and hence less erosion and associated P transport) than those with a higher *SPR* value.

Visual comparison between Figures 3.15 and 3.16 indicates that the overall spatial distribution is “paler” when *HER* is additionally considered compared to just crops, slope, cumulative area and soil type. This indicates that the P export from each cell has been reduced catchment-wide, as illustrated in Figure 3.19.

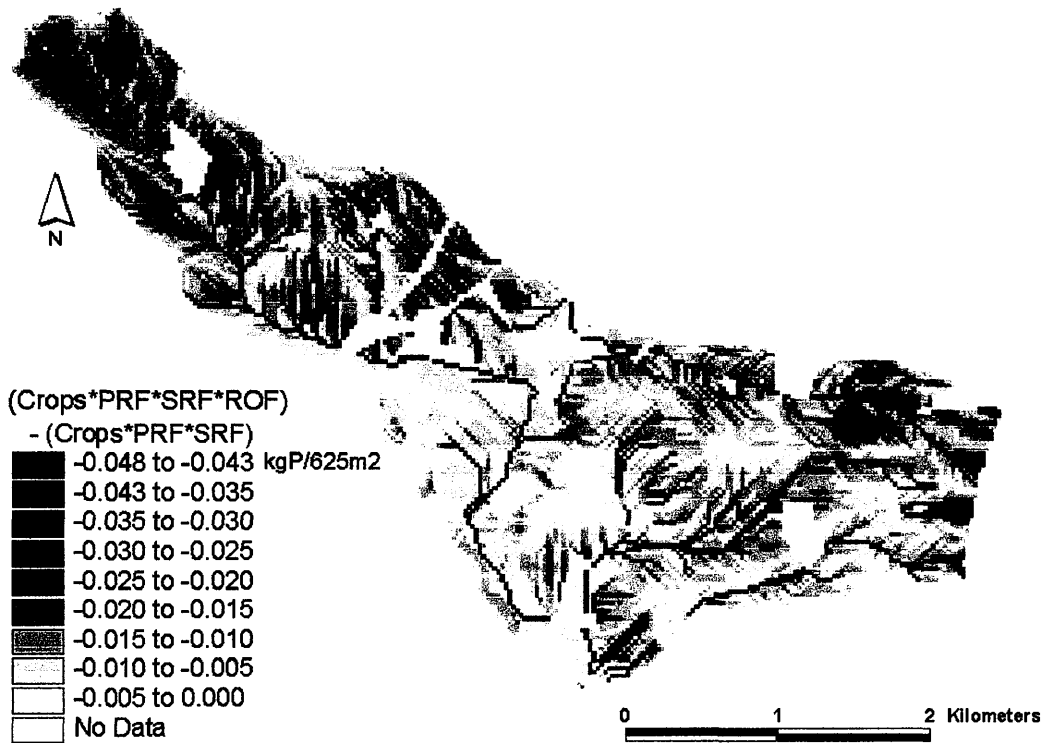


Figure 3.19. The difference in P export (in 1996) from each cell as a result of including *HER* in the model compared to considering cropping, slope, cumulative area and soil type (crops*PRF*SRF*ROF – crops*PRF*SRF).

From Figure 3.19, it can be seen that the P export from each cell has been reduced. The method of reduction (multiplying each cell by *HER*/average *HER*) means that cells with a higher export before the inclusion of *HER* are reduced by more than those which were previously exporting less P. 1996 is a drier-than-average year and so it is to be expected that the overall consequence of including the effect of *HER*/average *HER* will be a reducing one. In a wetter-than-average year (e.g. 1998), the reverse is true, with the P export being increased in each cell, as shown in Figure 3.20.

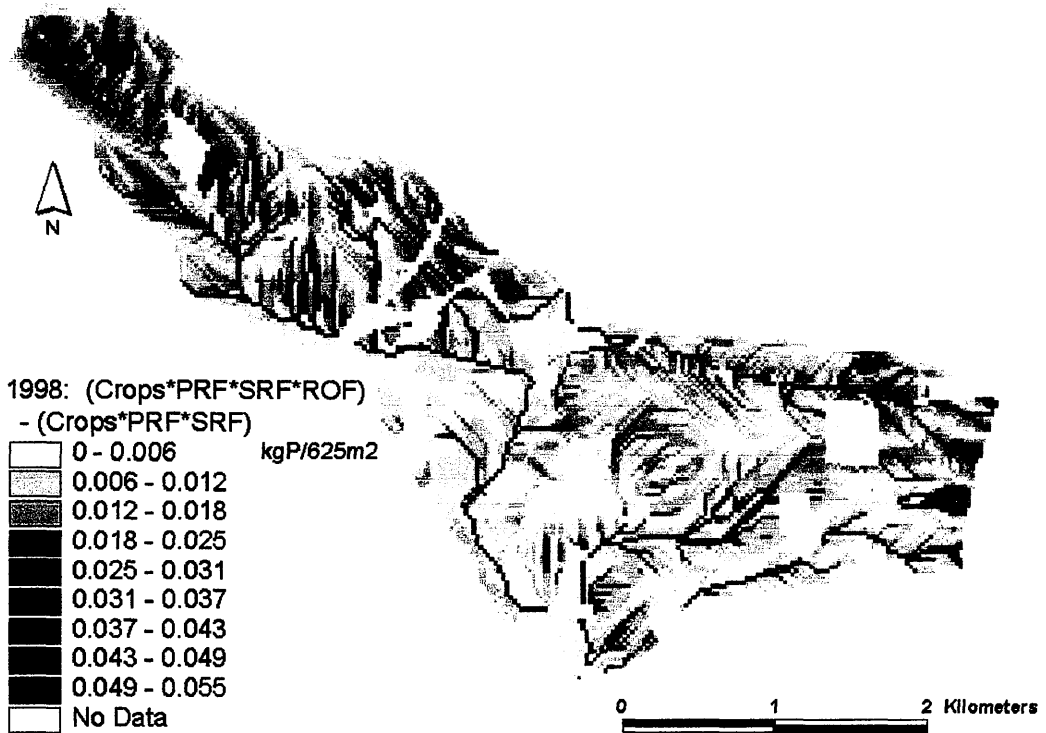


Figure 3.20. The difference in P export (in 1998) from each cell as a result of including *HER* in the model compared to considering cropping, slope, cumulative area and soil type (crops*PRF*SRF*ROF – crops*PRF*SRF).

The numerical results for each year (1996-99) from each stage of the model are shown in Table 3.5, along with the measured data for comparison.

Table 3.5. Numerical Results (1996-1999) from each stage of the model: P export (kgP a⁻¹) from just considering crops; from considering crops, slope and cumulative area (Crops*PRF); from crops, slope, cumulative area and soil type (Crops*PRF*SRF) and from crops, slope, cumulative area, soil type and *HER* (Crops*PRF*SRF*ROF) and the measured data for comparison.

Year	P Export kg P a ⁻¹				
	Measured Mean (SEM)	Crops Mean (SD)	Crops*PRF Mean (SD)	Crops*PRF*SRF Mean (SD)	Crops*PRF*SRF*ROF Mean (SD)
1996	519 (281)	2598 (659)	637 (158)	613 (152)	452 (112)
1997	574 (331)	2598 (642)	636 (156)	613 (148)	524 (128)
1998	665 (257)	2523 (738)	616 (181)	592 (172)	786 (229)
1999	529 (224)	2515 (696)	612 (173)	589 (164)	636 (177)

From Table 3.5, it can be seen that the variation in annual P export from the Greens Burn catchment in 1996-1999 as a result of considering the export coefficients alone is small. This implies that, although land use may have considerable impact on the local (field) scale, it may not be so vital for making predictions at catchment level. This shall be explored further in Chapter 5. Including slope and cumulative area into the model serves to produce more realistic annual P export results and supports their inclusion in the model. On the catchment scale, including the effect of soil type into the model makes little effect. This is to be expected given the method of inclusion into the model: at present it serves only as a within-catchment weighting. Including the effect of the change in *HER* year to year into the model (even in its currently simplistic manner) improves the predictions by correctly capturing the direction of change in annual P export from year to year.

3.2.3. Model Results

Figure 3.21 shows the frequency distributions of predicted P transfer produced for the Greens Burn catchment from 500 iterations for 1996 – 1999, along with the load estimated from measured concentration and discharge data (± 1 SEM). The distributions are approximately symmetrical with the mean fluxes standard deviations summarised in Table 3.6. From Figure 3.21, the similarity between the range of predicted loads and the measured load is evident.

Table 3.6. Summary of the mean and standard deviation of the distributions produced by the model predictions and the load estimated from the measured data for the Greens Burn catchment, 1996-1999.

Year	Predicted Flux		Measured Load
	kg P a ⁻¹ Mean \pm 1SD	kg P ha ⁻¹ a ⁻¹ Mean \pm 1SD	kg P a ⁻¹ Mean \pm 1SEM (n)
1996	452 \pm 112	0.42 \pm 0.10	519 \pm 281 (13)
1997	524 \pm 128	0.48 \pm 0.12	574 \pm 331 (12)
1998	786 \pm 229	0.73 \pm 0.21	665 \pm 257 (11)
1999	636 \pm 177	0.59 \pm 0.16	529 \pm 224 (11)

The high uncertainty in the measured load arises as a consequence of the high variability in measured concentrations and the low number of samples taken (n=11, 12, 13). It is important to recognise that the observed data with which the model output is compared are an estimate with a potentially high error, as explored in Chapter 2.

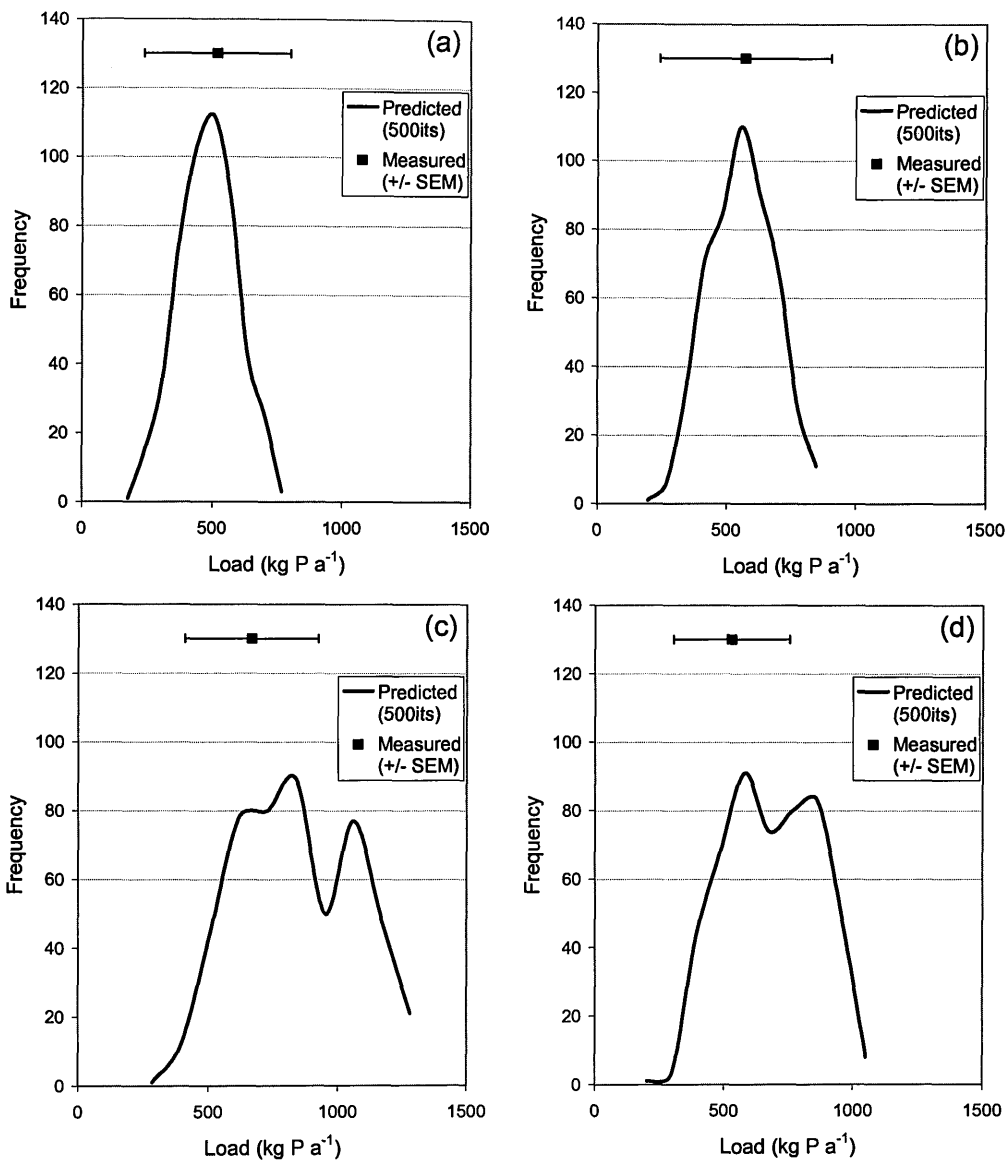


Figure 3.21. Frequency distribution of predicted TP loads (500 iterations) compared with an estimate of the load derived from measured data (± 1 SEM) from the Greens Burn catchment for 1996 (a), 1997 (b), 1998 (c) and 1999 (d).

The spatial distributions of predicted phosphorus export from the Greens Burn catchment for 1996 – 1999 are shown in Figure 3.22.

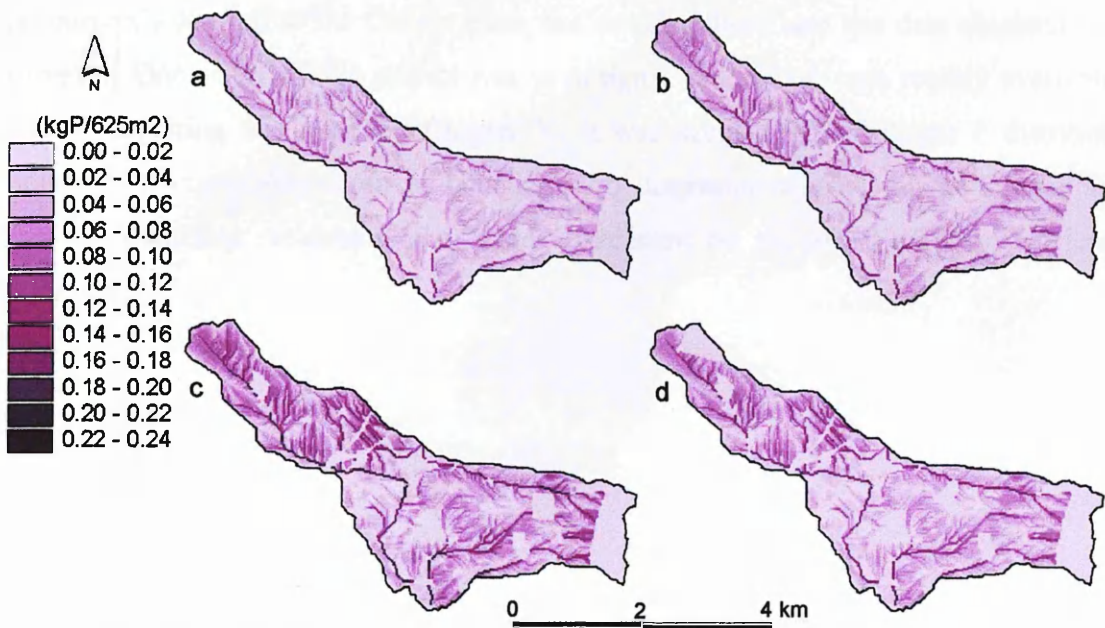


Figure 3.22. Spatial distributions of phosphorus export predicted by the SEPTIC model output from the Greens Burn Catchment in 1996 (a), 1997 (b), 1998 (c) and 1999 (d).

This shows the combined effects of land use, slope, proximity to watercourses, soil type and *HER*. Such a visualisation can help to show up “hot spots” for P loss. Worthy of note are the permanent grassland areas in the northwest of the catchment (Figures 2.11 – 2.14). According to the basic export coefficient model (e.g. Johnes, 1996) these areas should export relatively little phosphorus compared to arable land. However, they become significant when the export coefficient is selected from the published range for permanent grass (for a number of iterations) and subsequently adjusted for slope and cumulative area and soil type. Areas close to stream channels are also evident as disproportionately active sources of P due to high cumulative area. Again, this tallies with an expectation that P mobilised near to, or within, channels will be transported beyond the catchment outlet.

In general terms, a spatially explicit model allows the identification of “vulnerable” areas (i.e. those prone to P loss). This permits special management measures to be targeted to these areas and provides a vehicle to test out different management scenarios e.g. what is the impact of making a certain field “set aside”? This also provides a more robust justification for the effort, inconvenience and costs involved in such measures.

As currently applied to the Greens Burn, the model utilises land use data obtained via farm surveys. One remit of this project was to design a model that uses readily available data. Before exploring this issue (in Chapter 5), it was decided to investigate P distribution in fields, particularly deposition at boundaries to determine whether an additional layer of sophistication was required in the model to account for the effect of these barriers on P transport.

Chapter 4. Investigation into P distribution in fields

4.1. Introduction

4.1.1. Delivery of sediment-associated phosphorus to the watercourse

The SEPTIC model links soil erosion in fields to the export of P to watercourses. It assumes that the majority of phosphorus exported from catchments is associated with eroded sediment. Crop types with observed relatively high erosion rates, e.g. row crops, are given higher export coefficients than crops with less erosion risk. In addition, SEPTIC adjusts the coefficients for other variables (e.g. topography (slope and cumulative area from the divide), soil type and rainfall) observed to affect propensity for erosion.

Commonly, catchments do not export all eroded material due to the opportunities for sediment deposition between the eroded sediment source and the channel network. The average annual sediment yield (s) of a catchment is defined as

$$s = pe - qd$$

Equation 4.1

where

s = average annual sediment yield (measured as a volume, $m^3 a^{-1}$ or as a mass, $t a^{-1}$)

p = proportion of the catchment ($m^3 a^{-1}$ or $t a^{-1}$) that erodes at rate e (measured as a depth of erosion, $m a^{-1}$)

q = the proportion of the catchment ($m^3 a^{-1}$ or $t a^{-1}$) experiencing deposition at rate d (measured as a depth of deposition, $m a^{-1}$)

(From Richards, 1993).

The rate of yield to erosion is termed as the sediment delivery ratio (SDR), given by s/pe , and is usually expressed as a percentage.

The position of the eroding unit (e.g. a field or grid cell) with respect to the watercourse is important as the further the unit is from the stream, the greater the likelihood that the eroded

sediment will be deposited in the catchment, either in topographic hollows or by an encounter with a barrier such as downslope in-field vegetation or a field boundary.

Beuselinck *et al* (2000) studied the distribution of sediment deposits in a Belgium loam catchment and observed that the undisturbed aggregate-size distribution of sediment deposits in front of vegetation barriers was finer than for topographically-controlled deposits. However, when compared to the source material, it was found that the aggregate size of the vegetation-controlled deposits was not significantly different. For topographically-controlled deposits, there appears to be a selective process, with the preferential export of fines. Given that P is generally more associated with the clay fraction of the soil (e.g. Morgan, 1997), this would increase the relative importance of deposits at field boundaries compared with topographically-controlled deposits. Meyer *et al* (1995) performed flume studies to explore the effect of hedges further. They concluded that the sediment trapping resulted mostly from upslope ponding by hedges rather than by a filtering action. Depending on the vegetation (and its ability to retard flow), around 90% of coarse sediment ($>125\mu\text{m}$) was trapped, forming a delta. In comparison, approximately 20% of fines ($<32\mu\text{m}$) settled in the area between the delta and the hedge, with the rest moving into or through the hedge. In addition, the possibility for fines aggregating together, with the increased chance of settling out, should be considered. Beuselinck *et al* (2000) also calculated that 65% of the sediment deposited upslope of the barrier was due to settling in ponding at high flows. Hence, the rainfall duration and intensity and resultant runoff in the catchment will be important.

4.1.2. Distribution of phosphorus in the field

Different experimental research has concluded that when phosphorus is added to the soil surface, as fertiliser and manure additions over time, the result is surface P enrichment (Haygarth *et al*, 1998). A number of studies have shown that soil P content often reduces non-linearly with depth (e.g. Frossard *et al*, 2000, Nair *et al*, 1995).

Haygarth *et al* (1998) tested the Sodium Bicarbonate (Olsen) P fraction at various depths of cores taken from 1 ha plots. The results, shown in Figure 4.1, show a large change in Olsen-P status with depth, especially near the surface.

Eghball *et al* (1996) also measured the distribution of Olsen P with depth in alkaline soil (Nebraska, U.S.A.). Their results, which are shown in Figure 4.2, show that the application of P fertiliser to soil increases the P concentration in the surface horizons. The application of manure increases the P concentration further and to a greater depth, which may be explained by the increased movement of organic P in soils (e.g. Eghball *et al*, 1996; Caruso, 2000).

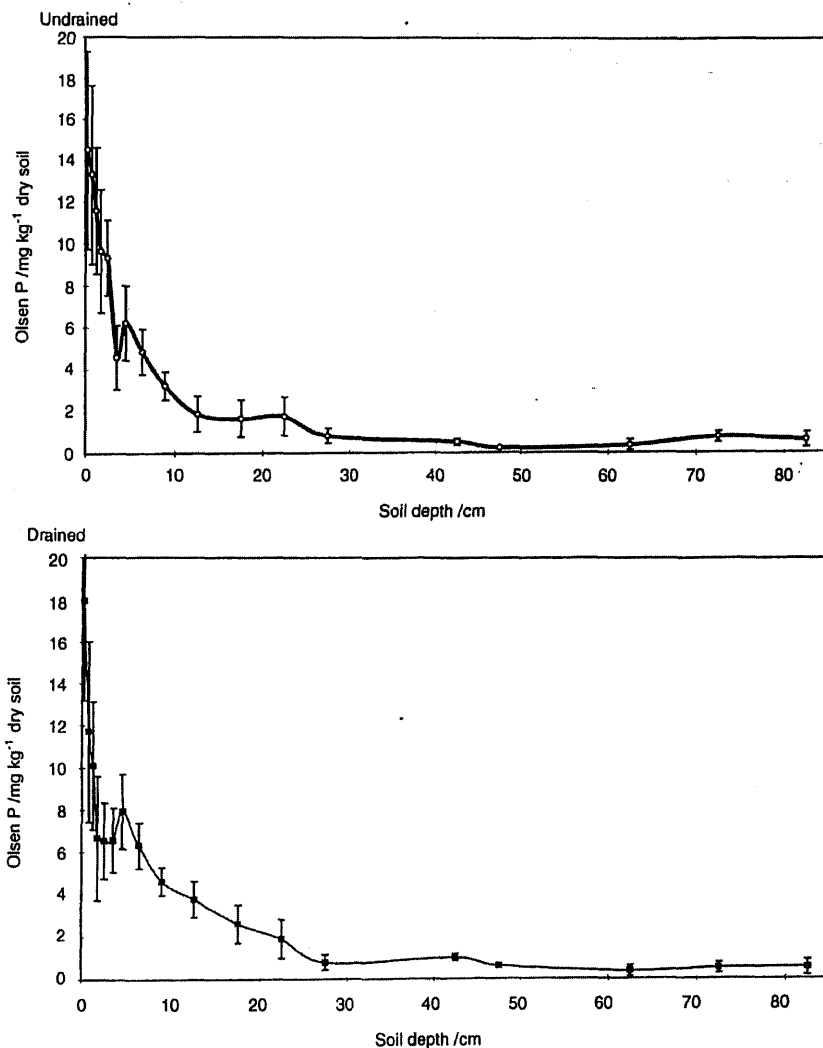


Figure 4.1. Olsen-P concentration in soil sampled between 0 and 85 cm depth, in drained and undrained plots (standard error bars are at the midpoint of the sample depth). (From Haygarth *et al*, 1998, p.68.)

4.2. Aims

The aims of the field work were to

- Assess the importance of both topographically-controlled deposits and those formed at boundaries (change in crop/vegetation) for the delivery of sediment-associated P to surface waters. From the literature, it was expected that topographically-controlled deposits, with their preferential export of fines, will be depleted in P compared to deposits formed at boundaries, where ponding may encourage the fines to settle out.
- Investigate the distribution of P in the different horizons of the soil from which the deposits were derived. It was expected that P concentration would decrease with depth. In addition, the spatial variability of P concentrations in the surface horizon was investigated. Large variations might challenge the method of assigning one export coefficient to a field, although on a catchment scale, other factors (such as land use or slope) may dominate over infield variations in P concentration.

4.3. Field Sites

Two fields in the Greens Burn catchment, Perth and Kinross, Scotland, were studied. The fields were selected on the basis that both fields have a history of infield erosion and deposition at field boundaries. The locations of the two fields are shown in Figure 4.3.

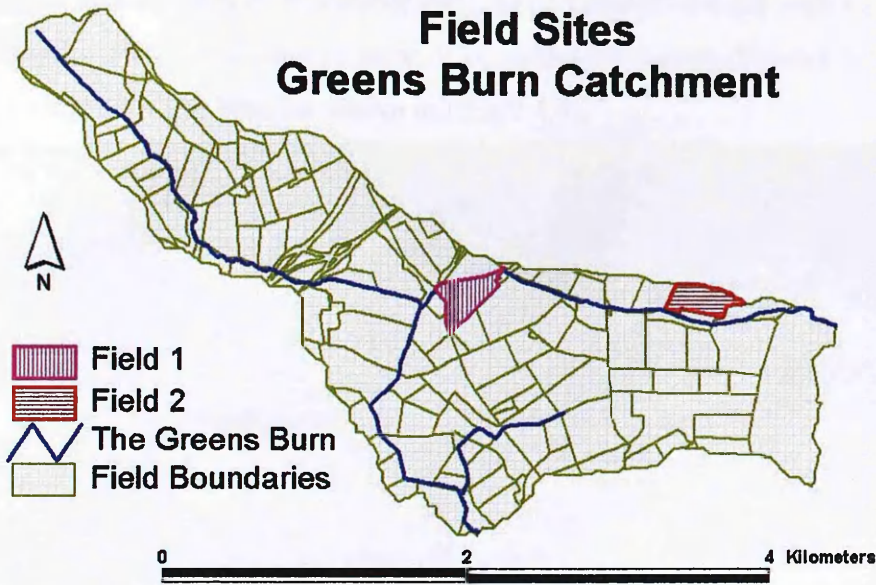


Figure 4.3. Location of fields sampled in the Greens Burn Catchment.

4.4. Field Site 1

The topographic and recent land use data for field 1 is given in Figure 4.4.

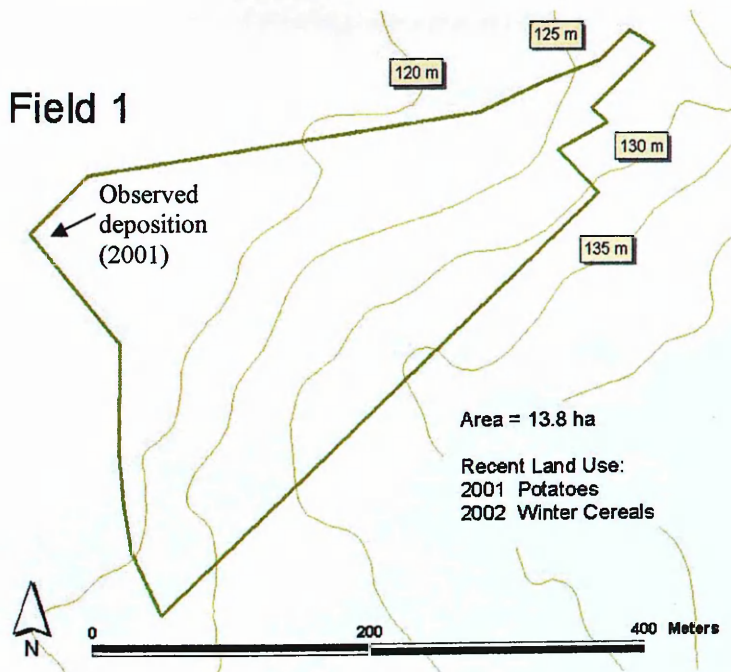


Figure 4.4. Topographic and recent land use data for field site 1. The location of boundary deposition observed in November 2001 is also depicted.

Field 1 was sampled in November 2001, as part of a pilot study with an undergraduate student (Higgins, 2002), and showed signs of boundary deposition (Figures 4.5 and 4.6) in the north-west corner of the field (as shown in Figure 4.4).



Figure 4.5. Evidence of boundary deposition in field 1 in November 2001.



Figure 4.6. Boundary deposition in field 1, November 2001.

The results from the study are shown in Figure 4.7 (data from Higgins, 2002).

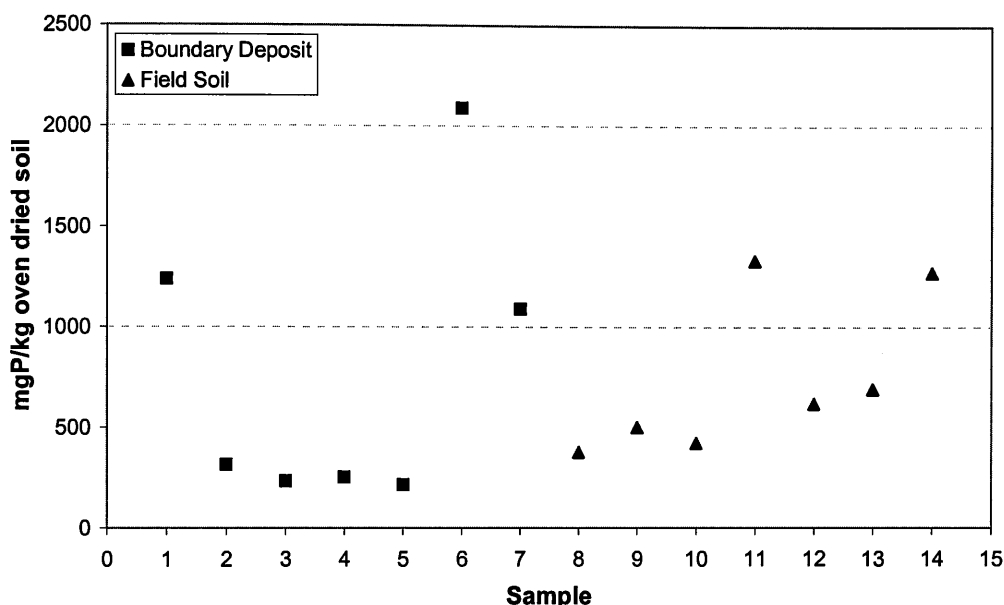


Figure 4.7. TP concentrations of surface soil (0-2cm) from samples taken from field 1 on 6 November 2001. Samples 1-7 were taken from the boundary deposit and samples 8-14 were taken from the surface horizon (0-5 cm) within the field.

There was a wide variation in P concentrations in both sets of samples. The mean P concentrations in the boundary deposit and field soil samples were 777 and 744 mgP /kg oven dried soil respectively. There was no significant difference between the deposit and the source soil samples, using the Mann-Whitney non-parametric test.

There was a wide variation in the texture of the deposit samples (see Figures 4.8 and 4.9). A possible explanation for this is the type of boundary, which consisted of tall, dense vegetation and partly a wall. It is likely that such a boundary would encourage ponding and particle settling, resulting in a graded texture.



Figure 4.8. Fine deposition in field 1, Nov 2001.



Figure 4.9. Coarser deposition in field 1, Nov 2001.

4.4.1. Sampling Strategy (October 2002)

A more thorough sampling campaign was conducted in October 2002. A systematic sampling scheme was employed in order to ensure a better spatial coverage. Since the field exhibits a clear topographic gradient, sampling along transects downslope in the field was employed as opposed to using a grid system. Care was taken to ensure a good, representative coverage e.g. the spatial sampling regime avoided sampling from just rows and not in-between rows in fields.

4.4.2. Number of samples

The number of samples required was estimated using the results of the pilot study (14 samples) carried out by Higgins (2002). The number of samples needed to approximate the true mean with a given tolerance and with a confidence interval of 95% can be calculated from the theory of standard errors (Rowntree, 1981):

$$n = \left(\frac{1.96 * s}{p * m} \right)^2$$

Equation 4.2

where

s = standard deviation

m = mean

p = tolerable error as a proportion of the mean (i.e. if it is required that the sample be within 10% of the mean, then p = 0.1)

n = number of samples required

However, since the statistics of the pilot sample will vary with the sample number used in the pilot study, the equivalent equation using the *t* statistic (rather than the standard normal parameter) is preferable (Petersen & Calvin, 1965):

$$n = \frac{t_{\alpha}^2 s^2}{D^2}$$

Equation 4.3

where

t_{α} = students t with (n-1) degrees of freedom at α probability level

D = specified limit (= $p \cdot m$)

Treating the 14 samples taken from Field 1 as a group (regardless of location i.e. boundary or in-field) and using the measured results for TP ($t_{0.95} = 2.16$ (for a sample size of 14), $s = 559.81$), the number of samples required to obtain certain specified limits are shown in Table 4.1.

Table 4.1. Number of samples (n) required to achieve the specified limit ($D = p \cdot m$)

p	n
0.1	253
0.2	63
0.25	40
0.3	28

As a compromise between effort and accuracy, it was decided to take 28 samples.

4.4.3. Conditions

Erosion and deposition in field 1 was very different in October 2002, compared November 2001 (see Figures 4.10 and 4.11) due to differences in cropping and rainfall patterns.



Figure 4.10. Field site 1 in November 2001. Potatoes lifted September 2001, Winter Wheat sown October 2001.



Figure 4.11. Field site 1 in October 2002. Winter Wheat cut September 2002.

In 2001, the field was in potatoes until September and then sown with winter wheat in October, the shoots of which can be observed in Figure 4.10. In 2002, the field was in winter wheat, which was cut in September and the remaining stubble is observed in Figure 4.11. Row crops such as potatoes are known to be a greater erosion risk (e.g. Morgan, 1997), which could explain the difference between the observed erosion/deposition in 2001 and 2002.

Rainfall is measured by SEPA at two gauges, at Balado and Portmoak, which are both situated approximately 5km from the centre of the catchment. The rainfall for the catchment is taken as the average of both gauges. Figure 4.12 shows the rainfall measured in the Greens Burn catchment for both 2001 and 2002 prior to the sampling days (6th November 2001 and 10th October 2002).

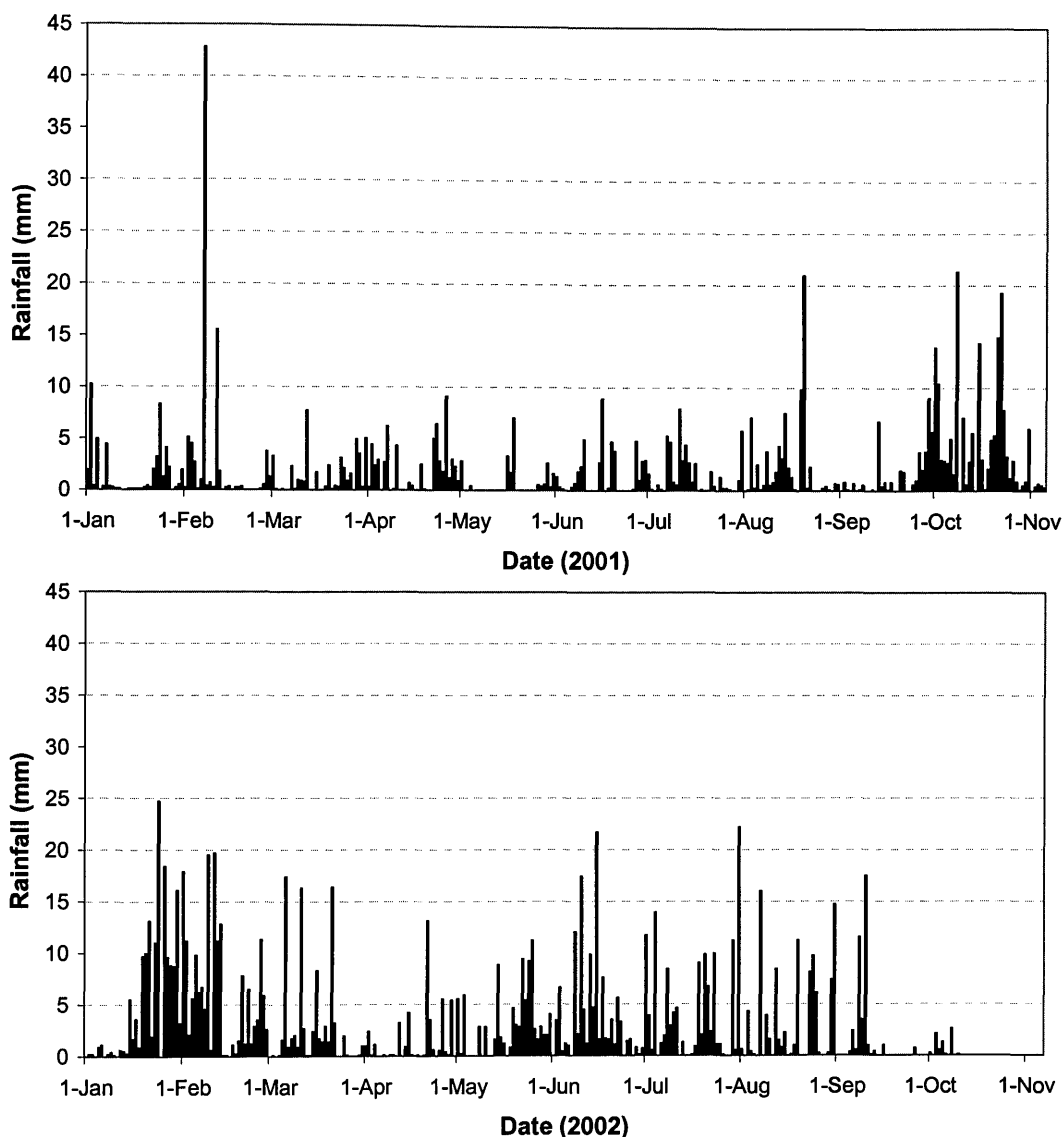


Figure 4.12. Daily rainfall measured in the Greens Burn catchment prior to the sampling dates (6th November 2001 and 10th October 2002), calculated as the average of the daily rainfall measured at the Balado and Portmoak rain gauge sites.

Overall, 2002 was a wetter year than 2001 (1275.6 compared with 719.2 mm/yr). However, in 2001 there was a large rainfall event on 7 February. Large storms are known to accelerate erosion, to the extent that most material moved in one year is moved by a small fraction of large events (e.g. Nash *et al*, 2000; Caruso, 2000). In addition, in the days immediately prior to sampling, there was greater rainfall in 2001, which coincided with recently disturbed ground (resulting from the lifting of the potato crop and the subsequent planting of winter wheat).

With the lack of field boundary deposit in 2002, effort was concentrated on sampling down transects in the field to investigate the distribution of P spatially on the surface and with depth and to ascertain the relationship between phosphorus and other soil factors. There were a few in-field deposits which were sampled for comparison with the source material.

4.4.4. Sampling Locations and Samples Taken

Figure 4.13 shows the sampling locations in field 1.

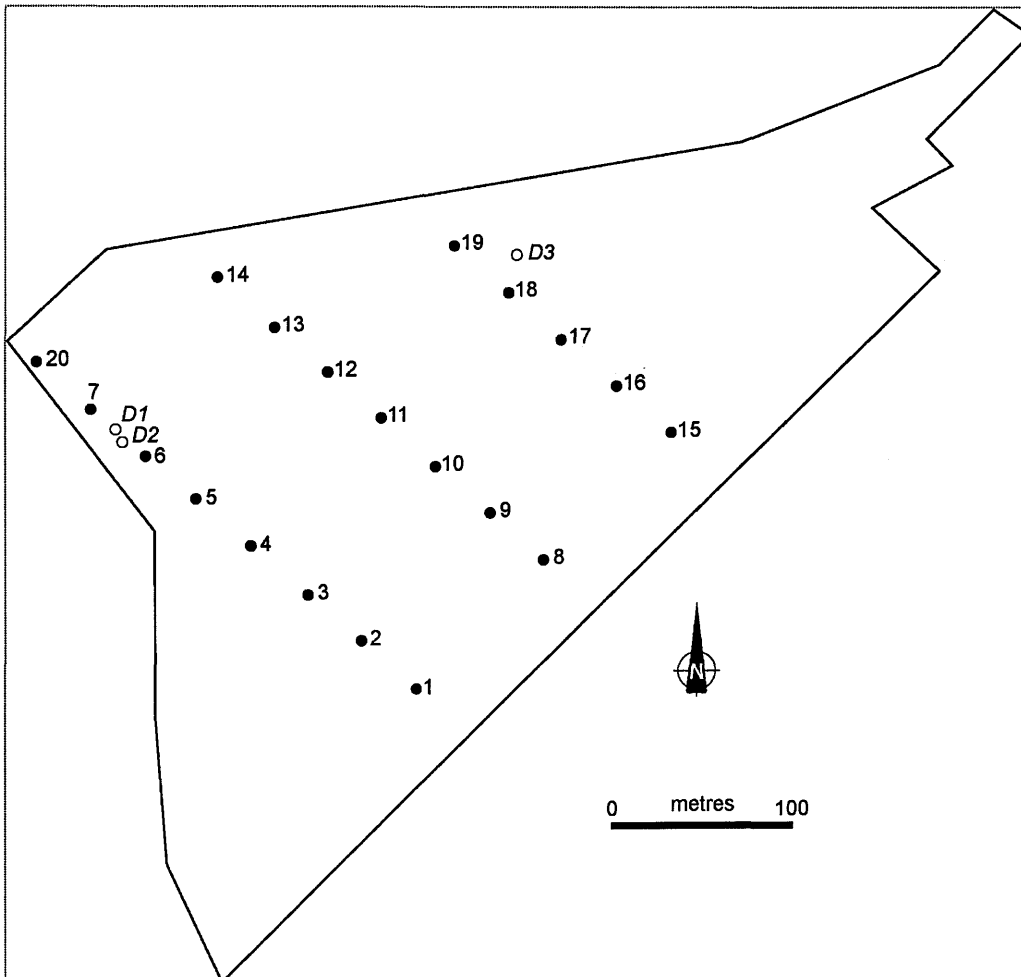


Figure 4.13. Sampling locations in field 1, for October 2002.

Samples were collected from the area that, according to the topography in the field, should contribute to any deposit in the bottom (north-west) corner of the field (where the deposit was observed in November 2001). To systematically sample from this source area, samples were taken along 3 transects (315° bearing) at 40m intervals. Surface samples (0-15cm) were collected from locations 1-20 to allow the surface distribution of P, infield, to be examined.

An auger was used to investigate the soil profile at regular (40m) intervals down the central transect (locations 8-14) and the results are shown in Figure 4.14.

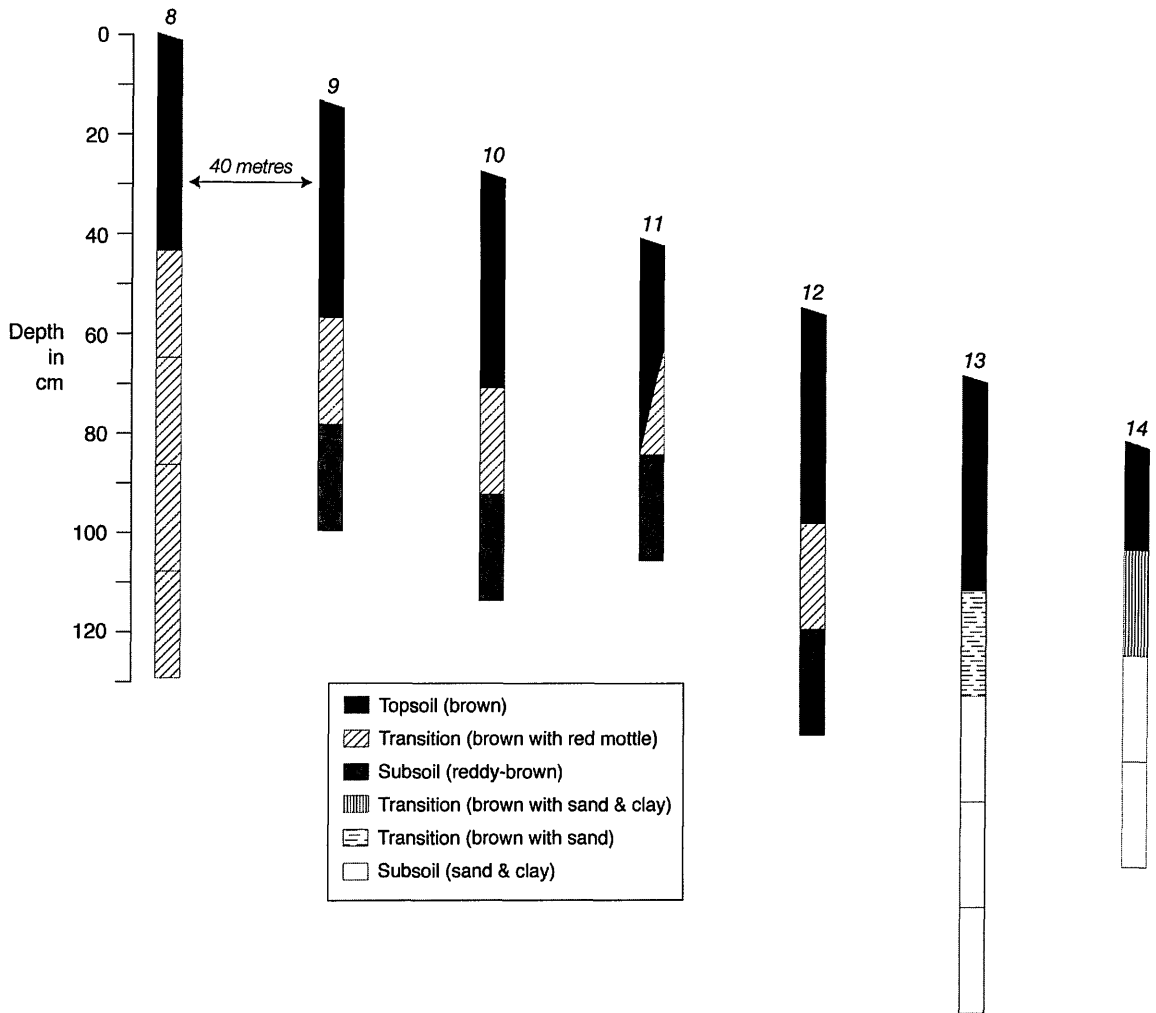


Figure 4.14. Qualitative description of the soil profile at sampling locations 8 to 14, with 8 being taken 40 m from the top of the slope and 40 m intervals between the samples until 14 at the bottom of the slope.

Cores (to 40cm depth) were taken at locations 8 (top of slope), 10 (mid-slope) and 14 (bottom of slope) and divided into 5cm depth sections for later analysis. The colour of the air-dried sub-samples of each section of the cores are shown in Figures 4.15 – 4.17. A change in colour can be observed in each core with depth and also between the core at the top of the slope (number 8) and the bottom of the slope (number 14), especially at depth. In all three cores, the surface samples are browner, indicating the presence of more organic matter. In the upslope and mid-slope cores (8 and 10), the colour becomes redder, which is consistent with the red sandstone parent material in the area. In the bottom slope core (14), the change is to a yellow/grey colour, consistent with the presence of more clay, which may have resulted due

to a history of erosion and the accumulation of finer particles towards the base of the slope or to variations in the clay content of the till parent materials.

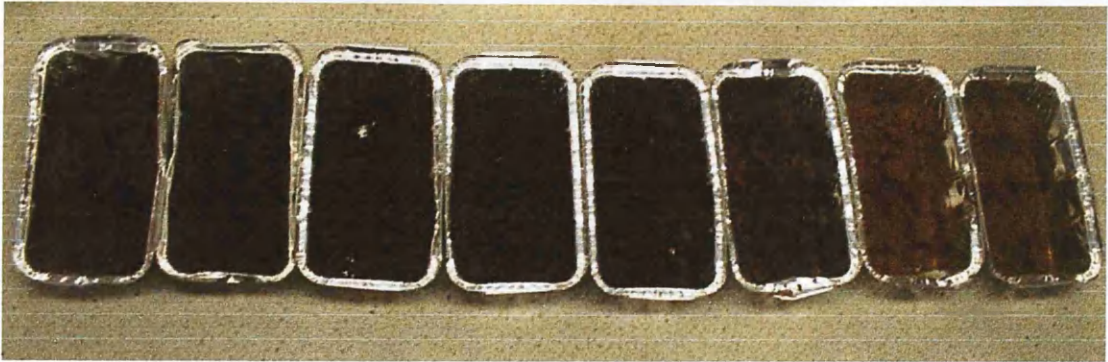


Figure 4.15. Visual comparison of soil colour changes with depth for core 8 at 0-5, 5-10, 10-15, 15-20, 20-25, 25-30, 30-35, 35-40 cm depths, dried at 30°C.



Figure 4.16. Visual comparison of soil colour changes with depth for core 10 at 0-5, 5-10, 10-15, 15-20, 20-25, 25-30, 30-35, 35-40 cm depths, dried at 30°C.



Figure 4.17. Visual comparison of soil colour changes with depth for core 14 at 0-5, 5-10, 10-15, 15-20, 20-25, 25-30, 30-35, 35-40 cm depths, dried at 30°C.

In the field in October 2002, there were little signs of deposition, compared to Nov 2001. There were three areas of non-boundary deposition (D1, D2, D3). Two small deposits (D1 and D2) accumulated at the end of tramlines, whilst a bigger deposit (D3) formed at the end of a rill (see Figures 4.18 – 4.21).



Figure 4.18. Deposit 1 (October 2002), formed at the end of a tramline, measuring 1.84 x 1.23 m, with an observed sandy layer (deposit) of 2cm. A sample (0-15cm) was taken from the centre of the deposit.



Figure 4.19. Deposit 2 (October 2002), formed at the end of a tramline, measuring 1.70 x 1.00 m, with an observed sandy layer (deposit) of 2 cm depth. A sample (0 - 15 cm) was taken from the centre of the deposit.



Figure 4.20. Deposit 3 (October 2002), formed at the base of a rill, measuring 12.60 x 10.10 m. A core (to depth 20 cm) was taken from the centre of the deposit and two samples (0 - 15 cm) were taken from opposite edges of the deposit.



Figure 4.21. View down a rill in field 1 (taken in October 2002), showing deposit 3 and the field boundary.

Surface samples were taken from all three deposits and a core (to a depth of 20cm) was taken from the centre of the largest deposit (D3). As with the transect cores, the core was divided into 5cm sections (Figure 4.22). The top two sections (0-10cm) are lighter than the two deeper sections (0-20cm), consistent with deposited sandy material in which finer particles (including organic matter) have been washed out beyond the deposit (cf. Beuslink *et al*, 2000).



Figure 4.22. Visual comparison of soil colour changes with depth for the deposit 3 at 0-5, 5-10, 10-15, 15-20 cm depths, dried at 30°C.

4.5. Laboratory Analysis

For each sample, the pH, water content, texture, organic matter content and total phosphorus concentration were measured. Total phosphorus was measured as this is consistent with model predictions. For the core samples, the dry bulk density was also determined.

4.5.1. pH

The pH was measured using the method described in Rowell (1994: p.160). The results are shown in Figures 4.23 and 4.24.

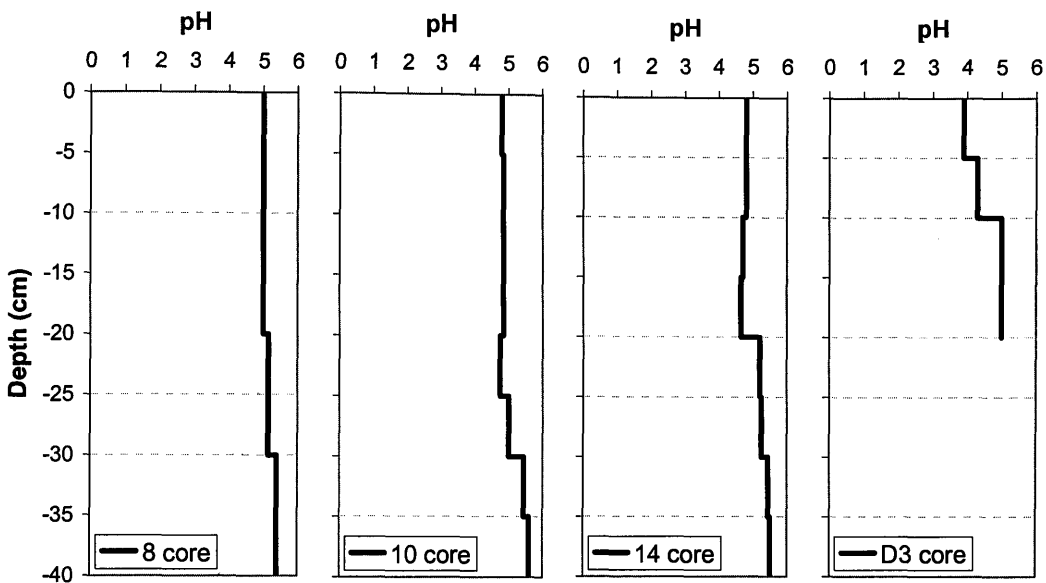


Figure 4.23. pH measured at depths down soil and deposit cores sampled from Field 1.

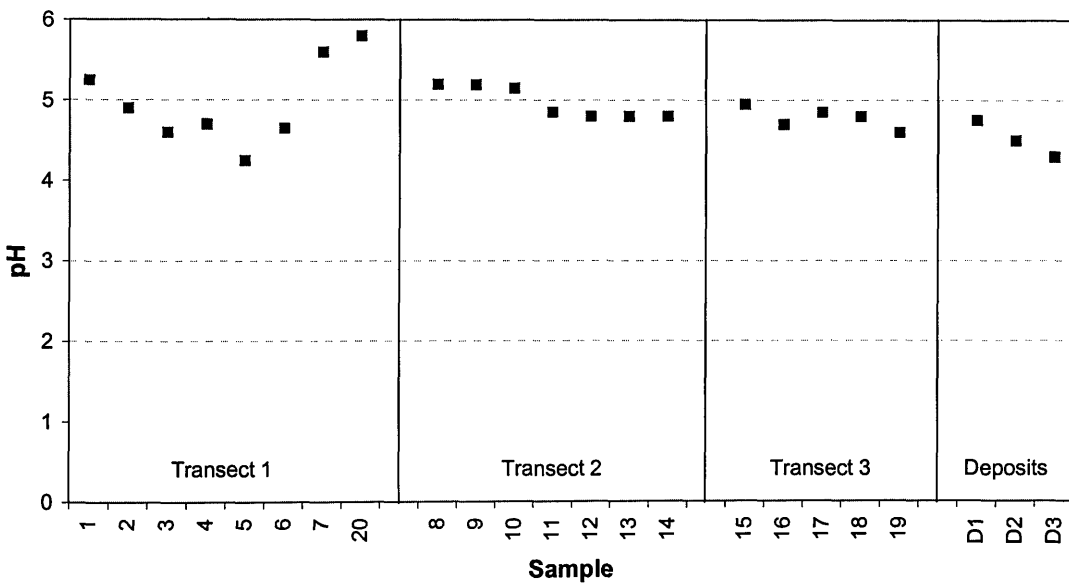


Figure 4.24. pH of surface soil (0-15cm) samples taken down three transects and deposits.

The pH remains fairly constant for the top 20 cm (corresponding to the plough layer) and then increases slightly (Figure 4.23). The pH in the samples taken from the deposit is lower than the transect deposits (i.e. about 4), in the top 10cm. In the 10-20cm depth range the pH is about 5 and is approximately equal to that in the plough layer of the soil. The depth of the sandy (deposit) layer was 2 cm. These changes in pH may be explained by different soil textures, with more clay rich soils having a greater pH probably due to less leaching of bases.

There appears to be no clear trend in pH with distance down the transects (Figure 4.24), although pH did decrease slightly in transects 2 and 3.

4.5.2. Water Content

The water content of each of the samples was measured and is shown in Table 4.2.

Table 4.2. Water content (expressed as a percentage of the oven dried (105°C) soil weight) of the soil samples.

Core samples							
		Core 8	Core 10	Core 14	Core D3		
Depth		%water	%water	%water	%water		
0-5 cm		18.88	20.96	24.09	18.21		
5-10 cm		18.09	21.52	20.35	9.51		
10-15 cm		18.79	22.42	23.53	37.97		
15-20 cm		18.54	22.40	23.71	25.20		
20-25 cm		19.75	22.51	23.46			
25-30 cm		19.15	24.61	21.63			
30-35 cm		16.56	18.95	16.39			
35-40 cm		14.67	10.46	22.20			
Surface samples							
Transect 1		Transect 2		Transect 3		Deposits	
Position	%water	Position	%water	Position	%water	Position	%water
1	20.39	8	18.86	15	21.67	D1	18.57
2	23.03	9	23.34	16	20.79	D2	17.47
3	24.64	10	22.36	17	15.80	D3	15.43
4	20.63	11	22.73	18	23.12		
5	18.01	12	20.76	19	23.94		
6	20.94	13	20.47				
7	28.58	14	23.23				
20	18.94						

With the surface samples, the deposits tend to have less water content compared to the source material taken from the transects. There is no clear trend in water content with depth for the transect cores, although with the deposit core, it is clear that the 0-10cm layer is drier than the 10-20cm layer.

4.5.3. Bulk Density

Observations of bulk density down the soil cores are shown in Figure 4.25. As expected, there was a general increase in bulk density with depth, although this increase was not consistent. There was also an increase in bulk density with depth in the core taken from the deposit. These results are consistent with general observations of changes in bulk density with depth in field soils (e.g. Soane, 1970).

The estimation of volume for each section of the core assumes that each section was exactly 5cm in length. Given the cores were divided in the field and the division point was observed to be uneven, this assumption is a source of error. In addition, a sub-sample (approximately one fifth of the total section) of the core section was used to determine the water content. This is another source of error as there will be some variability within the core section.

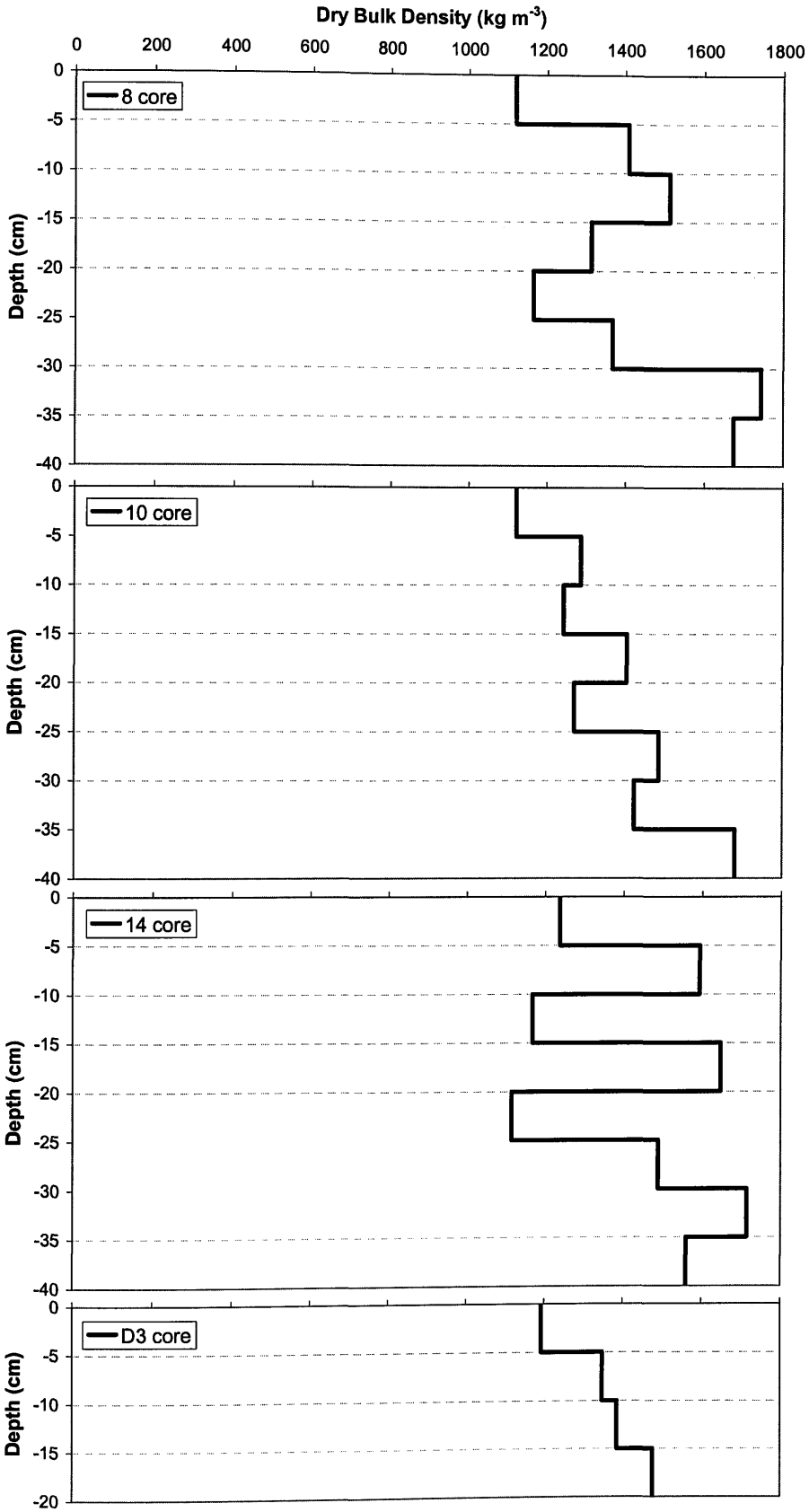


Figure 4.25. Change in bulk density with depth in soil cores.

4.5.4. Texture

Soil texture was ascertained using the “feel method” described in Foth *et al*, 1982, p.17. The constituent percentages of sand, silt and clay were then assigned using the “soil texture triangle” shown in Foth *et al*, 1982, p.15 and are shown in Table 4.3.

Table 4.3. Textural classes for the core and surface (0-15cm) soil samples taken in Field 1. The range (average) of the constituent sand, silt and clay for each textural class are: Loamy Sand: 70-90 (80), 0-30 (15), 0-15 (7.5); Sandy Loam: 43-85 (64), 0-50 (25), 0-20 (10); Sandy Clay Loam: 45-80 (62.5), 0-29 (14.5), 20-36 (28); Sandy Clay: 45-65 (55), 0-20 (10), 36-55 (45.5).

Core samples					
	Core 8	Core 10	Core 14	Core D3	
Depth	Textural Class	Textural Class	Textural Class	Textural Class	
0-5 cm	Sandy Loam	Sandy Loam	Sandy Loam	Loamy Sand	
5-10 cm	Sandy Loam	Sandy Loam	Sandy Loam	Sandy Loam	
10-15 cm	Sandy Loam	Sandy Loam	Sandy Clay Loam	Sandy Clay Loam	
15-20 cm	Sandy Loam	Sandy Clay Loam	Sandy Clay Loam	Sandy Clay Loam	
20-25 cm	Sandy Loam	Sandy Clay Loam	Sandy Clay Loam		
25-30 cm	Sandy Loam	Sandy Loam	Sandy Clay Loam		
30-35 cm	Sandy Loam	Sandy Clay Loam	Sandy Clay Loam		
35-40 cm	Sandy Loam	Sandy Loam	Sandy Loam		
Surface samples					
Transect 1		Transect 2		Transect 3	
Position	Textural Class	Position	Textural Class	Position	Textural Class
1	Sandy Loam	8	Sandy Loam	15	Sandy Loam
2	Sandy Loam	9	Sandy Clay Loam	16	Sandy Loam
3	Sandy Loam	10	Sandy Clay Loam	17	Sandy Loam
4	Sandy Clay Loam	11	Sandy Loam	18	Sandy Loam
5	Sandy Clay Loam	12	Sandy Clay Loam	19	Sandy Loam
6	Sandy Clay Loam	13	Sandy Loam	Deposits	
7	Sandy Clay Loam	14	Sandy Loam	Position	Textural Class
20	Sandy Loam			D1	Sandy Loam
				D2	Sandy Loam
				D3	Sandy Loam

The results show no clear trend with depth for the transect cores, although there was a slight increase in clay content in the lower layers of cores 10 and 14. With the deposit core, the top 10cm was much more sandy than soil from greater depth (10-20cm). With the surface samples, although the deposit samples have been classed the same as many of the source (transect) samples, they were observed to be more sandy.

4.5.5. Organic Matter Content

The soil organic matter (SOM) content was measured by loss on ignition (LOI). Oven dried soils (overnight at 105°C) were heated in a furnace at 500°C for 5 hours and the difference in weight taken as the organic matter content. Ignition at lower temperatures reduces the losses of inorganic constituents, such as free carbonates and structural water from clays, when the soil is ignited (Hesse, 1971). This method gives an approximate measure of organic content in sandy soils but may overestimate the organic matter content of heavily textured soils, due to the loss of appreciable quantities of structural water which can occur in clay and sesquioxides between 105 and 500°C (Rowell, 1994). Figure 4.26 shows the changes in LOI with depth in the cores sampled from field 1. Figure 4.27 shows the results from the surface soil samples.

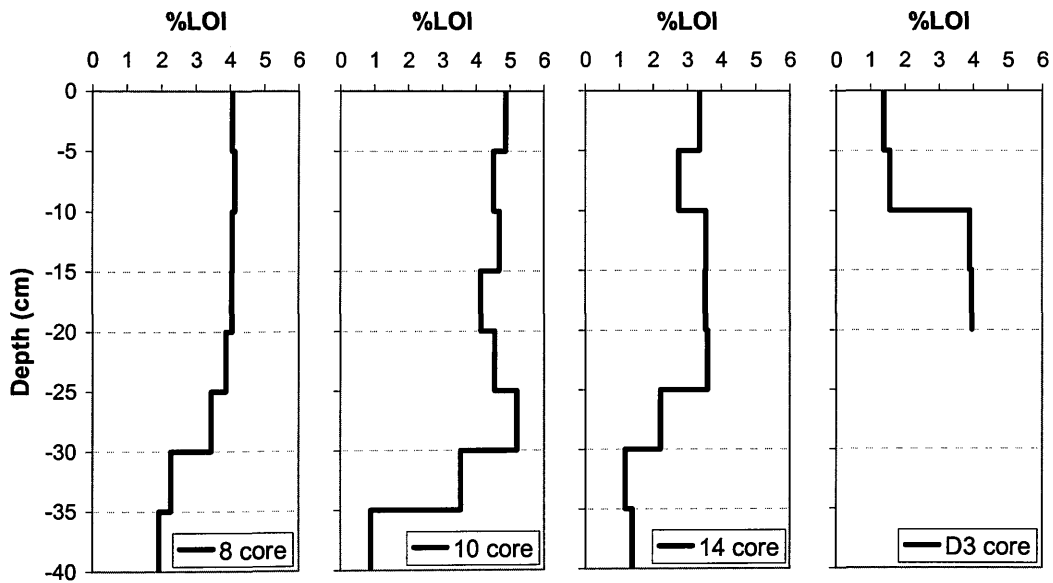


Figure 4.26 Organic matter content (measured as %LOI) of sub-samples with depth down three soil and one deposit cores in field 1.

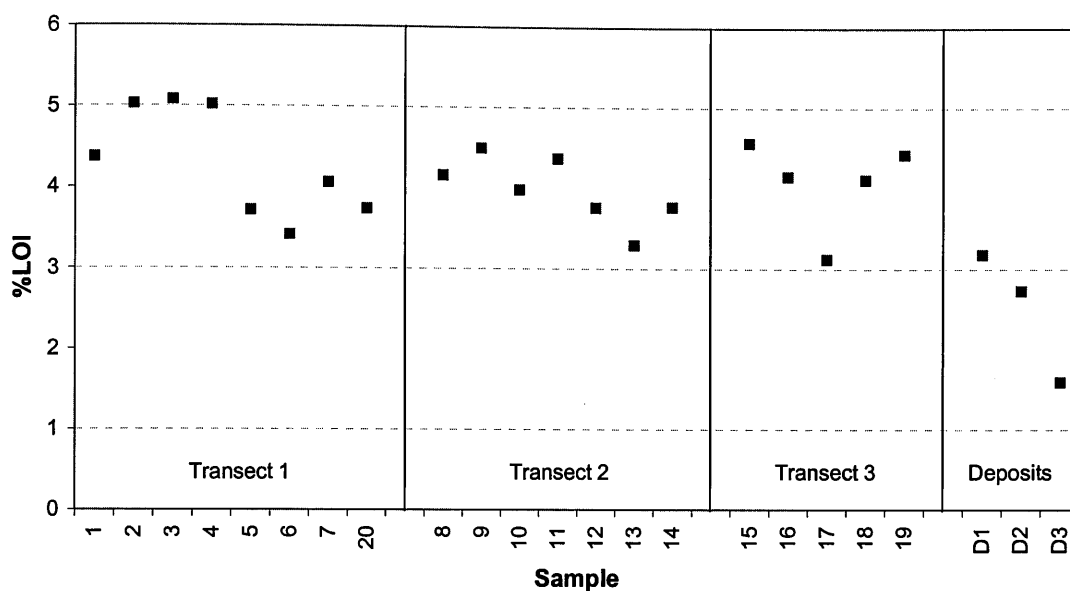


Figure 4.27. Organic matter content (measured as %LOI) of surface samples (0-15cm) taken down three transects and from deposits.

There is generally a constant concentration of soil organic matter in the plough layer (around 25cm) and a decrease at lower depths in the cores taken from the field soil. The core taken from the deposit shows an increase in LOI in the 15 – 20 cm layer consistent with a transition from deposit to the top of the soil. With the surface samples, there is an apparent slight decrease in LOI with distance downslope in the first two transects, although this is not reflected in the third transect. The LOI measured for the deposit samples are generally lower than the source (transect) samples.

4.5.6. Total Phosphorus

Total Phosphorus (TP) was determined using the Sulphuric Acid-Hydrogen Peroxide Procedure, as described in Allen (1989, pages 29, 59, 134-142). Once digested, the available phosphorus was measured colorimetrically using the molybdenum blue method as detailed in Appendix 2.

To determine the development time required before measuring the absorbance, an experiment, using aliquots containing 2 μ gP and 8 μ gP, was performed to study the loss of sample colour intensity with time. The results, graphed in Figure 4.28, show that aliquot with 2 μ gP reached maximum colour almost immediately and degraded steadily whereas the aliquot with 8 μ gP

took 43 minutes to reach maximum colour. The development time adopted for analysis of samples was set at 30 minutes, which was a compromise for low and high P. This also happens to be the recommended time in Forster (1995).

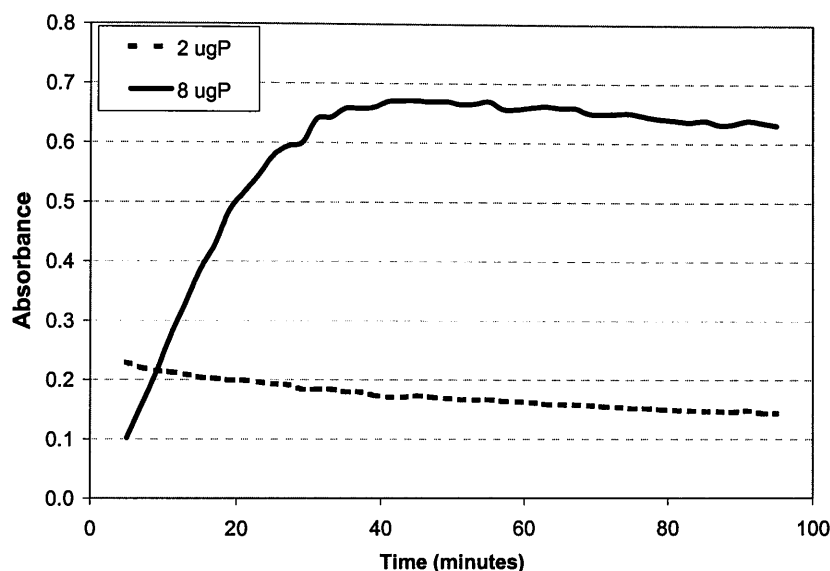


Figure 4.28. Graph showing the temporal variation in absorbance for molybdenum reactions for aliquots with 2 and 8 µgP.

The measured absorbances were then converted into the corresponding P concentration using the calibration curve formed by the standards. These concentrations ($\mu\text{g } 5\text{ml}^{-1}$) were then converted into mgP kgsoil^{-1} , using the knowledge that 0.2g soil had been digested and made up to 100ml. The reliability of these results was ascertained by digesting a reference soil of known chemical content along with the samples. Reference Material No. 142, Light Sandy Soil was used, which has a P concentration of $957 \text{ mgP kgsoil}^{-1}$. This matched well with the results of the current analysis, which gave a value of $987 \text{ mgP kgsoil}^{-1}$ for the reference material. In addition, the P content measured for the soils is within the typical range of 100 - 3000 mgP kgsoil^{-1} (Frossard *et al*, 2000).

The measured total P concentrations in the surface samples are shown in Figure 4.29. These are expressed as $\text{mgP kg oven dried soil}^{-1}$ using the measured water content of the air-dried soil used in the analysis.

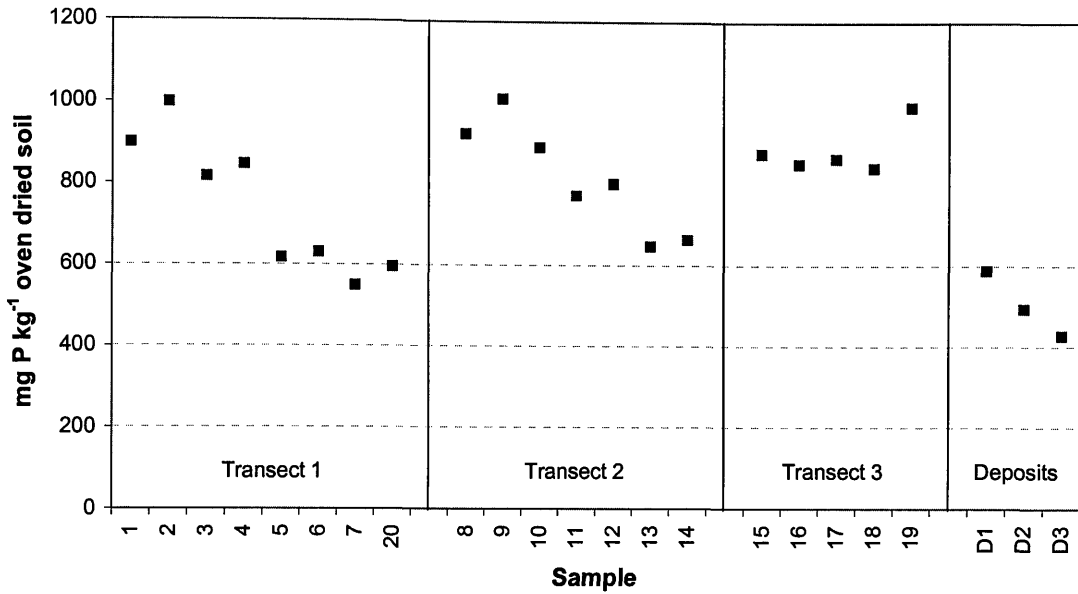


Figure 4.29. TP concentrations of surface soil (0-15 cm) down three transects and deposit samples (0-15 cm) in Field 1.

There appears to be a downslope decrease in TP concentrations in transects 1 and 2. However this is not evident in Transect 3. There are too few samples to be confident about the trend and in any case the high spatial variability makes it difficult to make firm conclusions. However, the downslope trend could suggest that P is increasingly removed from soils with increasing distance from the divide (i.e. increasing cumulative drainage area and consequently increased overland flow discharge).

Although there are only three deposit samples, all three samples had TP concentrations less than most of the soil samples. The texture of the deposits was sandy and the depletion of TP in coarser textured material is consistent with the observation that most P is associated with finer fractions (e.g. Morgan, 1997).

Figure 4.30 shows the variation of TP with depth in the cores taken. In all three source cores, TP concentrations were relatively constant down to a depth of 20cm (approximately the depth of the plough layer) and TP concentration consistently decreased at lower depths. These results are consistent with the findings of Haygarth *et al* (1998) and Eghball *et al* (1996) who observed a decrease in TP concentration with depth in grassland and arable land respectively. The decrease with depth in managed soils is generally thought to result from the application

of P in the form of fertiliser or manure to the soil surface and the limited translocation of P to greater depths because of various fixing processes. The core taken from the deposit (which was only taken to 20 cm) shows an increase in TP concentration with increasing depth. This reflects the observation made in the surface samples that these coarse deposits were depleted in TP with respect to the soil. The lower samples in the core taken from the deposit are likely to be a sample of soil material.

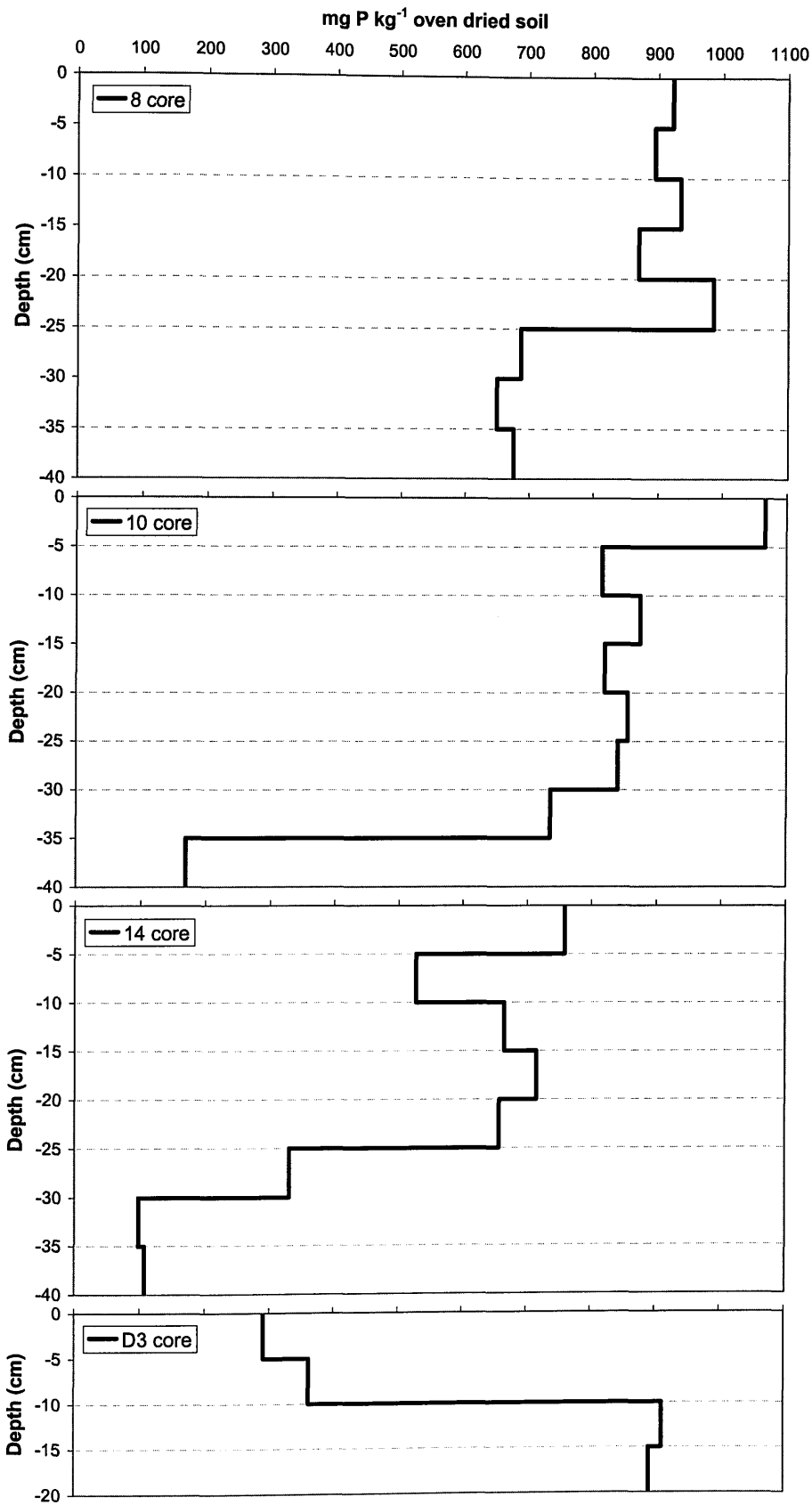


Figure 4.30. TP concentrations with change in depth down soil and sediment cores sampled from Field 1.

4.6. Statistical Analysis

4.6.1. Correlation

For all the samples (core and surface), statistical analyses were employed to assess the relationships between the measured variables (TP, %LOI, %water, pH). The Spearman rank correlation, which is more robust when sample numbers are low or when samples are not normally distributed, was employed on account of low sample numbers. The results are shown in Table 4.4. Significant positive correlations were observed between TP and organic matter content (%LOI), TP and water content (θ) and organic matter content (%LOI) and water content (θ).

Table 4.4. Spearman rank correlation coefficient (*p-value*) results for samples taken from Field 1.

	TP	%LOI	pH	θ
TP	1	0.788 (<0.01)	0.039 (0.786)	0.422 (<0.01)
%LOI	0.788 (<0.01)	1	-0.068 (0.634)	0.526 (<0.01)
pH	0.039 (0.786)	-0.068 (0.634)	1	-0.047 (0.741)
θ	0.422 (<0.01)	0.526 (<0.01)	-0.047 (0.741)	1

4.6.2. Difference between deposit and source samples

To assess whether there is a significant difference between the source and deposit samples, the non-parametric Mann-Whitney test was used on account of the low number of deposit samples ($n = 3$).

It is expected that TP_{sources} will be greater than TP_{deposits} due to the tendency for a preferential export of fines from topographically controlled deposits (Beuselink *et al*, 2000).

Values of TP, pH, SOM and θ were significantly greater than in the deposit samples according to a Mann Whitney test ($p < 0.05$).

4.7. Discussion

4.7.1. pH

Soil pH ranged between 4.25 and 5.80 for the surface source samples and between 4.30 and 4.75 for the surface deposit samples. In soil solutions, the pH determines the dominant form of phosphate present. The monovalent anion H_2PO_4^- dominates in acidic solutions. In addition, in acid soils, phosphate fixes with iron (Fe^{3+}), aluminium (Al^{3+}) and, to a lesser extent, manganese (Mn^{3+}) in precipitation reactions or exchange with hydroxyl anions on the surface of insoluble oxides of Fe, Al and Mn. For soils in the pH range 4.0 – 7.5, adsorption is the main mechanism of P retention (Heathwaite, 1997). There was no significant correlation between pH and TP. This may be explained by the fact that the range of pH is not big and within that range, the exchange processes are similar.

4.7.2. Organic Matter Content

The Spearman rank correlation coefficient between TP and organic matter content (%LOI) was 0.778 and was significant. This could be due to the incorporation of P in organic forms.

4.7.3. Total Phosphorus

There was a significant difference between the TP concentration in the source (median 1006.6 mgP/kg) and deposit samples (median 577.0 mgP/kg). This ties in with the expectation that P associated with fines can be preferentially exported from the topographically-controlled deposits (Beuselinck *et al*, 2000). Despite this P depletion, topographically-controlled deposits are still acting as P sinks although the consistency of low OM, TP, pH and clay suggests that the recent deposits are not likely to represent a significant barrier to P leaving the system. In addition, the total area of the three deposits identified in field 1 (approx. 0.013 ha) is small and thus retention is limited.

4.8. Field site 2

Field 2 was visited in February 2003. There was clear evidence of in-field erosion and deposition at the field boundary. Details of the topography and recent land use in Field 2 are

given in Figure 4.31. In 2002, the field was in potatoes with the following information given by the farmer:

May02: field fertilised with 180-120-320 (N-P-K) kg ha⁻¹.

Oct02: potatoes lifted

Dec02–Jan03: deposition observed from erosion

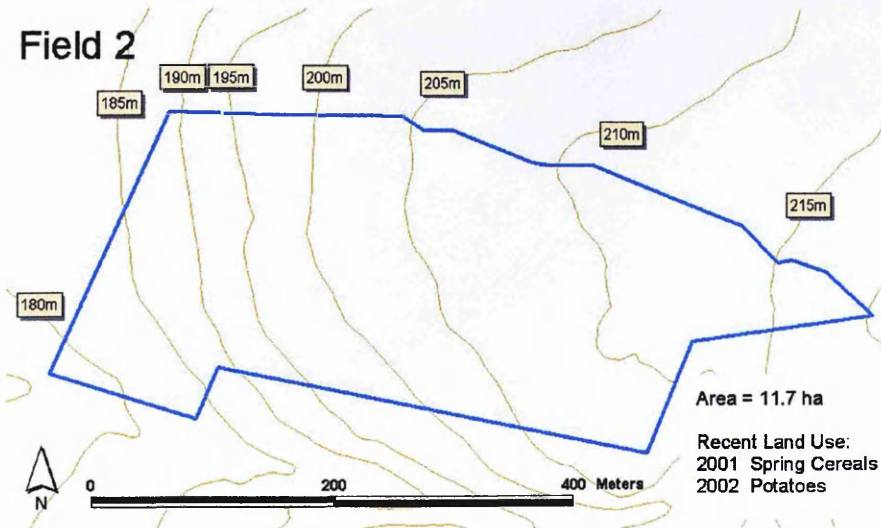


Figure 4.31. Topography and recent land use for field 2.

Figures 4.32 – 4.36 give an appreciation of the extent of the erosion and deposition in field 2.



Figure 4.32. View across the Greens Burn to field 2, showing source material being carried down a shallow (approximately 16 cm deep) gully (taken 14th February 2003).



Figure 4.33. Gully from upslope in Field 2 (taken 14th February 2003).



Figure 4.34. View from source area looking downslope to field boundary, along which sediment has accumulated (taken 14th February 2003).



Figure 4.35. Deposit along fence line, with buffer strip on other side (taken 14th February 2003).



Figure 4.36. The deposit in field 2 in the corner of the field (topographic low point) with a clear route for the eroded sediment from the boundary to the burn (taken 14th February 2003).

Unfortunately it was not possible to sample within this deposit as the farmer removed it and returned the sediment upslope (Figures 4.37 and 4.38). However, there was sufficient deposit remaining along the fence-line to allow some samples to be taken.



Figure 4.37. Corner of field 2, showing the removed deposit (28th February 2003).



Figure 4.38. Close up photograph, showing the depth of deposit removed (28th February 2003).

4.8.1. Sampling regime

Undisturbed deposited material was sampled on 28 February 2003. Surface samples (0-15cm) were taken at regular intervals (12m) along the fence line (Figure 4.39). The depth of the deposit was also measured at each sampling point.

The area of the field where gullies had formed was assigned as the main source area (Figure 4.32) for the deposit. Samples were also taken from this area and also from the main gully to the deposit (see Figure 4.39).

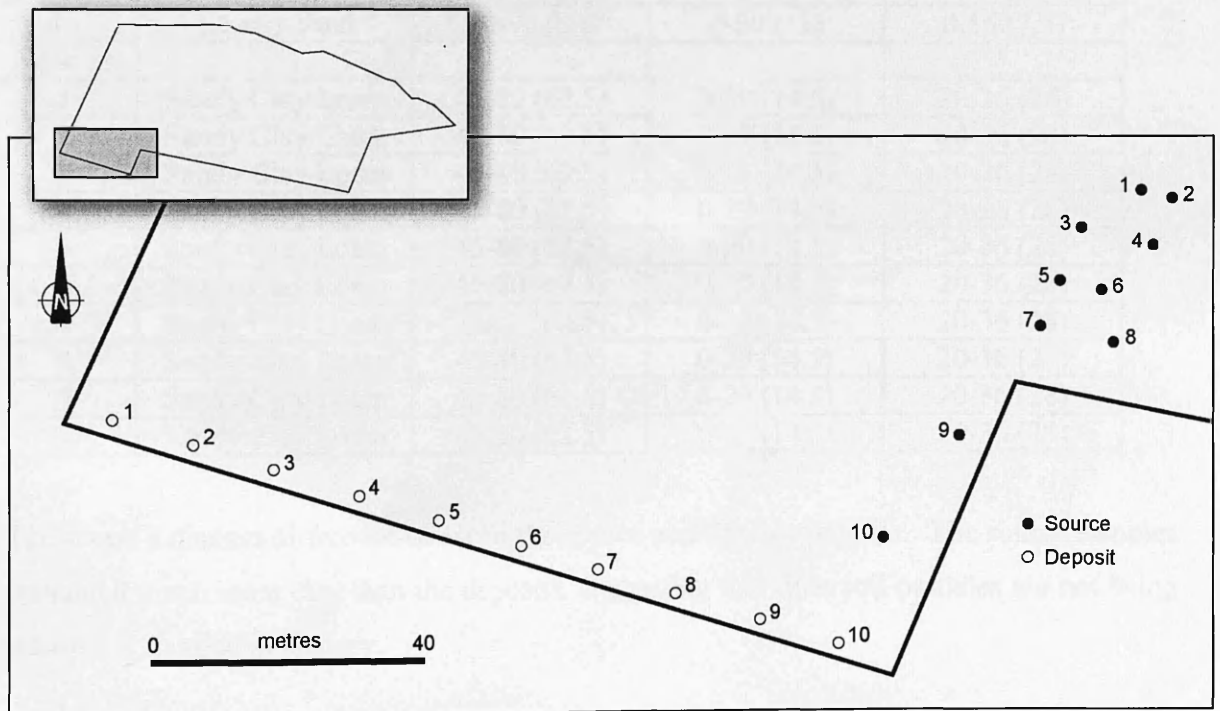


Figure 4.39. Sampling locations in field 2.

4.9. Analysis

4.9.1. Texture

The texture of the samples was estimated using the “feel method”. The results are shown in Table 4.5.

Table 4.5. Soil texture results for samples taken from Field 2.

Sample	Textural Class	% sand range (mean)	% silt range (mean)	% clay range (mean)
Deposits				
1	Loamy Sand	70-90 (80)	0-30 (15)	0-15 (7.5)
2	Loamy Sand	70-90 (80)	0-30 (15)	0-15 (7.5)
3	Loamy Sand	70-90 (80)	0-30 (15)	0-15 (7.5)
4	Loamy Sand	70-90 (80)	0-30 (15)	0-15 (7.5)
5	Loamy Sand	70-90 (80)	0-30 (15)	0-15 (7.5)
6	Loamy Sand	70-90 (80)	0-30 (15)	0-15 (7.5)
7	Loamy Sand	70-90 (80)	0-30 (15)	0-15 (7.5)
8	Loamy Sand	70-90 (80)	0-30 (15)	0-15 (7.5)
9	Sandy Loam	43-85 (61.5)	0-50 (25)	0-20 (10)
10	Loamy Sand	70-90 (80)	0-30 (15)	0-15 (7.5)
Sources				
1	Sandy Clay Loam	45-80 (62.5)	0-29 (14.5)	20-36 (28)
2	Sandy Clay Loam	45-80 (62.5)	0-29 (14.5)	20-36 (28)
3	Sandy Clay Loam	45-80 (62.5)	0-29 (14.5)	20-36 (28)
4	Sandy Clay Loam	45-80 (62.5)	0-29 (14.5)	20-36 (28)
5	Sandy Clay Loam	45-80 (62.5)	0-29 (14.5)	20-36 (28)
6	Sandy Clay Loam	45-80 (62.5)	0-29 (14.5)	20-36 (28)
7	Sandy Clay Loam	45-80 (62.5)	0-29 (14.5)	20-36 (28)
8	Sandy Clay Loam	45-80 (62.5)	0-29 (14.5)	20-36 (28)
9	Sandy Clay Loam	45-80 (62.5)	0-29 (14.5)	20-36 (28)
10	Sandy Clay Loam	45-80 (62.5)	0-29 (14.5)	20-36 (28)

There was a distinct difference between the source and deposit samples. The source samples contained much more clay than the deposits, suggesting that finer soil particles are not being retained at the field boundary.

4.9.2. pH

The pH of the soil was measured using the method described in Rowell (1994). The results are shown in Table 4.6.

Table 4.6. pH of samples taken from source area and deposited sediment.

Deposits	pH	Sources	pH
1	5.3	1	5.6
2	5.2	2	5.4
3	5.2	3	5.5
4	5.2	4	5.6
5	5.2	5	5.6
6	5.4	6	5.4
7	5.2	7	5.5
8	5.2	8	5.5
9	5.2	9	5.6
10	5.2	10	5.7
Mean	5.23	Mean	5.54
Median	5.20	Median	5.55

The median pH of the deposit and source samples was 5.20 and 5.55 respectively. There was a significant difference between the pH of the source and deposit samples, according to the Mann-Whitney two-sample test ($p < 0.05$). This may be explained by the reduced clay content of the deposits which will retain fewer base cations against leaching.

4.9.3. Total Phosphorus

Total Phosphorus was measured using the same method as that for the samples taken from Field 1. The results are shown in Table 4.7.

Table 4.7. TP concentrations ($\text{mgP kg oven-dried soil}^{-1}$) of the soil samples following digestion and Molybdenum Blue analysis.

Deposits	$\text{mgP kg oven-dried soil}^{-1}$	Sources	$\text{mgP kg oven-dried soil}^{-1}$
1	663.36	1	1042.98
2	481.00	2	1127.43
3	567.74	3	864.34
4	494.70	4	911.12
5	554.83	5	910.17
6	429.05	6	831.34
7	408.37	7	993.72
8	443.01	8	1010.84
9	628.68	9	928.63
10	452.16	10	869.37
Mean	512.29	Mean	948.99
Median	487.85	Median	919.87

There was a clear difference in TP between the source and deposit samples (significant at $P < 0.01$ according to the one-tailed Mann-Whitney test). The source samples contained nearly twice as much phosphorus as the deposited sediment, which were depleted in clay. This indicates that a large quantity of eroded sediment and associated-P is not being retained at the boundary and is being transported beyond the boundary with finer particles.

4.9.4. Deposit Depths and Estimation of Deposit Volume

At each sampling point along the deposit, the depth was measured and the results are shown in Table 4.8.

Table 4.8. Depth of deposit along fence-line.

Deposit Sample	Depth (cm)	Deposit Sample	Depth (cm)
1	14.0	6	6.0
2	20.0	7	4.5
3	13.0	8	7.0
4	2.5	9	7.0
5	4.5	10	5.0

As the deposit has been removed, it was not possible to measure the surface area of the deposit and construct a depth profile to allow the volume of deposit to be estimated. From the photographic evidence, with the knowledge that the average distance between the fence-posts is 2.5m, it has been estimated that the deposit was approximately 2m wide along the majority of the fence-line. The exception to this being in the corner of the field (at sample points 1 and 2), where the deposit was wider (approximately 5m) due to upslope input along the fence-line down to that point. Assuming that across the 2m wide strip, the deposit depth increased from zero to the depth measured at the sampling points, the volume was approximated.

Taking each section (between sampling points A and B) of the deposit in turn (as depicted Figure 4.40),

$$\text{Volume} = 0.5 * w * (0.5 * (d_A + d_B) * x)$$

Where d_A = depth at sample point A

d_B = depth at sample point B

x = distance between sample points = 12m

w = width of deposit = 2m (or 5m between samples 1 and 2)

Rough estimate of deposit volume along fence line = 12m^3 .

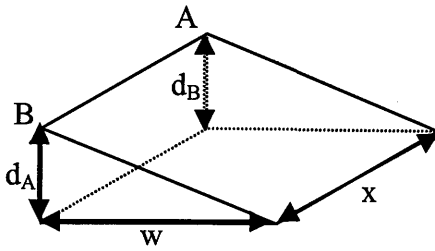


Figure 4.40. Diagram illustrating a section of the deposit used to estimate the volume.

Assuming ρ_B sediment = 1200 kg m^{-3} (consistent with surface ρ_B in Field 1, see Figure 4.25)

Mass = $\rho_B * V = 1200 * 12 = 14400 \text{ kg}$.

Area of field = 11.7 ha

So, deposited sediment is equivalent to $14400 / 11.7 = 1230 \text{ kg ha}^{-1}$

TP concentration is approximately 500 mgP kg^{-1} (from results in Table 4.7), which gives, $1230 * 0.0005 = 0.615 \text{ kgP ha}^{-1}$ deposited.

The range of typical export coefficient for row crops is $0.02 - 5.77 \text{ kgP ha}^{-1} \text{ a}^{-1}$ (mean $1.32 \text{ kgP ha}^{-1} \text{ a}^{-1}$), so the P deposited in field 2 represents approximately half of the mean potential P loss (mobilisation). Although this is just from one field, it does show the potential of P retention.

4.10. Correlation

The Spearman rank correlation coefficient between TP and pH for the samples taken in Field 2 was 0.750 ($p < 0.01$). This could be due to the fact that both pH and TP are related to clay content, although no such correlation was observed for field 1.

4.11. Discussion

This study has attempted to quantify the potential for P retention behind field boundaries. Although it was rather limited in extent, the results suggest that a significant fraction of P could be retained in some circumstances. Obviously both the amount of material eroded and retained will depend on site and time-specific conditions (soil moisture content, soil physical properties, antecedent and current meteorological conditions, topography and the nature of the field boundary). Soil under certain crops, such as potatoes, is known to be more susceptible to erosion than under other crops. It is, therefore, very difficult to draw out general conclusions about sediment and P retention. However, there is very little information in the literature about the amount of P which can be retained behind field boundaries. This study provides a useful insight into this process. Further work might involve a study of P availability in deposits vs. source soil e.g. water extractable P vs. Olsen P vs. TP.

4.11.1. Implications for modelling

The model currently estimates land-use specific erosion, with delivery adjusted for the position of the field relative to the watercourse. Few, if any models (physically-based or conceptual) make explicit estimates of nutrient retention at field boundaries. Some models do account for variations in the efficiency of sediment transfer from point of entrainment to the stream (either topographically controlled or via the concept of the delivery ratio). However, others (such as SWAT) assume that 100% of the eroded material reaches the stream network. This is clearly unrealistic. Despite the fact that field boundaries are unlikely to retain all the sediment mobilised and the fact that deposits are likely to be depleted in fine size fractions, and thus TP, P retention may be significant under some circumstances. With more permeable boundaries (e.g. fences or hedges), coarser material will settle out but the fines, with their associated P, will pass through the boundary.

In field site 2, the boundary was formed mainly by a change in vegetation as the wire fence did not impede flow at ground level, apart from where the fence posts were located. The deposited material was more sandy than the source material and also had a lower phosphorus concentration (mean of 512.3 mgP/kg soil compared with 949.0 mgP/kg soil), which indicates that a significant amount of P is being transported beyond this boundary. Using the rough

estimate of deposit volume calculated previously, 7 kg of P was retained at this boundary. On the local scale this is significant. However, on the catchment scale, there were only isolated boundary deposits and it is questionable whether they should be included in a catchment scale model, especially given the extra effort required in establishing the permeability of the boundary.

Erosion and deposition tend to be significant for specific combinations of row crops and heavy rainfall. Figure 4.41 shows the daily rainfall measured in the catchment for the year prior to sampling field site 2. The farmer stated that the field was fertilised in May 2002 and the potatoes were lifted in October 2002. In addition, he observed that the majority of the erosion/ deposition occurred after lifting. This is in agreement with the rainfall data, which shows increased rainfall in October, around/ just after the time of the disturbance caused by lifting the potatoes. It also concurs with evidence of erosion and deposition at field 2. This potential for high sediment and P transfer should be included in the frequency distributions sampled for this particular crop.

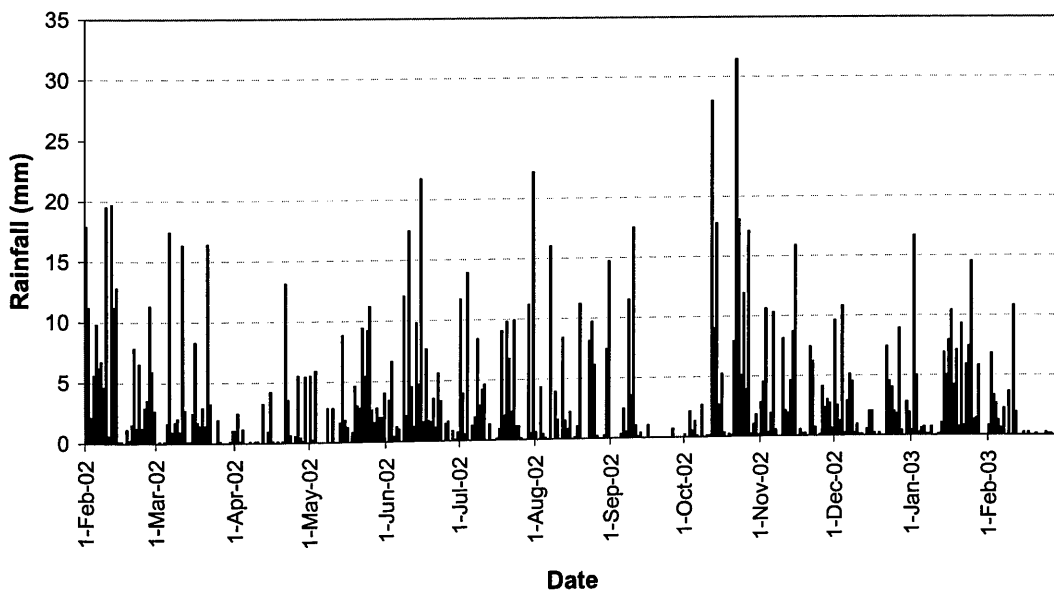


Figure 4.41. Daily rainfall measured in the Greens Burn catchment in the year prior to the sampling date of Field 2 (28th February 2003), calculated as the average of the daily rainfall measured at the Balado and Portmoak raingauge sites.

4.12. Conclusions

A limited field study was conducted in two fields in the Greens Burn catchment to ascertain the nature and extent of P retention behind field boundaries. Field boundaries are rarely, if ever, considered in models of diffuse-source P transfer. In both fields there was evidence of erosion and limited deposition although deposition was not restricted to field boundaries. The deposited material was always depleted (by approximately 50%) in P with respect to the source material (soil) and generally coarser in texture. This confirms the fact that a significant fraction of sediment-associated P is attached to finer size classes (clay and silt) which are more mobile and which probably penetrate all but the most impermeable of physical barriers.

However, the results of this study suggest that some P may be retained, at least temporarily, behind some field boundaries. The exact amount and form of this P retention will clearly depend on the nature of the erosive process, the condition of the source material (soil), the topography and the condition of the boundary. It will, no doubt, be variable temporally, even for the same boundary, and from field to field. The data collected here are insufficient to derive general conclusions but they do highlight the potential for a hitherto neglected process operating in many catchments.

Since field boundaries are a land management tool they do offer some potential for farmers to control P flux in areas where sediment associated P transfer is significant. More extensive studies are required to clarify this potential.

Chapter 5. Modelling using readily available data

In Chapter 3, it was shown that the SEPTIC model performs reasonably for the Greens Burn catchment for the years 1996-1999. The inputs required for this model included land use data which was obtained via time-intensive farm surveys. Given that one remit of this project was to design a model which could be used by land managers, it was decided to investigate the feasibility of applying the model to the Greens Burn catchment using more readily available data.

5.1. Alternative land use data

There are two main alternative sources of land use data: the agricultural census and land cover surveys.

5.1.1. Agricultural Census Data

Agricultural census data for the parishes covering the Greens Burn catchment is obtainable from the Scottish Executive Environment and Rural Affairs Department (SEERAD). Information is not available on a more detailed (e.g. farm-by-farm) basis due to data protection. Figure 5.1 shows the Greens Burn catchment in relation to the parishes in the area.

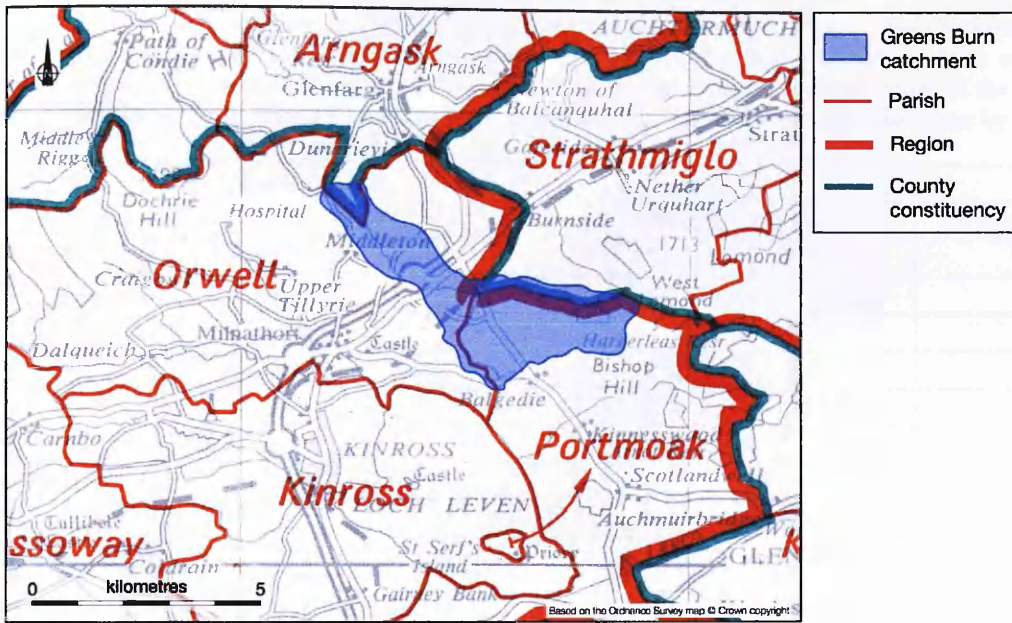


Figure 5.1. The Greens Burn catchment in relation to the Parishes in the area, reproduced from the Administrative Areas Diagram Scotland.

The majority of the Greens Burn catchment lies partly in Orwell parish and partly in Portmoak parish. The information that is obtainable for these parishes (for 2000 as an example) is shown in Table 5.1.

Table 5.1. Agricultural Census data for Orwell and Portmoak Parishes in 2000. (Note: To prevent disclosure of information about individual holdings, entries relating to less than five holdings, or those where two or less account for 85% or more of the information, have been replaced with an asterisk. Some of the data in the tables may not, by itself, be disclosive, but the information has been withheld to prevent disclosure by deduction.)

Information	Parish		
	Orwell	Portmoak	Orwell + Portmoak
Area of All Land (ha)	4667.20	3059.46	7726.66
Area of Set Aside (ha)	268.00	147.83	415.83
Area of Bare Fallow (ha)	*	*	14.92
Area of Total Cereals (ha)	1292.96	687.32	1980.28
Area of Other Combine Crops (ha)	133.53	83.97	217.50
Area of Potatoes (ha)	129.83	90.46	220.29
Area of Vegetables (ha)	*	*	65.84
Area of Fruit (ha)	*	*	*
Area of Glasshouses/protected crops (ha)	*	0.00	*
Area of bulbs/plants grown outside (ha)	*	0.00	*
Total Cattle (no)	2134	1132	3266
Total Sheep (no)	15571	4549	20120
Total Goats (no)	*	*	*
Total Horses (no)	57	28	85
Total Pigs (no)	0	*	*
Total Poultry (no)	*	*	94
Occupiers (no)	42	25	67
Occupiers with spouses working on farm (no)	16	9	25

The main problem with using the parish-level agricultural data is that the parishes cover a far wider area than the catchment and the spatial distribution of each land use is not available. Therefore, it is impossible to decide accurately what proportion of a certain land use falls within the catchment and its spatial distribution therein. Simple area-weightings could be used to apportion the area of the catchment covered by each land use but this would be inaccurate and would still not give any information of the distribution of land use. A more complex solution would be to stochastically assign land use to each field on the basis of probability and generate model outputs for a number of iterations. However, using the agricultural census data (with its limitations imposed by data protection and lack of spatial distribution) would probably not provide improvement on using an alternative source of land use data, e.g. the land cover surveys (LCM2000).

5.1.2. Land Cover Map 2000

The Land Cover Map 2000 (LCM2000), with 25m resolution, is a thematic classification of spectral data recorded by satellite images with the use of external databases to help refine the

spectral classification. This information was used to create 26 subclasses for a variety of land cover types (shown in Table 5.2). The output from LCM2000 for the Greens Burn catchment is shown in Figure 5.10.

Table 5.2. LCM subclasses (number and description).

1.1. Broad-leafwood	8.1. Acid	17.1. Built up areas, gardens
2.1. Coniferous woodland	9.1. Bracken	17.2. Continuous urban
4.1. Arable & horticulture	10.1. Dwarf shrub heath	18.1. Supra-littoral rock
4.2. Arable & horticulture	10.2. Open dwarf shrub heath	19.1. Supra-littoral sediment
4.3. Arable & horticulture	11.1. Fen, marsh, swamp	20.1. Littoral rock
5.1. Improved grassland	12.1. Bog	21.1. Littoral sediment
5.2. Set aside	13.1. Standing water	21.2. Saltmarsh
6.1. Neutral	15.1. Montane habitats	22.1. Sea & estuary
7.1. Calcareous	16.1. Inland rock	

On the whole, the distinction between the subclasses is deemed to be generally reliable. With regard to rough grasslands, LCM2000 initially allocated these as “6.1. Neutral” with contextual analysis with soil-acidity maps later changing the classification to “7.1. Calcareous” or “8.1. Acid”. It should be noted that built-up areas tend to be overestimated.

Field surveys (of 569 one km squares in Britain) were carried out in 1998-99 to assess the quality of LCM2000 (with an estimated 88% repeatability). A measure of non-correspondences associated with (1) the field survey’s greater original spatial resolution, (2) time differences in surveys, (3) class-definition differences and (4) errors in one or both surveys revealed an estimated per-pixel correspondence (between the field survey and LCM2000 land classes) of 54%. A more detailed discussion of the accuracy of LCM2000 is available in Fuller *et al* (2002).

The reliability of LCM2000 is questionable but there seems to be a lack of a better readily available alternative. In addition, the LCM is not available for every year so investigation is required to see if it is appropriate to use LCM2000 to model annual P export. The effect of using LCM2000 (with less detailed land classes) and whether LCM2000 can be used to predict annual P export in other years (apart from 2000) is explored in the next section.

5.2. Is it possible to use LCM2000?

In order to decide whether LCM2000 data could be used for P export modelling, SEPTIC was run, using the land use data (obtained via farm surveys) previously used but under constrained conditions.

5.2.1. The effect of using less detailed land classes

In the first instance, the model was run for each year (1996-1999) with no differentiation between cereal and row crops, instead lumping them together as “arable”. The export coefficient ranges used previously (in Chapters 2 and 3) for cereals (0.06 – 5.67) and row crops (0.02 – 5.77) were combined to give the range for the amalgamated “arable” class of 0.02 – 5.77.

The results for predicted annual total phosphorus exported from the Greens Burn catchment in 1996-1999 are shown in Figure 5.2, along with the results from the model when cereals and row crops are treated separately for comparison. As expected, given that the export coefficient ranges for cereals and row crops were similar, lumping cereals and row crops together does not have much impact on the predicted total phosphorus exported from the catchment in each year.

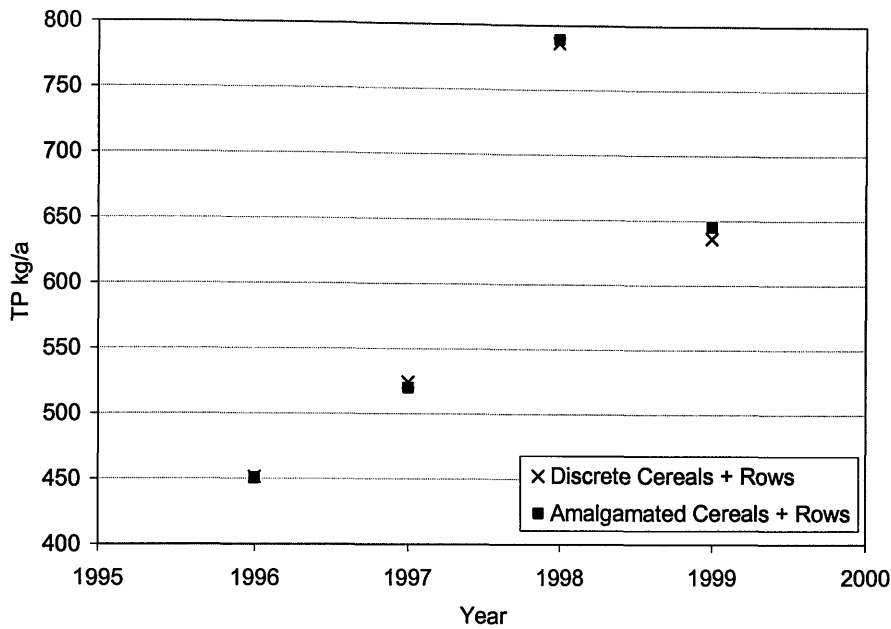


Figure 5.2. The predicted annual phosphorus export from the Greens Burn catchment in 1996-99 using discrete cereals and row crop export coefficients and an amalgamated “arable” coefficient.

Within the catchment, there were subtle spatial differences in the export of P predicted from individual cells with and without arable land use amalgamation, as shown in Figure 5.3. The maximum difference is $0.016 \text{ kgP}/625\text{m}^2\text{cell}$ (equating to $0.256 \text{ kgP}/\text{ha}$), which occurs in 1998. This should be viewed in the context of the range of possible export ($0.02 - 5.77 \text{ kgP}/\text{ha}$) from arable land. Although there may be differences of local importance, these differences are generally minimal compared to the maximum possible export from arable land. It should also be borne in mind that some differences will be a result of the stochastic nature of randomly selecting export coefficients for a number of iterations from a given range, because the start value (seed) was itself random. If a comparison was made between 2 runs (each of 500 iterations) of the model, keeping all inputs (e.g. range of export coefficients and land classes) the same, there would be differences between the model output from each of the 2 runs.

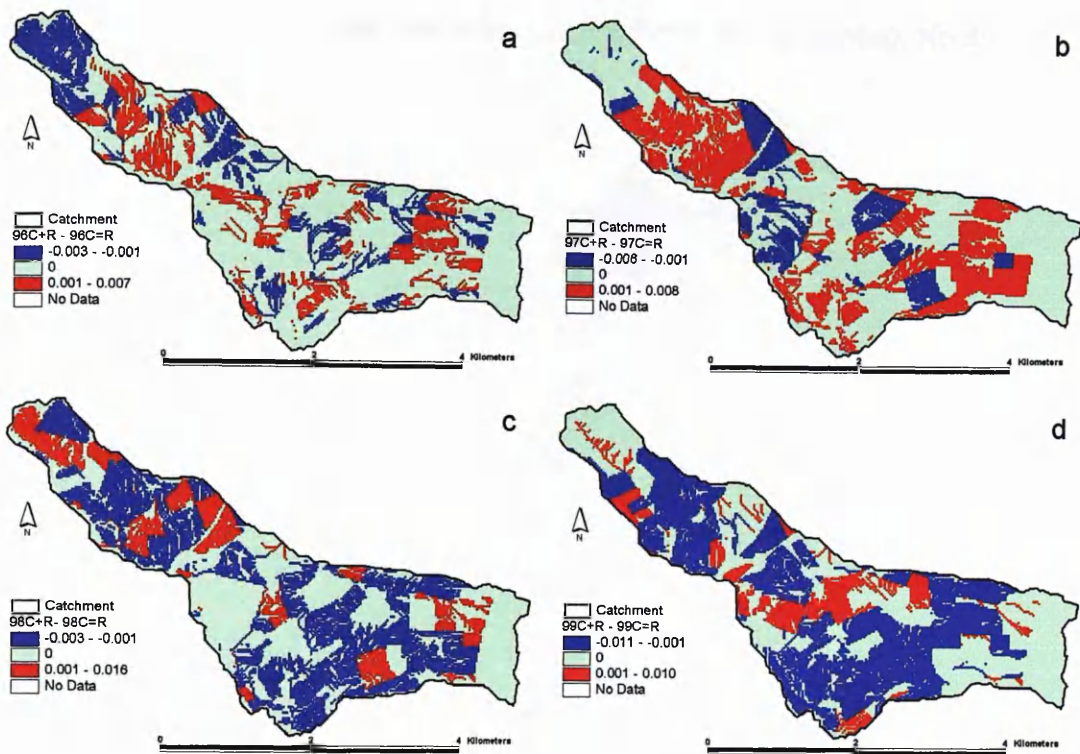


Figure 5.3. The difference in predicted P export from each cell (kg/625m² cell), when cereals and row crops are treated discretely (C+R) and when cereals and row crops are amalgamated (C=R) for a) 1996; b) 1997; c) 1998 and d) 1999. Positive values show areas where amalgamating arable crops underestimates export relative to the reference predictions. Negative values indicate overestimates.

5.2.2. Model sensitivity to land use change

The effect of using a constant land use over a number of years was investigated in order to ascertain model sensitivity to changes in land use. The model was run for 1997-1999, keeping land use constant at the 1996 pattern. The only input variation between years was *HER*. The results, along with those generated when land use changes from year to year, are shown in Figure 5.4. The model does not seem to be very sensitive to land use change. Predictions are similar in each year regardless of whether land use changes or not, implying that *HER* is the main driver behind inter-annual variability in predicted P export. The spatial differences between using the actual land use and the 1996 pattern for 1997-1999 are shown in Figure 5.5. The differences between simulations with and without land use change are small. Differences are rarely greater than 0.05 kgP/cell (0.8 kgP/ha).

Figure 5.5d shows that the variation resulting from the random selection of export coefficients (from given ranges) in a model run (500 iterations) is also very small, with a maximum

difference between two model runs being 0.007 kgP/cell (0.112 kgP/ha). No differences were observed for the majority of the catchment.

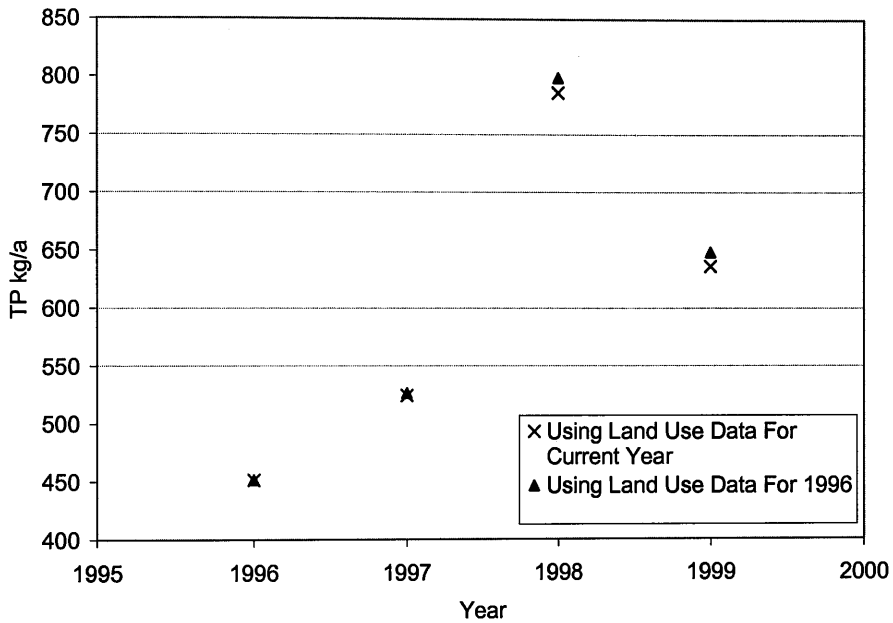


Figure 5.4. Predicted P export (kg/a) from the Greens Burn catchment for 1996-1999 when land use is kept constant (1996) and when land use is allowed to change between years.

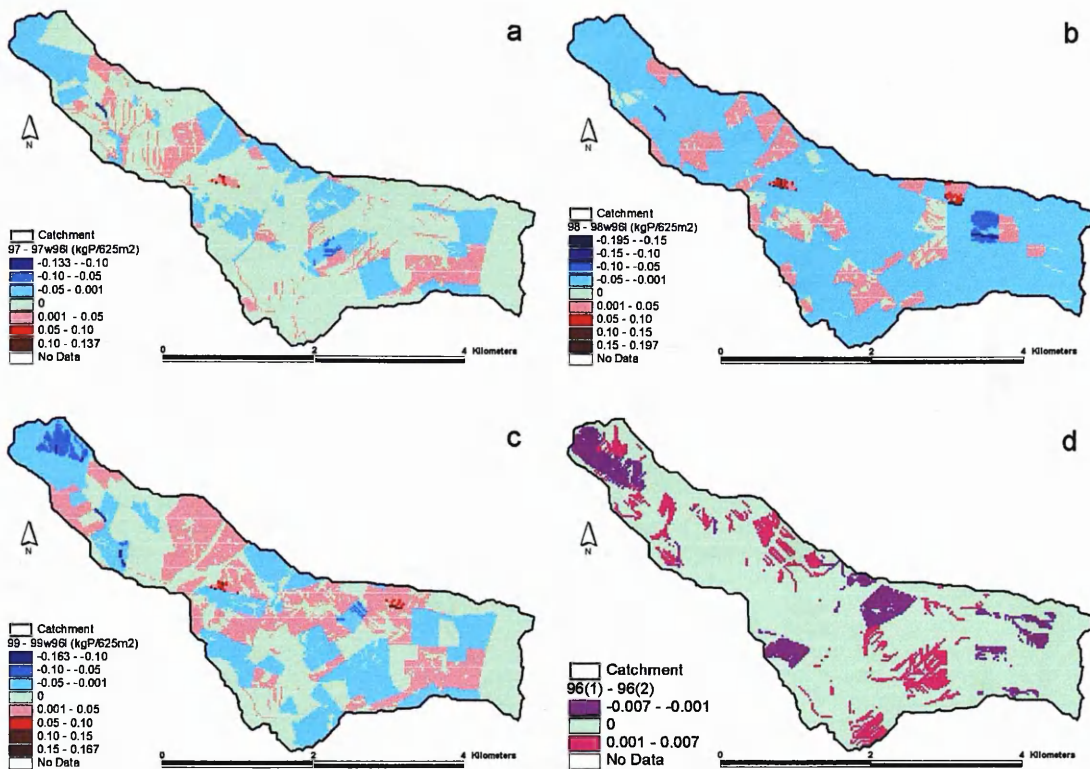


Figure 5.5. Spatial distributions of the difference between the model output (kgP/cell) obtained using land use data for the current year or land use for 1996 (given as P export using land use in current year – P export using land use in 1996) for a) 1997; b) 1998; c) 1999. d) shows the difference (resulting from stochasticity) between two “identical” runs of the model for 1996.

Given the relative insensitivity of the model predictions to inter-annual land use change and to the amalgamation of arable classes, it was decided that LCM2000 would be an acceptable land use input into the model for predicting annual P export, and spatial variations thereof, from the Greens Burn catchment.

5.3. Readily available data for the Greens Burn catchment

The SEPTIC model requires input data on land use, slope, cumulative area, HOST and *HER* for the catchment under consideration.

5.3.1. Catchment boundary

The boundary for the catchment draining to the gauging station (No. 17081, Grid Reference 37 (NO) 157 040) at Damley’s Cottage on the Greens Burn was obtained from CEH, Wallingford, UK. This boundary was derived using the IHDTM (Integrated Hydrological

Digital Terrain Model) drainage direction grid and is supplied in Arc/Info ungenerate format. The file was converted for use in ArcView and is shown in Figure 5.6, along with the catchment boundary derived from 5m contour data for comparison.

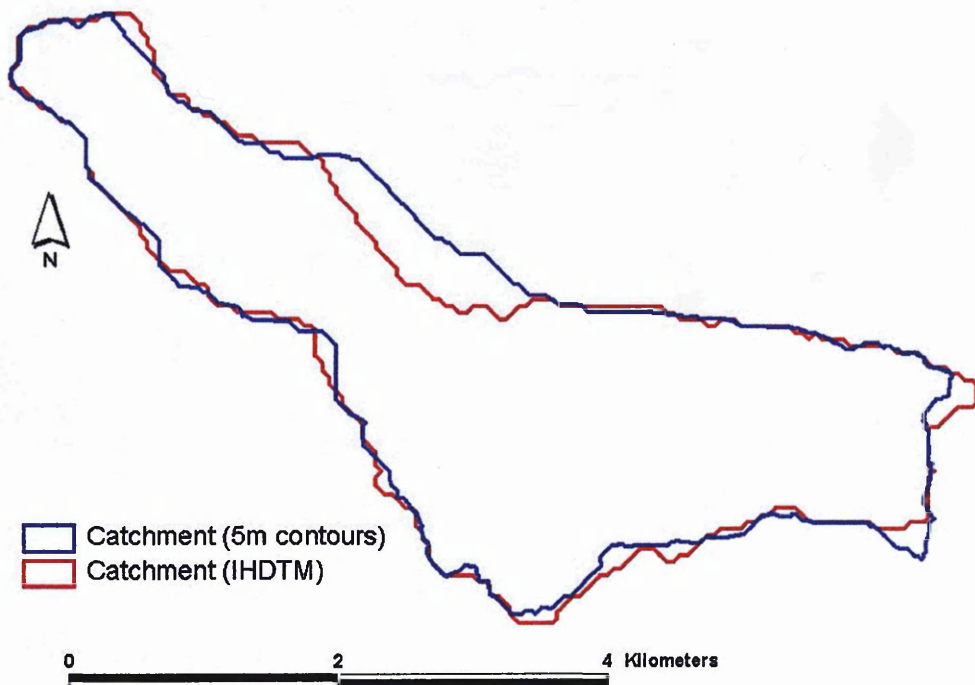


Figure 5.6. Greens Burn catchment boundary supplied by CEH (derived from IHDTM drainage direction grid) and the boundary derived from 5m contour data (as used in Chapters 2 and 3).

From Figure 5.6, it can be seen that for the most part, the catchment boundaries are in reasonable agreement. The main exception is in the centre north of the catchment where the CEH boundary decreases the catchment size. Ground truthing has already verified that the boundary derived from the 5m contour data is accurate. However, an environmental manager is more likely to use the ready-derived catchment boundary and perhaps not even be aware of its inaccuracies.

5.3.2. Slope and Cumulative Area (Digital Elevation Model)

IHDTM elevations (with a grid cell size of 50m) are also available from CEH, Wallingford, UK in Arc/Info GRIDASCII format. This was input into ArcView (Figure 5.7). The raw data were supplied with an inherent factor 10 so that the decimal elevations could be stored in integer format. The DTM was thus corrected using the Map Calculator function in Arc View.

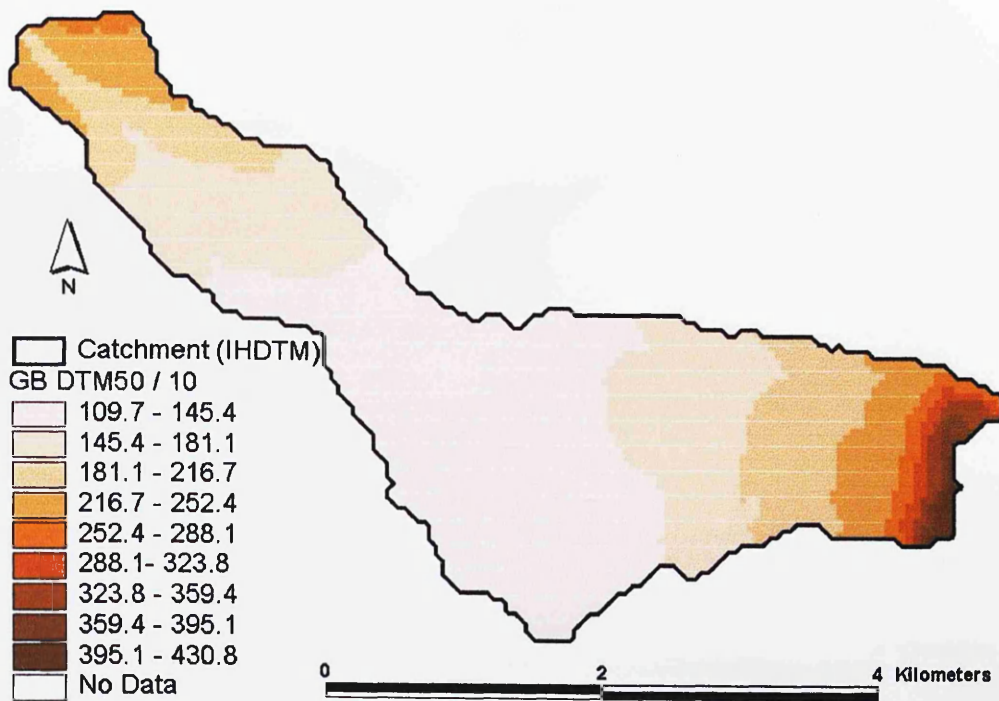


Figure 5.7. DTM for the Greens Burn data (using CEH boundary).

The CEH DTM was used to derive slope (Figure 5.8) and specific area drained (Figure 5.9) in Arc View, using the methods outlined in Chapter 3.

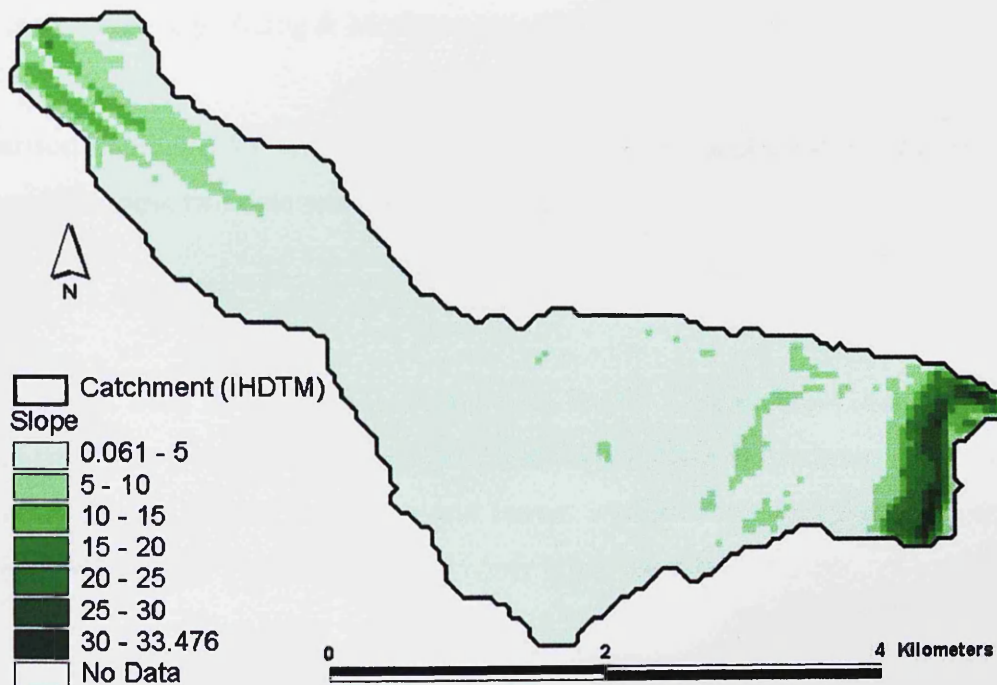


Figure 5.8. Slope in the Greens Burn catchment, derived from CEH DTM.

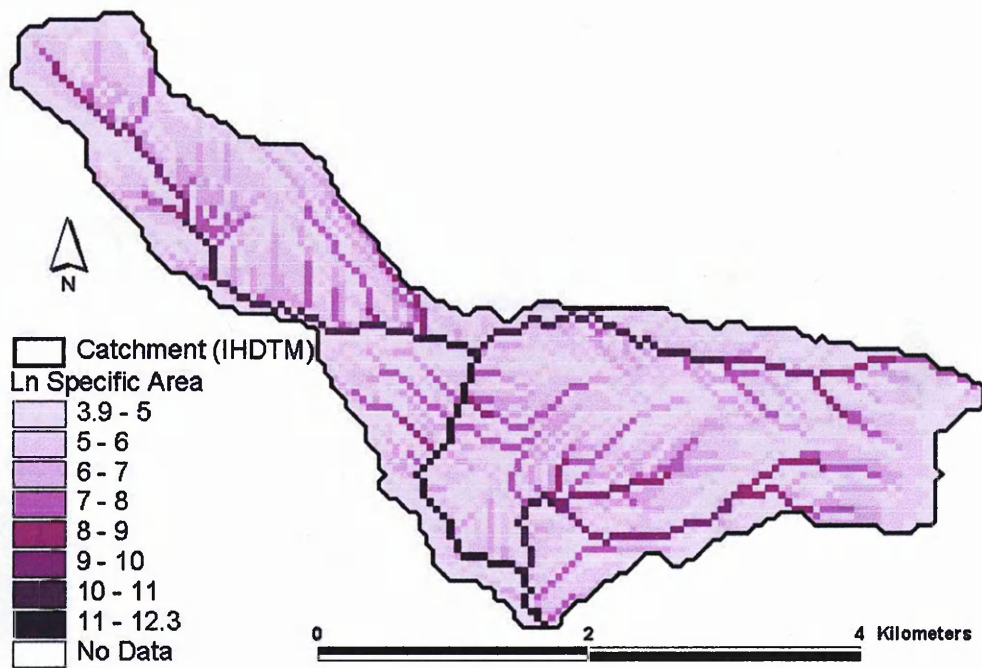


Figure 5.9. Natural logarithm of the specific area (calculated using flow accumulation derived using DTM).

A comparison of Figure 5.8 with the slope distribution used in Chapter 3 (Figure 3.1) shows an overall agreement. The maximum slope calculated using the 25m DTM (as used in Chapter 3) is 36° (in the east of the catchment) whereas the maximum slope derived from the CEH 50m DTM (located in the same area) is 33° . The slight decrease in slope with increasing cell size is expected (e.g. Zhang & Montgomery, 1994).

A comparison of Figure 5.9 with the distribution of specific area used in Chapter 3 (Figure 3.4), shows that these two data sets are very similar.

5.3.3. Land Use

The Land Cover Map 2000 Level 2 Vector data for the Greens Burn catchment area was purchased from The Centre for Ecology and Hydrology (CEH), Huntingdon, UK. The vector data was transformed (in ArcView) to a grid format with the same extent and cell size as the DTM provided by CEH. The resulting land cover is shown in Figure 5.10.

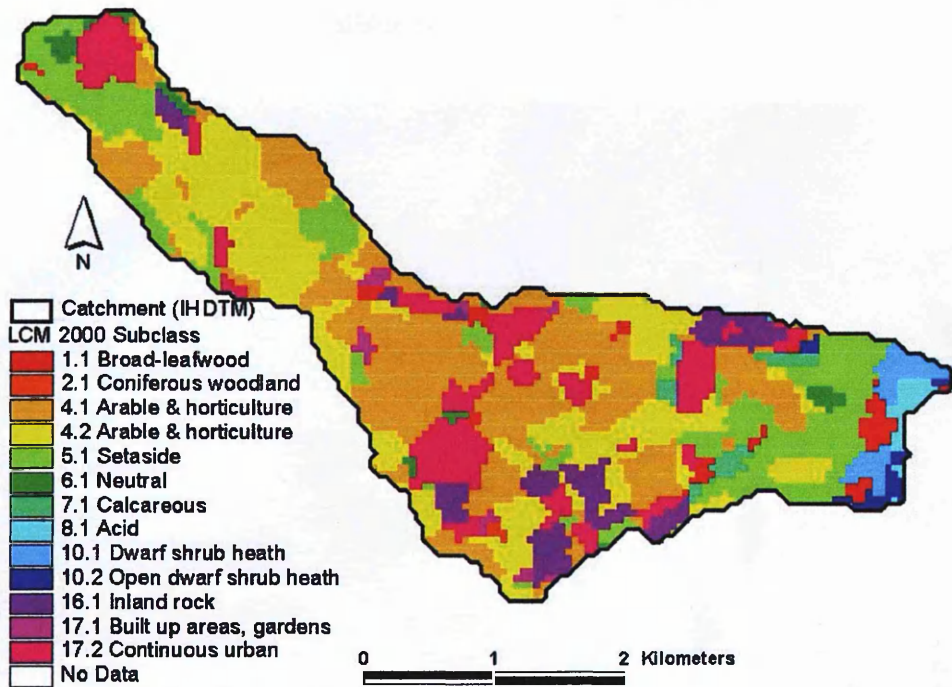


Figure 5.10. LCM 2000 Subclasses in the Greens Burn catchment.

5.3.4. HOST

HOST information is available from CEH, Wallingford, UK at the 1km grid cell scale (Figure 5.11). This data set was then converted to a 50m grid of the same extent as the DTM (Figure 5.12). Converting a large grid cell into smaller grid cells is not good practice, propagating errors in the spatial data set in a complex way (e.g. Thappa & Bossler, 1992). However, given the inaccuracies of the HOST class boundaries and the view that this additional HOST information was of benefit to the model, these errors are probably tolerable.

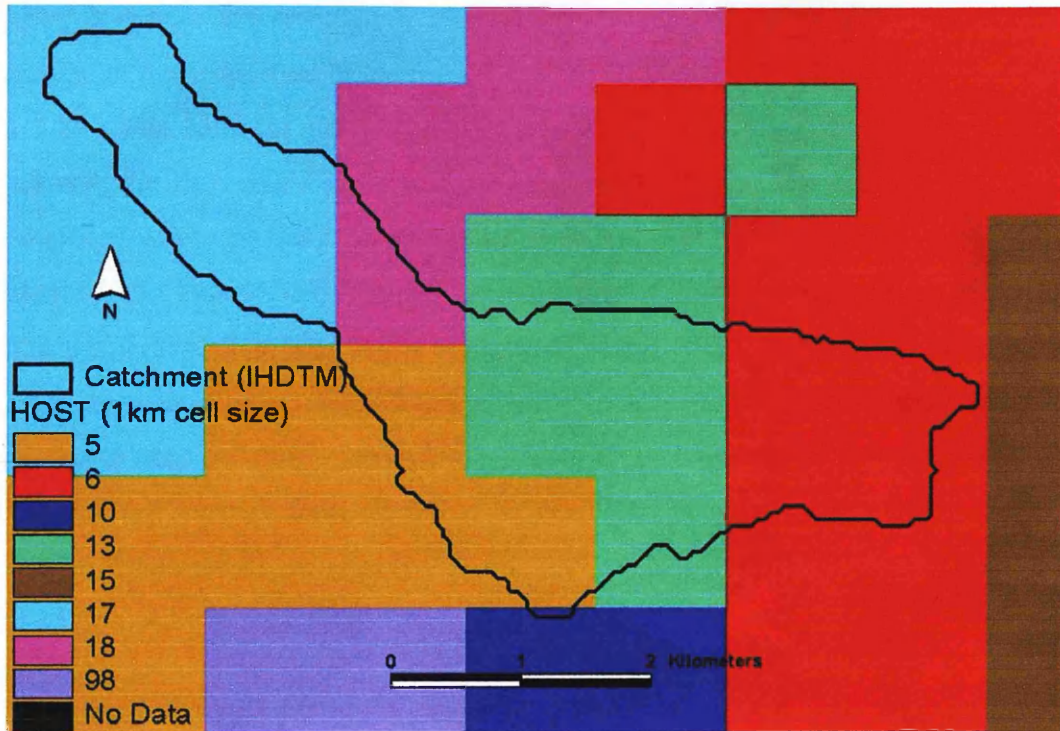


Figure 5.11. HOST data supplied by CEH (1km cell size).

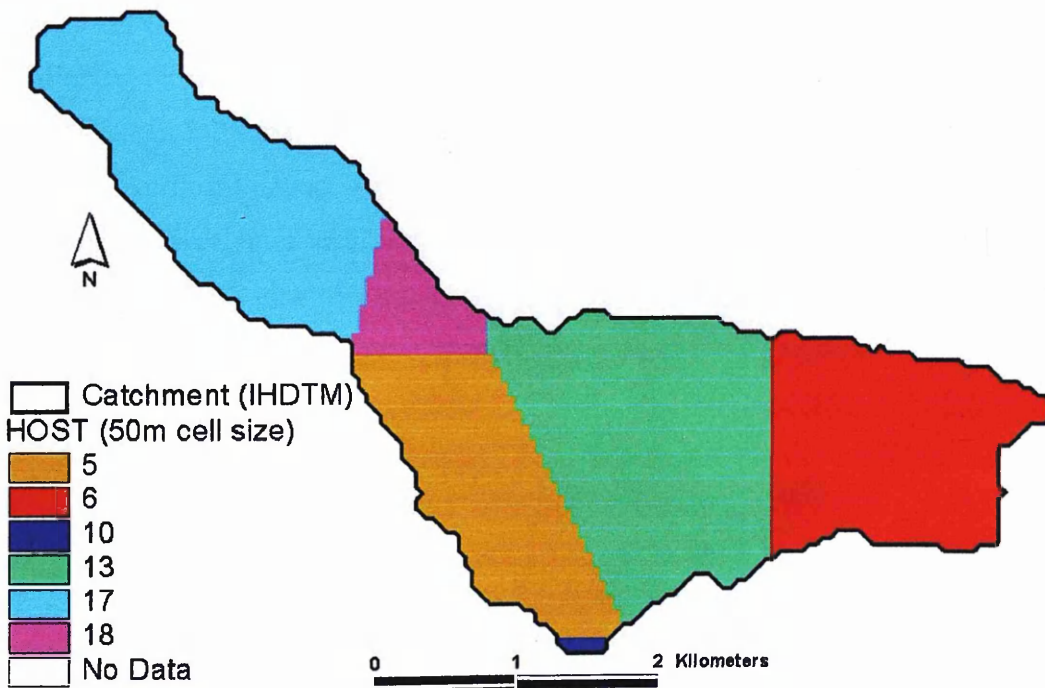


Figure 5.12. Host (50m cell size) derived from the 1km data set supplied by CEH.

The CEH HOST data only gives the dominant HOST class for each cell which means that the HOST values for each different soil area in the catchment will be different from those used in Chapter 3, where the resultant HOST and *SPR* values for each soil class were weighted according to the proportion of the constituent HOST classes in each soil class (see Figures 3.6 and 3.8). For some of the catchment, this is not a problem: in the North-west of the catchment, the 1km HOST class is given as 17 (with *SPR* = 29.2%) and the soil class (from the digitised soil map) is 472, which is 100% HOST class 17. However, in the middle of the catchment, the 1km HOST class is 13 (with *SPR* = 2%) and the soil class is 337 on the digitised soil map. Soil class 337 is made up of 50.5% HOST class 13 and 49.5% HOST class 17, which gives a weighted *SPR* value of 15.5%. As well as affecting the *SPR* value attributed to each cell, the overall range of the *SPR* values in the catchment (which is used by the model) will change from 15.5% – 43.2% when using the weighted *SPR* values derived from the digitised soil map (as in Chapter 3) to 2% – 47.2% when using the *SPR* values derived from the 1km dominant HOST classes map.

An additional inaccuracy, as a result of scaling up to 1km grid size, is that soil class 1 (see Figure 3.6) has not been registered. Instead it has been attributed to soil class 414, with dominant HOST class of 18. However, the overall trend of higher *SPR* values at the sides of the catchment (where slopes are steeper) and lower *SPR* values in the middle (where slopes are shallower) remains the same. Given the nature of how the effect of soil type is included in the model (as an intra-catchment weighting factor), it is not expected that these differences will have a significant impact on the overall annual phosphorus export from the Greens Burn catchment. However, on a local scale, cells may be deemed to export more or less P (when using the 1km HOST classification to attribute an *SPR* value to each cell) than when the model was applied using the digitised soil map to determine weighted *SPR* values for each cell.

5.3.5. *HER* (Rainfall and Actual Evapotranspiration)

As in Chapter 3, rainfall data were obtained from SEPA for the two raingauges near the catchment (at Balado and Portmoak) and the AET data was obtained from the NERC website (<http://www.nerc-wallingford.ac.uk/ih/nrfa/yb/>).

5.4. Model results using the readily available data in the Greens Burn catchment

The readily available data described above (land use from LCM2000, slope and specific area from the CEH DTM, *SPR* values derived from the CEH HOST 1km data set and *HER* being calculated from rain and *AET* data for the catchment) were used in the model for the years 1996-1999. The only variation in the input data between years was *HER*. The results for the predicted annual P export (kg a^{-1}) for each year are shown in Table 5.3, along with the results obtained using more detailed input data (see Chapter 3) and the measured annual P load for comparison.

Table 5.3. Comparison of predicted annual phosphorus export from the Greens Burn catchment using readily available data and more detailed data as input into the model (500 iterations were used in each run).

Year	Predicted P export (kg a^{-1}) Mean (SD)		Measured P load (kg a^{-1}) Mean (SEM)
	Model Using Readily Available Data	Model Using More Detailed Data (Chp 3)	
1996	453 (145)	452 (112)	519 (281)
1997	483 (153)	524 (128)	574 (331)
1998	741 (223)	786 (229)	665 (257)
1999	615 (205)	636 (177)	529 (224)

Using the readily available input data gave very similar predictions to those produced using detailed data.

With this small snapshot of success, it was decided to apply the model to a second catchment (the Leet Water) by sourcing the readily available data.

5.5. Application of SEPTIC to the Leet Water catchment

The SEPTIC model was set up for the Leet Water, which is a tributary of the River Tweed (Figure 5.13).

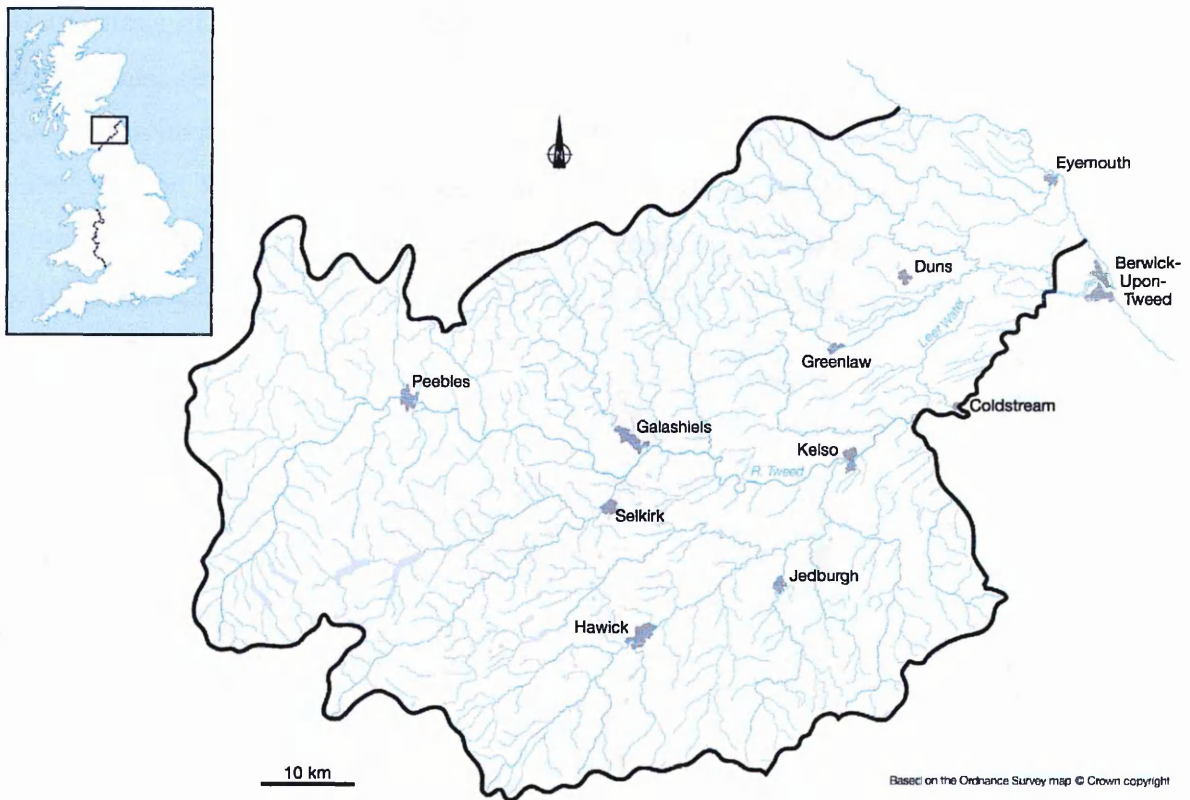


Figure 5.13. The Tweed Catchment.

5.5.1. The Tweed Catchment

The Tweed is a rural, mainly agricultural river system located in the eastern Scottish Borders. The catchment, delimited by the Moorfoot, Pentland and Lammermuir hills in the north and the Cheviot hills to the south, has an area of 4400km² (at Northam) and as such is the second largest river basin in Scotland and the sixth largest in mainland Britain (Clayton, 1997).

The climate is cool and temperate, with average monthly temperatures ranging from 1°C in January to 13°C in August (MORECS). Average annual rainfall ranges from 2200 mm in the headwaters of the Tweed to less than 650 mm in the lowlands of Berwickshire. (Fox & Johnson, 1997). Annual average evapotranspiration varies from more than 450 mm in the east to less than 400 mm in the south and west (Robson & Neal, 1997a). Thus annual hydrologically effective rainfall (precipitation – evapotranspiration) varies between 1800 and 200 mm, with a marked west – east gradient.

The geology of the catchment (Figure 5.14) includes a large area of Ordovician and Silurian greywackes, shales and mudstones together with Old Red Sandstones in the lowlands, Carboniferous sedimentary rocks and the igneous rocks of the Cheviot Hills (Robson *et al.*, 1996; Robson & Neal, 1997b). Soils range from well drained brown earth in the lowlands, gleys on the southern slopes, podzols (peaty podzols and humus-iron podzols) on higher land to peats on the hill tops and moors (Robson *et al.*, 1996; Robson & Neal, 1997b).

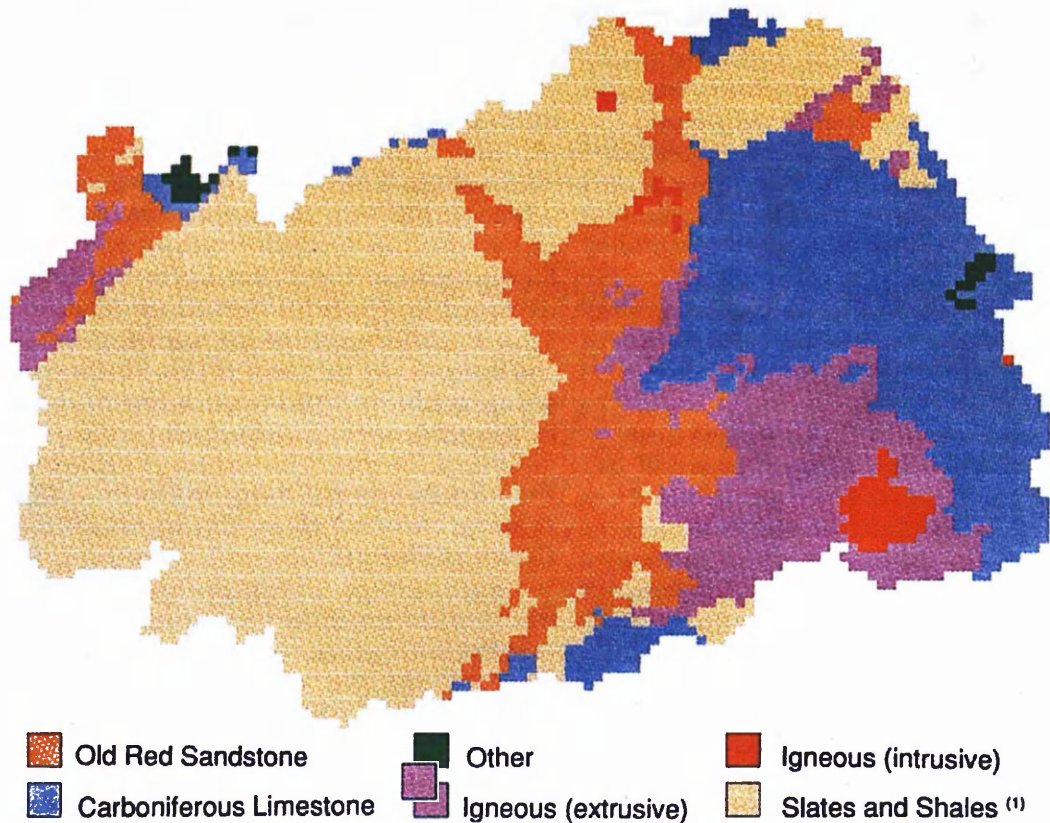


Figure 5.14. Geology of the Tweed Catchment (from Robson *et al.*, 1996, p.7).

Land use in the catchment ranges from sheep farming in the upland areas of moorland and rough pasture to cereal crops (mainly barley, wheat, oats and oilseed rape) and some potatoes in the lowland arable areas. Significant conifer plantations (16% of the land in 1996) are predominately located on the hills to the south and west of the region (Robson *et al.*, 1996).

The Tweed and its tributaries are largely clean and unpolluted, supporting a diverse biology. Over 99% of the waters in the Tweed are Class 1 (unpolluted – according to the Scottish chemical classification system) with only a few stretches being designated as Class 2 (fairly

good quality), usually as a result of sewage discharges or from natural causes (Robson *et al*, 1996). In April 1976, the Tweed was notified as a site of special scientific interest (SSSI), being described in the notification as “a nationally important example of a relatively nutrient rich river system showing characteristic hydrological and biological sequences along its length. It is one of the least polluted of the easterly flowing large eutrophic rivers with little or no water transfer from adjacent basins. Certain plant and animal species are at the northern edge of their British distribution” (Clayton, 1997). In addition, it supports one of the most important salmon fisheries in the UK which, along with its otter population and floating vegetation (*Ranunculus*), has resulted in it being designated as Special Area of Conservation (SAC) (Clayton 1997, W. Dryburgh *pers comm.*).

Eutrophication (with large growths of *Cladophora*, *Oedogonium* and *Hydrodictyon*) can occur in some of the smaller lowland water courses and diatom growth on the lower Tweed can be significant (Robson & Neal, 1997b; Clayton, 1997).

5.5.2. The Leet Catchment

The Leet Water (including the Lambden Water) is situated in the eastern lowlands of the Tweed catchment. The gauged catchment (at Coldstream, NT 839 396) has an area of 113km² and is shown in Figure 5.15.

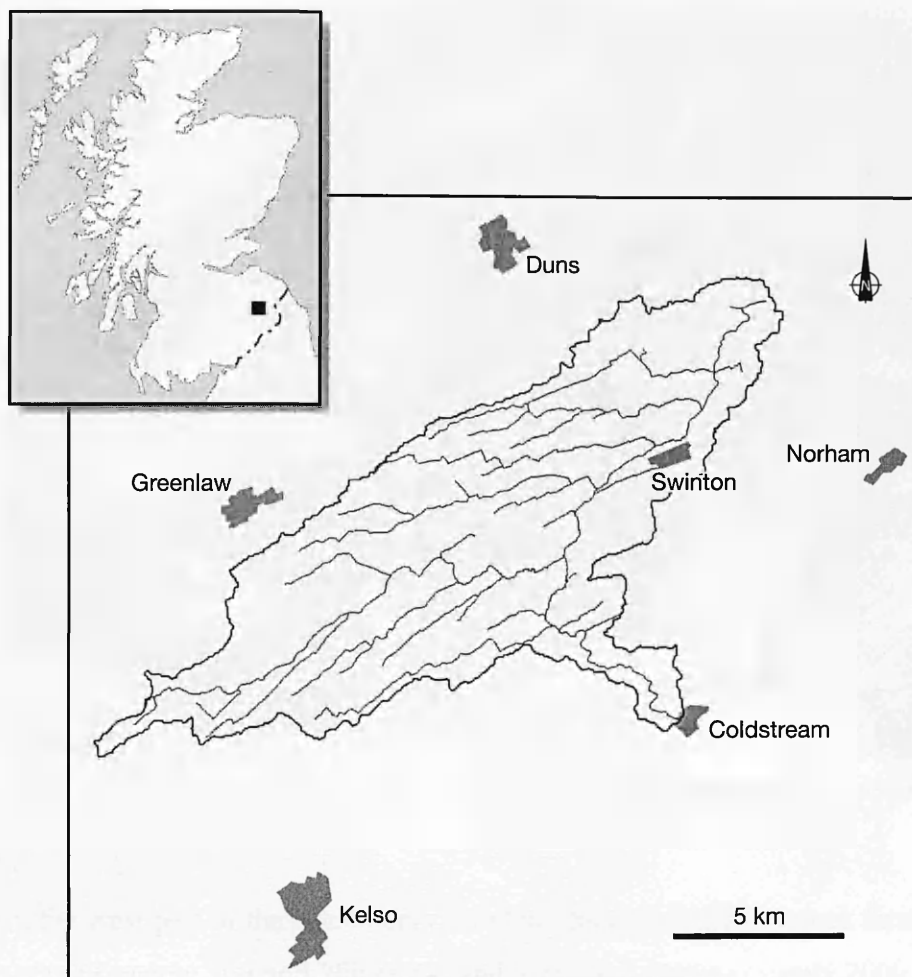


Figure 5.15. The Leet Catchment.

Land use in the catchment, especially in the east, is dominated by cereals with some sheep grazing, as can be seen in Figure 5.16.



Figure 5.16. The Leet catchment, taken from Hume Castle (NT 706 413) towards Hume, 23-03-06.

In the west part of the catchment (Lamden), there is some livestock farming with 2 dairy units (approximately 300 and 200 cows) and 1 pig unit (approximately 2000 pigs). Drainage from the dairy farm at Kennetsideheads used to go directly into the watercourse but since 2005, all drainage has been diverted via a wetland and settlement pond (Figure 5.17). As a result, the adjacent watercourse (Laprig Burn) is now fairly clean.



Figure 5.17. Kennetsideheads Dairy Farm (NT 729 412) - reed bed and settlement pond, 23-03-06.

In addition, there are two large poultry units (approx 300,000 chickens each) in the west of the catchment and one smaller unit (approx 9000 chickens) at Greenriggs in the east (Figure 5.18).



Figure 5.18. Greenriggs Poultry Unit in the Leet catchment (NT 833 482), 23-03-06.

A problem resulting from these large poultry units is that P rich dust from the ventilation system is washed by rain into the burn. This problem has been mitigated at the Greenriggs unit where rainwater and runoff from the roof is now diverted through a reed bed system, which has resulted in a 90% reduction in P loss to the watercourse from the unit. Efforts are being made to negotiate the installation of a similar system at the two large units in the west of the catchment (W. Dryburgh, *pers comm.*).

Approximately 1900 people reside in the Leet catchment (Dryburgh & Eastwood, 2005). Their sewage is treated either by four waste water treatment works (WWTW), in the relatively densely populated areas of Whitsome, Swinton, Leithom and Eccles, or by septic tank. The treatment works all underwent improvements (e.g. addition of reed beds with iron ochre in the medium) in the late 1990's. These improvements resulted in substantial reductions in P in the final effluents (W. Dryburgh, *pers comm.*).

The top 10km stretch of the Leet water was channelised (dredged) in the mid-1970s and the surrounding land was under-drained. Channelling has resulted in sedimentation (due to the

still water with lack of pool-riffle system) in the watercourse at Swinton Bridge (Figure 5.19a). Most erosion in this area occurs during floods at the end of the year when there is little ground cover. The resulting poor water quality has had a detrimental effect on the trout population, with serious fish mortalities in the mid-1990s. Inspired by a fly-tipped piece of corrugated iron dumped downstream of the bridge (which was observed to produce a pool-riffle system), revertsments were put in to create more pools/riffles in 1999-2002 (Figure 5.19b). The result has been an increase in the number of trout, otter and invertebrates (notably mayfly) in this stretch of the watercourse (W. Dryburgh, *pers comm.*).



Figure 5.19. The Leet Water at Swinton Bridge (NT 832 475) with views upstream (a) and downstream (b), 23-03-06.

Just beyond Swintonmill (NT 810 455), the artificial drainage ends and the river naturally meanders to Coldstream, where there is a gauging station operated by SEPA (Figure 5.20).



Figure 5.20. Gauging station at Coldstream (NT 839 396), 23-03-06.

A sample hydrograph for the gauging station at Coldstream is shown in Figure 5.21.

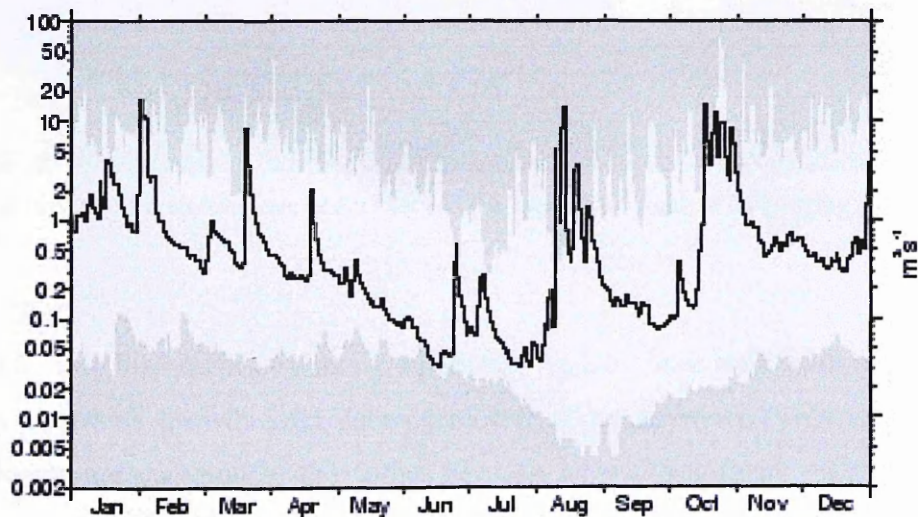


Figure 5.21. Maximum and minimum daily mean flows from 1970 to 2003 excluding those for the featured year (solid line), 2004: mean flow = $1.03 \text{ m}^3 \text{ s}^{-1}$ (2004 runoff = 288 mm). Sourced from http://www.nwl.ac.uk/ih/nrfa/station_summaries/021/023.html.

River discharge tends to be lower in summer and higher in winter, ranging from $0.003 - 51.667 \text{ m}^3 \text{ s}^{-1}$ (mean = $0.832 \text{ m}^3 \text{ s}^{-1}$), with a mean annual flood of $23 \text{ m}^3 \text{ s}^{-1}$ (for 1970-1995 in Fox & Johnston, 1997). The mean annual runoff (1970-1994) was 232 mm a^{-1} . At least once a year the river breaches the top of the wall in Figure 5.20b (W. Dryburgh, *pers comm.*).

However, high flows need to be treated with caution as the Tweed tends to “back-up” at Coldstream due to the angle of convergence between the Leet and the Tweed (Figure 5.22). The result is that discharge tends to be overestimated (J. Petry, *pers comm.*). There is one Combined Storm Overflow (CSO) which drains into the Leet just above the gauging station.



Figure 5.22. The convergence of the Leet and the Tweed, just south of the gauging station at Coldstream, 23-03-06.

Relatively high diffuse-source P inputs into the Leet have resulted in eutrophic conditions and an excessive growth (and decomposition) of macrophytes (Robson *et al.*, 1996). Diatom blooms are common in the spring and can have a significant effect on pH and dissolved oxygen concentrations. The Leet is considered to have a significant influence on the overall water quality of the Tweed.

5.6. Data for the Leet catchment – Model inputs

Readily available data for the Leet catchment were obtained from the same sources as for the Greens Burn catchment.

5.6.1. Data to derive slope and cumulative area

The boundary for the catchment draining to the gauging station (No. 21323, Grid Reference 36 (NT) 839 396) at Coldstream on the Leet Water is available from CEH, Wallingford, UK, along with the IHDTM elevations (with a grid cell size of 50m). The DTM was processed using ArcView and cut to the extent of the catchment boundary (Figure 5.23).

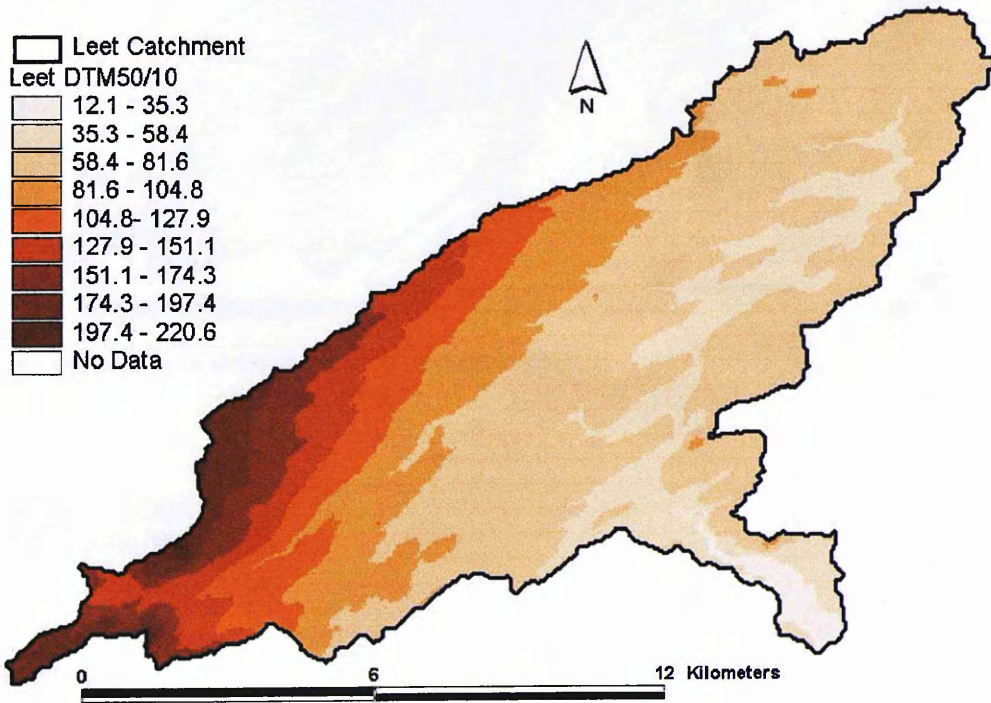


Figure 5.23. DTM of the Leet catchment. (Elevations are in metres above sea-level.)

Slope (Figure 5.24) and specific area (Figure 5.25) were derived from the DTM, using the methods outlined in Chapter 3.

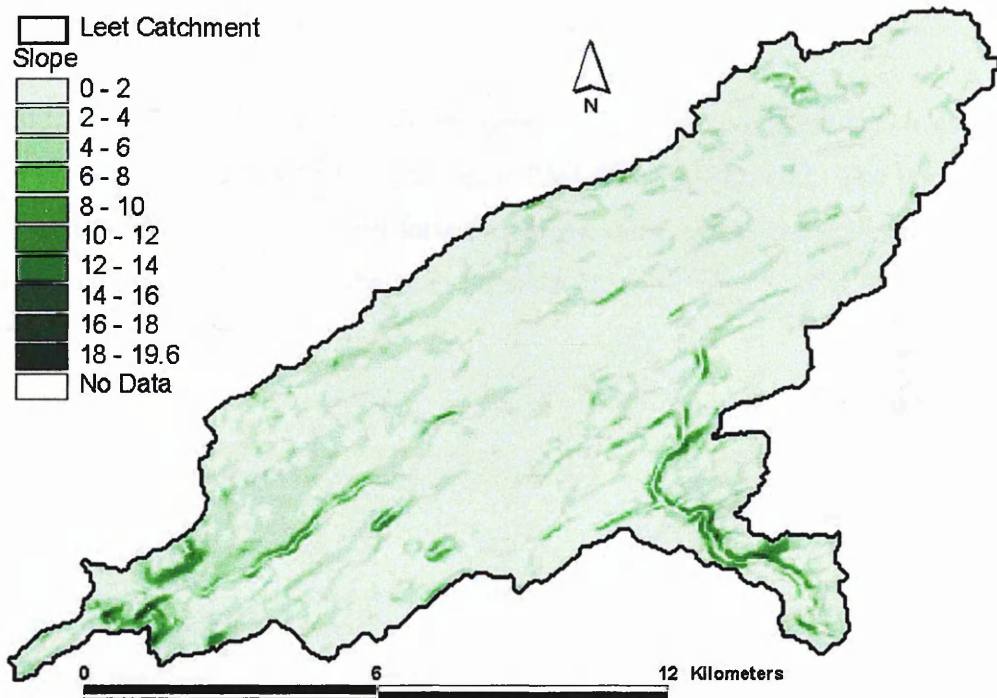


Figure 5.24. Distribution of slope (degrees) in the Leet Catchment.

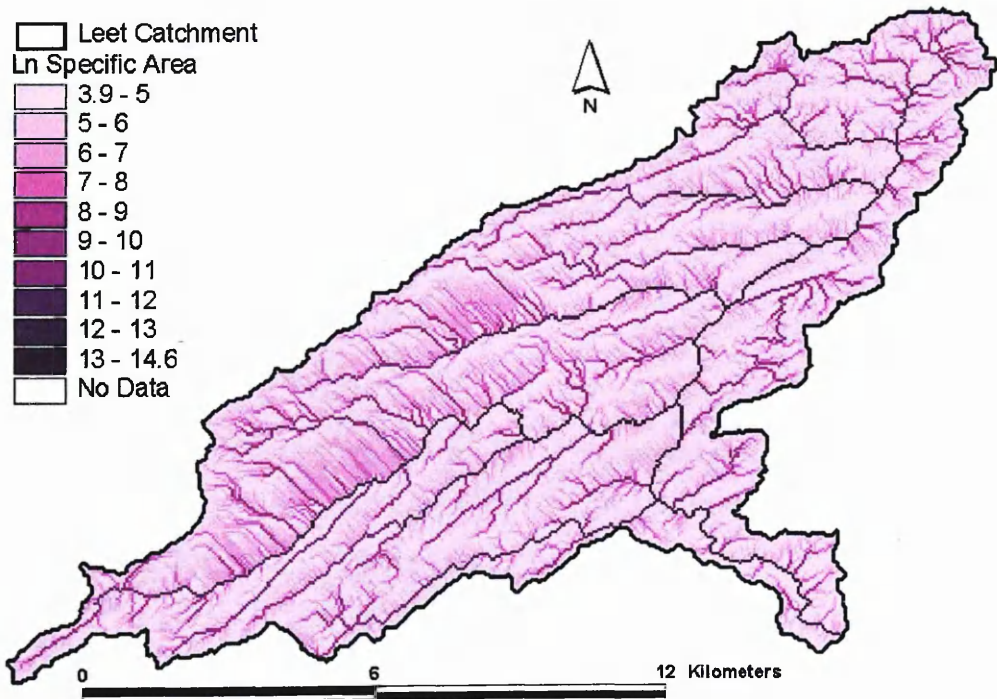


Figure 5.25. Distribution of the natural logarithm of specific area in the Leet Catchment.

5.6.2. Land use data

The Land Cover Map 2000 Level 2 Vector data for the Leet catchment area was purchased from The Centre for Ecology and Hydrology (CEH), Huntingdon, UK. The vector data was transformed (in ArcView) into a grid format with the same extent and cell size (50m) as the DTM. The resulting land cover is shown in Figure 5.26.

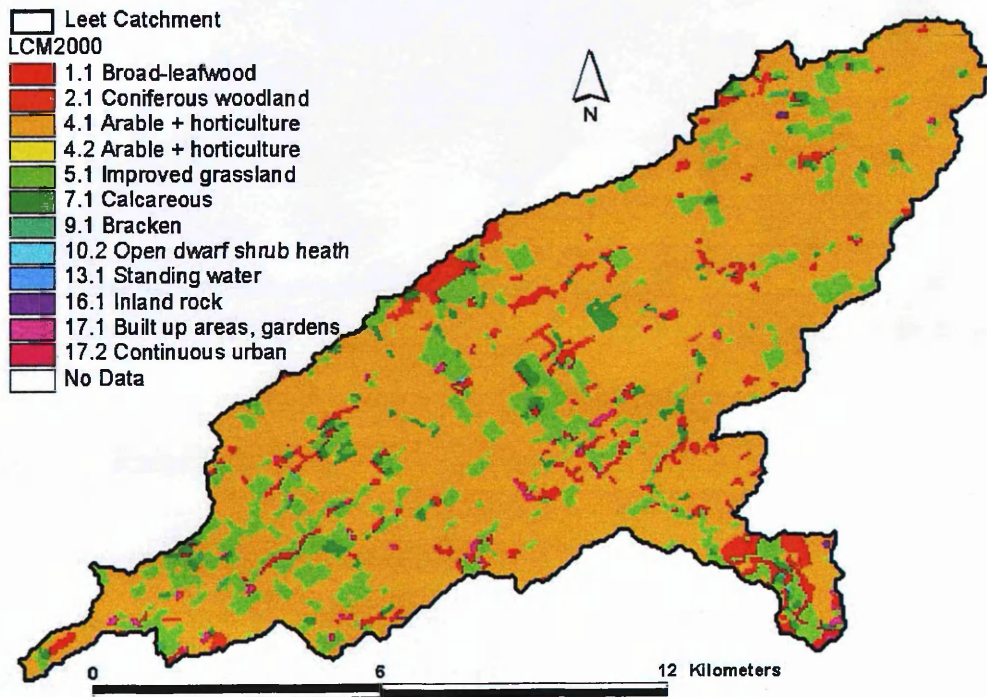


Figure 5.26. Distribution of land use (LCM2000) in the Leet catchment.

5.6.3. HOST data

Information on the dominant HOST classes in the Leet catchment is available from CEH, Wallingford, UK at the 1km grid cell scale. This data set was converted into a 50m grid of the same extent as the DTM (shown in Figure 5.27).

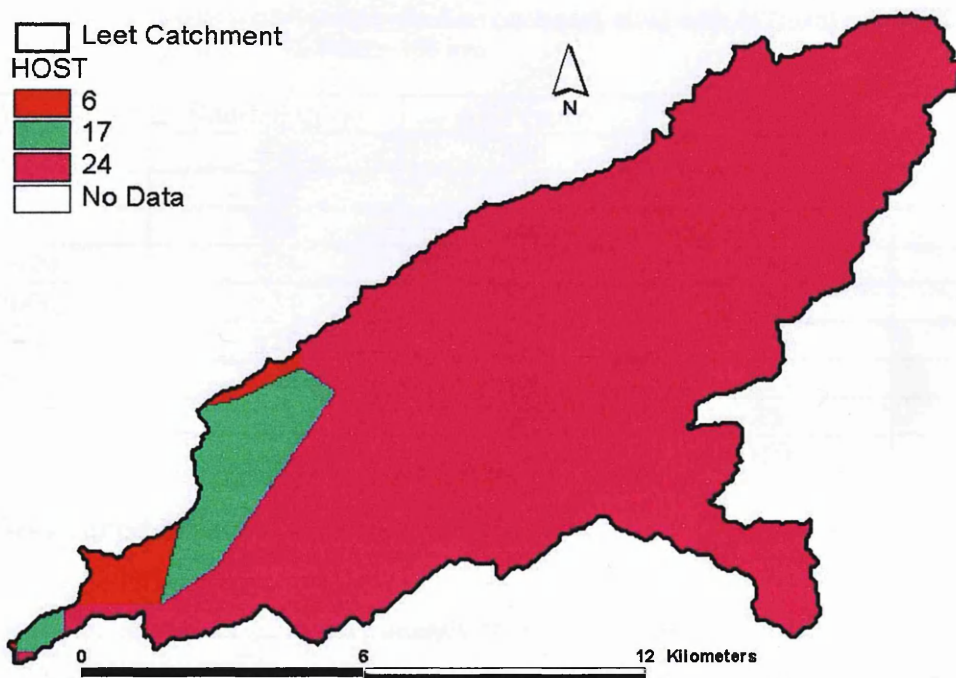


Figure 5.27. Distribution of HOST classes in the Leet catchment (Note: for each cell, only the dominant HOST class is given).

5.6.4. Rainfall data

Rainfall is measured by SEPA at Swinton (NT 832 475), in the north east of the catchment. Actual Evapotranspiration (*AET*) data were, again, obtained from <http://www.nerc-wallingford.ac.uk/ih/nrfa/vb/>. The Leet catchment is contained within the corners of 4 adjacent *MORECS* squares: 58, 59, 65 and 66. However, the rain gauge (at Swinton) is located in *MORECS* square 59 and so *AET* data for that square was used in the model. The measured annual rainfall and annual *AET* are shown in Table 5.4, along with the calculated Hydrologically Effective Rainfall (*HER*).

Table 5.4. Measured annual rainfall (mm) in the Leet catchment, along with *AET*(mm) and *HER*(mm) estimates for 1996-2004. Average *HER* (1996-2004) = 198 mm.

Year	Rainfall (mm)	<i>AET</i> (mm)	<i>HER</i> (mm)	<i>HER</i> /av <i>HER</i>
1996	589	480	109	0.55
1997	607	480	127	0.64
1998	824	540	284	1.44
1999	631	510	121	0.61
2000	834	510	324	1.63
2001	679	480	199	1.00
2002	903	480	423	2.14
2003	515	480	35	0.18
2004	689	530	159	0.81

5.7. Measured data for the Leet catchment

Water samples are collected approximately monthly at Coldstream gauging station. For the period of interest (1996-2004), only orthophosphate (o-P) analysis was undertaken. However, in 1990-1993 some TP analysis (monthly in 1990-1991 and less frequently in 1992-1993) was performed in addition to o-P (n=38). A regression was performed between the measured o-P and corresponding TP to see if any relationship existed between them to allow future estimates of TP on the basis of measured o-P. The result is shown in Figure 5.28.

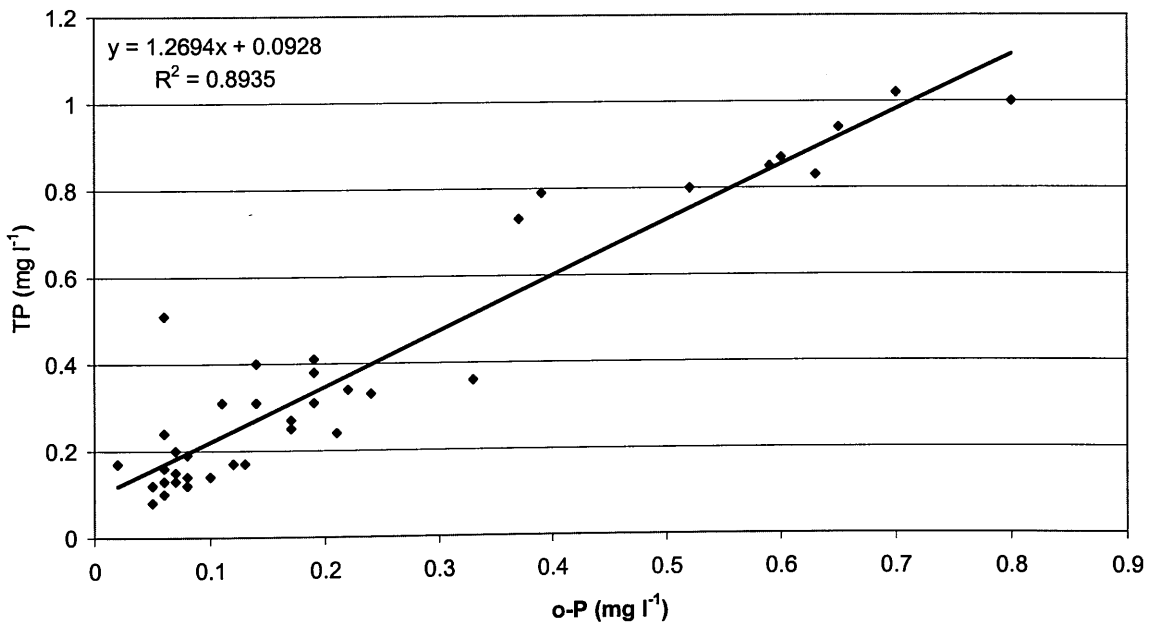


Figure 5.28. Regression between o-P and TP measured at Coldstream gauging station (n = 38).

There is a fairly strong relationship between o-P and TP ($R^2 = 0.89$) and this relationship was, therefore, used to make estimate of TP from the o-P data for 1996-2004. Obviously, this relies on the ratio of o-P to TP remaining constant which given the improvements to sewage treatment and animal waste loss in the catchment is unlikely. However, in the absence of better data and given the approximate nature of water quality characterisation based on monthly sampling, it is probably reasonable. The tendency of monitoring programmes (generally operated by environmental agencies) to analyse for o-P and not TP (presumably due to relative ease of analysis) means that this problem frequently occurs (e.g. Johnes, 1996; Johnes & Heathwaite, 1997). Reliance on TP derived from o-P is fairly common.

Flow data (DMF), measured at Coldstream gauging station, are also available from SEPA. As in Chapter 2, the flow data, TP data and TP estimated from o-P data were used to calculate the estimated annual TP load from the Leet catchment for 1990 and 1991 (years with complete data sets of TP and o-P). The results are shown in Table 5.5.

Table 5.5. Estimated annual TP load (kg P a^{-1}) from the Leet catchment in 1990 and 1991 using measured TP data and TP estimated from measured o-P data.

Year	TP load (kg P a^{-1}) using TP data			TP load (kg P a^{-1}) using TP estimated from o-P data		
	Average	Std Dev	SEM (count)	Average	Std Dev	SEM (count)
1990	4527	1466	423 (12)	4692	1913	552 (12)
1991	4208	2121	612 (12)	4153	3354	968 (12)

Differences between the TP load calculated using TP concentrations estimated from the o-P concentration data and the TP load calculated using the measured TP concentration data is small: 4% (calculated as difference divided by TP load from measured TP data) in 1990 and 1% in 1991. The calculated load using either method easily lies within the SEM of the other method.

In addition, annual TP load was calculated using TP concentrations estimated from o-P concentration data and also by using measured TP concentration for each day on which both o-P and TP were measured ($n=38$). The Mann-Whitney non-parametric 2-tailed test was performed with null hypothesis, H_0 : TP load using measured TP concentrations = TP load using TP concentrations estimated from o-P concentrations. At the 95% confidence interval, the null hypothesis cannot be rejected ($p = 0.6071$) and therefore there is no statistical

difference between TP load being calculated using measured TP concentrations and TP load being calculated using TP concentrations estimated from o-P concentrations.

The annual TP load for 1996-2004 was then calculated using TP estimated from o-P concentrations. The results are shown in Table 5.6.

Table 5.6. Estimated annual TP loads from the Leet catchment in 1996-2004 using measured TP concentrations estimated from o-P concentrations.

Year	Average P (kg a^{-1})	Standard Deviation (kg a^{-1})	SEM (count)
1996	3110	2247	425 (28)
1997	3057	1667	430 (15)
1998	3776	4505	1204 (14)
1999	2067	1002	163 (38)
2000	5000	5974	1889 (10)
2001	3733	1943	615 (10)
2002	3091	1321	381 (12)
2003	3133	4698	1356 (12)
2004	2590	1635	472 (12)

5.8. Application of the SEPTIC model to the Leet catchment

5.8.1. Numerical Results

The SEPTIC model was applied to the Leet catchment for 1996-2004. The results are shown in Figure 5.29. In most years, there is an overlap between the estimated average load and the mean \pm one standard deviation of the model predictions. There is also a fair match between the year-to-year trends. The exceptions are 2002 and 2003. The errors generated in these years are probably due to errors in the *HER* values used in SEPTIC. Figure 5.30 shows the comparison between the year-to-year trend in estimated load and *HER* for 1996-2004. The direction of change is the same for 1997-2001 but not prior to 1997 or after 2001. This brings into question the model assumption that the year-to-year change in *HER* is the driver in the year-to-year trend in P output from the Leet catchment. The disparity for 1996 and 2004 could possibly be explained by errors in the measured data. However, for 2002 (comparatively very big *HER*) and 2003 (comparatively very small *HER*), the model is failing to make reasonable predictions.

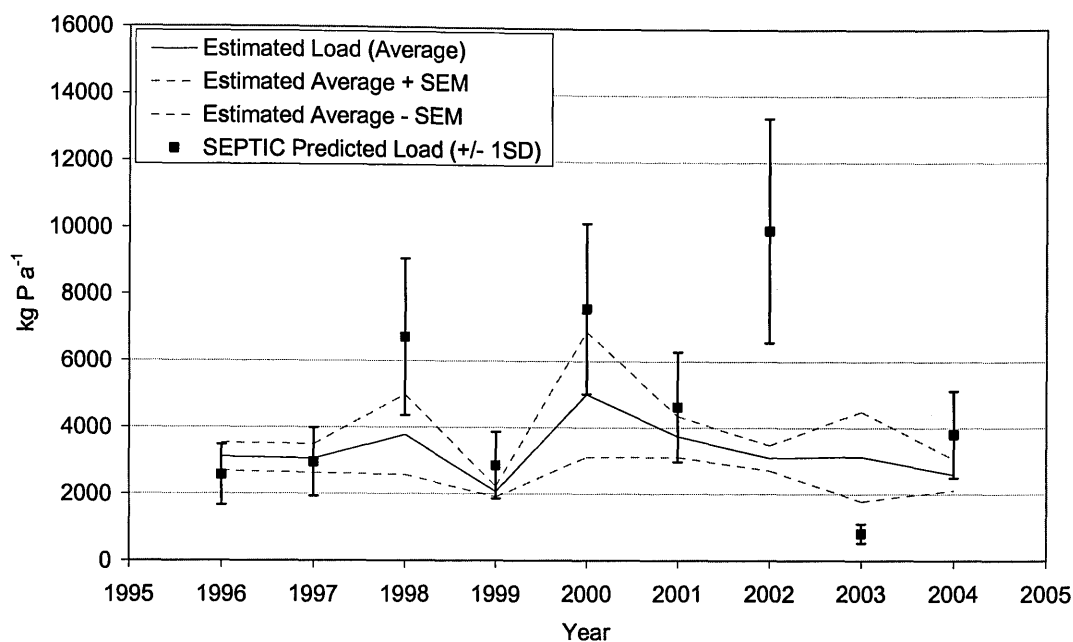


Figure 5.29. Comparison of SEPTIC model predictions with the estimated load, based on measured concentrations and flows, from the Leet catchment, 1996-2004.

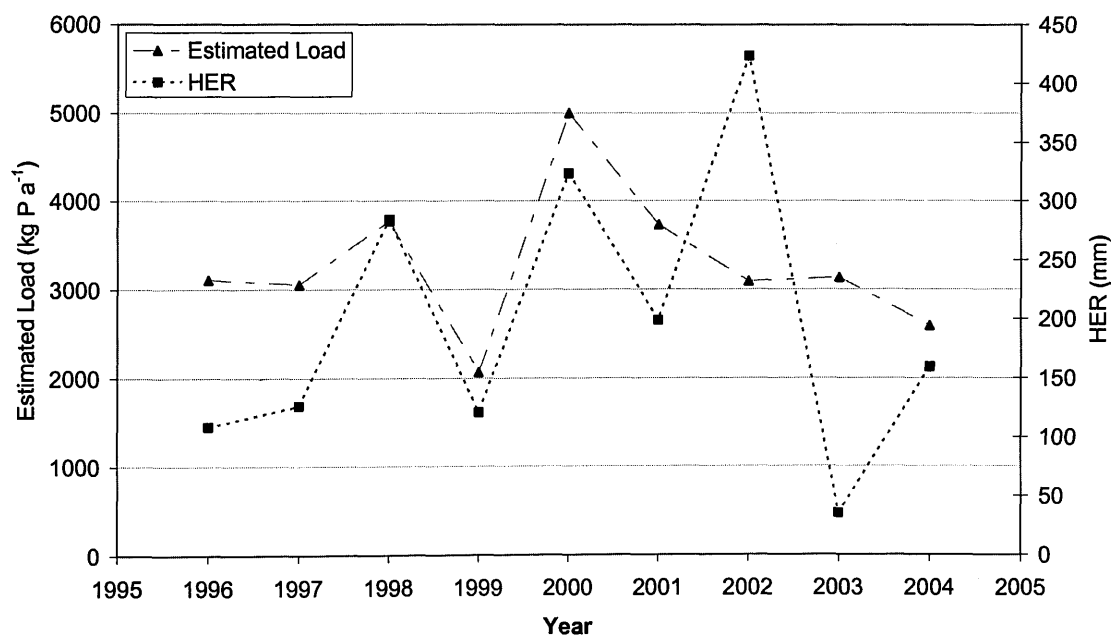


Figure 5.30. Comparison between the trends in estimated load (kg P a^{-1}) and *HER* (mm) for 1996-2004.

The annual runoff (mm) from the catchment was calculated (annual discharge divided by catchment area) and compared to annual *HER* (Figure 5.31). The inter-annual trend for runoff changes in the same direction as for *HER*, although the magnitude of change is more muted.

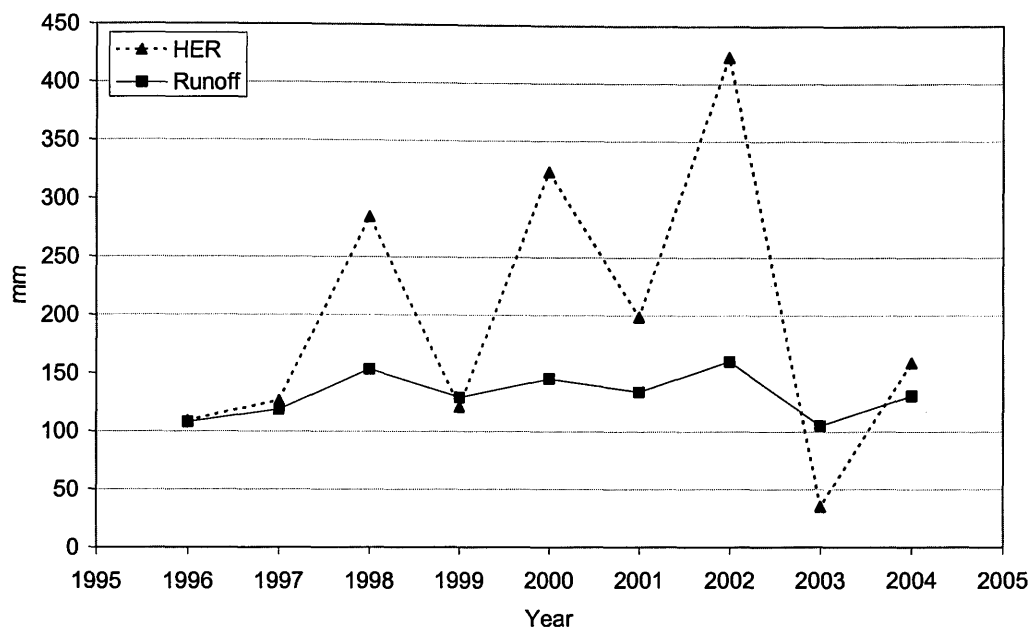


Figure 5.31. Comparison between *HER* (mm) and runoff (mm) for the Leet catchment, 1996-2004.

SEPTIC was applied to the Leet catchment, using annual runoff as the inter-annual change driver instead of *HER* (Figure 5.32).

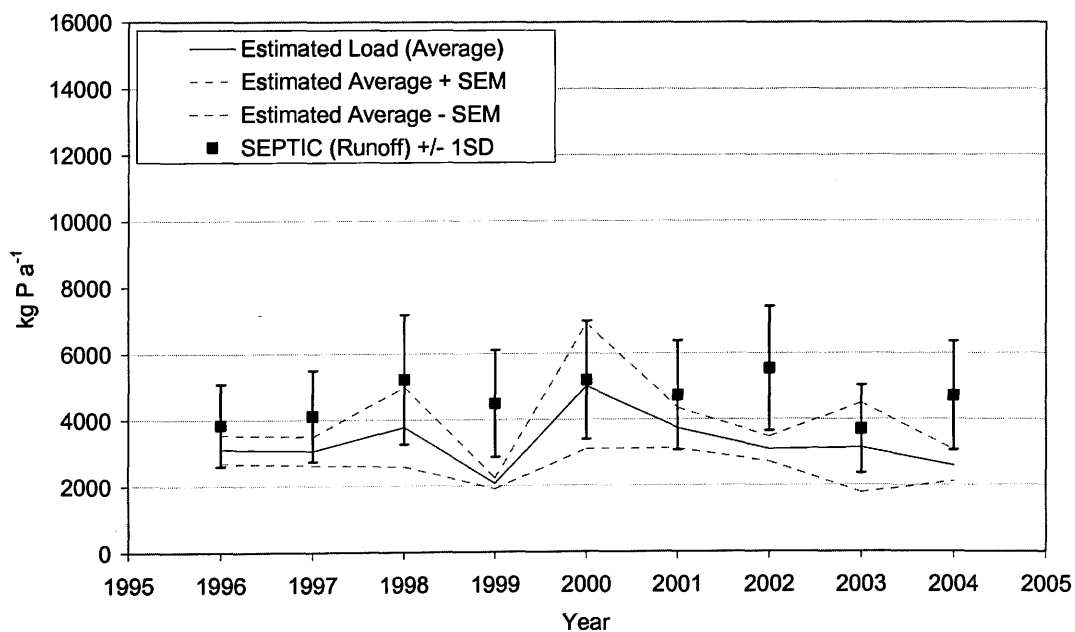


Figure 5.32. Comparison of SEPTIC model predictions (using annual runoff instead of *HER* as the inter-annual driver) with the estimated load, from the Leet catchment, 1996-2004.

As expected, the change in year-to-year predictions of P export is less extreme. The average predicted load is closer to the average estimated load in some years (1998, 2000, 2002 and 2003) but does not perform as well in the other years considered (1996, 1997, 1999, 2001 and 2004), as shown in Table 5.7.

Table 5.7. Comparison between SEPTIC outputs when using *HER* or annual runoff as the inter-annual driver. Average predicted loads are compared to the average estimated load, with the % difference (calculated as $((\text{predicted}-\text{estimated})/\text{estimated})\times 100$) shown for both outputs (using *HER* or annual runoff) for each year, 1996-2004.

Year	Average Estimated Load	Predicted Load using <i>HER</i> (% Difference)	Predicted Load using Runoff (% Difference)
1996	3110	2563 (-18)	3834 (23)
1997	3057	2958 (-3)	4117 (35)
1998	3776	6709 (78)	5212 (38)
1999	2067	2858 (38)	4485 (117)
2000	5000	7582 (52)	5185 (4)
2001	3733	4626 (24)	4729 (27)
2002	3091	9950 (222)	5530 (79)
2003	3133	819 (-74)	3700 (18)
2004	2590	3809 (47)	4703 (82)

The main improvement in using annual runoff instead of *HER* occurs in 2002, when using *HER* resulted in a large over-estimate of P load. However, this improvement is tempered by the result for 1999, when using annual runoff greatly increased the disparity between the predicted and estimated load, compared to using *HER*. In addition, the direction of change between 2002 and 2003 is still opposite to that for the estimated load. Annual runoff should be a more reliable inter-annual driver as *HER* does not account for water storage in the catchment and hence is not accurate for flow. If further study confirms that using annual runoff instead of *HER* results in significantly better model predictions, then annual runoff could be used as an alternative to *HER* in gauged catchments. In ungauged catchments, *HER* would still have to be used.

Frequency distributions for each year can be generated, showing the range of predicted loads and the most likely load (from 500 iterations). The results, using *HER* as the inter-annual driver, are shown in Figure 5.33, along with the estimated measured load (± 1 SEM) for comparison.

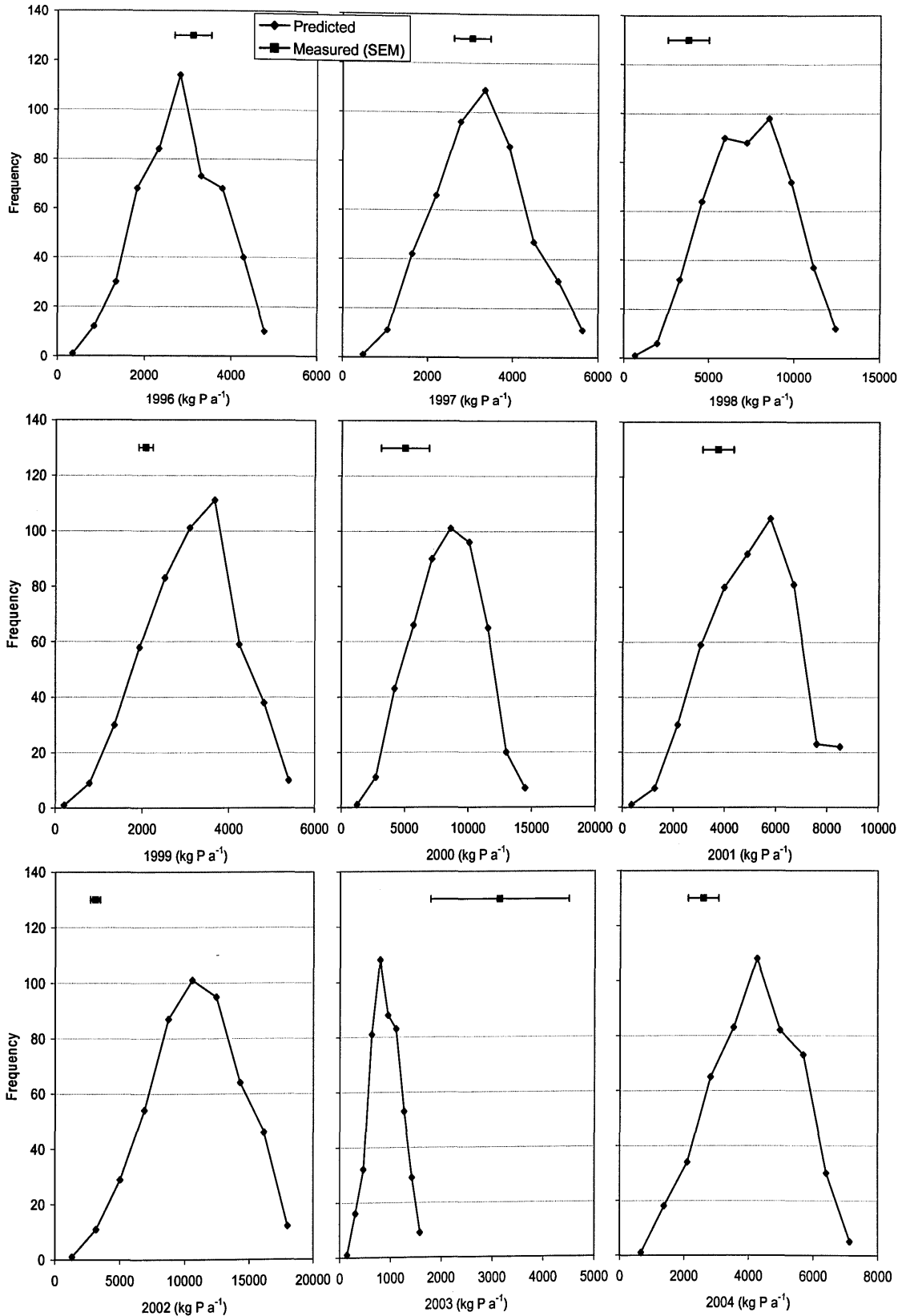


Figure 5.33. Histograms of the predicted model outputs (kg P a⁻¹) with the estimated measured load (kg P a⁻¹) for comparison, for the Leet catchment, 1996-2004.

Table 5.8 shows the output from the different steps in the model process. The predictions derived from the crop export coefficients alone grossly over-estimate the annual P load. Year-to-year, there is very little change in the crop output since the land use is assumed to remain constant (as LCM2000) throughout the years. The small variability is due to the stochastic nature of random sampling from the range of export coefficients for 500 iterations.

Incorporating the effect slope and cumulative area (Crops*PF) brings the model predictions into line with the estimated loads. However, given that topography remains constant from year-to-year, the small inter-annual variation is again due to random sampling from the range of export coefficients and their spatial distribution.

Table 5.8. Numerical results (1996-2004) from each stage of the model: P export (kgP a⁻¹) just considering crops; considering crops, slope and cumulative area (Crops*PF); from crops, slope, cumulative area and soil type (Crops*PF*SF) and from crops, slope, cumulative area, soil type and *HER* (Crops*PF*SF*RF).

Year	Crops Mean (SD)	Crops*PF Mean (SD)	Crops*PF*SF Mean (SD)	Crops*PF*SF*RF Mean (SD)
1996	29603 (10674)	4019 (1420)	4658 (1649)	2563 (907)
1997	29404 (10336)	3992 (1379)	4627 (1602)	2958 (1024)
1998	29652 (10534)	4029 (1409)	4668 (1636)	6709 (2352)
1999	29736 (10604)	4036 (1415)	4678 (1643)	2858 (1004)
2000	29452 (10157)	4002 (1354)	4638 (1573)	7582 (2571)
2001	29272 (10662)	3972 (1421)	4604 (1651)	4626 (1659)
2002	29536 (10215)	4012 (1362)	4650 (1581)	9950 (3384)
2003	29265 (10553)	3973 (1406)	4604 (1633)	819 (290)
2004	30089 (10492)	4083 (1402)	4732 (1628)	3809 (1311)

Incorporating the effect of soil type (as *SPR* determined by the dominant HOST class in each cell of the catchment) has the effect of increasing the overall export from the catchment. This is due to the fact that the majority of the catchment is one HOST class. The soil weighting factor (*SWF*) was defined in Chapter 3 as

$$SWF = \left(\left[\frac{\max SWF - \min SWF}{\max SPR - \min SPR} \right] * SPR \right) + SWFi$$

Equation 5.1

where

$\max SWF$ = maximum *SWF*, as defined by the model user; default = 0.8

$\text{min}SWF$	= minimum SWF , as defined by the model user; default = 1.2
$\text{max}SPR$	= maximum SPR value in catchment = 39.7 for Leet
$\text{min}SPR$	= minimum SPR value in catchment = 29.2 for Leet
SPR	= SPR value for specific cell
$SWFi$	= SWF intercept = -0.31 for Leet

In the Leet catchment, there are 3 dominant HOST classes. HOST class 6 (with $SPR = 33.8\%$, resulting $SWF = 0.97$) covers 3% of the catchment, HOST class 17 (with $SPR = 29.2\%$ and $SWF = 0.80$) covers 7% of the catchment and HOST class 24 (with $SPR = 39.7$ and $SWF = 1.20$) covers the remaining 90% of the catchment. Thus, P export is enhanced by soil type in 90% of the catchment. Given that the original intention was to use the effect of soil as a within-catchment weighting only, the method of inclusion needs to be reviewed and perhaps the area covered by each HOST class included into the calculation of the soil weighting factor. Since the HOST classes remain constant in the catchment between years, any variation is due to the random sampling of land use export coefficients.

Only when HER is considered, does the model generate any significant variation in year-to-year model predictions.

5.8.2. Spatial Results

The spatial distribution of P export from the catchment is shown in Figures 3.34 and 3.35 (for 1996 and 2000 as examples).

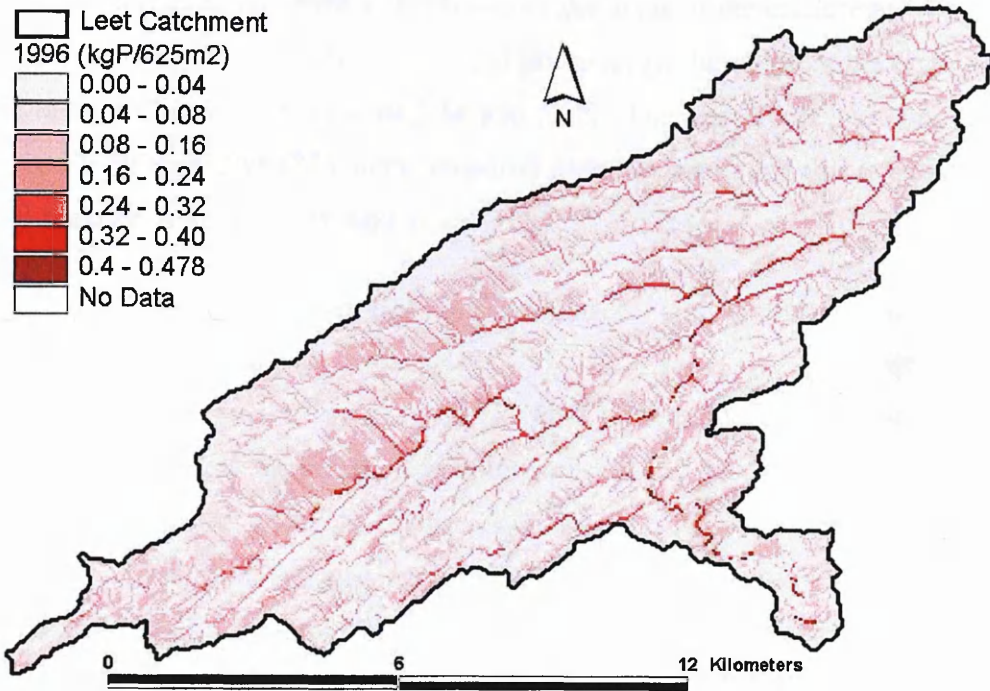


Figure 5.34. Spatial distribution of predicted P export from the Leet catchment, 1996.

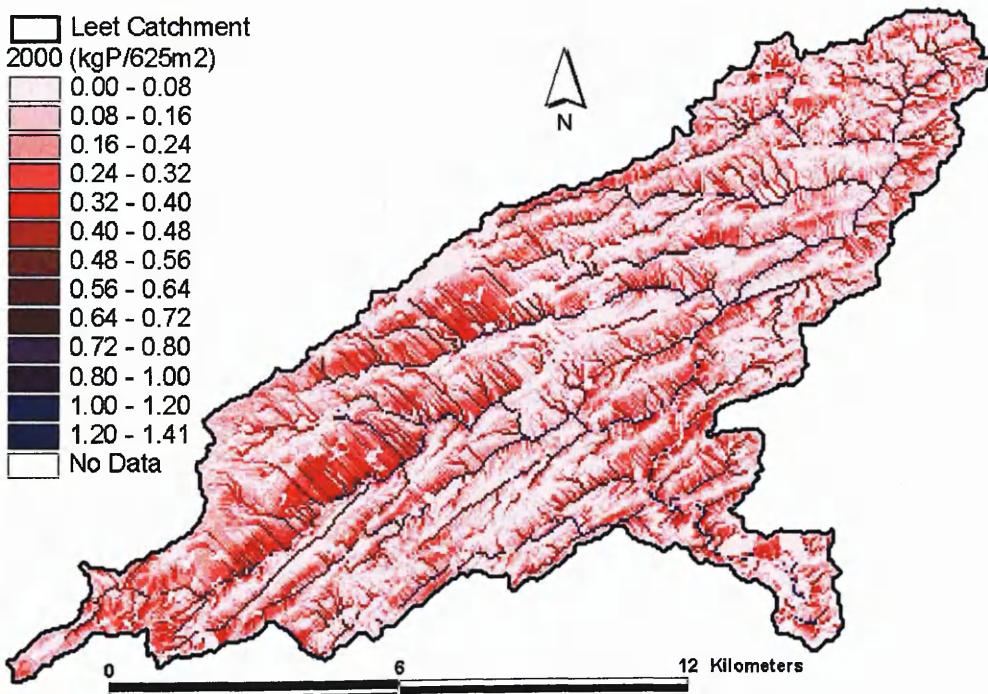


Figure 5.35. Spatial distribution of predicted P export from the Leet catchment, 2000.

In each year, the spatial distribution clearly shows the areas of the catchment where P export is most likely to affect watercourse exposure to phosphorus. In addition, the effect of rainfall can also be appreciated from Figures 5.34 and 5.35. The year 2000 had approximately 3 times as much *HER* as 1996 (323.5mm compared with 108.9mm) and this is manifested as an increased P export from the catchment as a whole.

5.8.3. Assessment of model performance

In considering model performance, it should always be remembered that the estimated measured annual load is uncertain. It is therefore difficult to assess the accuracy of the predictions with much confidence. However, assuming that the estimated loads are a fair representation of the actual annual loads, the SEPTIC model has mixed success in predicting the P load from the Leet catchment in 1996 – 2004. For most years, the model predicts annual P export and the inter-annual variability thereof reasonably well. There is a significant overlap between the standard deviation of the predicted load and the average estimated load in all years except 2002 and 2003. Given that this is an uncalibrated model with limited data input requirements, SEPTIC provides a good initial approximation of predicted annual P loads.

A main benefit of the SEPTIC model is its spatially distributed output. This identifies “sensitive areas” (i.e. areas where relatively large amounts of P exported are likely to contribute to the P load in the watercourse) in the catchment and allows land management strategies to be targeted appropriately.

There are areas of the model which would benefit from further consideration (e.g. the incorporation of the effect of soil type and *HER*) and this shall be discussed in Chapter 6.

Chapter 6. Discussion

6.1. Summary of overall aims

The aim of this work was to produce a model which will aid land managers in quantifying diffuse-source P losses from catchments. In doing so, secondary objectives included the potential for identifying catchments which have a high risk for relatively high diffuse-source P export and to identify areas within catchments which could generate disproportionately high fluxes. The starting point was the simple P export coefficient model. This model has been applied successfully to some UK catchments (e.g. the Windrush and Slapton catchments by Johnes & O'Sullivan, 1989; Johnes, 1996; Johnes et al, 1996; Johnes & Heathwaite, 1997). Owing largely to its simplicity, the export coefficient model has great value in identifying whether a catchment, as a whole, is likely to export P at levels which may be detrimental to the aquatic environment.

The basic export coefficient model described by Johnes (e.g. Johnes & O'Sullivan, 1989) is catchment-specific in that export coefficients selected for each land use within the catchment are calibrated to produce best agreement with measured export data. Provided land use is the most important driver for P export, the model can be used to explore the effects of land use change scenarios on future P exports and has also been used to explain historical changes in P losses associated with concurrent land use change. However, the calibration procedure precludes universal application of the model, except in a screening capacity, without a new fit for each catchment. This problem was addressed in this thesis by employing Monte Carlo simulation to randomly sample export coefficients for each land use from probability distributions constructed from the range of observed P exports, thus avoiding the need for calibration.

A further limitation of the basic model is the fact that it contains no spatial referencing. All areas of the catchment with identical land use are treated in the same way (regardless of slope, contributing area, proximity to water courses and soil type). As a result, it can provide no information of where in the catchment P hot-spots (areas which are most likely to export large amounts of P) are located. A fundamental feature of the work described here was the

application of GIS to allow the production of a spatial picture showing areas at most risk in terms of P loss, as governed by the influence of slope, contributing area, distance to stream and soil type.

Finally, the assumptions underlying the basic model do not explicitly recognise the role of hydrology in the movement of P, although it could be argued that this is implicit in the definition of the coefficients. This work aimed to address this issue, albeit rather simplistically, by including changes in annual rainfall and annual evapotranspiration.

6.2. Model performance

Before beginning to discuss model performance, it is valuable to re-iterate that caution must always be employed when assessing model predictions by comparison with measured data. P concentrations (which are used in conjunction with daily mean flow data to estimate P loads) tend to be measured infrequently and this can have a detrimental effect on the accuracy of the estimated annual P load. Of course, the issue of sampling error is not restricted to P nor to diffuse-source pollutants. Examples of papers highlighting the potential problems associated with grab sampling in systems dominated by point-source water quality controls include Whelan *et al* (1999) and Hazleton (1998). Webb *et al* (1997) have also highlighted the issue for suspended sediment sampling. Patterns of suspended sediments transport are likely to have many factors in common with TP transport. Rekolainen *et al* (1991) reported serious underestimation of annual P losses (especially PP) in small streams when utilising infrequent discrete sampling strategies compared to more intensive sampling. The episodic nature of P transport (particularly from diffuse-sources) means that intensive sampling is usually needed to give reliable estimates of P losses (Grant *et al*, 1996). However, with the exception of a limited number research sites, there is a general lack of long-term intensive sampling and consequently it is common to make annual load estimates from inadequate data. Any comparison of model predictions with measured data should therefore bear in mind that lack of agreement between model and measured loads could be a result of poor measured data and not necessarily poor model performance.

The first step in developing the basic export coefficient was to introduce a stochastic element into the selection of land use export coefficients. This had two benefits: (1) an avoidance of

using calibrated export coefficients and (2) an explicit recognition of the uncertainty in these coefficients. Referring to Table 2.5, when considering crops alone, the model grossly over-predicted (by approximately 5 times) the measured data. Including the effects of slope and cumulative area (which is a surrogate for proximity to watercourse), improved the model predictions such that they were within the same order of magnitude as the measured loads. Incorporation of soil type had little additional effect on the total load from the catchment because it was included in a way that provided primarily within-catchment weighting. Including hydrologically effective rainfall (*HER*) had the desired effect of capturing the majority of year-to-year variability in exported P, with model predictions now within the standard error on the mean of the measured loads in the Greens Burn catchment. These results were therefore encouraging and further work confirmed that it could also be applied using readily available data (i.e. the model is insensitive to many catchment-specific variables).

The SEPTIC model was then applied to a second catchment (The Leet), with mixed results. Given this model is entirely uncalibrated, there is some encouragement in the fact that, with the exception of 2002 and 2003, the model predictions are in the same order of magnitude as the estimated measured loads. In many years there is an overlap between the standard deviation of the predicted load and the standard error of the mean of the estimated measured load. The main points of concern were the incorporation of soil type and rainfall effects, as mentioned in Chapter 5 and discussed in more detail below.

It is important to underline that apparent model accuracy is not a guarantee that all salient drivers have been incorporated appropriately. A model can work well for the wrong reasons or may work well only within a limited range of application (Michaud & Sorooshian, 1994). Greater conviction in the performance of SEPTIC could be achieved from applying the model to additional years for the catchments considered (currently 4 years for the Greens Burn and 9 years for the Leet). In addition, the model should be applied to more catchments to allow performance and general applicability to be assessed.

In addition to eliminating the need for model calibration and the explicit recognition of uncertainties using Monte Carlo simulation, the main benefit delivered by the SEPTIC model

is the ability to identify a spatially-explicit measure of P export “risk” within a catchment through the incorporation of slope, cumulative area and soil type. The maps of within-catchment P export which are generated can give the land manager a visual idea of where management strategies aimed at minimising P loss should be targeted (Murdoch *et al*, 2005, see Appendix 4). This feature fills a gap in the toolset currently available to environmental managers for assessing and attempting to tackle diffuse-source P losses.

Recently published research (Heathwaite *et al*, 2005) outlines a tiered approach to predicting annual P loss from catchments, taking into account the quality and detail of available input data. This ranges from Tier 1 (a basic “risk screening” approach), which is based on export coefficients for different land cover and animal types, to Tier 2 (the “pressure delivery risk screening” (PDRS) matrix approach), which incorporates the effects of soil type, slope of land, rainfall and distance of the land from a watercourse, to Tier 3 (the “phosphorus indicators tool” (PIT)) which uses 108 coefficients to describe the process of annual P export in a three layer structure (loss potential P – transferred P – delivered P) at 1km² scale. The detail of PIT is described in Heathwaite *et al* (2003) and Lui *et al* (2005). Tier 2 of this modelling approach is very similar to SEPTIC in that it identifies areas within a catchment which are most at risk of significant P loss, although it only gives relative risk (0-9).

6.3. Further work on model

In applying the model to both the Greens Burn and Leet catchments, it has become clear that certain assumptions which have been made would benefit from further consideration and these are discussed below.

6.3.1. Soil type

The effect of soil type is included in SEPTIC as a relative moderator of P export. Each soil class in the catchment is distinguished by an *SPR* value defined by HOST (Boorman *et al*, 1995). With the readily available data, it is the dominant HOST class (and hence dominant *SPR* value) that is assigned to each soil class. The *SPR* values are then related to the others within the catchment to give a weighting factor such that soils with higher *SPR* values are likely to export more P than soils with lower *SPR* values. This method is simple to apply and

can be replicated easily for other catchments, at least in the UK. However although it captures the principal hydrological differences between soils, it fails to characterise other essential factors which may influence P loss, such as P availability (in solid or dissolved fractions).

Heathwaite *et al* (2003) also used the HOST classification. They attempted to apportion P transfer to surface and sub-surface pathways by calculating the volume of water moving along each pathway from *HER* multiplied by the proportion of flow along that pathway. Further investigation into whether HOST could be used in this way (i.e. multiply *HER* by *SPR*) in SEPTIC is desirable. This would give an absolute (as opposed to the currently relative) estimate of the propensity of the soil to generate surface runoff and, hence, sediment associated P.

6.3.2. Rainfall and runoff

Currently, SEPTIC includes the effect of rainfall by rather simplistically considering the annual *HER*. This approach has also been utilised elsewhere (e.g. Heathwaite *et al*, 2003). The assumption made in this work is that in wetter years, more surface and subsurface runoff is likely. Increased runoff is well recognised as an important regulator of P loss, both in dissolved and colloidal phases (principally in the subsurface) and attached to sediment (via overland flow). However, it is likely that high magnitude, low frequency storm events will transport a disproportionately high fraction of the total annual P export. This will not be captured using an estimate of annual total runoff. Nash *et al* (2000), for example, found that 72% of TP exported from the Darnum site, Australia, was transported in just 25% of storms. The results of the field work, documented in Chapter 4, also showed that a few high magnitude storms could generate significant erosion. It would therefore be more meaningful to include more detailed information about the nature of rainfall occurrence in the model. In addition to the size of storms, antecedent conditions and recent storm history are also important. Storms occurring when soils are dry are likely to move less P than those occurring when the soil is wet since less runoff will be generated.

One way in which these factors could be incorporated is to consider erosive storm energy. Soil detachment by incident rain has been found to be crucial in moving sediment-associated

P in surface runoff (James & Alexander, 1998; Heathwaite & Dils, 2000; Morgan, 2001) and in field drains (Addiscott *et al*, 2000). Detachment can be estimated as a function of rainfall kinetic energy (E_K). Using a well-established calculation (Marshall & Palmer, 1948), Davidson *et al* (2005) calculated rainfall E_K from hourly rainfall data for 11 Meteorological Office sites in England and Wales. When the resulting hourly E_K and rainfall quantities were summarised to daily totals, they found a close positive relationship existed between daily rainfall and daily E_K . Generally, they found that rainfall E_K per mm of daily rainfall was higher in autumn months (indicating that autumn rainfall events tend to be more intense) whilst in winter months, rainfall tends to be more prolonged but less intense. The variations in rainfall E_K between the 11 locations were largely attributable to the variations in total rainfall and not due to geographical location. This suggests that this approach would be transferable to other sites within the UK. If daily rainfall data are not available, Davidson *et al* (2005) also describe a method of estimating rainfall E_K from monthly climate data (monthly rainfall and number of rain days) which only increased the errors slightly compared to using detailed rainfall data for the same sites. Such an approach could be incorporated into the SEPTIC model. This would have the benefit of including seasonality, although it would be best accompanied by more detailed land use data detailing the extent crop cover throughout the year. The latter could be achieved using simple interpolations between marker values on key dates indicative of tillage, sowing, crop emergence, maximum growth and harvest dates.

An alternative method of incorporating more detailed rainfall information into the model is described by Kottegoda *et al* (2003) in which a disintegration model is used to produce storm-related rainfall from daily rainfall time series.

The potential of the climatic index for soil erosion potential (CSEP) for characterising rainfall-driven erosion could also be explored (Kirkby & Cox, 1995). This method integrates the effect of daily rainfall totals with a threshold-based prediction overland flow. A linear accumulation of discharge downslope and a power law relating sediment transport capacity to overland flow discharge are also assumed. The CSEP also considers analytical expressions for integrated runoff frequency distributions which could have been incorporated into SEPTIC using Monte Carlo simulation.

The inclusion of a more detailed characterisation of rainfall and runoff (and the introduction of seasonality) would be relatively straightforward and would not require unreasonable amounts of extra data. This activity should be explored as a priority in any further developments of the work, possibly as part of a more detailed set of predictions in a tiered P modelling framework (simple screening approach followed by more detailed, data intensive, analysis where required).

6.3.3. Connectivity

The routing of P from the point of mobilisation to the point of delivery to channelised flow is complex (e.g. Haygarth *et al*, 2005). For example, part of this work looked at the effect of field boundaries. Under the right circumstances (e.g. potatoes in a sloping field in a stormy year), there can be significant deposition which will retain P. On a local scale, these fields are important. However, on the catchment scale, their effects may be negligible (given the few number of fields in the catchment studied (Greens Burn) that exhibited substantial deposits) and it is questionable whether there is benefit to including extra detail in the model to account for them.

However, the presence of field boundaries will alter flow direction (and hence accumulation) in a catchment. Initial enquiries into this issue involved creating a 5m DTM with field boundaries added (the field boundaries were assumed to be 1.5 m high and solid). The flow accumulation (shown as the natural log of the specific area) in the North-east of the catchment resulting from using the DTM and the DTM with field boundaries are shown in Figures 6.1 and 6.2.

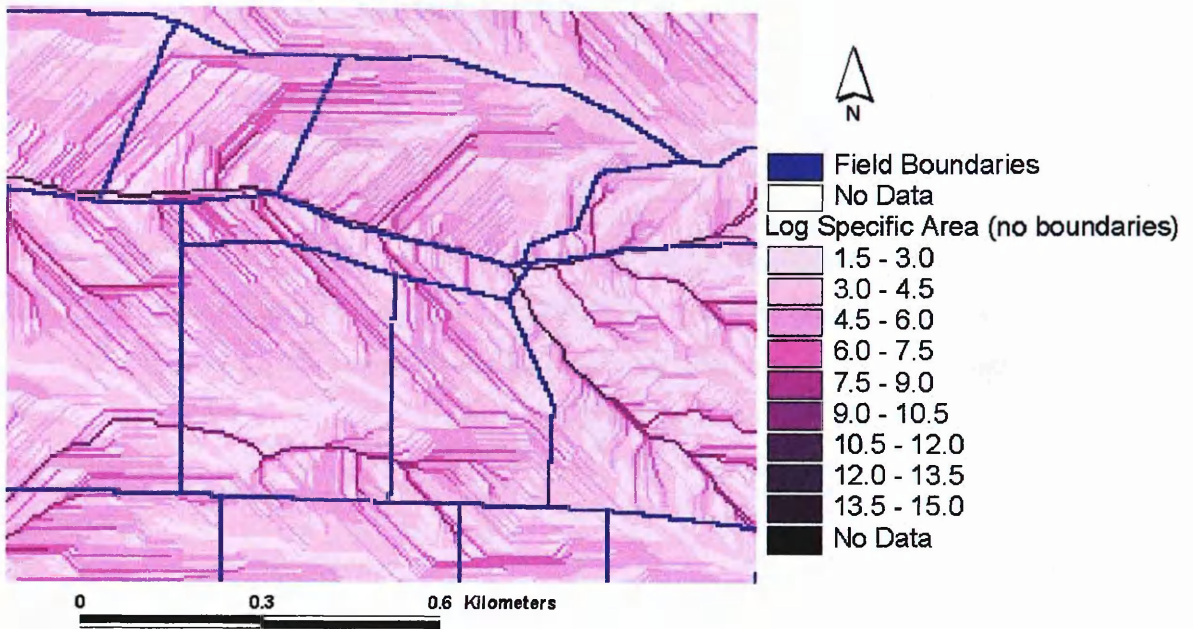


Figure 6.1. Natural log of specific area without including the effects of field boundaries in the DTM.

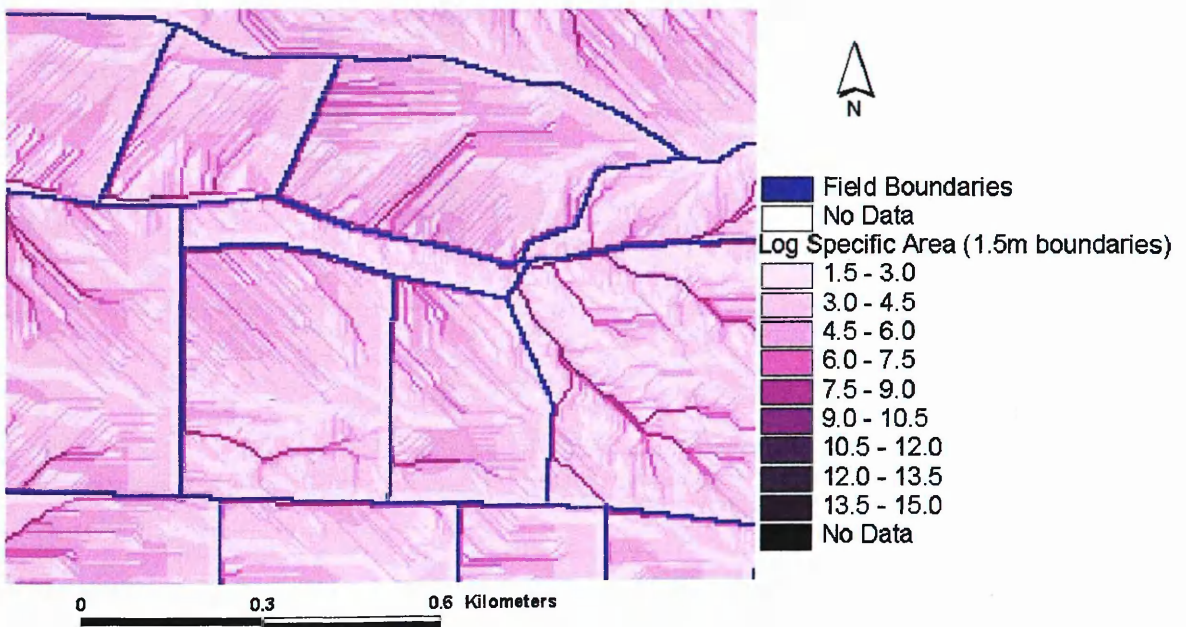


Figure 6.2. Natural log of specific area when field boundaries are added onto the DTM.

The effect of the field boundaries is to re-route flow and so change the pattern of flow accumulation. The assumption of solid, 1.5 m high boundaries is unrealistic and further work would need to include allowing the boundaries to vary in height and have different degrees of permeability. However, given that cumulative area is used in the model, it would be

interesting to model the P export for different cumulative area patterns (resulting from assuming different boundary conditions).

6.3.4. Selection of export coefficients – different distributions

In the absence of any catchment specific data and following the example of Hession & Storm (2000), the model assumed that the distribution of the measured export coefficients was uniform. Following the collation of additional measured coefficients, the distributions were plotted, as shown in Figures 6.3 and 6.4, for arable (cereals and row crops) and grassland respectively.

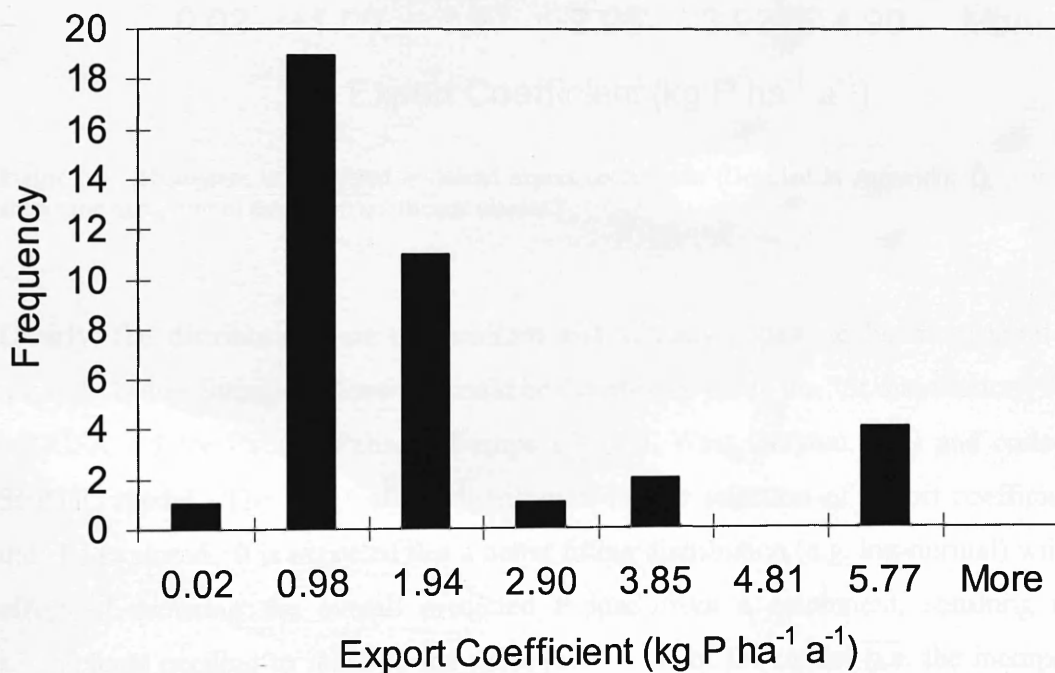


Figure 6.3. Histogram of measured arable (cereals and row crops) export coefficients (Detailed in Appendix 1), n = 38. (x-axis shows the mid-point of the export coefficient classes.)

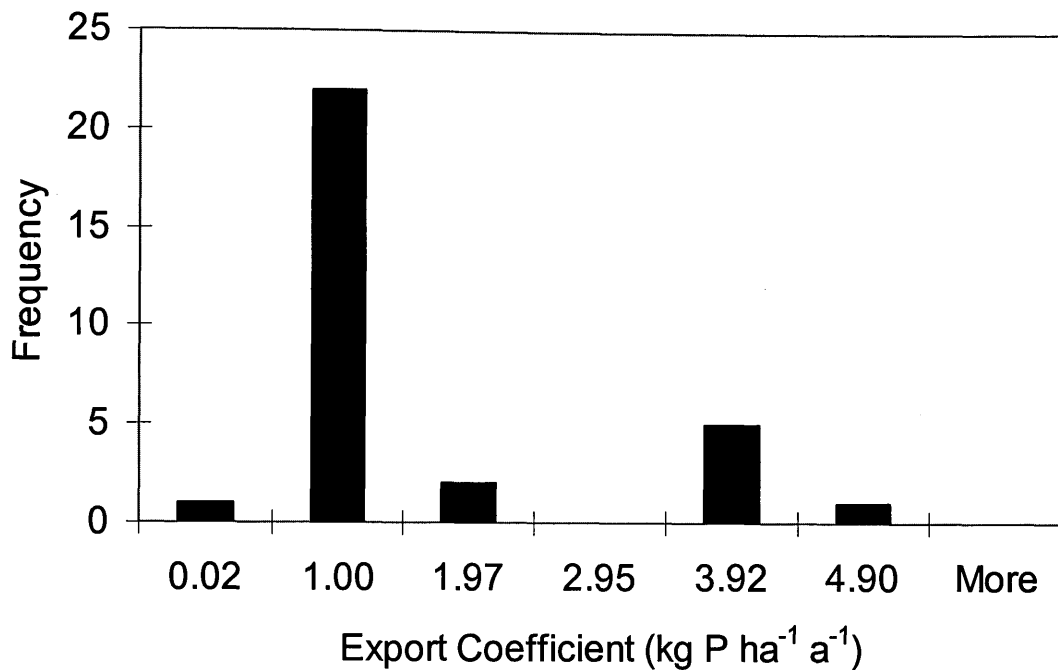


Figure 6.4. Histogram of measured grassland export coefficients (Detailed in Appendix 1), $n = 31$. (x-axis shows the mid-point of the export coefficient classes.)

Clearly, the distributions are not uniform and visually appear to be more similar to log-normal. Better fitting distributions could be determined using the “fit distribution” function in “@RISK 4.5 for Excel” (Palisade Europe UK Ltd, West Drayton, UK) and coded into the SEPTIC model. The effect of the distribution for the selection of export coefficients could then be explored. It is expected that a better fitting distribution (e.g. log-normal) will have the effect of reducing the overall predicted P load from a catchment, resulting in further adjustments needing to be made to the subsequent steps of the model (i.e. the incorporation of slope, cumulative area, soil type and rainfall).

6.4. Issues not included in model

6.4.1. Artificial drainage

The underlying assumptions employed in the SEPTIC model have been largely based (at least implicitly) on the received opinion of many workers in the field that the main pathway for P loss from agriculture is via surface runoff with eroded soil carrying adsorbed P with various degrees of availability (in terms of desorption) (Johnes *et al*, 1996; Johnes & Heathwaite, 1997; McGechan *et al*, 2005). It was generally believed that in the subsurface, most dissolved

P is efficiently sorbed to the soil solid matrix and thus cannot be transported to artificial drainage in leachate or to surface waters via throughflow. This assumption is supported by the research of Haygarth *et al* (1998), which showed that field drains can reduce the transfer of TP by approximately 30%, compared to undrained soil. More recent research, however, has shown that in some circumstances there can be appreciable losses of P via field drains (e.g. Addiscott *et al*, 2000; Gardner *et al*, 2002; McGechan *et al*, 2005). This has significant implications in the UK where most arable or improved grassland is artificially drained by mole-drains and tile-drains. Drains are now considered to be a major source of phosphorus in stream water in the UK (Gardner *et al*, 2002).

Heavy, clay-rich soils are liable to cracking and macropore formation, establishing preferential flow routes (Beven & Germann, 1982; Addiscott *et al*, 2000). Preferential flow can also take place in very wet conditions in well aggregated soils via water filled inter-aggregate spaces (e.g. McGechan, 2003). Macropores have a smaller solid surface area to volume ratio (wetted perimeter to cross-sectional area) so that they have faster flow and are less able to sorb dissolved phosphate and due to lower contact times. In addition, sorbed phosphate carried on small solid material detached from the soil matrix (clay and colloidal material) can also move through larger pores. Results from arable plot experiments show that, despite the expectation that heavy clay soils should retain phosphate effectively, appreciable losses via drains can be observed (Addiscott *et al*, 2000). These results contrast with grassland plot experiments which suggest that lower phosphate losses from field drains can be expected (Cooke, 1976, Haygarth *et al*, 1998). One reason for this difference could be that the cultivation of arable soils make them more vulnerable to detachment compared to grassland soils, which tend to have a more stable soil structure in the near surface horizons. However, if the grassland is grazed into late autumn, or given an application of slurry (when the soil is wet), substantial P losses can occur compared to almost negligible losses when the soil is dry (i.e. when colloids, and their associated P, enter smaller soil pores and become trapped) (McGechan, 2003).

Although, identifying the location and intensity of field drainage networks can be difficult and costly (Gardner *et al*, 2002), inclusion of a field drainage component could be considered using a conceptual approach (e.g. along the lines of the TOPMODEL-based ideas outlined Whelan *et al* (2002). Inclusion of field drains in the model would need to be justified against

the primary objective of allowing land managers to identify areas in a catchment most likely to be at risk of P loss. However, when assessing the performance of the model, the possible occurrence and effect of field drains should be considered.

6.4.2. In-stream changes

The SEPTIC model assumes that once P has reached the channel system, it will be transferred to the catchment outlet. In reality, however, a number of in-stream processes are likely to operate which can modify P concentrations in the water column. Many of these processes exhibit a strong seasonal pattern of P retention (e.g. biological uptake by growing macrophytes and algae in summer and release of stored material in winter). These interactions are likely to have a greater influence over P concentrations in the river in low-flow (summer) conditions than under high flow (winter) conditions (May *et al*, 2001). Cooper *et al* (2002a) detail an in-stream modelling approach which uses a kinematic wave equation to model in-stream flow, advection to approximate the transfer of suspended sediment and phosphorus components and includes mechanisms for in-stream source and sinks of P (SRP and PP). Inclusion of in-stream processes in the model would probably only make sense at temporal scales of less than one year (i.e. including seasonality). At the annual time-step currently used, seasonal adjustments to the in-stream flux should even out over the year to a large extent. This said, one issue which could still be important is the input which seasonal processes may have on measured P concentrations and the consequent impact on comparisons with model predictions. All things considered, in-stream processes are probably not as important as other factors, given the scope and level of complexity of SEPTIC.

6.5. The value of SEPTIC

Although complex processes are involved in P transfer, there is a need to limit this complexity in catchment-scale, management orientated, models. Such models should also be transferable and operate at an appropriate scale (Dunn & Ferrier, 1999; Dunn, 1999).

More complex models generally have more parameters and hence require more parameter estimation. Many models have parameters which are costly or difficult to estimate independently and consequently either default values are adopted or values are derived using

some sort of optimisation (calibration). In either case, but particularly in the latter, physically-based parameters can lose their meaning/relevance to the process they purport to represent and a mechanistic model can become more like a “black box”. This argument has been explored in important commentaries by Beven (1993) on the nature of physically based, spatially distributed hydrological models. Even where parameters can be estimated by independent, empirical means (e.g. derived using laboratory columns of homogenous soil), the conditions of the test system may not be representative of those in the field (Grayson *et al*, 1992). In some circumstances, simple models can be as accurate as complex models (e.g. Michaud & Sorooshian, 1994).

In discussing possible improvements/changes to the model, the purpose and benefits of the SEPTIC approach should not be forgotten. SEPTIC was constructed to use readily available data to predict P export from a catchment. The model is simple by design, allowing ease of application to existing and new catchments and computing time is very short, even when Monte Carlo simulation is used. The output gives a range of predicted P export (based on the uncertainty in the selection of export coefficients from the wide range published in the literature), with the range capturing the measured P load in the catchments and years investigated in this work. This allows an environmental manager a quick, first approximation of the potential P export from a catchment, including an idea of the uncertainty, and if this is deemed problematic, to investigate some of the factors which could be responsible. In particular, the spatial output from SEPTIC allows phosphorus hot-spots in the catchment to be identified and consequently can help remedial actions to be targeted accordingly. Various scenarios (management options e.g. arable areas converted to unimproved grassland) can be input into the model and their effectiveness evaluated before implementation. Hence a “screening” model such as this has value in that it allows resources (time and money) to be apportioned more appropriately.

Chapter 7. Conclusions

Phosphorus is a limiting nutrient in many surface waters. Increases in P loading from both point and diffuse sources can, therefore, result in increased primary productivity and associated problematic growth of algae and aquatic macrophytes. Numerical modelling can play an important role in understanding the factors controlling diffuse-source transfers of P and in exploring the potential changes which can be expected as a consequence of management (e.g. land use change, introduction of buffer zones etc.).

The model developed in this thesis (SEPTIC) is specifically designed to be used as a management tool and to be widely applicable (at least in the UK) using a minimal input dataset. It is based on extensions to the simple basic export coefficient approach which is commonly applied as a screening tool by UK environmental management authorities (e.g. The Environment Agency of England and Wales and The Scottish Environmental Protection Agency).

The basic export coefficient model has the advantage of requiring parsimonious input data to produce predictions of P export from catchments. However, in its original format, the selection of export coefficients was catchment specific, usually obtained by optimising the “fit” between predicted and observed fluxes. In order to avoid the need for calibration, and hence make the model more universally applicable, Monte Carlo simulation was employed to randomly select export coefficients from probability distributions constrained by the range of published export coefficient values. When run for a large number of iterations, the model output not only predicts the most likely P load from a catchment but also quantifies the uncertainty associated with the prediction. This gives land managers a more realistic perspective of the uncertainty about the model output and, in principle, allows them to better evaluate the effect of different management strategies within the context of other drivers (climate, topography etc.).

When run with uniform distributions of export coefficients, the unconstrained export coefficient model was found to significantly over-predict P export from the two catchments

studied. However, when key catchment variables known to govern P export were included i.e. topography (slope and cumulative area from the divide), soil type and hydrologically effective rainfall, the model gave reasonable agreement with estimated loads derived from measured concentration and flow data. The resulting model was called SEPTIC (Stochastic Estimation of Phosphorus Transfer In Catchments).

Most models of material transfer from land to water take little, if any, account of the connectivity between landscape elements and the receiving watercourse. This is the case for so-called process models (such as SWAT) as well as for simpler empirical approaches. However, it is believed by many that discontinuities in flow pathways can result in inefficient delivery of material to the catchment outlet, especially at short time scales (storm event to annual).

Field work was carried out to assess the need to explicitly include the effect of field boundaries into the model. Field boundaries have been hypothesised to act as filters for P along hillslope flow pathways. Although sediment (and associated P) deposition was observed in the fields studied and may be of local importance, on a catchment level the occurrence of field boundary deposits was limited. Field boundaries were deemed not to be important enough to require inclusion in the model.

The reasonable coincidence between model predictions and empirically derived annual P exports was encouraging, particularly given the unconstrained nature of the simulations (no calibration) and the relatively simplistic assumptions employed. However, confidence in the model could be improved by 1). Better measured data. There is a high degree of uncertainty in the estimated measured loads due to infrequent sampling and, in the case of the Leet, the absence of TP data meant that TP loads had to be estimated from o-P data); 2). Running the model for more years in each catchment and 3). Applying the model to more catchments.

There is room for improvement, namely in how soil type and hydrological controls are represented in the model and in the distributions used for the selection of the export coefficients, as discussed in Chapter 6. In addition, there is scope to include additional sophistication into the model by including, for example, the effects of seasonality, in-stream

processes and artificial field drainage systems. As the model is applied to a wider set of scenarios (catchments, years) with different conditions and controlling factors, details of the developments which will be required will become apparent.

In its present form, SEPTIC appears to provide a reasonable first approximation for the prediction of P loss from a catchment, including an appreciation of the uncertainty in the model predictions resulting from key uncertainties in the input variables. In addition, its spatially-referenced output allows P hot spots in the catchment to be identified, allowing the targeting of resources (be that more detailed modelling or practical mitigating measures) by land managers.

References

- Addiscott T.M., Brockie D., Catt J.A., Christian D.G., Harris G.L., Howse K.R., Mirza N.A. & Pepper T.J. (2000).** Vadose zone processes and chemical transport: phosphate losses through field drains in heavy cultivated soil, *Journal of Environmental Quality*, **29**, 522-532.
- Alexander R.B., Johnes P.J., Boyer E.W. & Smith R.A. (2002).** A comparison of models for estimating the riverine export of nitrogen from large watersheds, *Biogeochemistry*, **57/58**, 295-339.
- Allen S.E. (ed) (1989).** *Chemical Analysis of Ecological Materials*, 2nd Edition, Blackwell Scientific Publications, Oxford, U.K., pp. 368.
- Arheimer B. & Lidén. (2000).** Nitrogen and phosphorus concentrations from agricultural catchments – influence of spatial and temporal variables, *Journal of Hydrology*, **227**, 140-159.
- Arnold J.G., Allen P.M. & Bernhardt G. (1993).** A comprehensive surface-groundwater flow model, *Journal of Hydrology*, **142**, 47-69.
- Beaulac M.N. & Reckhow K.H. (1982).** An examination of land use – nutrient export relationships, *Water Resources Bulletin*, American Water Resources Association, **18**, (6), 1013-1024.
- Beuselink L., Steegen A., Govers G., Nachtergaele J., Takken I. & Poesen J. (2000).** Characteristics of sediment deposits formed by intense rainfall events in small catchments in the Belgium loam belt, *Geomorphology*, **32**, 69-82.
- Beven K. & Kirkby M.J. (1979).** A physically-based, variable contributing area model of basin hydrology. *Hydrological Science Bulletin*, **24**, 43-69.
- Beven K. & Germann P. (1982).** Macropores and water flow in soils, *Water Resources Research*, **18**, (5), 1311-1325.
- Beven K. (1993).** Prophecy, reality and uncertainty in distributed hydrological modeling, *Advances in Water Resources*, **16**, (1), 41-51.
- Beven K. (1997).** Topmodel: a critique. *Hydrological Processes*, **11**, 1069-1085.
- Boorman, D.B., Hollis, J.M. & Lilly, A. (1995).** *Hydrology of soil types: a hydrologically-based classification of the soils of the United Kingdom*, Report No. 126, Institute of Hydrology, Wallingford, U.K.
- Brady N.C. & Weil R.R. (1999).** *The Nature and Properties of Soils 12th Ed.*, Prentice Hall, New Jersey, U.S.A.
- Caruso B. S. (2000).** Integrated assessment of phosphorus in the Lake Hayes catchment, South Island, New Zealand, *Journal of Hydrology*, **229**, (3-4), 168-189.

- Cassell E. A. & Clausen J. C. (1993).** Dynamic simulation modeling for evaluating water-quality response to agricultural BMP implementation, *Water Science and Technology*, **28**, (3-5), 635-648.
- Clayton J.W. (1997).** The biology of the River Tweed, *Science of the Total Environment*, **194/195**, pp. 155-162.
- Cooke G.W. (1976).** A review of the effects of agriculture on the chemical composition and quality of surface and underground waters, *MAFF Technical Bulletin 32*, pp.5-57.
- Cooper D.M., House W.A., Reynolds B., Hughes S., May L. & Gannon B. (2002a).** The phosphorus budget of the Thame catchment, Oxfordshire: 2. Modelling, *Science of the Total Environment*, **282-283**, 435-457
- Cooper D.M., House W.A., May L. & Gannon B. (2002b).** The phosphorus budget of the Thame catchment, Oxfordshire, UK:1. Mass Balance, *Science of the Total Environment*, **282-283**, 233-251.
- Crawford A.** East of Scotland Water, *pers comm*, August 2000.
- Davidson P., Hutchins M.G., Anthony S.G., Betson M., Johnson C. & Lord E.I. (2005).** The relationship between potentially erosive storm energy and daily rainfall in England and Wales, *Science of the Total Environment*, **344**, 15-25.
- Desmet P.J.J. & Govers G. (1995).** GIS-based simulation of erosion and deposition patterns in an agricultural landscape: a comparison of model results with soil map information, *Catena*, **25**, 389-401.
- Dryburgh W.** SEPA, *pers comm*, March 2006.
- Dryburgh W. & Eastwood G. (2005),** *Leet Water Environmental Improvement Plan*, internal document, SEPA.
- Dunn S.M. & Ferrier R.C. (1999).** Natural flow in managed catchments: a case study of a modelling approach, *Water Research*, **33**, (3), 621-630.
- Dunn S.M. (1999).** Imposing constraints on parameter values of a conceptual hydrological model using baseflow response, *Hydrology & Earth System Sciences*, **3** (2), 271-284.
- Dunn S.M. & Lilly A. (2001).** Investigating the relationship between a soils classification and the spatial parameters of a conceptual catchment-scale hydrological model, *Journal of Hydrology*, **252**, 157-173.
- Eghball B., Binford G. D. & Baltensperger D. D. (1996).** Phosphorus movement and adsorption in a soil receiving long-term manure and fertiliser application, *Journal of Environmental Quality*, **25**, (6), 1339-1343.
- ESRI (1996).** *ArcView G.I.S.*, ESRI, California, U.S.A.

- Fisher P., Abrahart R. J. & Herbinger W. (1997).** The sensitivity of two distributed non-point source pollution models to the spatial arrangement of the landscape, *Hydrological Processes*, **11**, (3), 241-252.
- Forster J.C. (1995).** Soil Phosphorus, In Alef K. and Nannipieri P. (eds). *Methods in Applied Soil Microbiology and Biochemistry*, Academic Press, London, pp. 88-93.
- Foth H.D., Withee L.V., Jacobs H.S. & Thien S.J. (1982).** *Laboratory Manual for Introductory Soil Science, 6th Edition*, Wm. C. Brown Company Publishers, Dubuque, Iowa, U.S.A., pp.143.
- Fox I.A. & Johnson R.C. (1997).** The hydrology of the River Tweed, *Science of the Total Environment*, **194/195**, 163-172.
- Foy R.H. & Bailey-Watts A.E. (1998).** Observations on the spatial and temporal variation in the phosphorus status of lakes in the British Isles, *Soil Use and Management*, **14**, 131-138.
- Frossard E., Condon L.M., Oberson A., Sinaj S. & Fardeau J.C. (2000).** Processes governing phosphorus availability in temperate soils, *Journal of Environmental Quality*, **29**, (1), 15-23.
- Fraser A.I., Harrod T.P., Haygarth P.M. (1999).** The effect of rainfall intensity on soil erosion and particulate phosphorus transfer from arable soils, *Water Science and Technology*, **39**, 48-54.
- Frost A. (1993).** *Soil Erosion: Loch Leven Catchment*, SAC, Edinburgh, UK.
- Fuller R.M., Smith G.M., Sanderson J.M., Hill R.A., Thomson A.G. (2002).** The UK Land Cover Map 2000: construction of a parcel-based vector map from satellite images, *Cartographic Journal*, **39**, (1), 15-25.
- Gardner C.M.K., Cooper D.M. & Hughes S. (2002).** Phosphorus in soils and field drainage water in the Thames catchment, UK, *Science of the Total Environment*, **282-283**, 252-262.
- Grant R., Laubel A., Kronvang B., Andersen, H.E., Svendsen L.M. & Fuglsang A. (1996).** Loss of dissolved and particulate phosphorus from arable catchments by subsurface drainage, *Water Resources*, **30**, (11), 2633-2642.
- Grayson R.B., Moore I.D. & McMahon T.A. (1992).** Physically based hydrologic modelling 2. Is the concept realistic? , *Water Resources Research*, **26**, (10), 2659-2666.
- Haygarth P.M., Hepworth L. & Jarvis S.C. (1998).** Forms of phosphorus transfer in hydrological pathways from soil under grazed grassland. *European Journal Soil Science*, **49**, 65-72.
- Haygarth P.M., Condon L.M., Heathwaite A.L., Turner B.L. & Harris G.P. (2005).** The phosphorus transfer continuum: linking source to impact with an interdisciplinary and multi-scaled approach, *Science of the Total Environment*, **344**, 5-14.

- Hazelton C. (1998).** Variations between continuous and spot-sampling techniques in monitoring a change in river water quality, *Journal of the Chartered Institute of Water and Environmental Management*, **12**, 124-129.
- Heathwaite A.L. (1997).** Sources and pathways of phosphorus loss from agriculture. In *Phosphorus Loss From Soil To Water*, Tunney, H., Carton, O.T., Brookes P.C., Johnston, A.E. (eds), C.A.B. International, Wallingford, U.K., pp. 205-223.
- Heathwaite A.L. & Dils R.M. (2000).** Characterising phosphorus loss in surface and subsurface hydrological pathways, *Science of the Total Environment*, **215**, 523-528.
- Heathwaite A.L., Fraser A.I, Johnes P.J., Hutchins M., Lord E. & Butterfield D. (2003).** The phosphorus indicators tool: a simple model of diffuse P loss from agricultural land to water, *Soil Use and Management*, **19**, 1-11
- Heathwaite A.L., Dils R.M., Liu S., Carvalho L., Brazier R.E., Pope L., Hughes M., Phillips G. & May L. (2005).** A tiered risk-based approach for predicting diffuse and point source phosphorus losses in agricultural areas, *Science of the Total Environment*, **344**, 225-239.
- Hesketh N. & Brookes P.C. (2000).** Development of an indicator for risk of phosphorus leaching, *Journal of Environmental Quality*, **29**, 105-110.
- Hesse P.R. (1971).** *A Textbook of Soil Chemical Analysis*, William Clowes & Sons Ltd, London, pp. 520.
- Hession W. C. & Storm D. E. (2000).** Watershed-level uncertainties: implications for phosphorus management and eutrophication, *Journal of Environmental Quality*, **29**, (4), 1172-1179.
- Higgins P. (2002).** *The Effect of Field Boundaries on Particulate and Phosphorus Transfers*, B.Sc. Dissertation, University of Stirling, U.K., unpublished.
- Holden A.V. (1976).** The relative importance of agricultural fertilizers as a source of nitrogen and phosphorus in Loch Leven, *MAFF Technical Bulletin 32*, pp. 306-314.
- Hooda P.S., Moynagh M., Svoboda I.F., Edwards A.C., Anderson H.A & Sym G. (1999)** Phosphorus loss in drainflow from intensively managed grassland soils, *Journal of Environmental Quality*, **28**, 1235-1242.
- Hope E.G. (2000).** *Development of an export co-efficient model to predict the effects of land use on nutrient loadings from small catchments*, MSc Dissertation, University of Stirling, UK., unpublished.
- Hough M.N. & Jones R.J.A. (1997).** The United Kingdom Metrological Office rainfall and evaporation calculation system: MORECS version 2.0 – an overview, *Hydrological & Earth System Sciences*, **1**, (2), 227-239.

- James P.A. & Alexander R.W. (1998)**, Soil erosion and runoff in improved pastures of Clwdian Range, North Wales, *Journal of Agricultural Science*, **130**, 473-488.
- Jarvie H.P., Neal C. & Withers P.J.A. (2006)**. Sewage-effluent phosphorus: a greater risk to river eutrophication than agricultural phosphorus?, *Science of the Total Environment*, **360**, 246-253.
- Johnes P.J. & O'Sullivan P.E. (1989)**. Nitrogen and phosphorus losses from the catchment of Slapton Ley, Devon – An Export Coefficient Approach, *Field Studies*, **7**, 285-309.
- Johnes P. J. (1996)**. Evaluation and management of the impact of land use change on the nitrogen and phosphorus load delivered to surface waters: the export coefficient modelling approach, *Journal of Hydrology*, **183**, (3-4), 323-349.
- Johnes P., Moss B. & Phillips G. (1996)**. The determination of total nitrogen and total phosphorus concentrations in freshwaters from land use, stock headage and population data: testing of a model for use in conservation and water quality management, *Freshwater Biology*, **36**, 451-473.
- Johnes P.J. & Heathwaite A.L. (1997)**. Modelling the impact of land use change on water quality in agricultural catchments, *Hydrological Processes*, **11**, 269-286.
- Johnes P.J. & Hodgkinson P.A. (1998)**. Phosphorus losses from agricultural catchments. *Soil Use and Management*, **14**, 175-185.
- Johnston A.E. (1976)**. Additions and removals of nitrogen and phosphorus in long-term experiments at Rothamsted and Woburn and the effects of the residues on total soil nitrogen and phosphorus, *MAFF Technical Bulletin* 32, 111-144.
- Kirkby M.J. (1979)**. Implications for sediment transport. In *Hillslope Hydrology*, Kirby M.J. (ed), J. Wiley & Sons, Chichester, pp. 325-363.
- Kirkby M.J. & Cox N.J. (1995)**. A climatic index for soil erosion potential (CSEP) including seasonal and vegetation factors, *Catena*, **25**, 333-352.
- Kottogoda N.T., Natale L. & Raiteri E. (2003)**, A parsimonious approach to stochastic multisite modelling and disaggregation of daily rainfall, *Journal of Hydrology*, **274**, 47-61.
- Liu S., Brazier R. & Heathwaite L. (2005)**. An investigation into the inputs controlling predictions from a diffuse phosphorus loss model for the UK; the Phosphorus Indicators Tool (PIT), *Science of the Total Environment*, **344**, 211-223.
- LLCMP (1999)**. *The Loch Leven Catchment Plan*, March 1999, Perth & Kinross Council.
- Magid J. & Nielson N.E. (2000)**. Seasonal variation in organic and inorganic phosphorus fractions of temperature-climate sandy soils, *Plant Soil*, **144**, 155-165.
- Mainstone C.P. & Parr W. (2002)**. Phosphorus in rivers: ecology and management, *Science of the Total Environment*, **282**, 25-47.

- Maréchal D. & Holman I.P. (2005).** Development and application of a soil classification-based conceptual catchment-scale hydrological model, *Journal of Hydrology*, **312**, 277-293.
- Marshall J.S. & Palmer W.M. (1948).** The distribution of raindrops with size, *Journal of Meteorology*, **5**, 165-166.
- Marsden M.W., Fozzard I.R., Clark D., McLean N. & Smith M.R. (1995).** Control of phosphorus inputs to a freshwater lake: a case study. *Aquaculture Research*, **26**, 527-538.
- Mason C.F. (1996).** *Biology of Freshwater Pollution*, 3rd Edition, Longman, Harlow.
- May L., House W.A., Bowes M. & McEvoy J. (2001).** Seasonal export of phosphorus from a lowland catchment: upper river Cherwell in Oxfordshire, England, *Science of the Total Environment*, **269**, 117-130.
- McDowell R. & Trudgill S. (2000).** Variation of phosphorus loss from a small catchment in south Devon, UK, *Agriculture Ecosystems & Environment*, **79**, 143-157.
- McGechan M.B. (2003).** Phosphorus pollution implications of extending grazing into late autumn, *Grass and Forage Science*, **58**, 151-159.
- McGechan, M.B., Lewis D.R. & Hooda P.S. (2005).** Modelling through-soil transport of phosphorus to surface waters from livestock agriculture at the field and catchment scale, *Science of the Total Environment*, **344**, 185-199.
- Meyer L.D., Dabney, S.M. & Harmon W.C. (1995).** Sediment-trapping effectiveness of stiff-grass hedges, *Transactions of the ASAE*, **38**, (3), 809-815.
- Michaud J. & Sorooshian S. (1994).** Comparison of simple versus complex distributed runoff models on a mid-sized semiarid watershed, *Water Resources Research*, **30**, (3), 593-605.
- MLURI & FRPB (1995).** *PLUS. The Development of a GIS Based Tool for Calculating the Total Phosphorus Load from a Catchment*, The Macaulay Land Use Research Institute, Aberdeen.
- Monteith J.L. & Unsworth M.H. (1990).** *Principles of Environmental Physics*, 2nd Edition, Edward Arnold, pp. 291.
- Morgan, M.A. (1997).** The behaviour of soil and fertiliser phosphorus. In *Phosphorus Loss From Soil To Water*, Tunney, H., Carton, O.T., Brookes P.C., Johnston, A.E. (eds), C.A.B. International, Wallingford, U.K., 137-149.
- Morgan R.P.C. (2001).** A simple approach to soil loss prediction: a revised Morgan-Morgan-Finney model, *Catena*, **44**, 305-322.
- Murdoch E.G., Whelan M.J. & Grieve I.G. (2005).** Incorporating uncertainty into predications of diffuse-source phosphorus transfers (using readily available data), *Water, Science & Technology*, **51**, (3-4), 339-346.

- Nair V.D., Graetz D.A. & Portier K.M. (1995).** Forms of phosphorus in soil profiles from dairies of South Florida, *Soil Science of America Journal*, **59**, (5), 1244-1249.
- Nash, D., Hannah, M., Halliwell, D. & Murdoch, C. (2000).** Factors affecting phosphorus export from a pasture-based grazing system, *Journal of Environmental Quality*, **29**, (4), 1160-1166.
- NCC (1993).** *Loch Leven NNR Management Plan 1988-1993*, internal paper, SNH, Perth.
- Petersen R.G. & Calvin L.D. (1965).** Sampling In Black C.A. (ed). *Methods of Soil analysis. Part One. Physical and mineralogical properties, including statistics of measurement and sampling.* American Society of Agronomy Inc. Publisher, Madison, W.I., U.S.A.
- Petry J.** SEPA, *pers comm.*, March 2006.
- Prosser I.P. & Rustomji P. (2000).** Sediment transport capacity relations for overland flow, *Progress in Physical Geography*, **24**, (2), 179-193.
- Quinn P., Beven K., Chevallier P. & Planchon O. (1991).** The prediction of hillslope flow patterns for distributed hydrological modelling using digital terrain models. *Hydrological Processes*, **5**, 59-79.
- Rast W. & Lee G.F. (1983).** Nutrient loading estimates for lakes, *Journal of Environmental Engineering*, **109**, (2), 502-517.
- Reckhow K.H., Beaulac M.N. & Simpson J.T. (1980).** *Modelling Phosphorus Loading and Lake Response Under Certainty: A Manual and Compilation of Export Coefficients*, Clean Lakes Section, US Environmental Protection Agency, Washington, DC, USA.
- Rekolainen S., Maximilian P., Kämäri J., Ekholm P. (1991).** Evaluation of the accuracy and precision of annual phosphorus load estimates from two agricultural basins in Finland, *Journal of Hydrology*, **128**, 237-255.
- Richards K. (1993).** Sediment Delivery and the Drainage Network in Beven K. & Kirky M.J. (eds). *Channel Network Hydrology*, J Wiley & Sons, Ltd, Chichester.
- Robson A.J., Neal C., Currie J.C., Virtue W.A. & Ringrose A. (1996).** *Report No. 128 The water quality of the Tweed and its tributaries*, The Institute of Hydrology, U.K.
- Robson A.J. & Neal C. (1997a).** A summary of regional water quality for eastern UK rivers, *Science of the Total Environment*, **194/195**, 15-37.
- Robson A.J. & Neal C. (1997b).** Regional water quality of the River Tweed, *Science of the Total Environment*, **194/195**, 173-192.
- Rowell D.L. (1994).** *Soil Science: Methods and Applications*, Longman Scientific and Technical, Harlow, U.K., 350pp.

- Rowntree D. (1981).** *Statistics Without Tears: A Primer For Non-Mathematicians*, Penguin, Harmondsworth.
- The Royal Society (1983).** *The Nitrogen Cycle of the UK. A Group Study Report*, The Royal Society, London.
- RSPB (undated).** *Vane Farm Nature Centre And Reserve, Tayside*, RSPB, Edinburgh.
- Rustomji P. & Prosser I. (2001).** Spatial Patterns of Sediment Delivery to Valley Floors: Sensitivity to Sediment Transport and Hillslope Hydrology Relations, *Hydrological Processes*, **15**, 1003-1018.
- Shand C.A., Macklon A.E.S., Edwards A.C & Smith S. (1994).** Inorganic and organic P in soil solutions from three upland soils, *Plant*, **159**, 255-264.
- Sharpley A.N. (1985).** Phosphorus cycling in unfertilised and fertilised agricultural soils, *Soil Science Society American Journal*, **49**, 905-911.
- Smith A.M. (1959).** Soil analysis and fertilizer recommendation, *Proc. Fertilizer Society*, **57**, 1-40
- Smith R.M.S., Evans D.J. & Wheeler H.S. (2005)** Evaluation of two hybrid metric-conceptual models for simulating phosphorus transfer from agricultural land in the river Enborne, a lowland UK catchment, *Journal of Hydrology*, **304**, 366-380.
- SNH (2005).** *Loch Leven Citations*, internal document, SNH, Kinross.
- Soane B.D. (1970).** The effects of traffic and implements on soil compaction. *Journal and Proc. Of the Institute of Agric Engineers* **25**, 115-26.
- Sonneveld B.G.J.S. & Nearing M.A. (2003).** A nonparametric/parametric analysis of the Universal Soil Loss Equation, *Catena*, **52**, 9-21.
- Tarboton, D.G. (1997).** A new method for the determination of flow directions and upslope areas in grid digital elevation models, *Water Resources Research*, **32**, (2), 309-319.
- Thapa K. & Bossler J. (1992).** Accuracy of spatial data used in geographic information systems, *Photometric Engineering & Remote Sensing*, **58**, 835-841.
- Thompson N., Barrie I.A. & Ayles M. (1981).** The Meteorological Office Rainfall and Evaporation Calculation System: MORECS (July 1981), *Meteorological Office Memorandum*, **45**, Bracknell, UK.
- Tim U.S. & Jolly R. (1994).** Evaluating agricultural nonpoint-source pollution using integrated geographic information systems and hydrologic/water quality model, *Journal of Environmental Quality*, **23**, (1), 25-35.
- Vose D. (1996).** *Quantitative Risk Analysis: a guide to Monte Carlo simulation modelling*, John Wiley & Sons Ltd, Chichester, England.

- Weaver D.M., Ritchie G.S.P., Anderson G.C. & Deeley D.M. (1988).** Phosphorus leaching in sandy soils I, short-term effects on fertilizer applications and environmental conditions, *Australian Journal of Soil Research*, **26**, 177-190.
- Webb B.W., Phillips J.M., Walling D.E., Littlewood I.G., Watts C.D. & Leeks G.J.L. (1997).** Load estimation methodologies for British rivers and their relevance to the LOIS RACS (R) programme, *Science of the Total Environment*, **194/195**, 379-389.
- Whelan M.J., Gandolfi C. & Bischetti G.B. (1999).** A simple stochastic model of point source solute transport in rivers based on gauging station data with implications for sampling requirements, *Water Research*, **14**, 3171-3181.
- Whelan M.J., Hope E.G. & Fox K. (2002).** Stochastic modelling of phosphorus transfers from agricultural land to aquatic ecosystems, *Water Science and Technology*, **45**, 167-176.
- Wickham J.D., Riitters K.H., O'Neill R.V. Reckhow K.H., Wade T.G. & Jones K.B. (2000),** Land Cover as a framework for assessing risk of water pollution, *Journal of the American Water Resources Association*, **36**, (6), 1417-1422.
- Withers P.J.A., Davidson I.A. & Foy R.H. (2000).** Prospects for controlling diffuse phosphorus loss to water, *Journal of Environmental Quality*, **29**, 167-175.
- Worrall F. & Burt T.P. (1999).** The impact of land-use change on water quality at the catchment scale: the use of export coefficient and structural models, *Journal of Hydrology*, **221**, 75-90.
- Yoon K. S., Yoo K. H., Wood C. W. & Hall B. M. (1994).** Application of GLEAMS to Predict Nutrient Losses From Land Application of Poultry Litter, *Transactions of the ASAE*, **37**, (2), 453-459.
- Zhang W. & Montgomery D.R. (1994).** Digital elevation model grid size, landscape representation and hydrologic simulations, *Water Resources Research*, **30**, 1019-1028.

Appendices

Appendix 1. Literature Review of Export Coefficients

Appendix 2. Phosphate-Phosphorus in Water (Simplified Version)

Appendix 3. Stochastic Modelling of Phosphorus Transfers from Agricultural Land to Aquatic Ecosystems

Appendix 4. Incorporating Uncertainty into Predictions of Diffuse-Source Phosphorus Transfers (Using Readily Available Data)

Appendix 1. Literature Review of Export Coefficients

Table 1. Literature review of P exports ($\text{kg ha}^{-1} \text{a}^{-1}$) from different crops.

Land Use	Location	P Export Range kg/ha/a		Reference and Comments
		Minimum	Maximum	
Agriculture	Michigan, USA	0.1	0.8	Uttomark <i>et al</i> , 1974 in Johnes <i>et al</i> , 1994
Arable	Netherlands	0.06		Kolenbrander, 1972
Arable	Sweden	0.35		p317, Flevoland, Kolenbrander 1971, no animals
Arable	USA	0.06	2.9	Kolenbrander, 1972 p317, Uppsala reg, Brink 1971, no animals Loehr, 1974 in Johnes <i>et al</i> , 1994
Agriculture	UK	0.5	5	Cooke, 1976 Water erosion
Wheat	Oklahoma, USA	3.72		Smith <i>et al</i> , 1991 in Brady & Weil, 1999
Wheat	Oklahoma, USA	1.42		p545, 3% slope, Paleustolls, Conventional plow and disk, up to 23kgP fertiliser
Wheat	Oklahoma, USA	5.67		Smith <i>et al</i> , 1991 in Brady & Weil, 1999
Wheat	Oklahoma, USA	1.19		p545, 3% slope, Paleustolls, no till, up to 23kgP fertiliser
Wheat	Oklahoma, USA	0.06	0.7	Smith <i>et al</i> , 1991 in Brady & Weil, 1999
Agriculture Farm land	UK			p545, 8% slope, Ustochrepts, conventional sweep plow and disk, up to 23kg P fertiliser Cooke, 1976
Row crops - corn	Wisconsin, USA	1.22	1.49	Minshall <i>et al</i> , 1970 in Beaulac & Reckhow, 1982
Row crops - corn	Wisconsin, USA	1.03	5.77	0.004ha plot, silt loam, 0,0,0 NPK Minshall <i>et al</i> , 1970 in Beaulac & Reckhow, 1982
				0.004ha plot, silt loam, 109,39,99 NPK, fresh manure applied in winter

Row crops - corn	Wisconsin, USA	0.68	0.96	Minshall <i>et al</i> , 1970 in Beaulac & Reckhow, 1982 0.004ha plot, silt loam, 102,44,85 NPK, fermented manure applied in spring
Row crops - corn	Wisconsin, USA	0.76	1.18	Minshall <i>et al</i> , 1970 in Beaulac & Reckhow, 1982 0.004ha plot, silt loam, 78,33,114 NPK, liquid manure applied in spring
Row crops - corn	Wisconsin, USA	1	1.6	Hensler <i>et al</i> , 1970 in Beaulac & Reckhow, 1982 0.004ha plot, silt loam, 0,0,0 NPK
Row crops - corn	Wisconsin, USA	1.13	5.66	Hensler <i>et al</i> , 1970 in Beaulac & Reckhow, 1982 0.004ha plot, silt loam, 108,39,99 NPK, fresh manure applied in winter
Row crops - corn	Wisconsin, USA	0.73	0.9	Hensler <i>et al</i> , 1970 in Beaulac & Reckhow, 1982 0.004ha plot, silt loam, 108,39,99 NPK, fermented manure applied in spring
Row crops - corn	Wisconsin, USA	0.91	0.97	Hensler <i>et al</i> , 1970 in Beaulac & Reckhow, 1982 0.004ha plot, silt loam, 108,39,99 NPK, liquid manure applied in spring
Row crops - corn	Iowa, USA	0.092	2.118	Alberts <i>et al</i> , 1978 in Beaulac & Reckhow, 1982 30ha contour planting, deep loess, fine silty mixed mesics, 448,64,- NPK
Row crops - corn	Iowa, USA	0.083	1.288	Alberts <i>et al</i> , 1978 in Beaulac & Reckhow, 1982 33.6ha contour planting, deep loess, fine silty mixed mesics, 168,39,- NPK
Row crops - corn	Iowa, USA	0.024	0.613	Alberts <i>et al</i> , 1978 in Beaulac & Reckhow, 1982 60ha contour planting, deep loess, fine silty mixed mesics, 280,64,- NPK
Row crops - arable	USA	0.25	1.25	Sonzogni <i>et al</i> , 1980 in Johnes <i>et al</i> , 1994
Grassland-grazed	N. Carolina, USA	0.12	0.16	Kilmer <i>et al</i> , 1974 in Beaulac & Reckhow, 1982 1.88ha, moderate GRAZING, 37,16,8 NPK
Grassland-grazed	N. Carolina, USA	0.11	0.7	Kilmer <i>et al</i> , 1974 in Beaulac & Reckhow, 1982 1.48ha, heavy GRAZING, 149,64,12 NPK
Grassland-grazed	Oklahoma, USA	0.27	3.86	Menzel <i>et al</i> , 1978 in Beaulac & Reckhow, 1982 11.1ha, cts grazing, little bluestem cover, active gullies, silt loam, 0,0,0 NPK
Grassland-grazed	Oklahoma, USA	0.02	1.44	Menzel <i>et al</i> , 1978 in Beaulac & Reckhow, 1982 11.0ha, rotation grazing, little bluestem cover, good cover, silt loam, 0,0,0 NPK

Grassland-grazed	Oklahoma, USA	4.9	Olness <i>et al.</i> , 1980 in Beaulac & Reckhow, 1982 7.8ha, cts grazing, little bluestem cover, silt loam, 83,72,0 NPK
Grassland-grazed	Oklahoma, USA	3.09	Olness <i>et al.</i> , 1980 in Beaulac & Reckhow, 1982 7.8ha, cts grazing, little bluestem cover, silt loam, 87,76,0 NPK
Grassland-grazed	Oklahoma, USA	0.76	Olness <i>et al.</i> , 1980 in Beaulac & Reckhow, 1982 11.1ha, cts grazing, little bluestem cover, active gullies, silt loam, 0,0,0 NPK
Grassland-grazed	Oklahoma, USA	0.2	Olness <i>et al.</i> , 1980 in Beaulac & Reckhow, 1982 11.0ha, rotation grazing, little bluestem cover, silt loam, 0,0,0 NPK
Grassland-grazed	Iowa, USA	0.081	Schuman <i>et al.</i> , 1973 in Beaulac & Reckhow, 1982 42.9ha, Rotation grazing, 168,39,- NPK
Grassland-grazed	S Dakota, USA	0.25	Harms <i>et al.</i> , 1974 in Beaulac & Reckhow, 1982 6.28ha, Pasture, sandy clay loam
Grassland-grazed	Ohio, USA	3.6	Chichester <i>et al.</i> , 1979 in Beaulac & Reckhow, 1982 1ha winter grazed + summer rotational, orchard grass and blue-grass cover, silt loam, 56,0,0 NPK
Grassland-grazed	Ohio, USA	0.85	Chichester <i>et al.</i> , 1979 in Beaulac & Reckhow, 1982 1ha, summer grazed, silt loam, 56,0,0 NPK - major contribution from under ground spring
Grassland-grazed	Georgia, USA	1.35	Krebs & Golley 1977 in Beaulac & Reckhow, 1982 10ha, pasture for brood cattle, 0,0,0 NPK
Grassland-grazed	Maryland, USA	3.8	Correll <i>et al.</i> 1977 in Beaulac & Reckhow, 1982 351.2ha. Cts grazing, some winter feeding + hay production, well-drained sandy loams
Grassland	Netherlands	0.52	Kolenbrander, 1972 p317, Hupselsebeek, Kolenbrander 1971, no animals
Grassland	Switzerland	0.7	Kolenbrander, 1972 p317, Prealpine reg. Gachter/Furrer 1971, no animals
Grassland	USA	0.05	Sonzogni <i>et al.</i> , 1980 in Johnes <i>et al.</i> , 1994
Grassland	USA	0.05	Loehr, 1974 in Johnes <i>et al.</i> , 1994

Grassland	Europe	0.22	OECD, 1972 in Johnes et al, 1994
Grassland-grazed	UK	0.2 3	Cooke, 1976 Animal farming, conventional (0.2) - industrial (3)
Perm unfert grassland	UK	0.4	Crisp, 1966 in Heathwaite, 1997 Not clear if grazed
Grass - heavily grazed	Oklahoma, USA	0.24	Smith et al, 1991 in Brady & Weil, 1999 p545, 3% slope, Paleustolls
Grass - moderately grazed	Oklahoma, USA	0.09	Smith et al, 1991 in Brady & Weil, 1999 p545, 8% slope, Ustochrepts
Forest	Michigan, USA	0.02 0.4	Reckhow et al, 1980 in Johnes et al, 1994
Forest	USA	0.05 0.1	Sonzogni et al, 1980 in Johnes et al, 1994
Forest	USA	0.007 0.88	Loehr, 1974 in Johnes et al, 1994
Forest	Europe	0.01 0.06	OECD, 1972 in Johnes et al, 1994
Agriculture - Forest	UK	0.01 0.06	Cooke, 1976
Bare Fallow	USA	0.05 0.25	Loehr, 1974 in Johnes et al, 1994

Table 2. Literature review of P inputs ($\text{kg ca}^{-1}\text{a}^{-1}$) from various animals and humans.

Animal	Location	P Input Range kg/ca/a		Reference
		Minimum	Maximum	
Cattle	Bedfordshire, UK	10.6		Owens, 1976
Cattle	USA	17.6		Omernick, 1976 in Johnes <i>et al</i> , 1994
Cattle (steer, 450kg)	UK	8		Cooke, 1976
Cattle (dairy cow)	UK	10		Cooke, 1976
Cattle	Europe	7.65		Vollenweider, 1968
Cattle	UK	13.5		Richardson, 1976 in Johnes <i>et al</i> , 1994
Cattle FYM (dairy cow, 500kg)	Scotland	10.43		SAC, 1992
Cattle FYM (young cow, 250kg)	Scotland	3.13		SAC, 1992
Cattle FYM (fattening cow, 400kg)	Scotland	5.89		SAC, 1992
Cattle FYM	UK	15.6		Smith <i>et al</i> , 1998
Cattle	UK	9.56		McGechan, 2003
Pigs	Bedfordshire, UK	1.4		Owens, 1976
Pigs	UK	1.5		Richardson, 1976 in Johnes <i>et al</i> , 1994
Pigs	USA	3.23		Omernick, 1976 in Johnes <i>et al</i> , 1994
Pigs 125kg	UK	5.5		Cooke, 1976
Pigs	Europe	5.63		Vollenweider, 1968
Poultry - broiler poultry	UK	0.1		Cooke, 1976
Poultry - laying hens	UK	0.2		Cooke, 1976
Poultry	Europe	0.2		Vollenweider, 1968 in Johnes <i>et al</i> , 1994
Poultry	Bedfordshire	0.1		Owens, 1976
Poultry	USA	0.21		Omernick, 1976 in Johnes <i>et al</i> , 1994
Poultry	UK	0.3		Richardson, 1976 in Johnes <i>et al</i> , 1994
Sheep	Europe	1.5		Vollenweider, 1968
Sheep 75kg	UK	1.8		Cooke, 1976
Sheep	USA	1.47		Omernick, 1976 in Johnes <i>et al</i> , 1994
Human - septic tank	Michigan, USA	0.3	1	Reckhow <i>et al</i> , 1980 in Johnes <i>et al</i> , 1994
Human - sewage effluent	E Scotland	0.58	3.9	Stewart <i>et al</i> , 1982 in Johnes <i>et al</i> , 1994
Human - sewage effluent	USA	0.2	0.7	Sonzogni <i>et al</i> , 1980 in Johnes <i>et al</i> , 1994
Human - sewage produced	Europe	0.23	1.75	Devey & Harkness, 1973 in Alexander & Stevens, 1976

Human - sewage produced	England	0.91	1.5	Stewart <i>et al</i> , 1974 in Alexander & Stevens, 1976
Human - sewage produced	USA	0.8		Hetling & Carcich, 1973 in Alexander & Stevens, 1976
Human - sewage produced	Scotland	0.58		Stewart <i>et al</i> , 1974 in Alexander & Stevens, 1976
Human - sewage produced	USA	1.59		OECD, 1972 in Johnes <i>et al</i> , 1994

Note:

For animals, the export is calculated as: input * proportion applied to land * proportion estimated to reach surface waters. The proportion applied to land is assumed to be 70 – 100% for cattle and 100% for sheep (after Richardson, 1976 and Gostick, 1982 in Johnes *et al*, 1996). The proportion estimated to be lost to surface waters is 1 – 5% (after Vollenweider, 1968). Where slurry and hen manure are applied to the land, the inputs are taken as 10 kg P tonne⁻¹ hen manure and 7 kg P 1000 L⁻¹ slurry (after SAC, 1986).

REFERENCES

- Alexander G.C. & Stevens R.J. (1976).** Per capita phosphorus loading from domestic sewage, *Water Research*, **10**, 757-764.
- Beaulac M.N. & Reckhow K.H. (1982).** An examination of land use – nutrient export coefficients, *Water Resources Bulletin*, **18**, (6), 1013 – 1024.
- Brady N.C. & Weil R.R. (1999).** *The Nature and Properties of Soils 12th Ed.*, Prentice Hall, New Jersey, U.S.A.
- Cooke G.W. (1976).** A review of the effects of agriculture on the chemical composition and quality of surface and underground waters, *MAFF Technical Bulletin* 32, pp. 5-57.
- Heathwaite A.L. (1997).** Sources and Pathways of Phosphorus Loss From Agriculture. In *Phosphorus Loss From Soil To Water*, Tunney, H., Carton, O.T., Brookes P.C., Johnston, A.E. (eds), C.A.B. International, Wallingford, U.K., pp. 205-223.
- Johnes P.J., Moss B., Phillips G.L. (1994).** *Lakes – Classification and Monitoring. A Strategy for the Classification of Lakes.* National Rivers Authority R&D Project Record 286/6/A. U.K.
- Johnes P., Moss B., Phillips G. (1996).** The determination of total nitrogen and total phosphorus concentrations in freshwaters from land use, stock headage and population data: testing of a model for use in conservation and water quality management, *Freshwater Biology*, **36**, 451-473.
- Kolenbrander G.J. (1972).** Eutrophication from Agriculture with Special Reference to Fertilisers and Animal Waste, *Soils Bulletin*, **16**, 305-327.

- McGechan M.B. (2003).** Phosphorus pollution implications of extending grazing into late autumn, *Grass and Forage Science*, **58**, 151-159.
- Owens M. (1976).** Nutrient balances in rivers, *MAFF Technical Bulletin 32*, pp. 257-275.
- SAC (1986).** *Fertiliser Recommendations, Revised Edition*, Scottish Agricultural College, Edinburgh, UK.
- SAC (1992).** *Technical Note: Fertiliser Series No. 14. Fertiliser Allowances for Manures and Slurries*, Scottish Agricultural College, Edinburgh, UK.
- Smith K.A., Chalmers A.G., Chambers B.J., Christie P. (1998).** Organic Manure Phosphorus Accumulations, Mobility and Management, Soil Use and Management, 14, 154-159.
- Vollenweider R.A. (1968).** Scientific Fundamentals of the Eutrophication of Lakes And Flowing Waters, with Particular Reference to Nitrogen and Phosphorus as Factors in Eutrophication. OECD Technical Report No. Das/Dst/88. 182pp.

Appendix 2. Phosphate-Phosphorus in Water (Simplified Version)

Reagents:

1.2% stock ammonium molybdate reagent

Dissolve 6.0g ammonium molybdate and 0.150g antimony potassium tartrate in 300ml distilled water in a 500ml beaker. Carefully add, with mixing and cooling, 74ml concentrated sulphuric acid. When cool, transfer the solution to a 500ml volumetric flask and make to volume with distilled water.

Dilute the stock 1 volume to 8 volumes (0.15%) for the working reagent.

Both solutions should be stored in a cool and dark environment.

Phosphorus standard

Dry potassium dihydrogen orthophosphate in an oven at 105°C for an hour and cool in a dessicator. Weigh 0.4393g dry KH_2PO_4 and dissolve in 500ml distilled water in a beaker. Add 1ml concentrated HCl from a pipette. Transfer the solution to a 1000ml volumetric flask and make to volume with distilled water. Add 1 drop of toluene.

This stock solution has 0.1 mg P/ml.

On the day of use, dilute the stock standard solution 50 times (0.002 mg P/ml) with blank digest

1.5% ascorbic acid

NOTE : Prepare on the day of use.

Dissolve 1.5g in 60ml distilled water in a beaker. Transfer to a 100ml volumetric and make to volume with distilled water.

Standards:

Pipette 0, 1, 2, 3 and 4ml of the dilute phosphorus standard solution (0,2,4,6,and 8 μg P) into five 100ml conical flasks and make up to 5ml with blank digest. (Note: blank digest is used to ensure that the acidity of the standards and the samples are the same.) Add to each, 20ml 0.15% ammonium molybdate reagent and 5ml ascorbic acid solution. Swirl the flask to mix and allow the solutions to stand for 30 minutes to allow colour development. Transfer the solutions to a 40mm spectrophotometer cell and measure the absorbance at 880nm after

zeroing the spectrophotometer on 0 μ g standard. Prepare a calibration graph by plotting absorbance of standards against respective μ gP.

Samples:

Note: Although in strong acid solutions, colour development is suppressed, neutralisation is not required provided the acid digests are initially diluted to the equivalent of 1% sulphuric acid (v/v) before aliquots are taken for analysis the acidity of the standards and samples are the same (achieved through making up the standards with blank digest) (Allen, 1982). This is supplemented by Greenberg *et al* (1992, p.4-113) who advise that if a red colour develops on adding a drop of phenolphthalein indicator to the sample, 5N H₂SO₄ should be added to discharge the colour. A red colour will not develop if the pH is less than 8 (E. McQueen, *pers. comm.*) and hence there is no need to neutralise the acid digests (pH = 1).

Pipette 5ml of the sample into a conical flask. Add 20ml 0.15% ammonium molybdate reagent and 5ml ascorbic acid solution. Swirl the flask to mix and allow the solutions to stand for 30 minutes to allow colour development. Transfer the solutions to a 40mm spectrophotometer cell and measure the absorbance at 880nm (spectrophotometer zeroed using 0 μ g standard). Determine the concentration of the sample in μ gP from the calibration graph.

REFERENCES

Allen S.E. (ed) (1989). *Chemical Analysis of Ecological Materials, 2nd Edition*, Blackwell Scientific Publications, Oxford, U.K., 368pp.

Greenberg A.E., Clesceri L.S., Eaton A.D. (1992). *Standard Methods for the Examination of Water and Wastewater, 18th Edition*, American Public Health Association, Washington, U.S.A.

McQueen E. Chemistry Department, University of Stirling, *pers comm.*, November 2002.

Appendix 3. Stochastic Modelling Of Phosphorus Transfers From Agricultural Land To Aquatic Ecosystems

(This paper was presented at the 5th International Conference on Diffuse Pollution, Milwaukee, 2000 and subsequently selected for publication in *Water, Science and Technology*, **45**, (9), 167-175)

M. J. Whelan^{*}, E. G. Hope^{*} and K. Fox^{}**

^{*}Department of Environmental Science, University of Stirling, FK94LA, UK

^{**}Unilever Research, Port Sunlight, Wirral, CH633JW, UK

ABSTRACT

This paper describes a simple model of phosphorus (P) transfer from agricultural land to surface waters which incorporates the effects of spatial variability in catchment properties and uncertainty in model parameter values. TOPMODEL concepts are used to estimate water, solute and sediment fluxes to water bodies. The model predicts the spatial distribution of water table depth and saturation-excess overland flow based on topography. Dissolved P (DP) transfer is assumed to occur vertically in the unsaturated zone and laterally in the saturated zone. Readily soluble P is assumed to decrease exponentially with soil depth. Particulate P (PP) transfers are modelled by estimating overland flow discharge and associated sediment transport capacity. Uncertainty in the distribution of soil surface P concentrations and model parameters controlling the mobility of soil P are incorporated using Monte Carlo simulation. Predicted losses of DP are well correlated with discharge and those of PP are episodic. Highest losses of P tended to be predicted near to the stream where the water table is close to the surface. The combination of a deterministic model core with a stochastic generation of model parameters or state variables provides an attractive way of embracing variability and uncertainty in models of this kind.

KEYWORDS

Model; phosphorus; stochastic; surface waters; transfer

INTRODUCTION

Phosphorus (P) is a major limiting nutrient in many freshwater ecosystems (e.g. Foy and Bailey-Watts, 1998). Increases in its availability can result in enhanced primary productivity which can lead to eutrophication. Although simple export coefficient models of P transfers

from agricultural land to surface waters (e.g. Johnes and Hodgkinson, 1998) have some value in predicting annual fluxes on the basis of land use, they cannot predict intra-annual seasonality in P losses or provide information on the role of hydrological processes. Conversely, the utility of detailed physically-based models is often hampered by a lack of input data or model parameters at a suitable level of spatial and temporal resolution. Even where suitable input data exist, complex models often give little improvement in predictive capability over much simpler models. Furthermore, despite widespread recognition that some account should be taken of system variability and parameter uncertainty, relatively little attention has been devoted to incorporating these features into models of P transfer. An exception is the recent work of Hession and Storm (2000), who incorporated uncertainty estimates into a catchment-scale model of annual P loads, although their model is rather restricted in terms of temporal and spatial resolution. This paper describes a simple, process-based, parametrically parsimonious model of P transfer from catchments which uses readily available input data and which incorporates the effects of spatial variability in catchment properties and uncertainty in model parameters.

METHODS

Hydrological model

The model is based on TOPMODEL concepts (Beven and Kirkby, 1979; Beven, 1997) which attempt to incorporate the influence of topography on runoff response in a simple 'semi-lumped' fashion. In our model, the root zone is conceptualised as a single store with a maximum capacity equal to the integrated profile porosity. The water content of the root zone store is manifested in terms of a soil moisture deficit from saturation, δR (L), which is depleted by infiltration and augmented by evapotranspiration (ET) and drainage. Surface-atmosphere interactions (interception and ET) are accounted for using a procedure based on a modification of the UK MORECS (Meteorological Office Rainfall and Evaporation Calculation System: Thompson et al., 1981). Essentially, the scheme employs the simple "big leaf" concept combined with the Penman-Monteith equation although a simpler ET model (Hargreaves and Samani, 1982) may be employed if meteorological data are limited to mean daily temperatures and daily rainfall totals. Crop growth (height and leaf area index, LAI) throughout the year is accounted for by linearly interpolating between marker values typical for crops grown in the area under consideration. Infiltration rates are assumed to always exceed the rate of net precipitation (unless the soil becomes saturated), therefore precluding

the generation of infiltration-excess overland flow. This assumption is a direct result of the daily time step chosen for the model and the consequent lack of information on rainfall intensity.

It is assumed that root zone drainage occurs entirely in the vertical direction and that matric potential gradients in the root zone approach zero when the root zone moisture content is high enough to allow significant drainage. This allows the use of the one dimensional steady-state gravity flow equation for root zone drainage (Jury *et al.*, 1991) in which vertical discharge per unit area, r (LT^{-1}), is equal to the unsaturated hydraulic conductivity (K). The relationship between K and δ_R is approximated using the van Genuchten (1980) function which is based on parameters obtained from the moisture retention curve.

In TOPMODEL, discharge at the catchment outlet is assumed to be inversely proportional to a catchment-wide average deficit from saturation, $\bar{\delta}(t)$. This deficit is regularly updated by mass balance:

$$\frac{d\bar{\delta}}{dt} = Q - \bar{r} \quad (1)$$

where $Q(t)$ (LT^{-1}) is the saturated zone discharge per unit area per unit time and $\bar{r}(t)$ (LT^{-1}) is the average input to the saturated zone per unit time (i.e. vertical soil drainage). The lumped catchment water balance can be related to the spatial distribution of point values of the saturation deficit, $\delta(t,x,y)$, via the following equation (see Beven, 1997)

$$\delta(t, x, y) = \bar{\delta}(t) - m[\lambda(x, y) - \bar{\lambda}] \quad (2a)$$

where x and y are the co-ordinates of the point in question, m (L) is a curve parameter, which describes the rate of decrease in saturated hydraulic conductivity with depth, and $\lambda(x,y)$ is the topographic index

$$\lambda(x, y) = \ln\left(\frac{a}{\tan \beta}\right) \quad (2b)$$

in which a is the area drained per unit contour length (L) and β is the local slope angle for point (x, y) . $\bar{\lambda}$ is the catchment average of $\lambda(x,y)$. Note that the derivation of Equation (2) assumes a spatially uniform soil transmissivity when δ is zero.

For any value of $\bar{\delta}(t)$ there will be a range of point-specific values for $\delta(t,x,y)$, which will be determined according to values of $\lambda(x,y)$, scaled by the parameter m . Areas in which $\delta(t,x,y) \leq 0$ will generate saturation excess overland flow during storms. Similarly, areas where the root zone is regularly influenced by the saturated zone will have an increased likelihood for lateral transfer of dissolved material in the soil. The spatial distribution of λ can be derived automatically from a digital elevation model (*DEM*). Areas with similar values are considered to be ‘hydrologically similar’, such that calculations need only be made for classes of λ (obtained from its discrete probability density function [*pdf*]) rather than for every point in the basin.

Different crops have different sowing and harvest dates, and different phenologies which can affect the time course of the root zone water balance and average drainage rates to the saturated zone. Root zone water dynamics are, therefore, calculated separately for each land use in each class of λ . The proportion of each land use type in each class of λ is obtained by superimposing land use and λ layers in a GIS. The average daily (area-weighted) root zone water balance is calculated by

$$\frac{\Delta \bar{\delta}_R}{\Delta t} = \bar{r} + \bar{e} - \bar{n} \quad (3)$$

where \bar{r} is the catchment average drainage from the root zone, \bar{e} is the catchment average rate of ET and \bar{n} is net precipitation (after interception). All terms on the right hand side are rates (LT^{-1}). Values of δ are converted to equivalent water table depths by assuming an effective porosity for the “actively draining fraction” which can be considered equivalent to the pore space between “field capacity” and saturation (Quinn *et al.*, 1995).

Spatial distribution of soil phosphorus

Soil P concentrations will vary across the landscape in response to vegetation or cropping history, soil texture and drainage. In the absence of detailed information on the spatial distribution of P we assume that it is imperfectly correlated with λ . The *pdf* of λ can often be approximated by a log-normal model. In this case, for each point (x,y) the equivalent standard normal deviate, $z(x,y)$ is

$$z = \left(\frac{\ln(\lambda) - E[\ln(\lambda)]}{\text{s.d.}[\ln(\lambda)]} \right) \quad (4)$$

where $E[\ln(\lambda)]$ and $s.d.[\ln(\lambda)]$ are, respectively, the mean and standard deviation of the log-transformed *pdf* of λ . Given the mean and standard deviation for P content at the soil surface, $P(x,y,0)$ ($M M^{-1}$), along with the correlation coefficient (ρ) between $P(x,y,0)$ and $\lambda(x,y)$ and assuming a log-normal *pdf* for $P(x,y,0)$, then stochastic realisations of P content, $\hat{P}(x,y,0)$, can be obtained from:

$$\hat{P} = \exp\{E[\ln(P)] + s.d.[\ln(P)]\mu\} \quad (5)$$

where $E[\ln(P)]$ and $s.d.[\ln(P)]$ are, respectively, the mean and standard deviation of the log-transformed *pdf* of P and μ is a random normal deviate, correlated with $z(x,y)$ using

$$\mu = z \cdot \rho + \nu \sqrt{(1 - \rho^2)} \quad (6)$$

in which ν is an independent random normal deviate.

This procedure attempts to predict the global features ("texture") of P concentrations across the landscape (Deutsch and Journel, 1992) but is not conditional (i.e. it does not attempt to match specific, locally measured, values). The acceptability of the spatial representations produced is based on preserving (contemporaneously) the statistics of P content (mean, variance and shape of the distribution) and its correlation with λ . A number of model iterations will generate frequency distributions of P concentration for each cell which can then be used to indicate uncertainty (Deutsch and Journel, 1992).

Depth distribution of soil phosphorus

Soil P is assumed to decrease with depth (after Haygarth et al., 1998) according to a negative exponential function i.e.

$$P(x,y,z) = P(x,y,0) \exp(-k_p z) \quad (7)$$

where $P(x,y,z)$ is the concentration of P at depth z (L) and k_p is a curve parameter which describes the rate of decrease in P concentration with depth. If we assume a constant bulk density (ρ_B) with depth in the entire soil profile, then we can express $P(x,y,z)$ and $P(x,y,0)$ in terms of relative density (ML^{-3}) by multiplying by ρ_B . The total P content, $P_{TOT}(x,y)$ (ML^{-2}), in a soil profile with depth z_{MAX} is thus:

$$P_{TOT}(x,y) = \int_{z=0}^{z_{MAX}} P(x,y,z) \rho_B dz = \frac{P(x,y,0) \rho_B}{k_p} (1 - \exp(-k_p z_{MAX})) \quad (8)$$

If we know the depth to the water table (z_{SAT}) we can calculate the fraction (F_s) of total P which is beneath the water table:

$$F_s = 1 - \left(\frac{1 - \exp(-k_p z_{SAT})}{1 - \exp(-k_p z_{MAX})} \right) \quad (9)$$

The fraction of P_{TOT} which is in the unsaturated zone is thus $(1-F_s)$.

P losses

Dissolved P (DP) losses ($ML^{-2}T^{-1}$) from both the saturated (lateral) and unsaturated (vertical) zones (FDP_S and FDP_U respectively) for each class of λ are calculated from:

$$FDP_S = F_s \cdot P_{TOT} \cdot k_A \cdot \exp(-\delta(t, \lambda) / m) \quad (10)$$

$$FDP_U = (1 - F_s) \cdot k_A \cdot P_{TOT} \cdot \bar{r} \quad (11)$$

where k_A is the proportion of soil P which is in solution. Note that FDP_S is weighted to account for the exponential decrease in soil transmissivity with increasing depth and the consequent decrease in subsurface discharge. The assumption that DP is a constant proportion of total P is rather unrealistic and fails to account for the influence of important DP sinks such as plant uptake (which will be seasonal) and the occurrence of washout / exhaustion phenomena. In its current state the model can, therefore, be considered static in terms of soil P and variations in model output will largely be the result of hydrological processes. Concentrations of DP (C_{DP}) in the stream are simply:

$$C_{DP} = (FDP_S + FDP_U) / Q \quad (12)$$

Particulate P losses ($ML^{-2}T^{-1}$) are calculated from an estimate of wash erosion in overland flow. Neglecting the effects of rain splash and soil creep, we adopt the equation of Kirkby and Cox (1995)

$$S = k_s \tan \beta \left(\frac{q_s}{q_0} \right)^2 \quad (13)$$

where S is sediment transport per unit area ($ML^{-2}T^{-1}$), q_s (LT^{-1}) is the depth equivalent overland flow discharge and q_0 and k_s are fitted constants with dimensions of overland flow discharge (LT^{-1}) and sediment transport per unit area ($ML^{-2}T^{-1}$) respectively. Since hydrological calculations are only made for classes of λ rather than for every cell in the

catchment, the mean gradient for each class of λ was used in equation (13). Sediment associated P transfers (FPP , $ML^{-2}T^{-1}$) are assumed to be equal to the product of sediment transport rate and the P concentration at the soil surface. This ignores the possibility of P enrichment due to size-selective entrainment or deposition and/or aggregate stripping (e.g. Sharpley and Smith, 1990) but in the absence of catchment-specific data, the use of an enrichment ratio would only introduce additional uncertainty to an already parameter-rich model. Thus

$$FPP = S.P(x, y, 0) \quad (14)$$

Application To The Slapton Wood Catchment

The model was applied to the Slapton Wood catchment (Figure 1), a 0.93 km^2 instrumented basin in Devon, UK, with a mixed land use (cf Burt *et al.*, 1988).

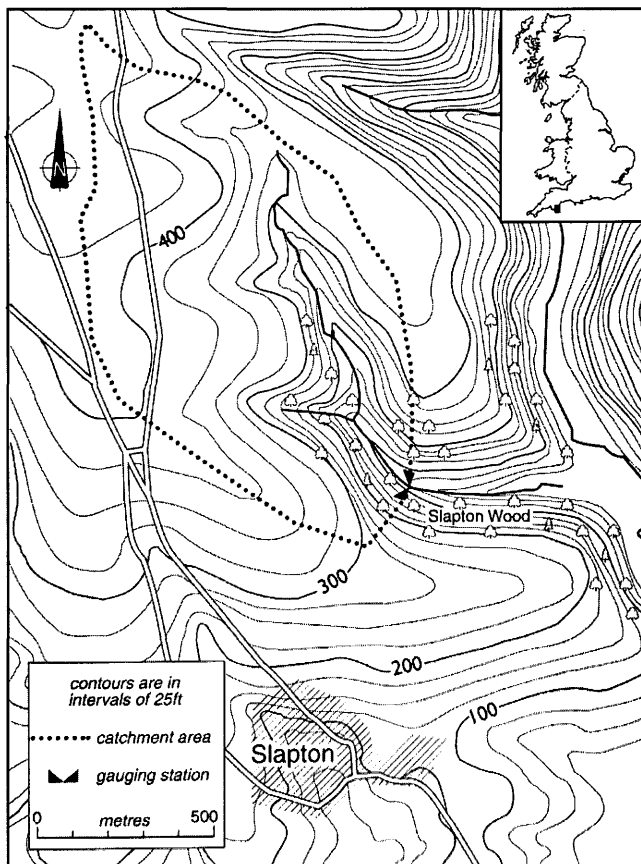


Figure 1. Location map of the Slapton Wood catchment.

The spatial distribution of λ was derived from a "depitted" 20 m *DEM* using a slight modification of the multiple flow direction algorithm described by Quinn *et al.* (1991). The

root zone hydraulic parameters used in the model were derived from measurements (e.g. Ragab and Cooper, 1993). Parameters for the subsurface flow component of the model were calibrated by minimising the error between predicted and observed daily discharge using data from the calendar year 1971. Root zone parameters were not changed during calibration. Once calibrated the model was run continuously for the period 1970 - 1985 (with no further adjustments) in four scenarios with different assumptions about the distribution of soil P at the soil surface (Table 1). Parameters describing the spatial distribution and availability of soil P and those describing P transfer were approximated from the literature. For those scenarios in which there is a stochastic element, thirty realisations of the model were performed so as to provide information about uncertainty in model output.

Since the hydrological component of the model has been calibrated and validated (and can, therefore, be considered to be a reasonable representation of the system) the P model parameters represent the largest degree of uncertainty in the model. The effect of including realistic uncertainty in the values of those parameters to which the model was most sensitive was therefore investigated in an additional model run for one year (1972) with 2000 iterations. Values of q_o , k_s , k_p , and k_A were incorporated as uniform probability distributions (see Table 2 for parameters).

Table 1. Details of scenarios for which the model was tested. In all cases Mean $P(x,y,0)$ was 15 mg P kg⁻¹.

<i>Scenario Name</i>	<i>CV for $P(x,y,0)$ (%)</i>	ρ
A	40	0.0
B	0	0.0
C	40	0.5
D	40	1.0

Table 2. Details of pdfs used to examine the impact of parameter uncertainty on model response. In each case a uniform pdf was used with the maximum value arbitrarily set at 4 times the minimum value.

<i>Parameter</i>	<i>Maximum</i>	<i>Minimum</i>
k_A	0.00002	0.000005
k_s	0.02	0.005
q_o	0.02	0.005
k_p	10	2.5

RESULTS AND DISCUSSION

Examples of predicted and measured daily stream hydrographs are shown in Figure 2. The results suggest that the hydrological model structure and most of its assumptions are reasonable for this catchment. On average, total annual predicted runoff was greater than measured runoff (Burt *et al.*, 1988) by just 8.3% (1971-1990). Model results suggest that surface saturation rarely occurs in more than 10 % of the total catchment area and is usually less than 5%, mostly in and around the stream channels.

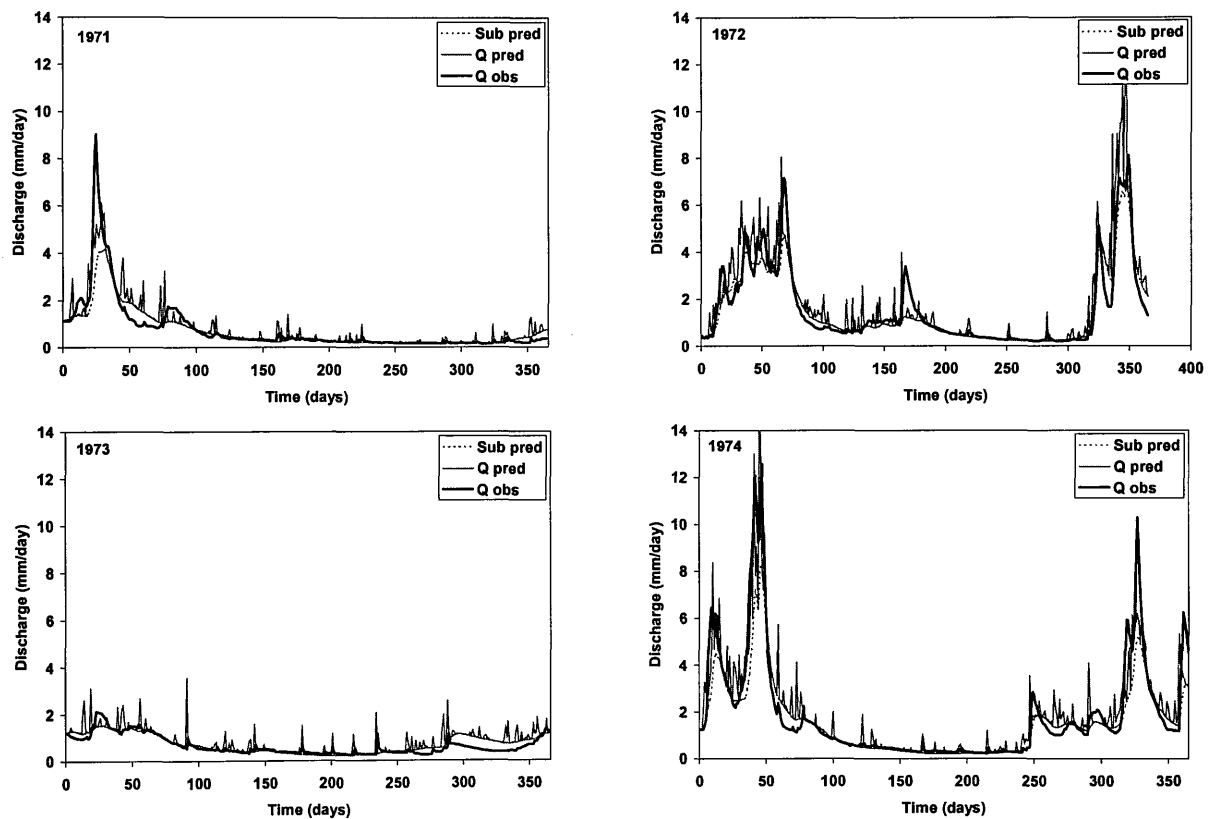


Figure 2. Examples of predicted (Q_{pred}) versus observed (Q_{obs}) daily runoff for the Slapton Wood catchment for 1971, 1972, 1973 and 1974. Sub pred is the predicted sub-surface flow component.

Predicted area-weighted DP, PP and TP losses from the Slapton Wood catchment are shown in Figure 3 for scenario A. In general predicted DP losses were greater than those for PP, although the relative importance of FDP and FPP would be altered during calibration of the P model. As expected, highest losses tended to be predicted in years with high annual precipitation. Average predicted loads for 1972 for each scenario are shown in Figure 4, as an example. Consistently higher values of were predicted for Scenario D ($\rho=1$) than for the other scenarios. This is to be expected since high soil P concentrations are always assumed to occur in hydrologically active areas (i.e. areas with high values of λ). In scenarios A and B

no relationship was assumed between soil P availability and topography. Even though a coefficient of variation of 0.4 was assumed in scenario A, the fact that soil P was randomly distributed in each stochastic realisation resulted in a very similar predicted average annual flux to scenario B (constant P concentrations throughout the catchment). Results for scenario C were intermediate between those for A/B and those for D. This is consistent with the assumptions of variable soil P and positive correlation, ρ , which tends to enhance P transfers by tending to predict coinciding high soil P concentrations, water table and a high incidence of overland flow.

The predicted pattern of mean daily DP concentration (with estimated uncertainty) and the predicted frequency distributions of DP, PP and TP loads resulting from a full incorporation of P parameter uncertainty are shown in Figure 5. It is clear that incorporating a realistic estimate of uncertainty generates wide uncertainty intervals which can only be reduced by better identification of model parameter values.

The results described in this paper were produced under the implicit assumption that the hydrological component of the model provides an adequate representation of the spatial and temporal variations in flow and water table depth in the Slapton Wood catchment. However, it is now widely recognised that there may be a number of different combinations of parameter values which produce reasonable fits to observed discharge (e.g. Beven, 1997), but relatively few which will also generate good predictions of water table depth variations. It is important to realise that without measurement of water table depths the model will always be poorly constrained and unique calibrations impossible.

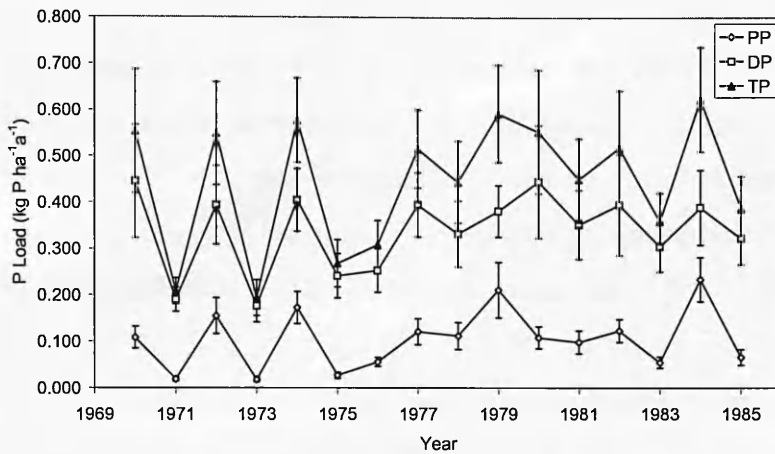


Figure 3. Predicted annual P losses from the Slapton Wood catchment (1970-85) for Scenario A. Error bars show mean \pm 1 SD for 30 realisations.

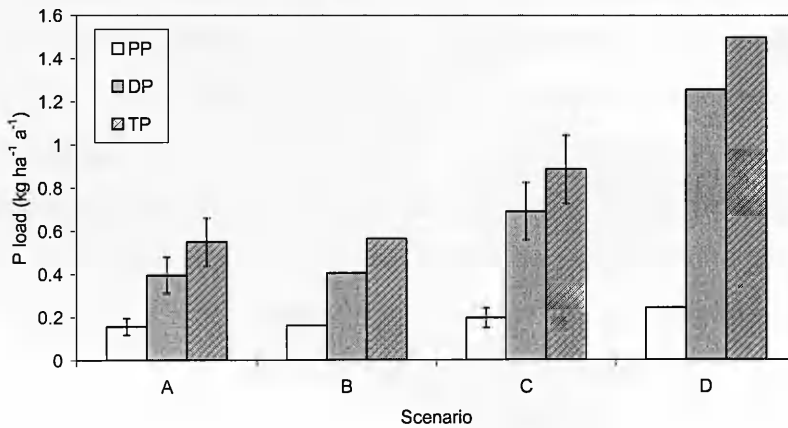


Figure 4. Predicted annual P losses from the Slapton Wood catchment (1972) - Scenarios A - D. Error bars show the mean \pm 1 SD for 30 realisations.

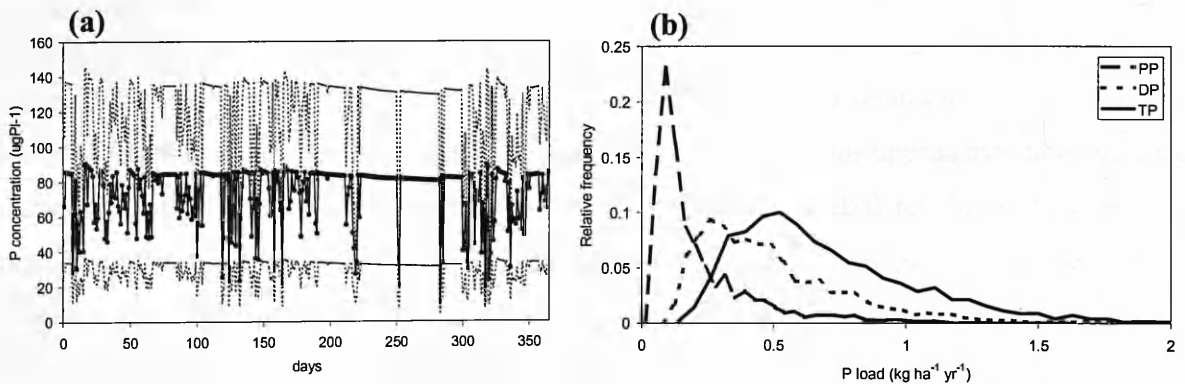


Figure 5. (a) Predicted mean daily DP concentration in the Slapton Wood stream \pm 1 SD and (b) frequency distributions of predicted annual DP, PP and TP loads for 1972 produced from 2000 iterations with values of $P(x,y,0)$ selected according to Scenario A and parameter values selected randomly from uniform *pdfs* (see Table 2).

The adoption of a daily time step (which permits model application to catchments with minimal meteorological data and which reduces run times for Monte Carlo simulations)

hinders the estimation of infiltration excess overland flow. This will be important in catchments where the generation of surface flow by this mechanism is common, although its impact in model applications in the UK (where infiltration rates are normally greater than rainfall intensities) will be limited. At present model output has not yet been compared with observed data on P transfers. The analysis presented here is not intended to evaluate model performance, although calibration and validation of the model will be essential prior to further development. Rather, emphasis is placed on the utility of incorporating state variable and parameter uncertainty using Monte Carlo procedures within a deterministic model framework, which is facilitated by a relatively simple structure and low number of parameters.

A number of simplifying assumptions and omissions have been made in the model which need to be addressed in further developments. The model does not simulate dynamic fluctuations in the sizes of soil P pools and is thus unable to take account of seasonal variations in soil P availability. Considerable seasonal variations in soil P levels have been reported in the literature (e.g. Sharpley, 1985) and will certainly have some control over soil P losses. Other important factors which have been omitted include the effects of land use and P amendments, the potential for P removal by deposition or plant uptake from surface or subsurface flows and the role of in-stream transformations and P input from stream bank erosion.

CONCLUSIONS

A simple model of P transfer from agricultural land to surface waters was presented. The model is appropriately-scaled for simulating processes in small to medium sized catchments and is parameter-efficient. It represents an improvement on previous approaches to modelling catchment-scale P transfer in providing greater temporal and spatial resolution than annual export-coefficient models and lower parameter and input data requirements than more complex, event-based, models. Although the model requires further development and has yet to be validated, the idea of combining a deterministic process-based model core with a stochastic generation of uncertain state variables and parameter values, along the lines described, is attractive since it embraces variability and uncertainty whilst maintaining a synthesis of our understanding of the system dynamics.

ACKNOWLEDGEMENTS

The authors would like to thank Unilever for funding and Claudio Gandolfi for comments on the model.

REFERENCES

- Beven K. (1997).** TOPMODEL: A Critique. *Hydrol. Procs.*, **11**, 1069-1085.
- Beven K. and Kirkby M.J. (1979).** A physically-based, variable contributing area model of basin hydrology. *Hydrol. Sci. Bull.*, **24**, 43-69.
- Burt T.P., Arkell B.P., Trudgill S.T. and Walling D.E. (1988).** Stream nitrate levels in a small catchment in south west England over a period of 15 years (1970-1985). *Hydrol. Procs.*, **2**, 267-284.
- Deutsch C.V. and Journel A.G., (1992).** *GSLIB. Geostatistical Software Library and User's Guide.* OUP, Oxford, UK
- Foy R.H. and Bailey-Watts A.E. (1998).** Observations on the spatial and temporal variation in the phosphorus status of lakes in the British Isles. *Soil Use and Man.*, **14**, 131-132.
- Hargreaves G.H. and Samani Z.A. (1982).** Estimating potential evapotranspiration. *J. Irrig. Drainage Engin.*, **108**, 225-230.
- Haygarth P.M., Hepworth L. and Jarvis S.C. (1998).** Forms of phosphorus transfer in hydrological pathways from soil under grazed grassland. *European J. Soil Sci.*, **49**, 65-72.
- Hession W.C. and Storm D.E. (2000).** Watershed level uncertainties: Implications for phosphorus management and eutrophication. *J. Env. Qual.*, **29**, 1172-1179.
- Jury W.A., Gardner W.R. and Gardner W.H. (1991).** *Soil Physics.* John Wiley and Sons, New York, USA.
- Johnes P.J. and Hodgkinson P.A. (1998).** Phosphorus losses from agricultural catchments. *Soil Use and Man.*, **14**, 175-185.
- Kirkby M.J. and Cox N.J. (1995).** A climatic index for soil erosion potential (CSEP) including seasonal and vegetation factors. *Catena*, **25**, 333-352.
- Quinn P., Beven K., Chevallier P. and Planchon O. (1991).** The prediction of hillslope flow patterns for distributed hydrological modelling using digital terrain models. *Hydrol. Procs.*, **5**, 59-79.

Quinn P., Beven K. and Culf A. (1995). The introduction of macroscale hydrological complexity into land surface-atmosphere transfer models and the effect on planetary boundary layer development. *J. Hydrol.*, **166**, 421-444.

Ragab R. and Cooper J.D. (1993). Variability of unsaturated zone water transport parameters: Implications for hydrological modelling. 1. In situ measurements. *J. Hydrol.*, **148**, 109-131.

Sharpley A.N. (1985). Phosphorus cycling in unfertilised and fertilised agricultural soils. *Soil Sci. Soc. Am. J.*, **49**, 905-911.

Sharpley A.N. and Smith S.J. (1990). Phosphorus Transport in Agricultural Runoff: The Role of Soil Erosion. In: *Soil Erosion on Agricultural Land*, Boardman J, Foster I.D.L. and Dearing J.A. (eds.), Wiley, Chichester, UK.

Thompson N., Barrie I.A. and Ayles M. (1981). *The Meteorological Office Rainfall and Evaporation Calculation System: MORECS (July 1981)*, Met. Office Memorandum No.45, Bracknell, UK.

Van Genuchten M.Th. (1980). Closed-form Equation for Predicting the Hydraulic Conductivity of Unsaturated Soils. *Soil Sci. Soc. Am. J.*, **44**, 892-898.

Appendix 4. Incorporating Uncertainty Into Predictions Of Diffuse-Source Phosphorus Transfers (Using Readily Available Data)

(This paper was presented at the 7th International Conference on Diffuse Pollution, Dublin, 2003 and subsequently selected for publication in *Water, Science and Technology*, **51**, (3-4), 339-346.)

Murdoch, Emma G¹., Whelan, Michael J²., & Grieve, Ian C¹.

¹*School of Biological and Environmental Sciences, University of Stirling, FK9 4LA, Scotland U.K.*

(Emails: e.g.murdoch@stir.ac.uk, i.c.grieve@stir.ac.uk)

²*Safety and Environmental Assurance Centre, Unilever Colworth Laboratories, Sharnbrook, Beds., MK44 1LQ, England, U.K. (Email: mick.whelan@unilever.com)*

ABSTRACT

Phosphorus (P) is a limiting nutrient in many freshwater ecosystems and increases in its availability can lead to eutrophication. Effective management of P in freshwaters requires quantitative estimates of P supply from all significant sources. A simple GIS-based model, capable of predicting total diffuse source phosphorus export from catchments using readily available data, has been developed. The model is based on the idea of export coefficients but includes the effects of topography (slope and cumulative area), soil type (using the UK Hydrology of Soil Types (HOST) classification) and climate (hydrologically effective rainfall) as well as land use. Uncertainty in key model parameters is accounted for using Monte Carlo simulation which involves random sampling from probability density functions in a large number of iterations. This reduces the need for subjective optimisation of export coefficients. The model has been applied to the Greens Burn catchment, Scotland and predicts P exports within the confidence limits of the measured values.

KEYWORDS

Phosphorus Export, GIS, Modelling, Monte Carlo

INTRODUCTION

There is wide concern relating to the eutrophication of surface waters and the associated enhanced growth of algae and aquatic macrophytes (e.g Vollenweider, 1968). Research indicates that phosphorus (P) is often the main limiting nutrient in freshwaters (e.g. Foy & Bailey-Watts, 1998) and consequently efforts have been concentrated on reducing P transfers to susceptible water bodies. Point sources are relatively easy to quantify, given information

on flow rates and concentrations or the number of people served by a particular sewage treatment plant. In addition, point sources can be treated with end of pipe abatement measures. As a result, there is now a focus on diffuse sources, of which agriculture can be the most important contributor. The influence of agriculture can be divided into P additions (fertiliser and animals) and soil management (e.g. tillage regime and crop type), both of which can affect P transfer.

Numerical models allow the prediction of surface water nutrient concentrations and loads on the basis of the most important controlling factors (e.g. land use, climate and soil type). Many different approaches (of varying complexity) have been developed, ranging from simple empirical models to distributed physically-based models. The problem with more complex models is that they have high data requirements and sometimes give little, if any, improvement on the predictions of simpler models. In this paper we describe a model which attempts to capture the most important factors controlling diffuse source P transfer to surface waters whilst retaining low and readily available input requirements.

METHODS

Our approach is based on the export coefficient model (e.g. Johnes & O'Sullivan, 1989). This is probably the simplest description of P export available and assumes that present land use is the most significant control on nutrient export. Total annual nutrient (nitrogen and phosphorus) loading to surface waters is predicted by estimating export coefficients from each of the constituent land uses in the catchment, such that, for phosphorus

$$P = \sum_{i=1}^n c_i A_i + \sum_{j=1}^m \omega_j v_j \quad (1)$$

where

P	=	estimated P load (kg a-1)
c_i	=	export coefficient for land cover type i (kg ha-1 a-1)
A_i	=	area of land cover type i (ha)
w_j	=	export coefficient for animal type j (kg ca-1 a-1)
v_j	=	number of animals of type j
n	=	number of land cover types in catchment
m	=	number of animal types in catchment

The export coefficients represent all controls on nutrient transfer (edaphic, hydrological and management). For phosphorus, the coefficients are expressed as mass ha⁻¹ a⁻¹ rather than as a proportion of the amount of P applied because phosphorus transfer is often independent of input rate in the short term.

The simplicity of this model has made it popular with regulators and policy makers. However, there are a number of problems: Firstly, no account is taken of the uncertainty in the selected export coefficients. For any particular land use, phosphorus export will vary from year to year and from location to location. This is reflected in a wide range of measured values of phosphorus export reported in the literature (e.g. Table 1) and means that the basis for selecting a meaningful coefficient for each of the constituent land uses of a catchment will always be highly uncertain, particularly in the absence of site-specific measurements. A common approach is to invoke a calibration procedure, which involves adjusting the coefficients so as to obtain a good match between the observed and measured fluxes. However, this will be poorly constrained as several different combinations of export coefficients may generate equally good fits to measured data. Alternatively, the selection of coefficients may be achieved subjectively, with expert opinion being sought to ascertain the likely export for land uses in a specific catchment. With both these approaches, the model parameters are set for a specific catchment and hence are not universally applicable.

Secondly, the position of each field in relation to receiving watercourses is not explicitly considered. The P transferred from all fields with the same land use is assumed to be the same, regardless of where the fields are in the catchment. However, it is reasonable to expect that P exported from a field far from a watercourse is more likely to be retained in the catchment (by deposition of sediment-associated P or adsorption of dissolved P) compared with a field adjacent to the receiving waterbody. Likewise, a field on a steep slope is more likely to export P than an otherwise identical field on a shallow slope. Finally, since P export is predicted solely on the basis of land use, the model cannot predict inter-annual variations in P losses due to changes in hydrological processes, although it is known that more phosphorus will generally be transferred in wet years than in dry years (e.g. Heathwaite, 1997).

In the model described here we have modified the export coefficient model by attempting to address these limitations. In addition to land use, the model requires information on topography (slope and cumulative area from the divide), soil type, annual precipitation and annual actual evapotranspiration, which are used to adjust export coefficients and to produce uncalibrated, catchment-specific predictions.

Catchments are represented, using a Geographical Information System (GIS), as a raster grid with boundaries defined using the digital elevation model (DEM). Each cell in the grid is characterised by its land use, soil type and its topographic attributes (slope and cumulative area drained from the divide).

Table 1. Range of export coefficients for crops and animals

Land Use	Export kg P ha ⁻¹ a ⁻¹		
	<i>Average</i>	<i>Minimum</i>	<i>Maximum</i>
Grass	0.52	0.02	4.90
Arable/Cereals	1.40	0.06	5.67
Row Crops	1.68	0.02	5.77
Animal	Input kg P ca ⁻¹ a ⁻¹		
	<i>Average</i>	<i>Minimum</i>	<i>Maximum</i>
Cattle	10.4	3.13	17.6
Sheep	1.59	1.47	1.80
Humans (Septic Tank)	0.65	0.30	1.00

(compiled from Vollenweider, 1968; Kolenbrander, 1972; SAC, 1992; Johnes et al, 1994; Smith et al, 1998; Brady & Weil, 1999; Turner & Haygarth, 2000; McGechan, in press). For animals, the export is calculated as: input * proportion applied to land * proportion estimated to reach surface waters. The proportion applied to land is assumed to be 70 – 100% for cattle and 100% for sheep (after Richardson, 1976 and Gostick, 1982 in Johnes et al, 1996). The proportion estimated to be lost to surface waters is 1 – 5% (after Vollenweider, 1968). Where slurry and hen manure are applied to the land, the inputs are taken as 10 kg P tonne⁻¹ hen manure and 7 kg P 1000 L⁻¹ slurry (after SAC, 1986).

In order to account for the uncertainty in the export coefficients selected for each land use, Monte Carlo simulation is employed. This involves making a large number of iterations of the deterministic model core. In each iteration, a value for each export coefficient is randomly selected from a probability distribution constructed from the range of published coefficients for that land use (see Table 1). Although calculations are made for each grid cell, the same export coefficient is used for cells of the same land use in each iteration. This is superior to the alternative technique of sampling from the relevant export coefficient distributions on a cell by cell basis as it results in a wider distribution of predicted P transfers which better reflects the constituent uncertainties. In the absence of information to suggest

otherwise, uniform distributions, with ranges defined in Table 1, are currently used for all export coefficients.

In addition to cropping, the contribution of animals to the total phosphorus (TP) load is included. To do this it is assumed that (1) animals are evenly distributed in all cells suitable for grazing (i.e. grass and rough grazing); (2) manure is spread evenly on all land use types and (3) where information on the position of sewage outlets (e.g. septic tanks) is not available, P resulting from humans is uniformly distributed over the catchment. Animal export coefficients are also selected randomly from probability distributions constructed using measured data.

In each iteration, the combined P export (cropping and animal) from each cell is corrected for topography (slope and cumulative area), soil type and annual hydrologically effective rainfall (HER). Slope is important in the erosion of sediment (e.g. Nash et al, 2000) so that, with all other factors remaining constant, steeper slopes pose a greater erosion risk and hence an elevated likelihood that sediment-associated phosphorus will be exported. Greater drainage area will result in greater surface and sub-surface discharge with more risk of erosion and a greater chance of both sediment-associated and dissolved P being transported. In addition, since upslope area increases as cells get closer to the channel network, it can also be used as an inverse surrogate for distance to streams. Topographic controls are included in the model using generic empirically-based equations summarised by Rustomji & Prosser (2001), i.e.:

$$q_s = k_1 \cdot q^\beta \cdot S^\gamma$$

where $q = k_2 \cdot a^\lambda$

i.e. $q_s = k_1 (k_2 a^\lambda)^\beta S^\gamma$

where

q_s = sediment flux per unit width of slope

q = discharge per unit width

S = local gradient

a = hillslope area per unit width of contour

$k_1, k_2, \beta, \gamma, \lambda$ = constants

(2)

The following parameter values were chosen for hillslope hydrological conditions in humid temperate climates, such as Britain (i.e. dominated by subsurface throughflow and the development of variable source areas) based on guidelines given by Rustomji & Prosser (2001): $k_1 = k_2 = \lambda = 1$; $\beta = \gamma = 1.4$. Since it is difficult to predict absolute sediment and phosphorus fluxes using a generic model, we have defined the relative flux (RF , 0-1) as:

$$RF = \frac{\ln(q_s + 1)}{\max [\ln(q_s + 1)]} \quad (3)$$

Soil properties (e.g. texture and organic matter content) are potentially important in the transfer of phosphorus (e.g. Morgan, 1997; Brady & Weil, 1999). To incorporate the effect of soil type into the model, we have adopted a well-tested and readily available soils classification system. The UK Hydrology of Soil Types (HOST) classifies UK soils into 29 classes on the basis of hydrology and geology (Boorman *et al*, 1995). Soils from different HOST classes will respond differently to rainfall, producing varying degrees of runoff. HOST predicts a standard percentage runoff (*SPR*) value for each HOST class. For each soil series, which may contain a number of different HOST classes, a weighted average for *SPR* can be calculated. These *SPR* values are used in the model to further adjust the export coefficients such that soils with greater *SPR* will have a greater likelihood of transferring dissolved and sediment-associated phosphorus than otherwise similar cells. The soil weighting factor (*SWF*) describing the relative transfer of P is defined as:

$$SWF = \left(\left[\frac{\max SWF - \min SWF}{\max SPR - \min SPR} \right] * SPR \right) + SWFi \quad (4)$$

where

- max*SWF* = maximum *SWF*, as defined by the model user; default = 0.8
- min*SWF* = minimum *SWF*, as defined by the model user; default = 1.2
- max*SPR* = maximum *SPR* value in catchment
- min*SPR* = minimum *SPR* value in catchment
- SPR* = *SPR* value for specific cell
- SWFi* = *SWF* intercept, defined by max*SWF*, min*SWF*, max*SPR*, min*SPR*

In addition to affecting hydrological response, soil type can also influence erodibility (the propensity of soil to erode). Whilst we recognise that this may be important in many circumstances, we believe that other factors probably outweigh erodibility in much of the UK and consequently it has not been included in the model for the sake of simplicity.

Climatic controls on the transfer of phosphorus to surface waters are incorporated using hydrologically effective rainfall (*HER*) for the catchment under consideration in each year. This is calculated by subtracting the actual evapotranspiration (*AET*) from the annual rainfall total. *AET*, which includes interception losses, is derived from predictions made by the Meteorological Office Rainfall and Evapotranspiration Calculation System - MORECS (Thompson *et al*, 1981). For each year a relative weighting factor is calculated by dividing the *HER* for that year by the average *HER* for all years. This is based on the reasonable assumption that annual P flux (although not necessarily concentrations) will be directly proportional to *HER* (see for example Figure 3b).

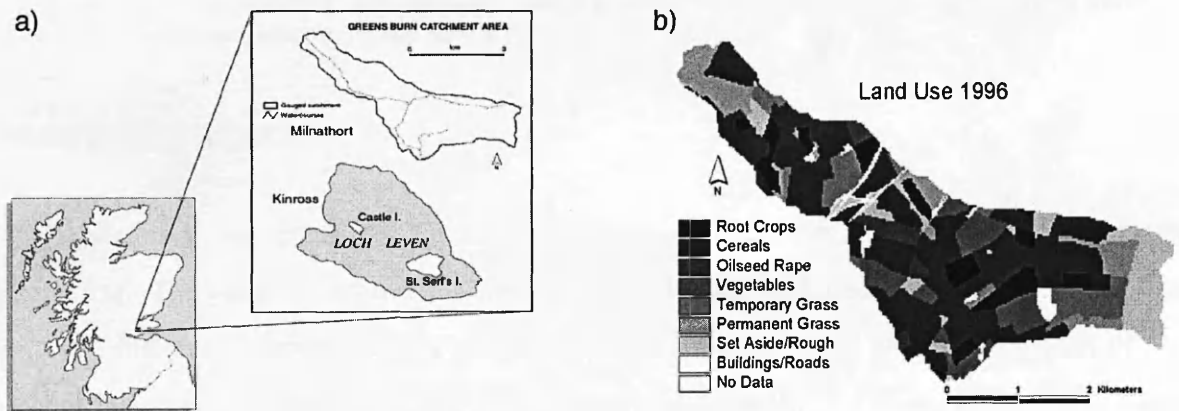


Figure 1. a) Location of the Greens Burn catchment, b) Raster grid of land use in the Greens Burn catchment for 1996.

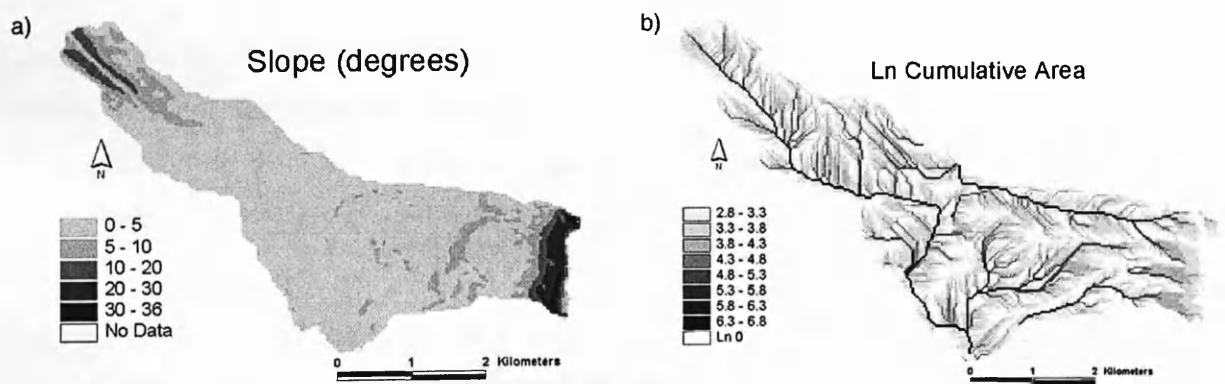


Figure 2. a) Slope and b) Natural Log of Cumulative Area for the Greens Burn catchment.

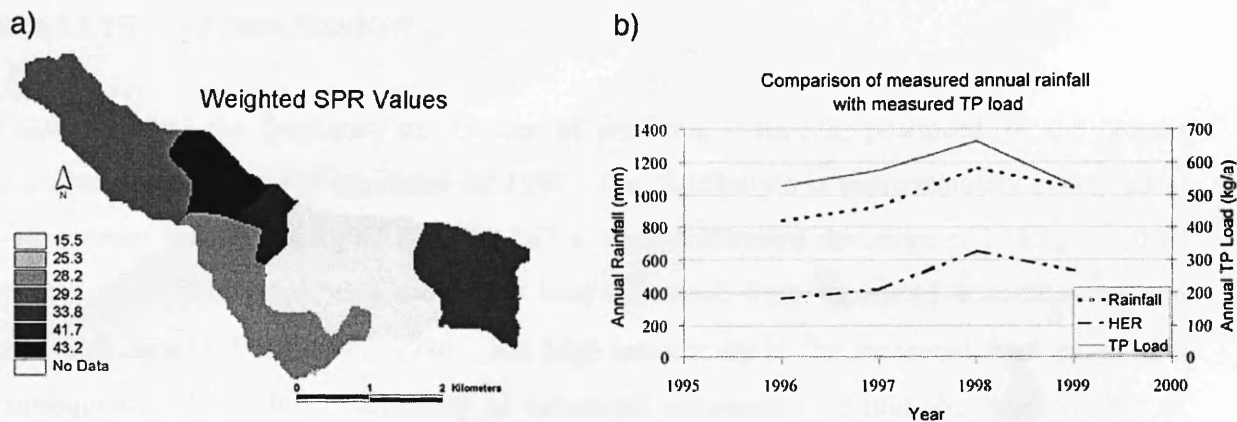


Figure 3. a) Weighted SPR coefficients for each soil class (as defined by the Soil Survey of Scotland, 1:250,000, The Macaulay Inst. for Soil Research, Aberdeen, 1982), derived from HOST. b) Comparison of measured average annual rainfall and HER with measured average annual TP loading, 1996-1999, for the Greens Burn catchment. Correlation between TP and *HER* is 0.997 (p -value = 0.003).

MODEL APPLICATION

The model was applied to the Greens Burn catchment, Scotland, UK (location shown in Figure 1a). The gauged catchment is approximately 10 km² and drains into Loch Leven. The loch has historically shown signs of eutrophication, which led to the establishment of the Loch Leven Area Management Advisory Group (LLAMAG) in 1992. Since then, major reductions in point sources of phosphorus have been achieved (LLCMP, 1999) and an appraisal of measures to reduce diffuse sources is currently being carried out.

Land use data and stocking densities for the catchment were obtained by interviewing farmers (shown for 1996 in Figure 1b). Slope and cumulative area were derived from a raster grid DEM with a 25m grid cell resolution (Figure 2) using standard routines in ArcView GIS (ESRI, 1996).

Soil type for the Greens Burn catchment is detailed in the Soil Survey of Scotland, 1:250,000. Using HOST, a map of weighted SPR values for the catchment was created (Figure 3a). Soils in the centre of the catchment are predicted to produce less runoff than those to the east and west, all other factors remaining constant.

RESULTS AND DISCUSSION

Figure 4 shows the frequency distribution of predicted P transfer produced for the Greens Burn catchment from 500 iterations for 1996. The distribution is approximately symmetrical with a mean flux of 486 kg a^{-1} ($0.45 \text{ kg ha}^{-1} \text{ a}^{-1}$) and a standard deviation of 111 kg a^{-1} ($0.10 \text{ kg ha}^{-1} \text{ a}^{-1}$). The graph also shows the load estimated from measured concentration and discharge data ($\pm 1 \text{ SEM}$) for 1996. The high uncertainty in the measured load arises as a consequence of the high variability in measured concentrations and the low number of samples taken ($n=14$). It is important to recognise that the observed data with which the model output is compared is, itself, an estimate with a potentially high error. From the graph, the similarity between the range of predicted loads and the measured load is evident.

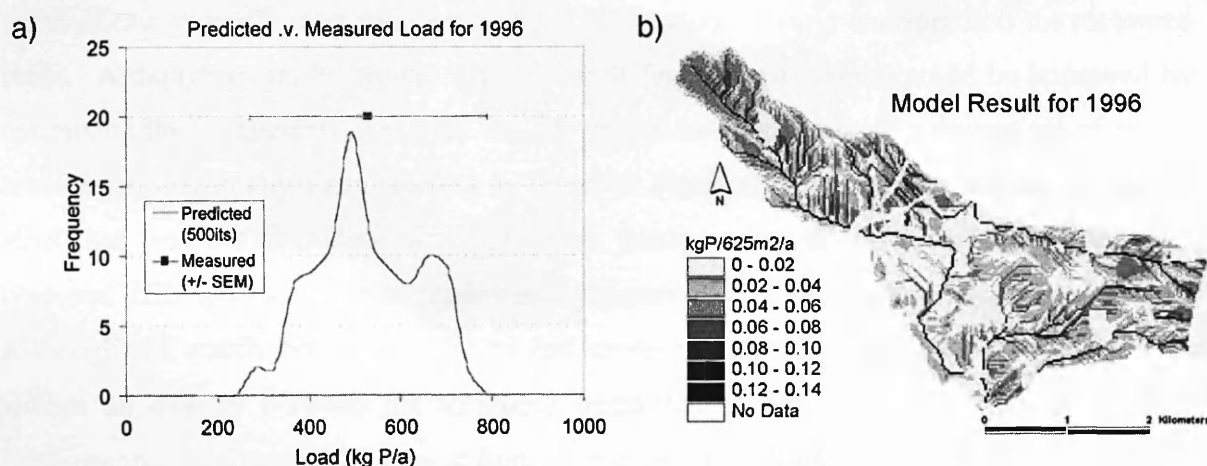


Figure 4. a) Frequency distribution of predicted TP loads (500 iterations) compared with an estimate of the load derived from measured data ($\pm 1 \text{ SEM}$) for the Greens Burn catchment. b) Spatial distribution of P losses from the Greens Burn catchment for 1996.

The spatial distribution of predicted phosphorus export from the Greens Burn catchment for 1996 is shown in Figure 4b. This shows the combined effects of land use, slope, proximity to watercourses and soil type. Such a visualisation can help to show up "hot spots" for P loss which can be targeted for special management measures. Worthy of note are the grassland areas in the northwest of the catchment. According to the basic export coefficient model these areas should export relatively little phosphorus compared to arable land. However, they become significant when adjusted for slope, cumulative area and soil type. Areas close to

stream channels are also evident as disproportionately active sources of P due to high cumulative area. Again, this tallies with an expectation that P mobilised near to, or within, channels will be transported beyond the catchment outlet.

Table 2. Comparison of TP loads (1996-1999) from the Greens Burn catchment predicted by the basic export coefficient model and the modified model (Mean, Mean-1SD, Mean+1SD) with measured data (SEM).

Year	Measured (SEM) (kg P a ⁻¹)	Basic Model (kg P a ⁻¹)	Modified Model Mean (kg P a ⁻¹)	Mean – 1SD (kg P a ⁻¹)	Mean + 1SD (kg P a ⁻¹)
1996	527 (260)	1810	486	376	597
1997	574 (330)	1607	542	422	662
1998	664 (257)	1614	860	632	1087
1999	528 (224)	1639	678	459	898

Table 2 shows the model results for 1996-1999, along with the measured loads in these years. Also shown are the results from the original export coefficient model, applied using the mean value of export coefficients shown in Table 1. This model clearly over-predicts the measured loads. Although it can be argued that the result for the basic model could be improved by optimising the coefficients, there are too few measurements to justify a unique set of export coefficients, especially since changes in observed fluxes may be due to a number of factors other than land use (including sampling error). Incorporating the effects of topography, soil type and *HER* produces better predictions suggesting that these adjustments are sensible. Although the match between predicted and measured mean is not always good, there is always an overlap between the measured mean \pm SEM and mean predicted flux \pm 1SD. Furthermore, the direction of change from year to year is captured by the modified model but not by the original export coefficient model.

CONCLUSIONS

The model presented is an improvement on the basic export coefficient model. The inclusion of additional controls (topography, soil type and *HER*) describing TP transfer and the use of Monte Carlo simulation (to preclude the need for poorly constrained optimisation or subjective selection of coefficients) greatly improves the utility of this approach for predicting phosphorus transfer, whilst retaining low, readily-available input data requirements. Although further testing of the model in other catchments is required, it represents a

promising screening tool for evaluating diffuse source P transfers, particularly in data poor catchments.

ACKNOWLEDGEMENTS

This project is being financed by The University of Stirling and Unilever.

REFERENCES

- Boorman, D.B., Hollis, J.M. & Lilly, A. (1995). *Hydrology of Soil Types: A Hydrologically-Based Classification of the Soils of the United Kingdom*, Report No. 126, Institute of Hydrology, Wallingford, U.K.
- Brady, N.C. & Weil, R.R. (1999). *The Nature and Properties of Soils 12th Ed.*, Prentice Hall, New Jersey, U.S.A.
- ESRI (1996). *ArcView G.I.S.*, ESRI, California, U.S.A.
- Foy, R.H. & Bailey-Watts, A.E. (1998). Observations on Spatial and Temporal Variation in the Phosphorus Status of Lakes in the British Isles, *Soil Use and Management*, **14**, 131-138.
- Heathwaite, A.L. (1997). Sources and Pathways of Phosphorus Loss From Agriculture. In *Phosphorus Loss From Soil To Water*, Tunney, H., Carton, O.T., Brookes P.C., Johnston, A.E. (eds), C.A.B. International, Wallingford, U.K., pp. 205-223.
- Johnes, P.J. & O'Sullivan, P.E. (1989). Nitrogen and Phosphorus Losses from the catchment of Slapton Ley, Devon – An Export Coefficient Approach, *Field Studies*, **7**, 285-309.
- Johnes P.J., Moss B., Phillips G.L. (1994). *Lakes – Classification and Monitoring. A Strategy for the Classification of Lakes*. National Rivers Authority R&D Project Record 286/6/A. U.K.
- LLCMP (1999). *The Loch Leven Catchment Management Plan, March 1999*, Perth & Kinross Council.
- Kolenbrander, G.J. (1972). Eutrophication from Agriculture with Special Reference to Fertilisers and Animal Waste, *Soils Bulletin*, **16**, 305-327.
- McGechan, M.B. (in press, 2003). Modelling Phosphorus Leaching to Watercourses from Extended Autumn Grazing, *Grass and Forage Science*.
- Morgan, M.A. (1997). The Behaviour of Soil and Fertiliser Phosphorus. In *Phosphorus Loss From Soil To Water*, Tunney, H., Carton, O.T., Brookes P.C., Johnston, A.E. (eds), C.A.B. International, Wallingford, U.K., pp. 137-149.

- Nash, D., Hannah, M., Halliwell, D., Murdoch, C. (2000). Factors Affecting Phosphorus Export from a Pasture-Based Grazing System, *Journal of Environmental Quality*, **29**, (4), 1160-1166.
- Rustomji, P. & Prosser, I. (2001). Spatial Patterns of Sediment Delivery to Valley Floors: Sensitivity to Sediment Transport and Hillslope Hydrology Relations, *Hydrological Processes*, **15**, 1003-1018.
- SAC (1986). *Fertiliser Recommendations, Revised Edition*, Scottish Agricultural College, Edinburgh, UK.
- SAC (1992). *Technical Note: Fertiliser Series No. 14. Fertiliser Allowances for Manures and Slurries*, Scottish Agricultural College, Edinburgh, UK.
- Smith, K.A., Chalmers, A.G., Chambers, B.J., Christie, P. (1998). Organic Manure Phosphorus Accumulations, Mobility and Management, *Soil Use and Management*, **14**, 154-159.
- Thompson, N., Barries, I.A. & Ayles, M. (1981). *The Meteorological Office Rainfall and Evaporation Calculation System: (MORECS)*, Hydrological Memorandum No. 45, The Met Office, Bracknell, UK.
- Turner, B.J. & Haygarth, P.M. (2000). Phosphorus Forms and Concentrations in Leachate Under Four Grassland Soil Types, *Soil Science Society of America Journal*, **64**, (3), 1090-1099.
- Vollenweider, R.A. (1968). Scientific Fundamentals of the Eutrophication of Lakes And Flowing Waters, with Particular Reference to Nitrogen and Phosphorus as Factors in Eutrophication. OECD Technical Report No. Das/Dst/88. 182pp.